IDENTIFICATION AND EVALUATION OF ANTIGENS FOR SARCOMA IMMUNOTHERAPY

HARSIMRAT KAUR BIRDI

Thesis submitted to the University of Ottawa
in partial Fulfillment of the requirements for the
Doctorate of Philosophy in Microbiology and Immunology

Department of Biochemistry, Microbiology and Immunology
Faculty of Medicine
University of Ottawa

Abstract

Cancer immunotherapies focused on tumor-specific T cell responses are promising alternatives to chemotherapy/radiotherapy for various cancers as they can be engineered to specifically target tumours and establish long-term surveillance against relapsing tumours. The premise for the application of active immunotherapies is the recognition of tumor-specific and/or tumor-associated antigens by the immune system. Approaches that have been explored to this end include cancer vaccines and gene therapy/autologous cell transfer (T-cell receptor (TCR) or chimeric antigen receptor (CAR)-based).

This study evaluated the use of oncolytic rhabdovirus-based vaccines (ORV) for the treatment of sarcoma with a focus on rhabdomyosarcoma (RMS). Sarcomas are amenable to to oncolytic virus (OV) infection and generate robust T-cell responses against tumour antigens. The ORV strategy undergoing clinical evaluation uses a prime-boost vaccine whereby a non-replicating adenovirus serotype 5 vector (Ad5) encoding an antigen is administered as a priming agent and boosted with a rhabdovirus encoding the same antigen (NCT02285816). However, the prevalence of pre-existing immunity to Ad5 in patients serves as an exclusion criterion and limits its effectiveness as a priming agent. To this end, we have shown that an alternative priming agent and antigen delivery vehicle, anti-DEC205 (aDEC205), targets antigens directly to dendritic cells (DCs), inducing robust immune responses. However, a lack of targetable antigens and methods to identify antigens is a limiting step for the application of ORVs for sarcoma. Thus, the identification of immunogenic sarcoma antigens is a critical step for the study ORVs. Current methodologies have important drawbacks in that they can be prohibitively time-consuming, complex or are ineffective in coupling antigen discovery and immunogenicity. Presented herein is the study of a novel methodology for the discovery of immunogenic antigens by probing for T cell activation

marker CD107a and isolation by flow cytometry. In parallel, RMS antigen discovery was also performed via peptide elution and mass spectrometry resulting in the identification of 24 novel murine RMS antigens. Ultimately, therapeutic vaccination with a subset of these antigens encoded into DEC205 and ORV did not yield immune responses in a pre-clinical model; however, this research established immunization tools for further study of immunotherapy in RMS.

Acknowledgements

The work presented herein truly would not have been possible without the aid and mentorship of several people. Firstly, I would like to thank my supervisor Dr. Jean-Simon Diallo for all of the motivation, understanding and support for a particularly difficult and highly ambitious project. I would also like to thank Dr. Fanny Tzelepis for her unrelenting guidance, support, and patience throughout my studies. Dr. Tzelepis' mentorship was paramount to my sustained passion for the study of immunology. I would like to acknowledge the aid, insight and counsel given by my thesis committee members, Dr. Seung-Hwan Lee, Dr. Michele Ardolino and Dr. Carolina Ilkow, who have played a significant part in my scientific training. Additionally, this work would not have been possible without the advice and contribution of our collaborators Dr. Silvia Boscardin, Dr. Shashi Gujar and Dr. Robin Parks.

Thank you to all of my lab mates at the OHRI and Cancer Center. I have learned a lot from all of your unique experiences both in life and science. There are several of my peers, both past and present, I would like to thank for their moral and technical support: Dr. Nicole Forbes, Dr. Daniel Serrano, Dr. Elena Godbout, Dr. Serge Neault, Andrew Chen, Michael Phan, Anabel Bergeron, Boaz Wong, Nouf Alluqmani, Anne Landry, Keara Sutherland, Zaid Taha, Naveen Haribabu, Dr. Rozanne Arulanandam, Dr. Ramya Krishnan, Dr. Mohsen Hooshyar, Dr. Nader El-Sayes, and Dr. MOhammed Selman. Most importantly, I would like to acknowledge Anna Jirovec who has been with me from the start through every failed experiment, late nights, early mornings, manuscript writings, collaboration and immunological banter.

Finally, these last 5 years certainly would not have been possible without the love and support of my closest and dearest friends and family. The one person who is truly the proudest of my work is my father Paramjit Singh Birdi who has been my greatest example of tenacious work

ethic and perseverance. There were many times in my career when I felt like giving up and selling myself short but my father knew how much I can truly accomplish and this is all because he never gave up on me. The emotional support from my mother, Manjinder Kaur Birdi, really kept me afloat on the days when I was sure I would give up. I owe my parents everything I am today as they've allowed me to flourish in a country in which they were not born but one they made for themselves with hard work and sheer determination. They gave me all the freedom that allowed me to truly be myself and stand up for myself, both critical life lessons. Lastly, I thank my sister Manreet Kaur Birdi for adding her touch of humor and unyielding life talks as we both grew together in a time when we were physically apart but always a phone call away.

Table of Contents

List of Abbreviations

7-AAD	7-Aminoactinomycin D
APC	Antigen presenting cell
Ad	Adenovirus
CAF	Cancer associated fibroblast
CAR	Chimeric antigen receptor
cDNA	Complimentary DNA
CDR3	Complementarity determining region 3
CFU	Colony-forming unit
CLR	C-type lectin receptor
CTL	Cytotoxic T cell
CTLA-4	Cytotoxic T-lymphocyte-associated protein-4
DAMP	Danger associated molecular pattern
DC	Dendritic Cell
DEC205	Cluster of differentiation 205
DCIR	Dendritic cell immunoreceptor
ECM	Extracellular matrix
ELISA	Enzyme-linked immunosorbent assay
ELISPOT	Enzyme-linked immunospot assay
FACS	Fluorescence-activation cell sorting
FSC-A	Forward scatter height
FSC-H	Forward scatter width
GFP	Green fluorescent protein
GIST	Gastrointestinal stromal tumour
GM-CSF	Granulocyte macrophage colony stimulating factor
GzmB	Granzyme B
HIV	Human immunodeficiency virus
HLA	Human leukocyte antigen
ICD	Immunogenic cell death
ICS	Intracellular staining
ICV	Infected cell vaccine
IFN-γ	Interferon-gamma
IHC	Immunohistochemistry
IT	Intratumoural
IV	Intravenous
ITAM	Immunoreceptor tyrosine-based activation motif
JX-594	Pexastimogene devacirepvec
LPS	Lipopolysaccharide
MG-1	Maraba virus 1
MOI	Multiplicity of infection
MHC	Major histocompatibility complex
MMR	Macrophage mannose receptor
NFAT	Nuclear factor of activated T cells
NK	Natural killer
ORF	Open reading frame

ORV	Oncolytic rhabdovirus vaccine
OV	Oncolytic virus
OVA	Ovalbumin
PAMP	Pathogen associated molecular pattern
PBMC	Peripheral blood mononuclear cells
PCR	Polymerase chain reaction
PD-L1	Programmed cell death protein 1
PFU	Plaque forming units
PI	Propidium iodide
PRR	Pattern recognition receptor
pMHC	Peptide/major histocompatibility complex
qPCR	Quantitative polymerase chain reaction
RFP	Red fluorescent protein
RMS	Rhabdomyosarcoma
scFv	Single-chain variable fragment
SSC-A	Side scatter area
SSC-H	Side scatter height
SSC-W	Side scatter width
STS	Soft tissue sarcoma
TAA	Tumour associated antigen
TCR	T cell receptor
TIL	Tumour infiltrating lymphocyte
TLR	Toll-like receptor
TNFα	Tumour necrosis factor alpha
Tregs	Regulatory T cell
VSV	Vesicular stomatitis virus
Wt	Wild-type
β-2M	Beta-2-microglobulin

List of Figures

List of Tables

Copyright Statement

This thesis contains published and unpublished work.

The introduction, materials and methods, Figures 2-1 to 2-9, associated figure legends, text and discussion of Chapter 2 are included in the following publication:

> Tzelepis, F.,*__Birdi, H.K.,*__ Jirovec, A.,* Boscardin, S., Tanese de Souza, C., Hooshyar, M., Chen, A., Sutherland, K., Parks, R., Werier, J., Diallo, JS. "Oncolytic rhabdovirus vaccine boosts chimeric anti-DEC205 priming for effective cancer immunotherapy." *Molecular Therapy Oncolytics*. 19; P240-252 (December 2020) doi: 10.1016/j.omto.2020.10.007.
>
> *Equal contribution

Some modifications to the text and formatting of figures have been made in this thesis. The original article is attached as Appendix IV and is also available here:

https://www.cell.com/molecular-therapy-family/oncolytics/fulltext/S2372-7705(20)30158-3

Chapter 1 - General Introduction

1.1 Immune System

The immune system is a complex but coordinated defense mechanism in animals whose sole purpose is to protect the host from harm and maintain homeostasis. This system is incredibly complex, ranging an entire organism and constantly scanning tissues for anything awry. Research into such a field can be a daunting task but key discoveries in the past century have truly expanded our range of understanding of its basic tenets, the physiology of the immune system and also its larger role in human disease. T cells, a critical component of this system, provide insight into the ever-expanding diversity of vertebrate immunity. The adaptive immune system typically works in harmony with the whole of an organism to orchestrate the diverse mechanisms required to fight pathogens and potentially dangerous self-derived components; the latter being the most notorious for representing the development of cancer. This body of work delves deeper into the intricacies of T cell-mediated immunity in the context of cancer.

1.2 Antigen processing and generation of peptide-MHC complexes

T cells carry out their immunologic activity upon recognizing antigens, which are byproducts (peptides) of cleaved proteins. Peptides are presented in the context of major histocompatibility complexes (MHC) I or II, creating the peptide-MHC complexes (pMHC).[1,2] CD8+ T cells recognize peptides presented by MHC class I and CD4+ helper T cells (herein referred to simply as CD4+ T cells) recognize peptides in the context of MHC class II.[3,4] A third class of antigen presenting machinery also exists, called CD1, presenting lipid-derived antigens to specific classes of T cells and will not be discussed here.[5] All vertebrate animals express MHC molecules; in humans, these are called human leukocyte antigens (HLA), the genes of which are

located on chromosome 6. There are many subclasses of MHC arising from gene duplication events in evolution. Class I proteins consist of a heterodimer of an α-chain (*HLA-A, HLA-B, HLA-C* genes) bound to the ubiquitous β2-microglobulin (β2M) subunit. Class II proteins consist of α- and β- heterodimers encoded by the *HLA-DP, HLA-DM, HLA-DOA, HLA-DOB, HLA-DQ,* and *HLA-DR* genes.[6]

MHC I and II present different types of peptides dependent on the origin of the protein itself. MHC II typically present peptides derived from exogenous proteins. In the endoplasmic reticulum (ER), the α- and β- chains associate with an invariant chain (CD74) that blocks unstable peptide-binding within the ER and translocate to mature endosomes through the trans-Golgi network.[7] In parallel, exogenous proteins are internalized through either phagocytosis, endocytosis or macropinocytosis. Exogenous proteins are cleaved in the vesicular pathway by lysosomal proteolysis mediated by the action of cathepsins.[8] Cleaved peptides are also translocated to the late endosomal compartment, now called the MHC-II compartment (MIIC). Following invariant chain processing, high affinity peptides of 11-15 amino acid length are loaded onto mature MHC II molecules.[9]

MHC I, present on all cells in the host, excluding erythrocytes, typically present peptides of cytosolic origin from self or viral proteins. Cytosolic proteins arising from defective ribosomal products (DRiPs), native proteins and exogenous proteins are transported to proteasomes and cleaved. These peptides are trafficked to the endoplasmic reticulum (ER) through the transporter associated with antigen processing (TAP) heterodimer.[10] ER aminopeptidases (ERAP/ERAP1, ERAP2) further process and trim ER peptides. Occurring in parallel in the ER is the association of the peptide loading complex (PLC) proteins calreticulin (CRT) and ERp57 with the MHC-I/B2M heterodimer and TAP1/2, stabilizing the empty MHC I prior to peptide loading. The binding of

high affinity peptides into the MHC I groove induces dissociation of MHC-I/B2M heterodimer and translocation to the cell surface through the Golgi apparatus.[11] However, MHC I does not only present intracellular proteins. Mechanisms in dendritic cells (DC), a class of professional antigen-presenting cells (APC), allow for proteins of exogenous origin to be trafficked into the ER through retro-translocation from phagosomes and thus be loaded onto MHC I. This process is called cross-presentation and is crucial for mounting a strong and coordinated immune response against various antigens.[12]

1.3 T lymphocytes

1.3.1 T Cell Receptor

The T cell antigen receptor (TCR), an elusive protein and regarded as the "Holy Grail of Immunology," was discovered in the 1980s by Tak Wah Mak and Mark M. Davis and revolutionized the study of the adaptive immune system.[13,14] A TCR consists of clonotypic αβ heterodimers associated with the CD3 proteins CD3δ, CD3ε, CD3γ and CD3ζ.[15] The individual proteins of the TCR-CD3 complex form first as subunits of TCRα and TCRβ in complex with CD3εδ or CD3εγ. These subunits transport to the Golgi where they combine with CD3ζ. All 6 components of the TCR-CD3 complex are transported to the plasma membrane for cell surface expression.[16] Upon T cell activation, the mature TCR-CD3 complex then recruits intracellular components to carry out functional activity (discussed in section 1.5.4)

Owing to the similarity of TCRs to immunoglobulin, further research led to elucidation of the basic structure, function and diversity of TCRs. TCR gene diversity is defined by genetic recombination of the highly divergent variable (V), diversity (D) and joining (J) domains of chromosome 14 by the V(D)J recombinase complex in early T cell development. The output is the

translation of a hypervariable region on the TCR that codes for the complementarity determining region 3 (CDR3) which bind to pMHC.[17] The allelic constant region (C) variants are far less diverse and are genetically conserved.[18] Unlike immunoglobulins that recognize whole proteins/antigens, TCRs recognize short peptides processed in APCs and presented in the context of MHC I or MHC II molecules. A key difference between immunoglobulins and TCRs is their avidity for antigens. Immunoglobulins continue to modify their affinity for an antigen through a process called somatic hypermutation, in which the CDR3 region undergoes cumulative point mutations, allowing for its adaptation to foreign antigen and enhanced recognition ability.[19] Contrarily, once developed in the thymus, TCRs do not undergo somatic hypermutation and thus retain affinity to their cognate pMHC complexes. However, the mechanisms governing TCR-ligand interactions are far more complex owing to the presence of additional co-signaling proteins which, ultimately strengthen T cell activity.[20] A great majority of T cells (>95%) express the αβ heterodimeric TCR, but a small subset of T cells express a less defined γδ heterodimer TCR hypothesized to recognize lipid antigens.[21]

1.3.2 T Cell Development

During T cell development, an extensive process prunes the milieu of precursor T cells to ensure reactivity of appropriate cells and deletion of auto-reactive cells. A process of positive and negative selection takes place to edit bone-marrow-derived T cell progenitors in the thymus.[22] The thymus is a unique compartment in that it possesses thymic antigen-presenting cells and expresses a large array of tissue-specific self-antigens that guide the editing of T cell progenitors.[23] T cell precursors first commit to either the αβ or γδ lineage while remaining both CD4 and CD8 negative (double negative, DN). From the αβ DN cells arise double-positive (DP) cells which acquire CD4+

and CD8+ expression and undergo somatic recombination at this stage resulting in a broadly heterogeneous population of DP T cells.[22]The TCR repertoire is highly diverse and mediated by processes of genetic recombination, random insertions, deletions and substitutions during T cell development. In theory, there is a potential to encode for a possible 10^{15} to 10^{20} different clonotypes, truly defining the level of diversity of this key adaptive immune compartment.[24] Of the many TCR combinations created, several DP cells arise that lack binding capacity to host MHC (in the context of self-peptide) and thus undergo apoptosis. Functional T cells, those that appropriately bind to the host MHC, but have low affinity for self-peptides, are selected for in the process of positive selection. These selected T cells eventually becoming single positive (SP) CD4+ or CD8+ T cells. SP cells that then bind too strongly to self-peptide-MHC complexes i.e. autoreactive cells that can cause harm to the host, are clonally deleted or induced towards anergy.[25] Anergic CD4 single positive T cells later function as regulatory cells that operate in the periphery to monitor and control other autoreactive immune mechanisms carried out by the activity of T regulatory (Treg) cells for example.[26]All the selected SP, differentiated, naïve CD8+ or CD4+ T cells then enter the blood stream, arriving at the spleen. They may also enter secondary lymph nodes by passing through high endothelial venules (HEVs).[26] Naïve T cells have limited functionality and require T cell priming at these lymphoid organs by APCs and to be activated.

1.3.3 T cell activation

T cell activation in lymphoid organs determines the fate of antigen specific T cells. T cell priming is mediated by professional APCs, of which the best example are conventional DCs. Once activated, CD4+ and CD8+ T cells undergo phenotypic changes, clonally expand and gain their effector function. T cell phenotypes can be characterized by the cytokines they secrete for example,

activated CD4+ T cells can secrete IFNγ or IL-4, depending on specific cell type, and CD8+ T cells secrete IL-2, TNFα and IFNγ.[27,28]

T cell priming requires a minimum of two signals to become activated: TCR binding to pMHC on an APC and binding of co-stimulatory ligands of DC (CD80/CD86) to costimulatory receptor (CD28) of T cells.[29] Receiving either signal alone is insufficient for T cell priming and may lead to the generation of anergic cells or T cell ignorance. Furthermore, a balance between activating and inhibitory signals, e.g. the inhibitory signal CTLA-4 on APCs, ultimately regulates T cell priming.[30]

The engagement of TCR to a cognate pMHC is a dynamic process orchestrated by a number of accessory proteins enabling the close 15nm interaction of a T cell and target cell.[31] In the initial moments of T cell and target cell binding, distant pMHC and TCRs form microclusters with weak intracellular signalling capacity.[32] A current understanding of this interaction suggests the formation of a "bulls eye" like structure at a central location composed of several accumulating microclusters that move centripetally through dynein and actin mediated transport.[33] The accumulation of microclusters creates a central synaptic region called the central supramolecular activation cluster (cSMAC) which facilitates sustained signalling mediated by highly concentrated intracellular Lck, a cytosolic protein tyrosine kinase (PTK).[32] Distally from this central location, the interaction between integrins such as LFA-1/ICAM-1, also called the peripheral supramolecular activation cluster (pSMAC), further mediate cytoskeletal adhesion and stabilization to facilitate T cell signalling at the cSMAC.[34] Furthest from the cSMAC is the distal ring of SMAC composed of CD45 that plays a role in signal regulation.[35]

Intracellular signalling at the cSMAC begins with the phosphorylation of immunoreceptor tyrosine-based activation motifs (ITAMs) on, CD3ε and CD3ζ by Lck (associated intracellularly

with CD4 or CD8).[36] Phosphorylated CD3ζ, in particular, serves as a recruitment site for ZAP-70, a member of the Syk kinase family.[37] Zap70 is a critical protein that carries out a downstream activation pathway by first phosphorylating LAT and SLP-76, which then associate with Gads. These adaptor proteins recruit PLC-γ, which then cleaves PIP_2 to form diacylglycerol (DAG) and inositol triphosphate (IP_3).[38] These proteins, as well as the Ca^{2+}-release activated Ca^{2+} (CRAC) channel which function to free intracellular and extracellular calcium Ca^{2+}, respectively, activate the nuclear factor of activated T cells (NFAT), activate NFκB and activate the MAP kinase cascade.[39,40] Notably, TCR binding to its ligand is insufficient to promote this signaling cascade and is aided extensively by the downstream, and parallel, activity of the co-receptor CD28. APCs present the ligands B7.1/CD80 and B7.2/CD86 that ligate with CD28. Intracellular effector proteins then mediate a host of complementary and highly essential functions in T cells such as cell survival, T cell differentiation, promoting production of cytokines (the most significant being IL-2) and promoting progression of the cell cycle.[41] The most distinguishing characteristic of T and B cells is the ability to acquire a trained response, or memory, to the antigen against which they are primed. Early data suggested that upon an antigen re-challenge, these adaptive cells are activated without the need for antigen presentation by DCs and co-stimulation resulting in hastened proliferation, release of cytokines, cytotoxic function and differentiation into antibody-secreting plasma cells.[42] However, many groups have challenged this idea and suggest that indeed some CD28 co-stimulation is necessary for the generation of a recall response from memory T cells.[43,44] The principles of memory formation in T and B cells are discussed in greater detail in chapter 1.7 (Vaccines).

1.3.4 Cytotoxic T cells

CD8+ T cells, also referred to as cytotoxic T lymphocytes (CTLs) are distinct from CD4+ T cells in that their effector functions include the release of cytotoxic molecules in addition to cytokines. Although research suggests that CD4+ T cells also have some capacity for cell lysis,[45] CD8+ T cells are much more adept at this function. CD8+ T cell priming is aided enormously, indirectly and directly, by the milieu of secreted cytokines and stimulatory signals by CD4+ T cells.[46] Helper T cells express the ligand (CD40L) for the CD40 receptor presented on DCs.[47] The ligation of the CD40L with CD40 upregulates the co-stimulatory proteins CD80 and 4-1BBL on DCs rendering them fully mature and activated. Only then can a CD8+ T cell be effectively primed to recognize pMHC in the periphery.[48] The fully activated CD8+ T cell proliferates by the autocrine and paracrine function of IL-2 and subsequently traffics to the periphery.[49] An antigen presenting cell can be induced to undergo apoptosis by its association with and recognition by cognate antigen-specific CD8+ T cells which then secrete directed cytotoxic granules and/or interact with death ligand receptors like Fas. CD8+ T cells store the cytotoxic granules, granzyme B (GzmB), a serine protease, and perforin, in intracellular vesicles until a calcium influx event, facilitated by TCR signal transduction, leads to vesicle fusion at the cell membrane and release of GzmB and perforin at the cytotoxic synapse.[50] Perforin creates pores in the antigen presenting cell through which GzmB permeates. There, GzmB targets pro-caspase 3 (which activate caspase mediated cell death) and BID (a member of the Bcl-2 family pro-apoptotic proteins).[51] The death ligands, FasL and TRAIL, also induce cell death upon engaging death receptors and inducing apoptosis in parallel in the same fashion as GzmB.[52] As all immune cells are incredibly skilled at cell-cell communication, another key function of effector CD8+ T cells is the recruitment of other immune components to the site of inflammation. This is accomplished by the release of two key

cytokines: interferon-γ (IFN-γ) and tumor necrosis factor-α (TNF-α). These cytokines have varying functions including immune cell recruitment, further CD8+ T cell proliferation, and macrophage activation.[53]

1.4 Cancer

Cancer is highly heterogeneous, with more than 100 distinct types, and is one of the most complex diseases affecting humans.[54] The complexity of cancer is attributed to the biological capabilities acquired during its multistep evolution, influenced by both intrinsic (genetic/epigenetic), local (tissue), and systemic (host) factors. The key hallmarks of cancer include sustained proliferation and evasion of growth suppressors, resistance to cell death, induction of angiogenesis, capacity to metastasize, and evasion from the immune system.[55] The Canadian Cancer Society predicts that 1 in 2 Canadians will develop cancer in their lifetime and 1 in 4 will die of it, indicating a need for the development of therapies that are able to tackle this growing national health problem.[56] However, cancer is not only prevalent in the aging population; it also manifests in children. Based on origination tissue type, there are 6 major categories that classify cancer, based on originating tissue type, and include: carcinoma, sarcoma, myeloma, leukemia, lymphoma and mixed.[57] Among these, sarcoma is a relatively rare and heterogeneous malignancy that arises from mesenchymal tissue and accounts for less than 1% of adult solid cancers but 20% of pediatric solid cancers.[58] Sarcomas occur frequently in bone, fat, joints and muscles and are divided into two major types: >50 subtypes of soft-tissue sarcoma (STS) and 3 subtypes of bone sarcoma (osteosarcoma, chondrosarcoma and Ewing's sarcoma).[58–60] Rhabdomyosarcoma (RMS), a sarcoma of muscle tissue, represents nearly 50% of all STS cases in which diagnoses are made in children from the ages of 1 and 9 years old.[61] Two common

histological subtypes of RMS exist: the embryonal (ERMS) subtype, typically common in the head and neck region, and the alveolar subtype (ARMS) found in the torso and extremities.[62] Molecularly, most RMS tumours display the aberrations characteristic of tumours, such as mutations in the *p53* and *Rb1* tumour suppressor genes and dysregulation of *RAS* genes.[63] ARMS, in particular, display chimeric transcription factors indicative of a translocation event leading to the fusion of the forkhead transcription factor (FKHR/FOXO1) to PAX3 (PAX3-FOXO1) or PAX7 (PAX7-FOXO1) transcription factors.[64] The presence of these transcription factors is a major determinant of RMS subtype and drives prognosis and therapeutic intervention.

1.4.1 Tumour Microenvironment: Non-immune Components

A tumour is far more complex than a mass of infinitely dividing cells. Multiple factors in its immediate environment help to feed, communicate, protect and provide growth signals to the malignant tissue allowing it to truly flourish and evade host defenses. These inter- and intracellular interactions of cancer cells with other host factors are termed the tumour microenvironment (TME). Gaining an understanding of the components within an individuals' TME will help to guide a full understanding of disease state and therapeutic outcome.

Firstly, the physical scaffolding, or the extracellular matrix (ECM) of a tumour is greatly influenced by the activity of cancer associated fibroblasts (CAFs). Fibroblasts generally play a role in producing the components of the ECM, such as connective tissue, and are invariably important in tissue repair.[65] It is speculated that normal fibroblasts in the TME can be transformed by factors secreted by tumours such as inflammatory cytokines (IL-6, TNF, TGFβ, epidermal growth factor (EGF))[66], induction of physiological stress by way of metabolic disruption and generation of reactive oxygen species (ROS)[67], and cell to cell interactions via ICAM1 and VCAM1.[68]

Differentiated fibroblasts, in turn, induce further tumour growth through the secretion of EGF and hepatocyte growth factor (HGF). Furthermore, CAFs stimulate angiogenesis and lymphangiogenesis through the secretion of vascular endothelial growth factor (VEGF) and PDGF, fueling the cancer with nutrients, oxygen and circulating immune suppressive factors.[69] With the advent of vasculature and lymphatic vessels, CAFs can mediate tumour metastasis to distant tissues such as lung, liver and lymph nodes.[70] CAFs also secrete key pro-inflammatory chemoattractant signals, such as CXCL12, which stimulate the recruitment of immune cells.[71]

The cells that make up the newly formed blood vessels, the vascular endothelial cells, respond to angiogenic cues (VEGF, FGF, PDGF) present in the TME and produce additional neovasculature around tumours. This neovasculature defies normalcy, as they contain extensive branching and leaky channels leading to uneven distribution of nutrients and oxygen creating hypoxic regions within the tumour.[72]

The major structural component of tumours, the ECM, makes up the structural units that function as a scaffold for the various cell types present within the tumour. The structural building blocks include a complex network of proteins, proteoglycans and glycoproteins. Some examples of these components include collagenous fibrils and fibronectin making up the scaffolding and producing the tensile strength and contributing to elasticity of tumours.[73] Matrix metalloproteases (MMPs), proteases and cathepsins remodel ECM components contributing to the continuous evolution of cancer.[74]

1.4.2 Tumour Microenvironment: Immune Cells

The TME consists of numerous immune cells that contribute greatly to the malignancy of the tumours which they support. Immune cells exert both pro-inflammatory and anti-inflammatory

pressures on the tumour and define the behavior of the other TME components. Tumour associated macrophages (TAMs) have been extensively studied and are well characterized. There exist both pro-tumorigenic, called M2, and anti-tumorigenic, M1, TAMS. TAMs are polarized by the presence and absence of various signals within the TME. M2 macrophages are characterized by the secretion of IL-10 and TGF-β and exert anti-inflammatory effects in the TME leading to the recruitment of other anti-inflammatory immune cells and contributing further to angiogenesis and metastasis leading to poor therapeutic prognosis.[75]

Myeloid-derived suppressor cells (MDSCs), a class of immature myeloid cells, are another population of inhibitory immune cells found in the TME. MDSCs are much less studied than TAMs nevertheless what is known is that they may be a key player in mediating global immunosuppression. MDSCs can deplete amino acids, more specifically regulating the levels of L-arginine, that is necessary for T cell activity. Additionally, MDSCs produce IL-10 and TGF-β, which affect the antitumour T cell responses and recruit regulatory T (Treg) cells. Taken together, MDSCs can severely impair antitumour immune responses.[76]

There are a variety of lymphocytes that traffic to the TME. As tumours are highly immunosuppressive and concentrated with anti-inflammatory chemokines and cytokines, the majority of T lymphocytes trafficking to tumours are effectively inhibited by these compounds. The presence of antigen experienced CTLs in the TME is associated with better prognosis as they have the capacity to kill antigen expressing tumours. CD4+ T cells of the Th1 phenotype that secrete IL-2 and IFN-γ support the activity of CTLs in the TME.[77] The role of Th2 in a pro or anti-tumorigenic capacity is heavily debated and is generally thought that they secrete anti-inflammatory cytokines such as IL-4, IL-5 and IL-13.[78] B cells are also widely debated in terms of their role in influencing anti-tumour immunity especially with research into tertiary lymphoid

structures (TLS) harbouring a great proportion of tumour associated B cells. B cells, apart from secreting anti-tumour antibodies, provide activation signals similar to CD4+ T cells in the TLS and the TME.[79] On the other hand Tregs and Bregs (B regulatory cells similar to Tregs) have been extensively studied for their role in suppressive immune responses as they secrete IL-10 and TGF-β. Furthermore, Tregs express the immune checkpoint inhibitor (ICI) CTLA-4 that inactivate effector CTLs in the TME.[20] Altogether, the presence of Tregs and Bregs in the TME indicate a poor patient prognosis and greater immune suppression of any draining CTLs or Th1 cells.[21]

1.5 Cancer Immunotherapy

Immunotherapy has emerged in the last few decades as a treatment option for cancer as we expand our knowledge on the important role played by the immune system to prevent tumour growth in healthy individuals. However, the tumor microenvironment is a complex array of supporting cells composed of cancer associated fibroblasts, vasculature, and immune components that contribute to cancer growth.[77,80] Of the immune components, there exist both anti-tumour and pro-tumour responses which compete with one another involving an interplay of regulatory T cells, myeloid-derived suppressor cells (MDSCs), and tumour associated macrophages.[81] The suppressor cells can induce anergy of effector cells through secretion of immunosuppressive cytokines such as IL-10 and TGF-β, and also delete tumor-specific T cells. The localization of the tumor also affects T cell response because it can impair the access of circulating T cells.[82]

In addition, a selective pressure imposed by effector T cells influence tumor immunogenicity by triggering evasion mechanisms in a process called immunoediting. Initially, neoplastic growth is relatively controlled by the innate and adaptive components of the immune system during the phase termed elimination. However, as cancer cells are defined by rapid mutational rates, some cell clones emerge that effectively resist immunological pressure. In this

case, the immune system and cancer fight head-to-head with little elimination of one or the other, thus an equilibrium is formed. Finally, as more resistant cells grow, they outcompete the immunological pressure and escape from control.[83] The mechanisms by which tumors evade active immune responses include down-regulation of MHC class I molecules from tumor cell surface, loss of tumor antigens and upregulation of immune checkpoint blockade, among many.[84]

Cancer immunotherapy strives to manipulate the balance between pro-tumour and anti-tumour immune responses. There are many ways in which this can be accomplished which include, but are not limited to, breaking immune tolerance, passive immunotherapy involving the administration of anti-tumour antibodies and immunomodulatory drugs, and active immunotherapy involving the deliberate generation of stronger effector T cell responses in a patient.[85,86] As such, immunotherapies based on mounting a long lasting immune response by tumour specific T cells are one form of treatment that has attained clinical success and has the potential to be used for the treatment of cancer. Sarcoma specifically can benefit from the advent of immunotherapies as a number of recent advancements from pre-clinical research to Phase I-II clinical trials show promise in this disease setting.[87] The next subsection discusses these therapies in detail.

1.5.1 Vaccines

The study of immunity was accelerated by the advent of vaccines by the fathers of immunology, Edward Jenner and Louis Pasteur.[88] Vaccines have been one of the most important contributors to the eradication of some of the most lethal human infectious diseases. The basic tenets of vaccination, also called immunization, is the generation of protective and long-lasting immunity. The type of immunization necessary for the development of a robust immune response

varies according to each pathogen and thus a variety of vaccine strategies exist which include: RNA, live-attenuated, inactivated, subunit/conjugate vaccines and toxoid vaccines for SARS-CoV-2, tuberculosis, polio, hepatitis B, and tetanus, respectively.[89] Protective immunity against most pathogens can be generated by inducing the production of neutralizing antibodies. However, for some pathogens such as tuberculosis, malaria and HIV, neutralizing antibodies are insufficient and protective immunity must be complimented with cell-mediated immunity. In the latter case, cellular components of the adaptive immune system are mobilized against a vaccine formulation conjugated to peptide or protein subunits, aptly named conjugate vaccines. These vaccines convert a T-cell independent immune response to a T-cell dependent response as the conjugated protein/peptide can be processed and presented to T cells in the context of MHC on APCs. Important caveats to this approach are generating a suitable response and in the appropriate cell type. As such, adjuvants, substances that augment immunogenicity, are crucial for alerting the innate immune response and recruiting adaptive compartments. Inorganic aluminum salts (alum), Freund's adjuvant (oil-in-water emulsion containing component of mycobacteria), bacterial polysaccharides (CpG and LPS) are all examples of adjuvants that trigger innate immunity by signaling through TLRs and NOD-like receptors.

A commonality between all of these vaccine types is the need for multiple immunizations consisting fundamentally of priming and boosting doses generally done with homologous and heterologous vectors. A priming dose, as the name suggests, primes an adaptive immune response to the primary antigen encounter, leading to efficient antigen presentation by DCs, presentation to CD4+ and CD8+ T cells, of which the former encourages B cell priming, and the development of immune memory. In a homologous context, a boosting dose consists of the same elements as a priming dose and functions as both a secondary antigen challenge to increase antibody titer and a

means to improve antibody affinity as well as the population of memory CD4+ and CD8+ T cells. Research suggests that heterologous prime-boost vaccines, which employ dissimilar prime and boost vectors, are more effective than homologous vaccines described in models of HIV, *Plasmodium falciparum* and *Mycobacterium bovis* vaccines.[90] The exact mechanism by which this occurs is still unknown, but the recently described phenomenon of trained immunity may provide some clues and is an avenue of research that will aid in the design of effective vaccines for infectious disease and cancer.[91,92]

1.5.2 Cancer Vaccines

There is an intricate relationship between the immune system and tumour. The existence of tumour antigens (discussed below) and tumour specific T cells has provided the basis for many immunotherapies. Prophylactic vaccines against the viruses HPV and HBV, the causes of cervical and liver cancer respectively, have shown success in their ability to induce immune responses to viral antigens and act, in the traditional sense, as anti-cancer vaccines.[93,94] Therapeutic vaccines for developed tumours have unique challenges including: 1) circumventing immune suppressive mechanisms, 2) possible low immunogenicity or low antigen burden of some tumours and 3) physical barriers of an established tumour. A successful cancer vaccine requires that an appropriate tumour antigen is selected, displayed in a suitable vector and administered in the relevant site overcoming immunological challenges. As cancer is a highly heterogeneous disease, research is still ongoing to understand the diverse biological mechanisms governing the interplay of the immune system with each disease type. There currently exist 3 vaccine platforms which will be discussed below: 1) cellular vaccines, 2) virus vector vaccines and 3) molecular vaccines (peptides, DNA or RNA).[95]

Apart from pathogenic cell vectors (BCG for the treatment of bladder cancer) for delivery of antigenic payloads, the other two widely studied examples of cellular vaccines for cancer are immunization with killed (irradiated) tumour cells or autologous APCs.[96] Currently in clinical trials is the GVAX vaccine consisting of whole tumour cells genetically induced to produce the cytokine GM-CSF by transduction with viral or non-viral vectors.[97] Theoretically, there is a potent secretion of GM-CSF at the site of immunization rendering the site pro-inflammatory and leading to, not only the recruitment of immune cells, but also to the uptake of a milieu of tumour associated antigens by DCs.[98] This in turn is hypothesized to prime an adaptive immune response against a variety of antigens in a natural process of antigen uptake, processing and presentation. Although successful in promoting tumour regression in murine models, the results for melanoma, prostate cancer, lung cancer and pancreatic cancer are quite varied.[74]

Another method for delivering tumour antigens in the form of a vaccine is the immunization with *ex vivo* antigen loaded autologous DCs.[99] This technique ensures efficient antigen uptake by DCs and eliminates the additional physical and immunological barriers of inducing antigen presentation that may arise by immunizing with irradiated tumours alone. The first instance of the use of such a vaccine in human disease was for metastatic and castration-resistance prostate cancer (Provenge, Sipuleucel-T). First autologous DCs are collected via leukapheresis and purified by magnetic-bead purification. Purified DCs are then loaded *in vitro* with prostatic acid phosphatase (a prostate cancer antigen) and activated by GM-CSF, expanded and infused back into the patient. Bearing the burden of a complicated procedure, high cost and most importantly, only a modest median overall survival (25.8 vs. 21.4 months in infused vs. placebo patients), the trial was deemed unsuccessful.[100] Another small clinical trial using an

$MART_{27-35}$ antigen pulsed autologous DC vaccine was employed for the treatment of melanoma and yielded some promising results indicating the involvement of T cells in the response.[101]

Alternatively, antigens may be provided independently of a cellular carrier by way of protein or peptide vaccines given with adjuvant. Peptides themselves do not require antigen processing and can be presented on MHC I by both APCs and other non-DC APCs quite effectively priming CD8+ T cells.[102] However, presentation without co-stimulation, as mediated by any nucleated cells that uptake and present the antigen, leads to tolerance to antigens and may have the opposing effect of tolerizing CD8+ T cells to the immunizing agent and promoting tumour growth.[103] This hurdle may be overcome by involving imperative players of the antigen processing machinery: DCs and CD4+ T cells that both work together to effectively prime CD8+ T cells. This can be accomplished by immunizing instead with a synthetic long-peptide (SLP) consisting of MHC I and MHC II tumour specific/associated epitopes in tandem and separated by cathepsin and protease specific linkers. This strategy has the advantage of ensuring SLP processing and presentation on DCs to both T-helper and cytotoxic cells when administered with adjuvants.[104] However, the rate limiting step in this mechanism is effective targeting to the appropriate DCs which cannot be ensured when peptides are simply administered to patients without a vehicle.

An alternative mechanism of delivering antigenic peptides and proteins directly to conventional DCs is by employing a specific DC targeting vehicle.[105] This is accomplished by exploiting the characteristic cross-presentation mechanism of DCs that allows antigen presentation on both MHC II and MHC I, leading to a more holistic immune response. The mechanism by which extracellular, endocytosed antigens enter stable early endosomes and is presented on MHC I are still unclear but research has alluded to the most effective endocytic receptors that drive this process.[106] As such, specific cross-presentation associated endocytic receptors include the

macrophage mannose receptor (MMR), dendritic cell immunoreceptor (DCIR2), dendritic cell-specific intercellular adhesion molecule-3-grabbing non-integrin (DC-SIGN), Dectin-1 and cluster of differentiation 205 (CD205 or DEC-205).[107]

1.5.3 DEC-205 Antigen Targeting

DEC-205 is a 205kDa, type I (outward pointing N terminus) cell surface receptor of the C-type lectin receptor (CLR) family and is expressed on activated DCs, thymic epithelial cells and Langerhans cells. The CLR class of receptors contain carbohydrate binding domains (CRD) that bind to carbohydrate motifs in a calcium dependent manner however DEC-205, containing 10 CRDs, differs from the prototypical CLR, a mannose receptor, as its CRDs do not show actual carbohydrate binding. The true physiological ligand of DEC-205 has remained largely unknown; however, some studies have alluded to its binding to keratin on apoptotic cell bodies and synthetic CpG oligonucleotides.[108,109] DEC-205 contains a cytoplasmic tyrosine based motif that mediates internalization by clathrin-coated vesicles.[110] Evidence suggests that there is differential expression of CLRs in DCs dependent on their activation status, indicating that activated cells largely express DEC-205 whereas immature DCs express MMR and DC-SIGN.[111] Most CLRs are internalized in coated vesicles and recycle ligand-receptor molecules to and from cells in early endosomes. DEC-205 is unique in that it is internalized in coated vesicles and recycles through the late endosome/lysosomal vacuoles and is particularly poised to present/cross-present antigens to MHC I and MHC II much more efficiently than MMR.[112] The efficiency of cross-presentation led to extensive research into the utilization of this receptor to mediate effective antigen specific T cell responses in a vaccine platform. One method of achieving this goal is targeting DEC-205 via recombinant monoclonal antibodies that carry an antigenic payload.[113] Antigen delivery using this

mechanism leads to cross-presentation of antigens and production of potent cytokines, such as IFN-γ, that will activate all compartments of the adaptive immune response including CD8+ T cells, Th1 cells and B cells.[114] Pre-clinical immunization studies that entail the delivery of a monoclonal anti-DEC205 (aDEC205), conjugated to the model antigen ovalbumin (OVA) via its Fc portion, with an anti-CD40 and LPS adjuvant, shows enhanced protection against infectious disease, delays in tumour growth and improved survival of tumour bearing mice.[103] Other studies have assessed targeting of various antigens to DEC-205 in this manner such as an HLA-DP4 restricted epitope from MAGE-A3, survivin, HER2/*neu*, and CD8+ HIV epitopes.[115–118] The advantage of such a vaccine strategy combines the effects of an *ex vivo* antigen loaded autologous DC vaccine and *in vivo* delivery of antigenic peptides. This lends the aDEC205 targeting strategy as an attractive vaccination approach in combination with appropriate adjuvants and has implications for the development of effective T cell responses in the context of infectious disease and cancer.

1.5.4 Viral Vector Vaccines

Antigens can also be delivered in a vector, that is inherently foreign, to efficiently alert the immune system without the need for suitable adjuvants. This is accomplished by delivering antigenic payloads in the form of a viral vector that serves as PRRs and triggers TLRs and NOD-like receptors thus, employing a holistic immune response recruiting innate and adaptive systems while also delivering specific cancer antigens to APCs.[119,120] Furthermore, viruses are fundamentally diverse and contain sufficient flexibility to allow for the insertion of chosen genetic material intended for a particular outcome ranging from specific antigens, immune modulators, and effector proteins[121,122] Commonly studied recombinant viruses used as cancer vaccines include

iterations of vaccinia virus (encoding PSA, MUC1, CEA, or 5T4 antigens)[123], adenoviruses (encoding MART-1 or gp100)[124], Semliki forest virus (encoding HPV E6 and E7 genes)[125], Sindbis virus (encoding NY-ESO-1 antigen)[126], and Herpes simplex virus, HSV (encoding gp100, MART-1, tyrosinase antigens or IL-12, GM-CSF immunomodulators).[127] A key limitation to the use of viral vectors as antigen delivery vehicles is that they cannot be administered as multiple doses in a homologous prime-boost method to boost antigen specific T cell responses. As such, the advent of a heterologous prime-boost strategy has been a tremendous benefit for the induction of primary and secondary T cell responses, in which variations of DNA plasmids, recombinant viruses, recombinant proteins or bacterial vectors are given. PROSTVAC®-VF/Tricom™ is one such example of a vaccine strategy for prostate cancer, employing a vaccinia virus prime encoding PSA followed by booster immunizations with fowlpox encoding the same antigen.[128] A phase 1 clinical trial reported tolerability to a prime-boost vaccination of plasmid DNA priming immunization encoding HER2 and GM-CSF followed by a booster vaccine with adenovirus encoding HER2.[93] The current hurdle in the approval of such vaccine strategies is a lack of the induction of a robust immune response that is able to overcome inherent immunosuppression in the TME. Thus, studies of heterologous prime-boost are being assessed as combination therapies with checkpoint inhibitors against CTLA-4, PD-1 and PD-L1.

1.5.5 Oncolytic Viruses

Another form of immunotherapy that has gained recent regulatory approval employs oncolytic viruses (OVs). OVs are a class of live biologicals used to preferentially target and kill cancer cells while leaving healthy cells relatively unharmed. Cancers exhibit many characteristics that overlap with those that are conducive to successful viral replication such as resistance to

apoptosis, increased nucleotide synthesis, and an impaired antiviral response.[129] Many different viruses have been clinically evaluated for their potential as OVs including measles virus, herpes simplex virus (HSV), and the rhabdoviruses vesicular stomatitis virus (VSV) and Maraba virus.[130] Additional attenuating genetic modifications are generally introduced into OVs to increase the safety profile. For example, oncolytic rhabdoviruses are attenuated by deletion of the matrix protein in vesicular stomatitis virus (termed VSVΔ51) and mutation of components of the matrix and glycoproteins in Maraba (MG-1).[131] In addition, OVs can be genetically manipulated to encode proteins that either help to establish a productive infection of cancer cells or encode cytokines and/or immunogenic antigens. For example, FAST proteins are a group of fusogenic proteins found among non-enveloped reoviruses that function as virulence factors that enable fusion of the virus infected cell to a neighbouring host cell allowing for local viral dissemination.[132] A recombinant oncolytic VSVΔ51 expressing FAST protein has been generated and was found to increase viral replication and spread in *in vivo* tumours.[133]

While they can be effective as monotherapies (such as the recently FDA approved HSV-based Imlygic encoding the transgene GM-CSF), OVs have the potential for combination with other therapies that enable anti-tumour immune responses.[134] It is known that OVs can elicit cancer vaccine effects on their own. Indeed, infectious virions specifically target tumour cells, cause lysis and relieve local immunosuppression. In this environment, DCs can phagocytose dead/dying infected tumour cells and prime an anti-tumour, as well as anti-viral, immune response in the draining lymph node.[135] This effect can be further exploited as autologous cancer vaccines where cells are infected *ex vivo* and re-administered as a vaccine following irradiation.[136]

Vaccine strategies are generally not limited to a single dose and can be made more effective by multiple immunizations. This can involve the administration of additional homologous

(matched vaccine) or heterologous (unmatched vaccine) doses.[90] In the context of cancer vaccines, it has been recently shown that a heterologous prime-boost strategy, where an initial priming dose of a virus encoding an antigen of interest is administered then followed by a boosting dose of a different oncolytic virus encoding the same antigen, can be effective to eradicate tumors. This novel prime-boost vaccination strategy is of particular interest as an immunotherapy as it has been shown to induce robust and long-term effector T cells responses.[137] A phase I/II clinical trial is currently underway for the treatment of patients with MAGE-A3 expressing tumours. The regimen being evaluated utilizes a non-replicating adenovirus serotype 5 vector to elicit a priming response to MAGE-A3 ahead of an oncolytic rhabdovirus vaccine (ORV) expressing MAGE-A3 to maximize T-cell response (NCT02285816). A variety of sarcomas have previously been shown to be particularly sensitive to oncolytic rhabdoviruses MG-1 and VSVΔ51 and the ORV strategy generates robust T-cell responses against tumour antigens.[138] Furthermore, ORVs have an added feature in which efficient infection of splenic B cells provides an additional source for antigen presentation to dendritic cells (DCs) and secondary expansion of T cells.[139] However, one potential limitation in the current prime-boost strategy employing adenovirus serotype 5 is that it may be less effective in patients who are seropositive for the adenovirus, representing nearly 30-40% of the North American population.[140] Ad5 neutralizing antibody titres are even higher among populations in Asia, South America and Africa further decreasing the effectiveness of Ad5 based vaccine platforms around the globe.[141] Therefore, many viral vectors in various contexts are currently being explored to seek an alternative prime-boost strategy that can overcome the existence of pre-existing immunity to adenovirus vectors.

1.6 Tumour antigens

A necessity in the development of anti-cancer vaccines is the identification and use of appropriate tumour antigens. The process by which a tumour interacts with the host immune system is multifactorial however, one of the crucial factors, especially for the adaptive immune response, is the recognition of tumour as a dangerous entity. Bacterial, viral or parasitic pathogens inherently harbor non-self-components called pathogen-associated molecular patterns (PAMPS) which interact with host pattern recognition receptors (PRR) to elicit an innate pro-inflammatory response, effectively alerting the immune system of danger and ridding the host of the foreign challenge.[142] Host cellular components can also mount an innate immune response when danger associated molecular patterns (DAMPs), such as HMGB1, heparan sulfate or calreticulin is released by apoptotic cells.[143] DAMPs in the TME often function as a double-edged sword. A tumour which is fundamentally a host tissue, may retain the capacity to elicit an innate immune response but likely in the context of immunogenic cell death (ICD). However, the secretion of DAMP associated pro-inflammatory cytokines such as many IL-1, IL-6 and HSPs may aid tumour progression.[144] Therefore, a highly specific response from the innate immune system is not possible for such a disease.

The adaptive immune system, namely T cells, respond to a host invasion in a very specific manner, as CTLs and effector CD4+ T cells recognize a presented antigen rather than a conserved PAMP or DAMP. All cells in the human body, including tumours, present their own processed antigens on MHC class I; however, the adaptive immune system does not consistently respond to host antigens due to a mechanism called tolerance.[145] There exist both central and peripheral tolerance mechanisms. Central tolerance is established during the development and maturation of lymphocytes in the bone marrow and thymus in a process called negative selection. Essentially,

any autoreactive T cells that bind too strongly to self-antigen presented by medullary thymic epithelial cells or dendritic cells, undergo apoptosis or remain in an anergic state.[22] Peripheral tolerance, mediated by mainly Tregs and Bregs, exists to regulate auto-reactive T cells that may have escaped negative selection.

Understandably, it is difficult for T cells to mount a tumour specific immune attack, owing to the tumours' presentation of endogenous antigens. However, cancer is characteristically highly mutated, and in many cases, dedifferentiated, which alters its presentation of 'endogenous' antigens. However, ever evolving tumours do present specific antigens that indeed are capable of recognition by autologous reactive T cells.[146] There are 5 main types of antigens that cancer cells can present to be recognized by T cells (cancer germline, mutated, viral, overexpressed and differentiation) and are divided in terms of whether they are tumour-specific antigens (TSA) or tumour-associated antigens (TAA). The first TSAs are cancer germline antigens which are proteins expressed typically in germline (such as cancer testis antigens) or trophoblastic cells (such as oncofetal antigens), not in normal differentiated tissue. This class of antigens emerges due to demethylation of promoter sequences and includes the melanoma-antigen encoding gene (MAGE family), NY-ESO-1 and SSX genes which are shared among many patients.[147] Trophoblastic and germline cells do not express MHC I and antigens are not expressed in these tissues. Therefore, developing T cells are not negatively selected against and any presentation of germline antigens is deemed as atypical to T cells.[148]

The second class of TSA are mutated antigens derived from mutated genes that give rise to altered proteins which are cleaved and presented on MHC I. In many cases, point mutations in ubiquitously expressed genes or frameshift mutations give rise to misfolded proteins that may either be destroyed or, upon proteolytic cleavage, enable the presentation of new epitopes not seen

anywhere else in the host.[149] Since tumours mutate continuously and adapt to their toxic environment, their tumour-specific mutations are constantly changing, giving rise to many new antigens, called neoantigens. Therefore, neoantigens are strongly correlated with the mutational burden of cancers and thus are more immunogenic, which is the case for lung cancer, melanoma and bladder cancer.[150] However, these antigens are rarely shared between patients due to the heterogeneity of the mutations in each disease.

A third class of TSA are viral antigens. Cervical cancer, hepatocarcinoma and nasopharyngeal carcinoma have viral origins and therefore any viral proteins translated in the cell can be presented on MHC I.[151] They are evidently foreign antigens and are thus detected by T cells. Many antigens have been discovered from human papillomavirus proteins E6 and E7.[152]

One class of TAA are overexpressed peptides that are due to the increased transcription and translation of proteins in cancer. Although these proteins are found in healthy tissue as well, tumours simply have very high levels of these proteins therefore, they present more of them endogenously. A complication of such antigens is determining the threshold by which overexpression is considered abnormal. Some examples of shared overexpressed antigens include peptides from the *PRAME* gene, survivin, ERBB2 (Her-2/*Neu*) and p53.[153]

The fifth and final class of TAA are differentiation antigens which are proteins expressed in both the malignant tissue and its corresponding healthy tissue. However, expression in healthy tissue typically occurs during differentiation of that tissue. The most well-known example is in melanoma in which proteins involved in melanin synthesis, such as tyrosinase, Melan-A/MART-1 and TRP2 are highly expressed in tumours.[154] Carcinoembryonic antigen (CEA) is also expressed in various epithelial tissue in the gastrointestinal tract but can be expressed in colorectal cancers.[155]

1.7 T cell antigen discovery

Vaccine based approaches for the treatment of cancer rely heavily on the selection of appropriate antigens that will elicit strong and long-term T cell immune responses. A majority of early vaccine studies for cancer employed overexpressed proteins and was not based necessarily on the ability of antigens to induce T cell responses. Due to the high degree of polymorphisms of HLA in humans and the diversity of cancers, the identification of individual-specific and immunogenic antigens can be daunting and challenging. As it currently stands, it is imperative to identify a diverse array of antigens that may be expressed across a wide range of patients and tumours and induce immune responses. Many different approaches have been employed over the past few decades that identify MHC I and MHC II restricted epitopes as well as surface antigens that may serve as target antigens for T cell immunotherapy.

1.7.1 cDNA library functional screening

The early technologies to identify T cell antigens relied on screening cDNA libraries with CD8+ T cells by assessing their functional activity in response to an array of pMHC molecules expressed in a target cell line. This technology was highly used for melanoma due to the amenability of this cancer to *in vitro* culture methods. In this genetic approach, a cDNA library is first created from autologous tumour cells and tumour reactive CTLs are isolated. The cDNA library of interest is transfected into cells with suitable antigen-presenting capability and amenable to genomic library transfections. As such, COS-7 (monkey kidney fibroblasts) and 293T (human embryonic kidney) cells were used as targets for this purpose. Screening of the target cell library is then performed by co-culture with a pool of autologous CTLs purified from patient blood. Positive target cell clones are identified based on cytokine release, namely IFN-γ or TNF-α, by CTLs.[156,157] Sequential limiting dilutions are necessary to isolate the specific target from the

selected pools. The well-known MAGE-1, -2, -3 antigens were discovered in this way.[158] An advantage of this method is that immunogenic antigens that elicit a CTL response can be isolated. However, one of the major challenges with this method is the difficulty in generating T cell clones and the necessity to re-clone the selected pools of target cells that will undergo the second step of sequential limiting dilutions. Furthermore, these T cell clones may not necessarily represent the full repertoire of tumour specific CTLs present in the patient.[159]

Similar to CTL screening, serological analysis of recombinant cDNA expression libraries (SEREX) is also used to identify tumour antigens. This method uses serum isolated from patients to screen phage display libraries expressing tumour derived cDNA proteins. This technique involves the creation of a cDNA library from the tumour of interest and expression in a phage display system. The phage library is then probed for antibody recognition using sera derived from the same tumor bearing patient as well as control sera. A secondary IgG reactive antibody (autoantibody) is then added to assess binding of IgG to target cell clones. DNA from the positive clones is sequenced and used for downstream screening to assess T cell reactivity to proposed antigens.[160] The NY-ESO-1 cancer testis antigen was discovered in this way.[161] Although this approach is simpler than the CTL screening approach, the identified proteins deemed to induce B-cell responses are not indicative of CD8+ T cell responses present in the patient. If a CTL response is to be determined, this must be further validated *in vitro* which can be tedious.

1.7.2 Reverse immunology

Newer technologies make use of *in silico* algorithms programmed to reflect the antigen processing machinery to predict peptides likely to be loaded onto MHC I or MHC II based on anchor-motif residues. This method involves assessing bioinformatics algorithms and using

molecular methods to identify tumour-specific transcripts. Then prediction of proteasomal cleavage sites and HLA binding is required in order to finally experimentally validate the immunogenicity of the antigen. The peptides most likely to serve as a tumor specific antigen are then screened *in vitro* using patient derived CTLs by assessing cytokine release in ELISPOT assays to truly confirm the presence of responding T cells.[162] Mesothelin, expressed in pancreatic cancer, was discovered in this way.[163] A major advantage of this method is that it does not rely on long-term *in vitro* T cell culture or the availability of autologous patient tumor cells. The prediction algorithm can also be programmed to assess any HLA type. Some disadvantages of this approach are that the screening method cannot accurately predict receptor binding affinity, post-translational modification of these MHC ligands *in vitro* or indicate immunogenicity of the identified peptide.[164]

1.7.3 MHC Pulldown

The immunoaffinity chromatography method of identifying therapeutic target for CD8+ T cell based therapies and cancer immunotherapy is biochemically-based and relies on the isolation of peptide-MHC (pMHC) complexes using MHC specific monoclonal antibodies (mAB) from lysed fresh tumour tissue, frozen tissue, cell lines or blood. A lysing process purifies MHC from the surface of cells and the resulting lysate is then centrifuged and filtered. The lysate is then passed onto pan mAbs (W6/32 for HLA-A, -B, -C or L243 for HLA-DR) sepharose beads for binding.[165,166] Bound MHC complexes are washed with high pressure liquid chromatography (HPLC) and resulting peptides are isolated by ultrafiltration that filter molecules of 10kDa or less. The filtrate, containing a variety of proteins and peptides, is then assessed downstream for sequence analysis. Mass spectrometry (MS) is one such technology used to identify the amino acid sequence of the resulting peptides. For this type of analysis, peptides are fragmented and the mass

of the analyte molecules is assessed to deduce the identity of the peptide sequence.[119] Currently, MS of eluted peptides is considered the gold-standard technology for the rapid identification of MHC I or MHC II peptides. This method also has limitations such as the large amount of mABs needed for isolation, methodological and analytical complexity, and incapacity to distinguish between intracellular pMHC and extracellular pMHC, of which only the latter is expressed and is capable of being immunogenic. Again, immunogenicity is not certain as surface pMHC expression is not always indicative of the presence of a corresponding CTL response. Importantly, it is not known if the T cell response elicited by these antigens could attribute to autimmunity.[167]

1.9 Rationale and Aims

Although RMS is incredibly rare, it still represents more than half of all STS cases in children. From 2013-2017, 40 children between 0-14 years of age were diagnosed with STS of which 30% were diagnosed with RMS in Canada.[168] A large majority of patients are within the low or intermediate risk group with a 5-year survival rate of greater than 70%. However, high risk patients, those with stage III or IV disease, characterized by metastasis to lymph nodes and lungs, have a 5-year survival rate of less than 20%.[169] The standard of care for RMS currently is chemotherapy consisting of a combination of the drugs vincristine, dactinomycin and cyclophosphamide (VAC), radiation and surgery, a treatment regimen that has remained largely unchanged.[170] The rarity of this disease in relation to the highly prevalent cancers (melanoma, lung, breast, prostate) contributes to the lack of improved therapies in the last 3 decades.

Alternative therapeutic approaches for all types of pediatric sarcomas are currently being studied, the most notable being immunotherapy. Immunotherapy in the form of antigenic vaccines, immune checkpoint blockade, adoptive cell transfers and immune modulators are only now

starting to be studied for subclasses of STS including Ewing's sarcoma, gastrointestinal stromal tumour (GIST), synovial sarcoma, liposarcoma and leiomyosarcoma. These STS subtypes have well characterized expression of CTAs such as NY-ESO-1, MHC independent/cell surface ganglioside antigens (G2, G3, GM2), SSX, survivin and MAGE family antigens.[171]

Immunological profiling of RMS is only now beginning to be executed. In a recent study, ganglioside antigens were described in 4 out of 16 RMS patient samples. Ultimately, the study alluded to the targeting of ganglioside antigens in an antibody specific therapy.[172] Furthermore, PD-L1 expression was assessed in patient tissue by immunohistochemistry (IHC) and found to be present in 15 out of 25 patient samples.[173] This study also suggests the possibility of assessing checkpoint inhibitors as a therapeutic strategy for RMS. Other TAA or TSAs, the tumour microenvironment, and the immunological landscape are still far less characterized in RMS; this limits the exploration of novel immunotherapy strategies for this disease.

To this end, the objectives of the research presented herein were to explore the applicability and efficacy of a therapeutic vaccine in the context of a pre-clinical model of RMS. The design of such an immunotherapy is dependent upon a variety of factors that must be taken into consideration for an immunotherapy to emerge for specific diseases. In the context of a T cell based immunotherapy, as is the case with the use of a therapeutic vaccine, the choice of antigen, adjuvant, and delivery vehicle that leads to an effective anti-tumour T cell response must all be considered. The study presented herein assesses these various aspects of a prime-boost immunotherapy vaccine design including the discovery of novel antigens, the immunogenic activity of the antigen-specific and tumour-specific T cells and the efficacy of a novel prime-boost vaccine consisting of a combination of unique antigen delivery vehicles. As proof of concept, this study evaluated a heterologous prime-boost vaccine strategy employing an anti-DEC205 (aDEC205) antibody

conjugated to novel RMS antigens as a priming agent followed by a boost with matched-antigen expressing oncolytic rhabdovirus in an experimental model of RMS. This type of comprehensive and diverse study informs, guides and assesses the potential limitations of novel immunotherapy approaches and also paves the road for the study of immune based therapeutics RMS.

The following chapters explore, in depth, the components required for the generation of a therapeutic vaccine for RMS:

Chapter 2: A proof of concept study assessing the efficacy of a novel heterologous prime-boost vaccine, aDEC205+VSVΔ51, in the context of a well characterized antigen model.

Chapter 3: The development of a novel approach to discover RMS TSAs. This approach was an attempt to improve the cDNA functional library method by employing flow cytometry as a means to assess CD8+ functional T cell activity.

Chapter 4: The discovery of differentially expressed MHC I epitopes from murine RMS tumour tissue using the gold standard MHC I pulldown method leading to the development and assessment of an aDEC205+VSVΔ51 prime boost vaccine in the context of a murine RMS model.

Chapter 2- Oncolytic rhabdovirus vaccine boosts chimeric anti-DEC205 priming for effective cancer immunotherapy

Fanny Tzelepis[1]*, Harsimrat Kaur Birdi[1,2]*, Anna Jirovec[1,2]*, Silvia Boscardin[3,4], Christiano Tanese de Souza[1], Mohsen Hooshyar[1], Andrew Chen[1], Keara Sutherland[1,2], Robin Parks[2,6], Joel Werier[5], Jean-Simon Diallo[1,2*]

1. Centre for Innovative Cancer Research, Ottawa Hospital Research Institute, Ottawa, Ontario, Canada. 2. Department of Biochemistry, Microbiology and Immunology, University of Ottawa, Ottawa, Ontario, Canada. 3. Laboratory of Antigen Targeting to Dendritic Cells, Department of Parasitology, University of Sao Paulo, Sao Paulo, Brazil. 4. Institute for Investigation in Immunology (iii)-INCT, Sao Paolo, Brazil. 5. Department of Surgery, The Ottawa Hospital, Ottawa, Ontario, Canada. 6. Regenerative Medicine Program, Ottawa Hospital Research Institute, Ottawa, Ontario, Canada.

Contribution

Conception and design: F.T. Data acquisition, analysis and interpretation: F.T., H.K.B., A.J. Animal Work: A.C. and C.S. Writing and Review: H.K.B., A.J., F.T., and J.S.D. Antibody plasmids and production protocol: S.B. Viral Construction and Rescue: M.H., and K.S. Adenovirus production: R.P. Supervision: J.S.D.

Published in: Molecular Therapy Oncolytics October 2020.

2.1 Introduction

As knowledge of the important role played by the immune system in preventing tumor growth in healthy individuals has expanded over the last decades, immunotherapy has emerged as a viable treatment option for cancer.[174] One form of immunotherapy that has gained recent regulatory approval employs oncolytic viruses (OVs). OVs are live replicating viruses selected or genetically modified to preferentially target and kill cancer cells while leaving healthy cells relatively unharmed.[175] This is possible owing to the fact that cancers exhibit many characteristics that are conducive to successful viral replication such as resistance to apoptosis, increased nucleotide synthesis, and an impaired antiviral response.[129] OVs elicit their anti-cancer effects through multiple mechanisms and following tumor cell lysis and immunogenic cell death, can trigger anti-cancer immune responses.[176] In addition to Imlygic, an intratumorally delivered oncolytic HSV-1 strain approved for treatment of late stage melanoma, many different viruses have been clinically evaluated for their potential as OVs including many that can be delivered intravenously such as (but not limited to) measles virus,[177] coxsackie virus,[178] and rhabdoviruses like vesicular stomatitis virus (VSV) and the closely related Maraba virus.[130] Additional attenuating genetic modifications are generally introduced into OVs in order to increase their safety profile. For example, oncolytic rhabdoviruses are attenuated by deletion of the matrix protein in vesicular stomatitis virus (termed VSVΔ51) and mutation of components of the matrix and glycoproteins in Maraba (MG-1).[131] In addition, OVs can be genetically manipulated to encode proteins that either help to establish a productive infection of cancer cells or encode cytokines and/or immunogenic antigens, such as cancer antigens.

It is known that OVs can elicit *in situ* cancer vaccine effects and relieve local immunosuppression through the induction of immunostimulatory cytokines. In this environment,

dendritic cells (DCs) can phagocytose dead/dying infected tumor cells and prime an anti-tumor as well as antiviral immune response in the draining lymph node.[135] However, the heterogeneous nature of cancer has resulted in limited efficacy of OVs as monotherapies and has steered researchers to investigate combinations of these biologics with other therapies that not only enhance OV infection of tumors but also enable anti-tumor immune responses.[179,180]

Typical vaccination regimens are generally not limited to a single dose and can be made more effective by multiple immunizations. This can involve the administration of additional homologous (matched vaccine) or heterologous (unmatched vaccine) doses.[90] In the context of cancer vaccines, it has been recently shown that a heterologous prime-boost strategy, where an initial priming dose of an adenovirus virus encoding a cancer antigen is administered followed by a boosting dose of an oncolytic rhabdovirus encoding the same antigen, can be effective to eradicate tumors.[181] This strategy has been shown to induce robust and long term effector T cell responses [137,138] and is currently undergoing clinical evaluation for multiple antigens and indications (NCT02285816, NCT02879760, NCT03618953, NCT03773744).

As a boosting component, oncolytic rhabdoviruses are thought to be uniquely effective because in addition to infecting tumor and breaking local immunosuppression, they efficiently, but non-productively, infect splenic B cells which provides an additional source for antigen presentation to DCs resulting in secondary expansion of T cells.[139]

To prime the oncolytic rhabdovirus boost, current clinical trials employ a non-replicating adenovirus serotype 5 (Ad5) vector expressing a shared cancer antigen (e.g. MAGE-A3, NCT02285816). Questions regarding the importance of vector seropositivity were raised recently following Merck's failed phase II clinical trial of a trivalent human immunodeficiency virus (HIV) vaccine delivered in an Ad5 vector.[182] Indeed, Ad5 seropositivity is sometimes an exclusion

criterion in vaccine and gene therapy clinical trials employing this vector.[183] Approximately 30-40% of the North-American population is seropositive for Ad5 and this proportion approaches an 85% average globally, posing a potential limitation to the widespread use of Ad5 as a priming vector for the oncolytic rhabdovirus heterologous prime-boost cancer immunotherapy strategy.[184–186]

DEC-205 is a C-type lectin endocytic receptor highly expressed on certain DC subtypes.[187] Chimeric antibodies specific to DEC-205 fused with an antigen of interest (anti-DEC205) have been shown to be an effective strategy to target fused antigens directly to DCs, inducing robust cellular and humoral responses when combined with adjuvants.[188,189] To overcome potential issues with Ad5 and other viruses that could be used as priming vectors but that may have the potential to be affected by pre-existing immunity, we hypothesized that chimeric anti-DEC205 antibodies could provide an effective alternative. In this study, we modeled and evaluated the impact of pre-existing immunity on Ad5-based priming. As proof of concept, we also evaluated a heterologous prime-boost vaccine strategy employing anti-DEC205-OVA (aDEC205-OVA) as the priming agent followed by a boost with OVA-expressing oncolytic rhabdoviruses in an experimental model of OVA-expressing B16 melanoma to provide a proof-of-concept for this therapeutic vaccine. The regimens employed in the B16 melanoma model were also explored in the context of a therapeutic RMS vaccine. This vaccine consisted of aDEC205-769 priming vector antibody conjugated to RMS specific CD8+ T cell epitopes discovered in the pMHC pulldown experiments in Chapter 4. The heterologous boosting vector consisted of a VSVΔ51 ORV encoding matched epitopes.

2.2 Results

2.2.1 Pre-existing immunity to wtAd5 impairs generation of SIINFEKL specific immune response to rAd5-SIINFEKL

We hypothesized that pre-existing immunity to wild-type Ad5 (wtAd5) may negatively affect priming of the immune response induced by recombinant Ad5 expressing antigens. To investigate this, we evaluated the capacity of Ad5 encoding the ovalbumin (OVA) epitope SIINFEKL (rAd-SIINFEKL) to generate an antigen specific immune response in mice with pre-existing immunity to wtAd5. To model pre-existing immunity, we immunized naive C57BL/6 mice with 10^{10} plaque-forming units (pfu) of wtAd5 virus. After 35 days, mice were administered 10^{8} pfu rAd5-SIINFEKL intramuscularly (i.m.) (Figure 2-1A). Generation of anti-adenovirus neutralizing antibodies (AdNAbs) in sera of pre-immunized mice 40 days post administration of wtAd5 was confirmed by neutralization assay and was elevated in pre-immunized mice (Figure 2-1B). SIINFEKL-specific CD8+ T-cell responses were measured 10 days after rAd5-SIINFEKL immunization; the peak time of the adaptive immune response elicited by adenovirus vectors.[190] We observed a statistically significant decrease from 10% to approximately 5% of splenic SIINFEKL-specific CD8+ T cells, depicted by H-2Kb-SIINFEKL pentamer staining, from pre-immunized mice compared to control PBS mice (Figure 2-1C, D). To assess CD8+ T cell functionality, splenocytes from pre-immunized mice and PBS mice were re-stimulated with SIINFEKL peptide *in vitro* and followed by intracellular (ICS) staining for IFNγ and TNFα. Again, there was a reduction from, an average of, 6% to 2% of IFNγ and TNFα-producing CD8+ T cells specific to SIINFEKL detected in the splenocytes from pre-immunized mice compared to control PBS (Figure 2-1E, F). Together, these results indicate that modelled pre-existing immunity to

wtAd5 limits the generation of SIINFEKL-specific cellular responses following rAd-SIINFEKL immunization in C57BL/6 mice.

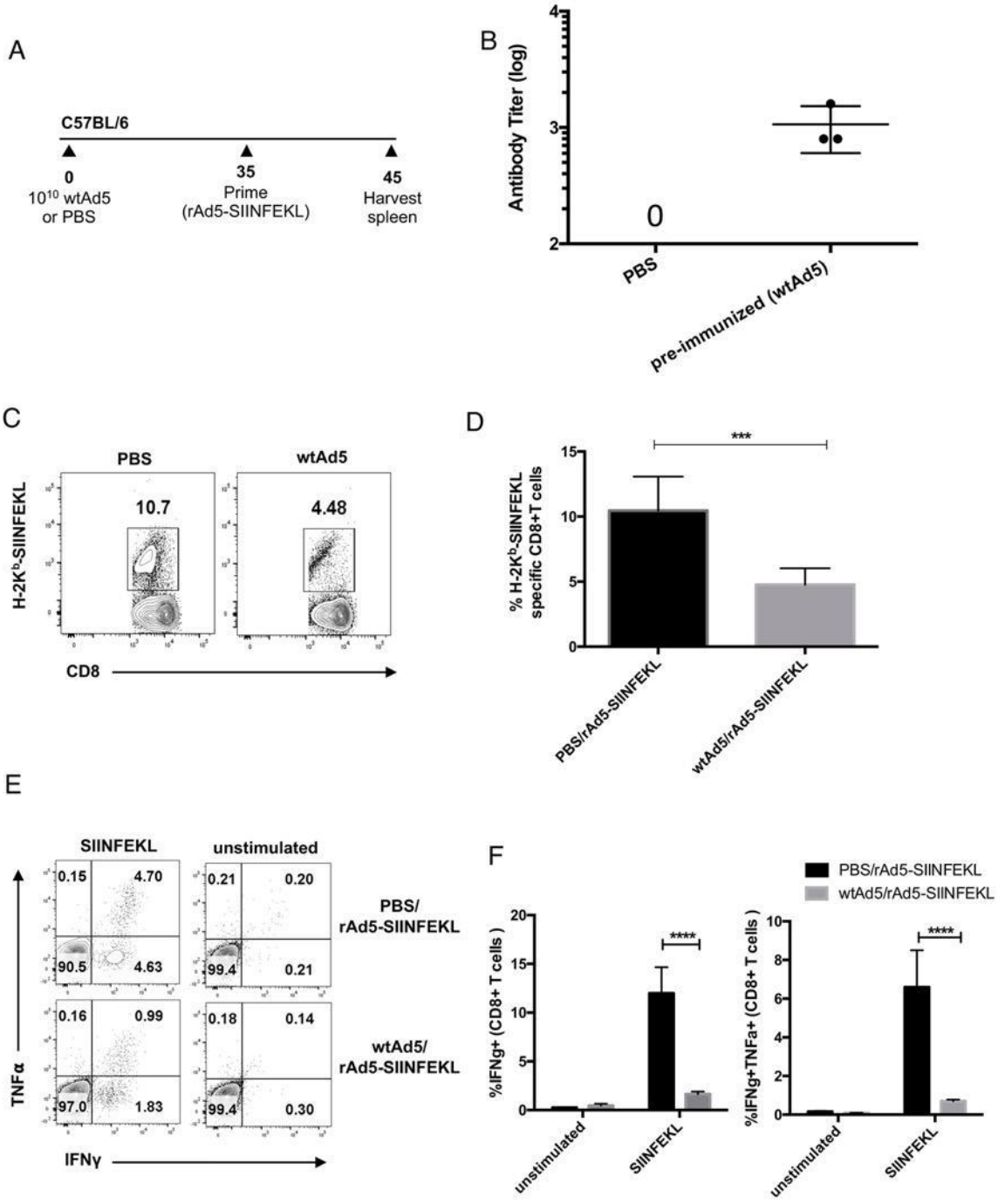

Figure 2-1. Comparing SIINFEKL-specific T cell response after i.m. injection of priming agent rAd-SIINFEKL in mice modelling pre-existing immunity to wtAd5. A. Naïve C57BL/6 mice were injected i.m. on day 0 with 10^{10} pfu of wtAd5 (n=7) or PBS (n=5). After 35 days, mice were injected i.m. with rAd5-SIINFEKL. **B.** Anti-adenovirus neutralizing antibody (AdNAbs) titers in mouse sera (n=3) were determined by neutralization assay 40 days after administration of wtAd5. **C, D.** 10 days after prime, the percentage of SIINFEKL-specific $CD8^+$ T cells in the spleen was determined by H-2Kb-SIINFEKL pentamer staining. **E, F.** The percentage of OVA-specific T cells producing IFNγ and TNFα in the spleen was evaluated by flow cytometry. Briefly, splenocytes were stimulated *in vitro* with MHC-I epitope (SIINFEKL) for 5 hours, subsequently stained for intracellular production of IFNγ and TNFα, and assessed by flow cytometry. ***$p <$ 0.001 and **** $p <$0.0001 (two-way ANOVA).

2.2.2 Production and Characterization of aDEC205-OVA

Impaired SIINFEKL-specific immune responses following rAd-SIINFEKL immunization of C57BL/6 mice modeling pre-existing immunity led us to consider employing an alternative priming agent that would be better able to overcome pre-existing immunity to wtAd5 and other potential alternative viral vectors. Several studies have shown the ability of chimeric aDEC205 antibodies fused to antigens such as OVA (aDEC205-OVA) or tumor antigens, to elicit strong antigen specific immune responses in mice when administered with an adjuvant.[114,117] To evaluate the use of antigen-fused aDEC205 antibodies as alternative priming agents for heterologous boosting with ORV vectors, we used aDEC205 fused to the model antigen OVA.

To generate the aDEC205 antibodies used in this study, HEK293T cells were co-transfected with plasmids containing the mouse aDEC205 kappa light chain and the aDEC205 heavy chain fused to the full OVA protein sequence at the carboxyl terminus (or no antigen as a control, aDEC205-empty). The recombinant antibodies produced following transient transfection in HEK293T cell were purified on protein G sepharose columns. The resulting antibodies were characterized by western blot using anti-IgG antibodies on SDS-PAGE under reducing conditions (Figure 2-2A). Figure 2-2A shows that heavy and light chains of the purified recombinant antibodies had the expected size for both the fused antibody aDEC205-OVA (~95kDa and 25kDa, respectively) and control antibody aDEC205-empty (50kDa and 25kDa, respectively). The capacity of the aDEC205-OVA and aDEC205-empty antibodies to bind to its receptor on the surface of splenic DCs CD11c+CD8a+ was confirmed with a binding assay.[191] Incubation of splenocytes from naïve C57BL/6 mice with different concentrations of aDEC205-OVA (0.1, 1 or 10μg/mL) resulted in a dose-dependent binding (Figure 2-2B) on the surface of splenic CD11c+CD8a+ DCs (gating depicted in Appendix Figure 1) expressing the DEC205 receptor. These results indicate that

aDEC205-OVA and aDEC205-empty were successfully purified from culture supernatants, and that aDEC205-OVA and aDEC205-empty (Figure 2-2C) retain binding capacity to the DEC205 receptor as expected.

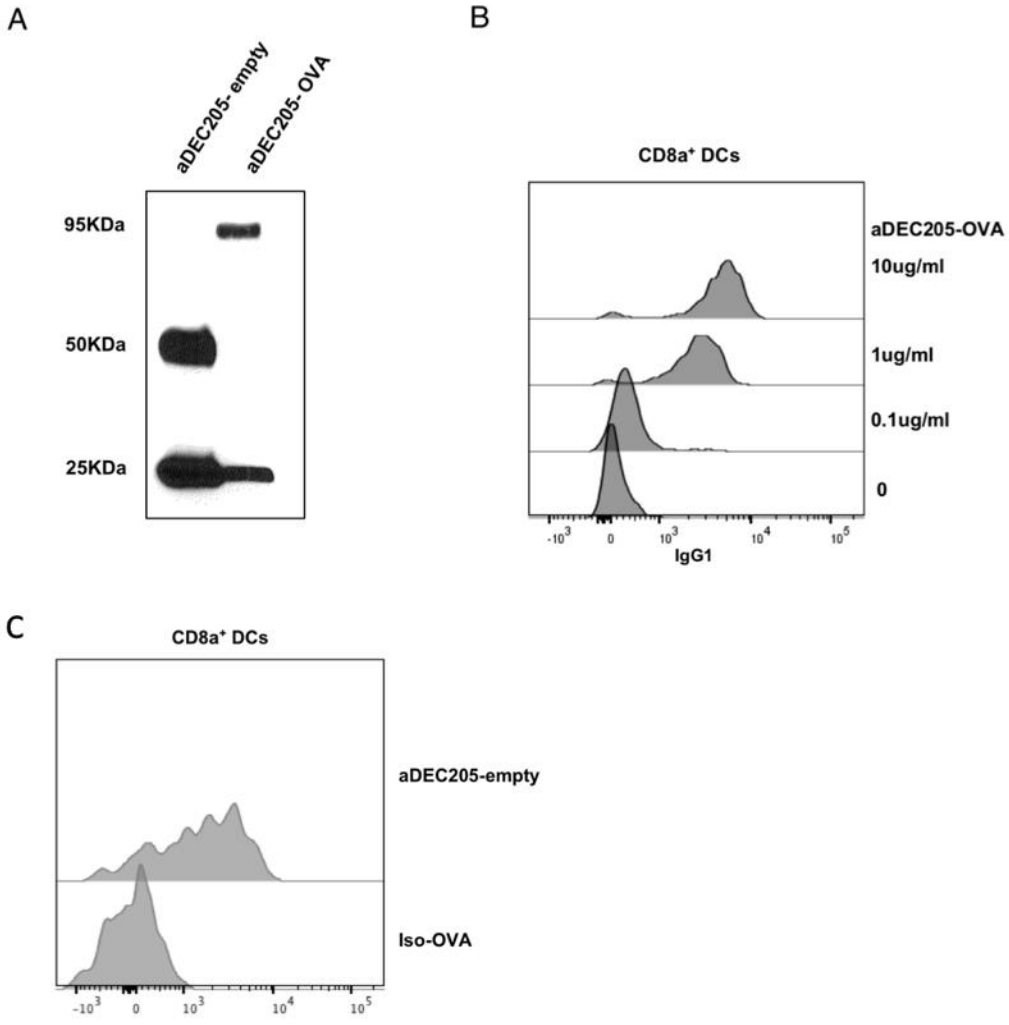
A
aDEC205- empty
aDEC205- OVA
95KDa
50KDa
25KDa
B
CD8a+ DCs
aDEC205-OVA
10ug/ml
1ug/ml
0.1ug/ml
0
IgG1
C
CD8a+ DCs
aDEC205-empty
Iso-OVA

Figure 2-2. Production and characterization of aDEC205-OVA A. aDEC205-OVA and aDEC-empty were generated by transfection of 293T cells in vitro, and subsequent purification of the antibody. **A.** Final antibody product was reduced by β-mercaptoethanol and verified by immunoblotting for the heavy and light chains. aDEC205-empty shows a heavy chain at 50kDa and light chain at 25kDa. aDEC205-OVA shows the heavy chain linked with OVA at 95kDa; indicating presence of OVA antigen, and a light chain at 25kDa. A binding assay was performed to verify effective binding of **B.** aDEC205-OVA or **C.** aDEC205-empty or isotype control IgG, to the DEC205 receptor on $CD11c^{+}CD8^{+}$ dendritic cells (DCs) isolated from murine splenocytes. aDEC205-OVA is probed with an anti-IgG1-APC antibody and detected by flow cytometry. The histogram overlay depicts high binding of aDEC205-OVA to $CD11c^{+}CD8^{+}$ DCs at concentrations of 10μg/mL and 1μg/mL, and low binding at 0.1 μg/mL.

2.2.3 aDEC205-OVA administered via intraperitoneal and intravenous routes generates cellular immune responses against SIINFEKL

Several studies demonstrated the influence of the route of immunization on immune response and disease outcome.[192] To determine which route of aDEC205-OVA administration leads to the most potent T cell response systemically, we immunized naïve C57BL/6 mice intraperitoneally (i.p) or intravenously (i.v) with 10μg aDEC205-OVA or aDEC205-empty, both in combination with 50μg poly:IC and 50μg anti-CD40. SIINFEKL-specific T cells were evaluated by flow cytometry at 10 and 21 days post-immunization (Figure 2-3A 2-4A, gating strategy shown in Appendix Figure 2). Intracellular cytokine staining after *in vitro* re-stimulation of lymphocytes with SIINFEKL peptide showed that i.v. and i.p. routes of administration elicited statistically similar percentages of IFNγ and TNFα-producing CD8+ T cells in the lung and spleen of mice immunized with aDEC205-OVA at days 10 and 21 post-immunization (Figure 2-3B-D, 2-3B-D). Additionally, staining with H-2Kb-SIINFEKL pentamer showed statistically similar percentages of SIINFEKL-specific CD8+ T cells at day 21 in the spleen and lung of mice immunized with aDEC205-OVA when comparing i.v. and i.p. routes of administration (Figure 2-3E, 2-4E). As expected, no SIINFEKL-specific CD8+ T cells were detected in the spleen or lungs of animals immunized with control aDEC205-empty. These results indicate that either route of administration elicits a strong anti-SIINFEKL primary immune response. Ultimately, to model a preferred route of administration in humans, we proceeded to administer aDEC205-OVA intravenously for the remainder of this study.

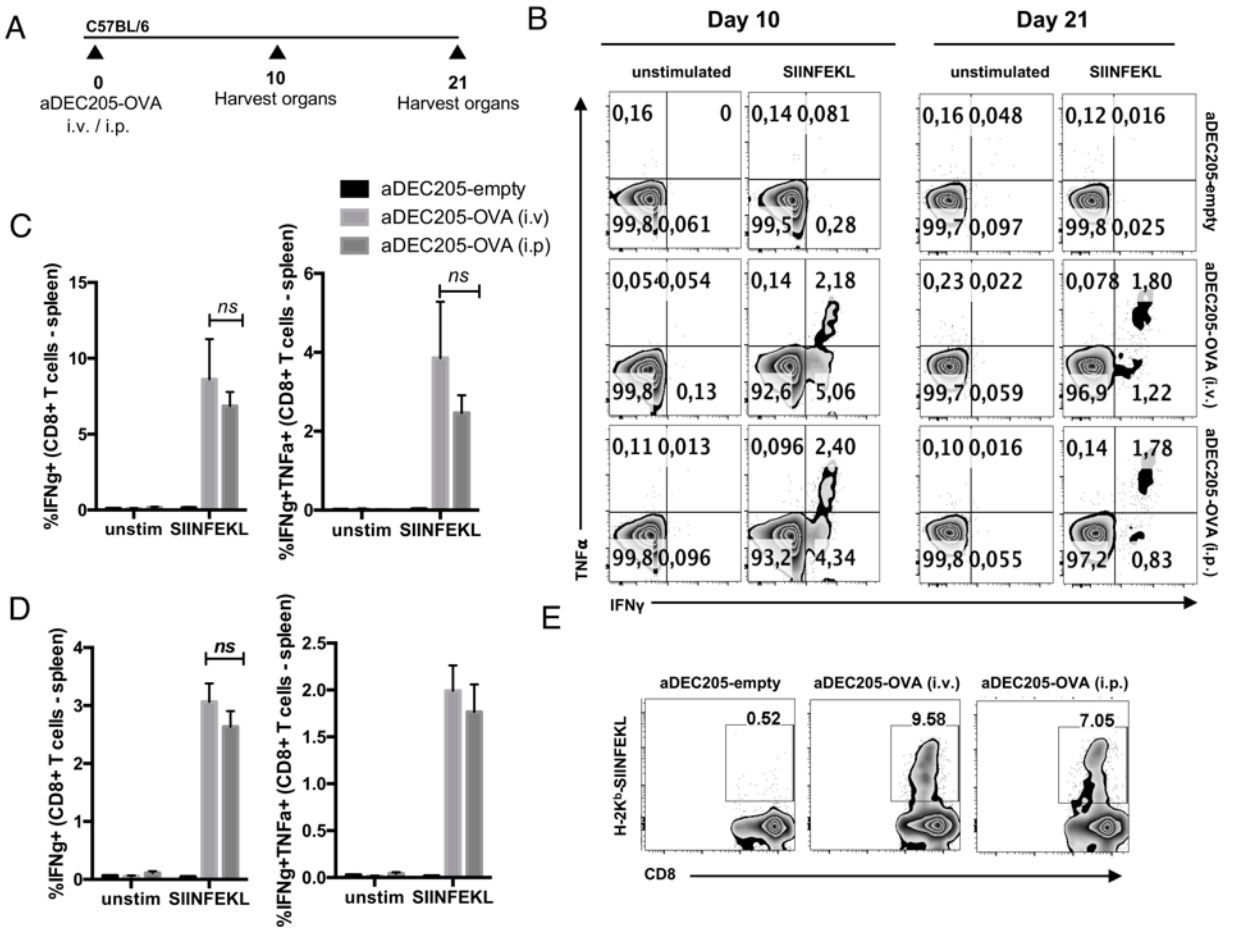
A
C57BL/6
0
aDEC205-OVA
i.v. / i.p.
10
Harvest organs
21
Harvest organs
B
Day 10
Day 21
unstimulated
SIINFEKL
aDEC205-empty
aDEC205-OVA (i.v.)
aDEC205-OVA (i.p.)
TNFα
IFNγ
C
aDEC205-empty
aDEC205-OVA (i.v)
aDEC205-OVA (i.p)
%IFNg+ (CD8+ T cells - spleen)
%IFNg+TNFa+ (CD8+ T cells - spleen)
ns
unstim
SIINFEKL
D
E
H-2Kb-SIINFEKL
CD8

Figure 2-3. aDEC205-OVA administered i.v. or i.p. elicits OVA specific T cells in the spleen of immunized mice. A. Naïve C57BL/6 mice were primed with 10μg of aDEC205-OVA or aDEC205-empty + 50μg poly:IC + 50μg anti-CD40 i.v. or i.p. The percentage of SIINFEKL-specific T cells producing IFNγ and TNFα in the spleen (**B, C** (D10), **D** (D21)) was evaluated by flow cytometry. Quantification of SIINFEKL specific T cells by pentamer staining (H-2K^{b}-SIINFEKL) was also assessed in the spleens **E.** by flow cytometry at day 21 post injection. *P*-value considered nonsignificant (NS) when >0.05 (two-way ANOVA).

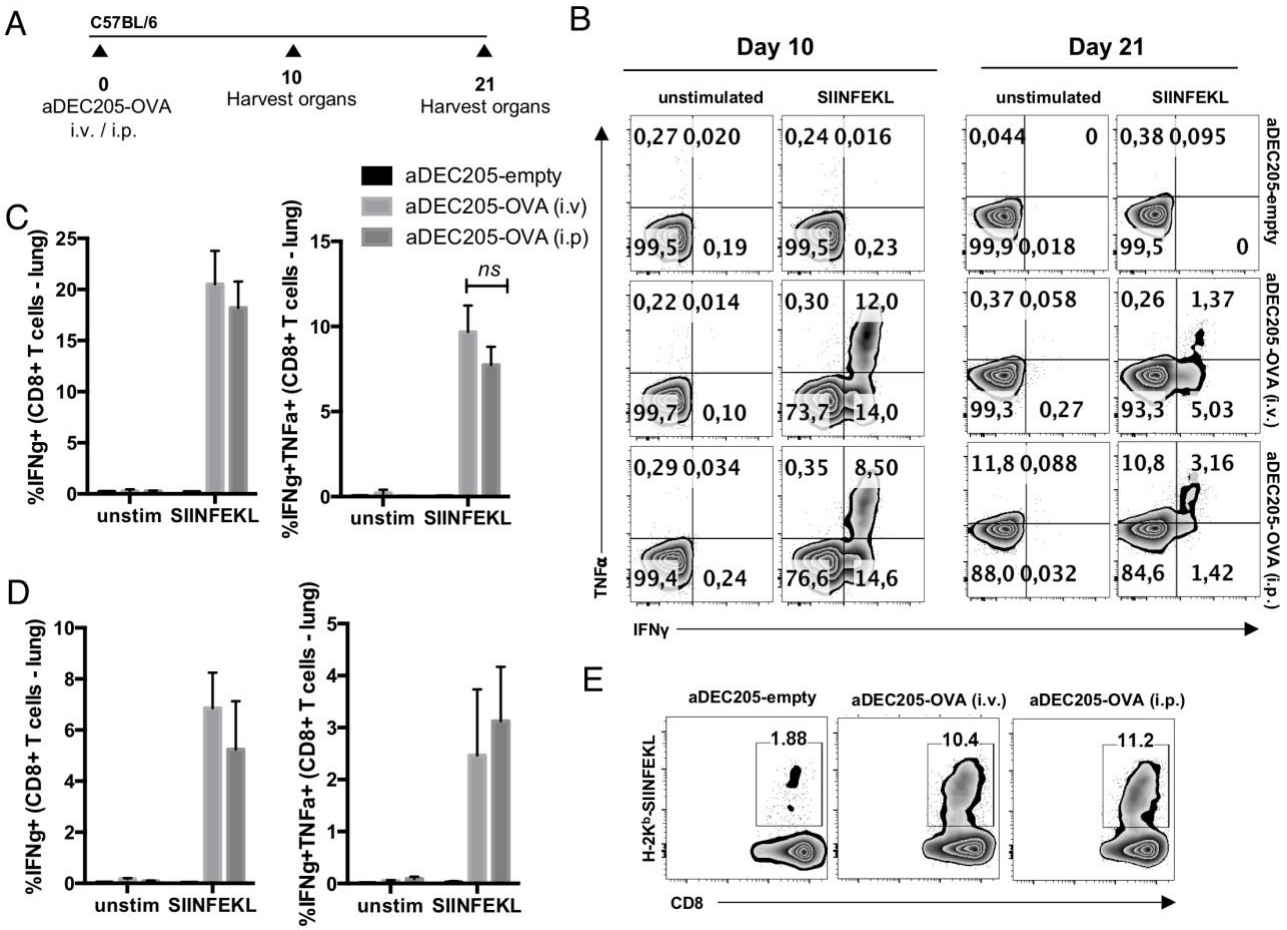
A
C57BL/6
0
aDEC205-OVA
i.v. / i.p.
10
Harvest organs
21
Harvest organs
B
Day 10
Day 21
unstimulated
SIINFEKL
aDEC205-empty
aDEC205-OVA (i.v.)
aDEC205-OVA (i.p.)
TNFα
IFNγ
C
aDEC205-empty
aDEC205-OVA (i.v)
aDEC205-OVA (i.p)
%IFNg+ (CD8+ T cells - lung)
%IFNg+TNFa+ (CD8+ T cells - lung)
ns
unstim
SIINFEKL
D
E
H-2Kb-SIINFEKL
CD8

Figure 2-4. aDEC205-OVA administered i.v. or i.p. elicits OVA specific T cells in the lungs of immunized mice. A. Naïve C57BL/6 mice were primed with 10μg of aDEC205-OVA or aDEC205-empty + 50μg poly:IC + 50μg anti-CD40 i.v. or i.p. The percentage of SIINFEKL-specific T cells producing IFNγ and TNFα in the lungs (**B, C** (D10), **D** (D21)) was evaluated by flow cytometry. Quantification of SIINFEKL specific T cells by pentamer staining (H-2Kb-SIINFEKL) was also assessed in the **E.** lungs by flow cytometry at day 21 post injection. P-value considered nonsignificant (NS) when >0.05 (two-way ANOVA).

2.2.4 aDEC205-OVA overcomes barriers posed by pre-existing immunity and generates cellular and humoral immunity against OVA

We next evaluated the ability of aDEC205-OVA to overcome pre-existing immunity to wtAd5 in a C57BL/6 murine model. To model pre-existing immunity, all naive C57BL/6 mice were immunized with wtAd5 35 days prior to the injection of priming agents (Figure 2-5A). As previously observed, AdNAbs were detected by neutralization assay in mouse sera 40 days post administration of wtAd5 and were elevated in pre-immunized mice around time of prime (Figure 1B). Pre-existing immunity to wtAd5 did not affect priming with aDEC205-OVA; approximately 9% of SIINFEKL-specific CD8+ T cells were observed in the spleen of pre-immunized mice and control PBS mice 10 days after prime (Figure 2-5B and C). Furthermore, a similar percentage of splenic IFNγ and TNFα-producing CD8+ T cells specific to SIINFEKL were also detected by intracellular staining (Figure 2-5D, E). Together with Figure 2-1, these results suggest that adjuvanted aDEC205 is an effective prime in the face of pre-existing immunity to wtAd5.

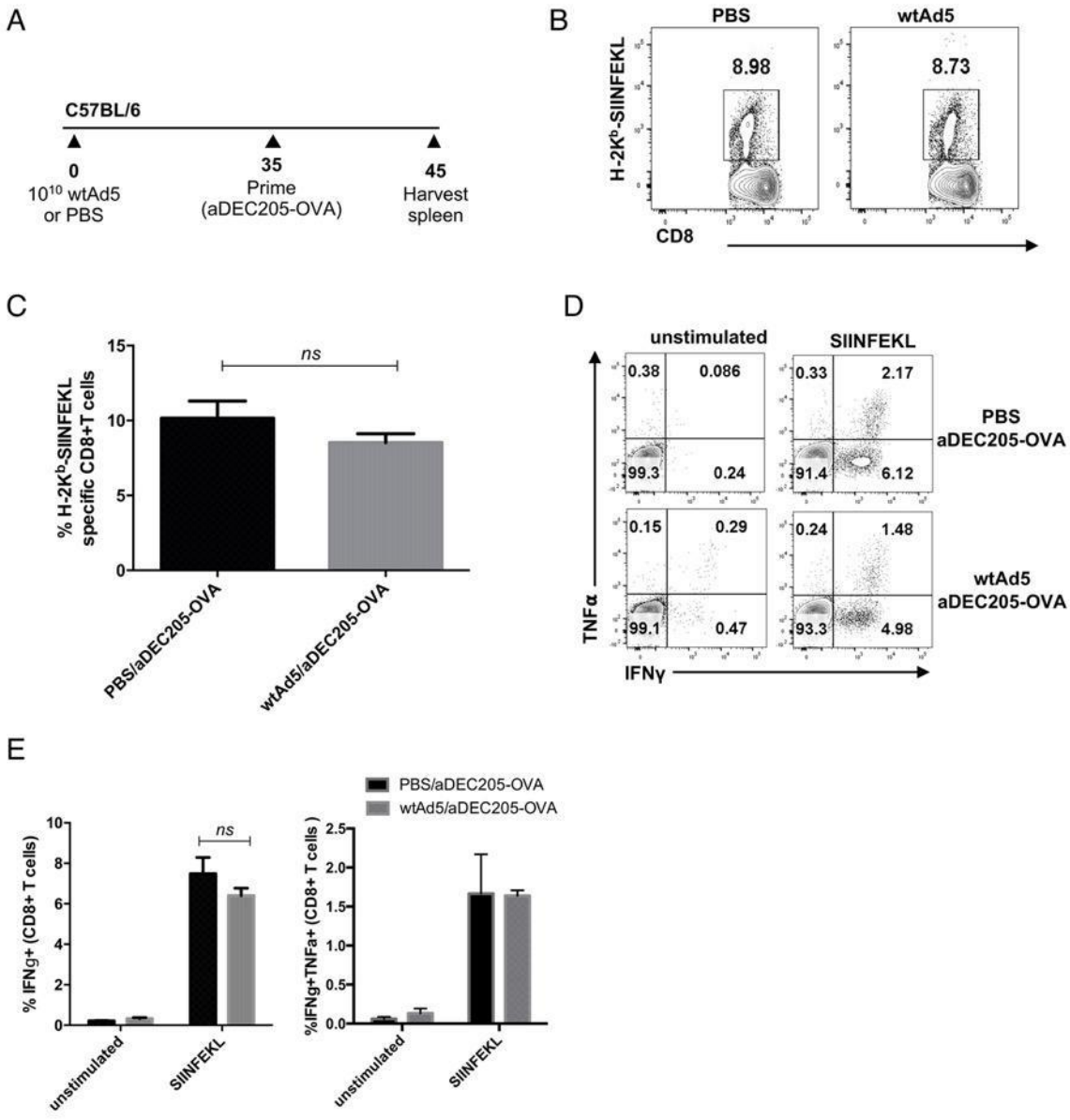
A
C57BL/6
0
10^10 wtAd5
or PBS
35
Prime
(aDEC205-OVA)
45
Harvest
spleen
B
PBS
wtAd5
8.98
8.73
H-2K^b-SIINFEKL
CD8
C
% H-2K^b-SIINFEKL
specific CD8+T cells
ns
PBS/aDEC205-OVA
wtAd5/aDEC205-OVA
D
unstimulated
SIINFEKL
0.38
0.086
99.3
0.24
0.33
2.17
91.4
6.12
PBS
aDEC205-OVA
0.15
0.29
99.1
0.47
0.24
1.48
93.3
4.98
wtAd5
aDEC205-OVA
TNFα
IFNγ
E
PBS/aDEC205-OVA
wtAd5/aDEC205-OVA
% IFNg+ (CD8+ T cells)
ns
unstimulated
SIINFEKL
%IFNg+TNFa+ (CD8+ T cells)
unstimulated
SIINFEKL

Figure 2-5. Pre-existing immunity to adenovirus does not affect immune response elicited by aDEC205-OVA prime. A. Naïve C57BL/6 mice (n=5 per group) were injected i.m. on day 0 with 10^{10} pfu of wtAd5 or PBS. After 35 days mice were injected i.v. with 10μg of aDEC205-OVA+50μg poly:IC+ 50μg anti-CD40 **B,C.** 10 days after priming, the percentage of SIINFEKL-specific $CD8^+$ T cells in the spleen was determined by H-2Kb-SIINFEKL pentamer staining. **D,E.** The percentage of SIINFEKL-specific T cells producing IFNγ and TNFα in the spleen was also evaluated by ICS and flow cytometry. *P*-value considered nonsignificant (NS) when >0.05 (two-way ANOVA).

2.2.5 Heterologous boosting of aDEC205-OVA prime with rhabdovirus encoding OVA potentiates cellular and humoral immune response

Priming with Ad5 encoding a cancer antigen followed by boosting with ORV vectors such as MG1 or VSV expressing the same antigen induces strong antigen specific responses, providing survival benefit in various tumor models.[90,137,138,180,181] Therefore, we tested the ability of the combination aDEC205-OVA prime and MG1-OVA boost in the generation of SIINFEKL-specific T cell response. To this end, naive C57BL/6 mice were primed (i.v) with 10μg aDEC205-OVA or aDEC205-empty, both in combination with 50μg poly:IC and 50μg anti-CD40 and boosted (i.v) 14 days later with 10^8 pfu of MG1-OVA or 10μg aDEC205-OVA with 50μg poly:IC and 50μg anti-CD40, or PBS. Seven and 14 days after boost, lymphocytes were harvested from the spleen and lung and then stained with H-2Kb-SIINFEKL pentamer. At days 7 and 14 post-boost, the greatest expansion of SIINFEKL-specific T cells was observed in the spleen (Figure 2-6A-C) and lungs (Figure 2-7) of animals boosted with MG1-OVA. Similar results were obtained using VSV-OVA (Figure 2-8). Although boost with aDEC205-OVA expanded the antigen specific cells compared to the group only primed with aDEC205-OVA, the level of expansion was significantly lower compared to MG1-OVA. Humoral immunity was also assessed using mouse sera to quantify OVA-specific IgG by ELISA. The combination of aDEC205-OVA / MG1-OVA prime-boost generated the highest anti-OVA antibody titers compared to other combinations and control groups (Figure 2-6F).

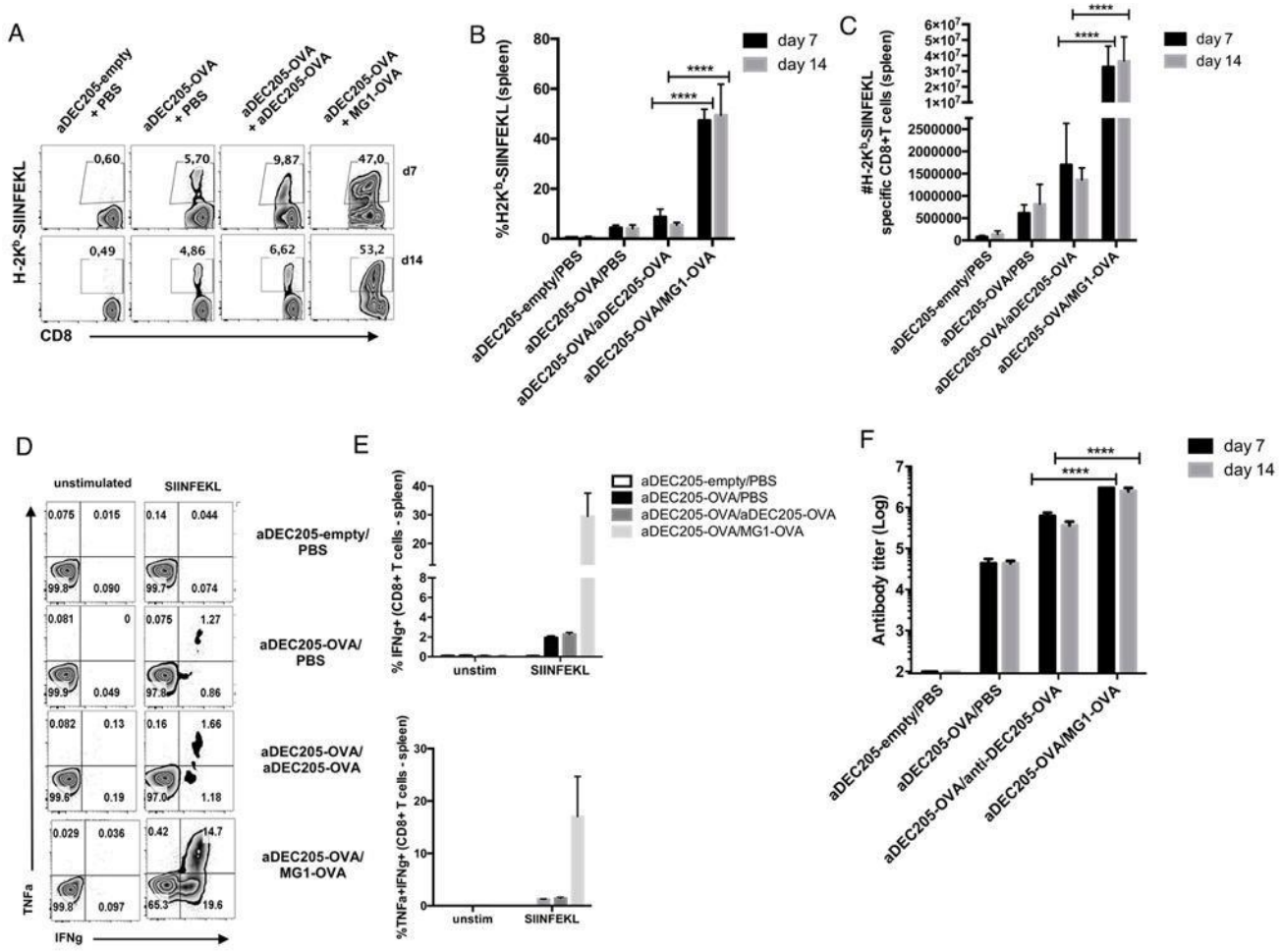
A
aDEC205-empty + PBS
aDEC205-OVA + PBS
aDEC205-OVA + aDEC205-OVA
aDEC205-OVA + MG1-OVA
H-2Kb-SIINFEKL
0,60
5,70
9,87
47,0
d7
0,49
4,86
6,62
53,2
d14
CD8
B
%H2Kb-SIINFEKL (spleen)
day 7
day 14
****
****
aDEC205-empty/PBS
aDEC205-OVA/PBS
aDEC205-OVA/aDEC205-OVA
aDEC205-OVA/MG1-OVA
C
#H-2Kb-SIINFEKL specific CD8+T cells (spleen)
day 7
day 14
****
****
aDEC205-empty/PBS
aDEC205-OVA/PBS
aDEC205-OVA/aDEC205-OVA
aDEC205-OVA/MG1-OVA
D
unstimulated
SIINFEKL
aDEC205-empty/ PBS
aDEC205-OVA/ PBS
aDEC205-OVA/ aDEC205-OVA
aDEC205-OVA/ MG1-OVA
TNFa
IFNg
E
% IFNg+ (CD8+ T cells - spleen)
aDEC205-empty/PBS
aDEC205-OVA/PBS
aDEC205-OVA/aDEC205-OVA
aDEC205-OVA/MG1-OVA
unstim
SIINFEKL
%TNFa+IFNg+ (CD8+ T cells - spleen)
unstim
SIINFEKL
F
Antibody titer (Log)
day 7
day 14
****
****
aDEC205-empty/PBS
aDEC205-OVA/PBS
aDEC205-OVA/anti-DEC205-OVA
aDEC205-OVA/MG1-OVA

Figure 2-6. Induction of potent cellular and humoral OVA-specific immune response in the spleen after aDEC205-OVA prime and MG1-OVA boost. C57BL/6 mice (n=10 per group) were immunized i.v with 10μg of aDEC205-OVA or aDEC205-empty+50μg poly:IC+50μg anti-CD40 at day 0 (D0). Fourteen days later, mice were immunized with a boosting dose of either, PBS, 10μg aDEC205-OVA i.v +50μg poly:IC+50μg anti-CD40 or 10^8 pfu of MG1-OVA. Spleens were harvested 7 and 14 days following boost to evaluate cellular immune response to prime-boost regimens. **A,B,C**. The percentage and total number of SIINFEKL-specific $CD8^+$ T cells was determined by H-2Kb-SIINFEKL pentamer staining. **D, E.** At day 14, the percentage of splenic IFNγ and TNFα-producing $CD8^+$ T cells in response to *in vitro* stimulation with 5uM SIINFEKL peptide was evaluated. **F.** The titers of anti-OVA antibodies in the sera of mice were determined by ELISA at day 7 and day 14 after boost. These results are representative of two independent experiments. **** p <0.0001 (Two-way ANOVA).

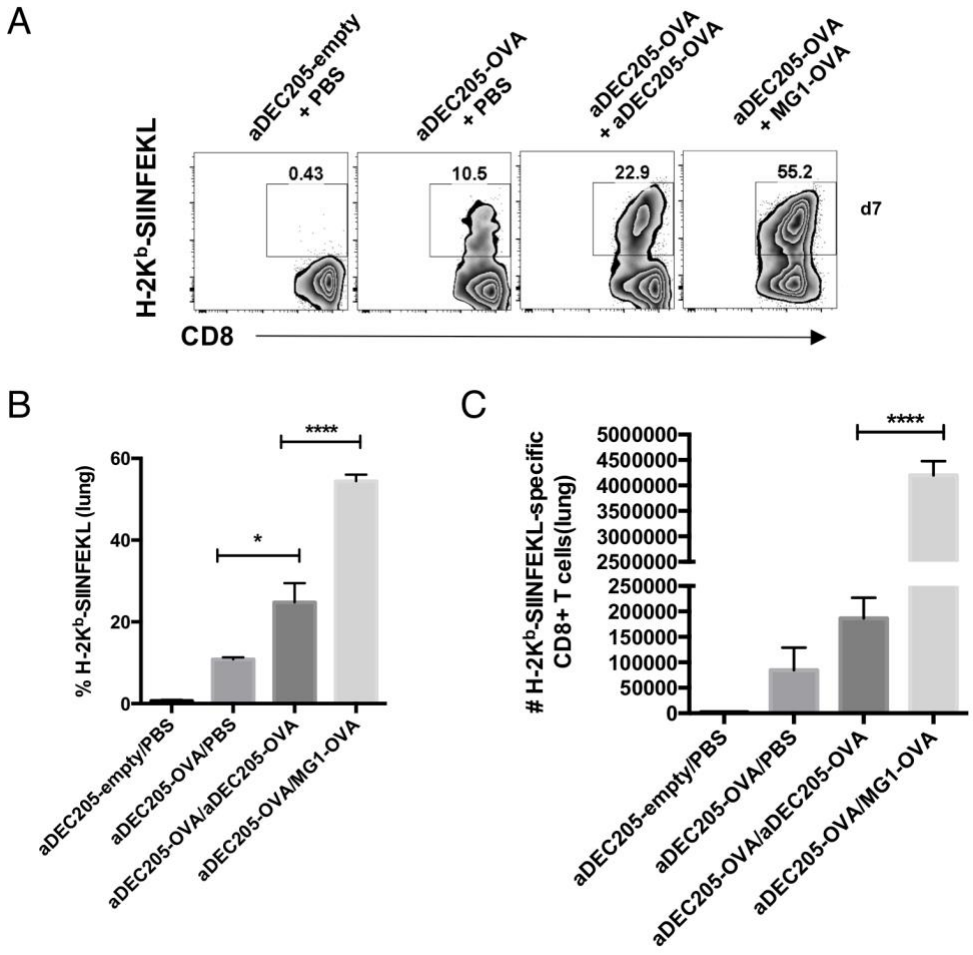
A
aDEC205-empty + PBS
aDEC205-OVA + PBS
aDEC205-OVA + aDEC205-OVA
aDEC205-OVA + MG1-OVA
H-2K^b-SIINFEKL
0.43
10.5
22.9
55.2
d7
CD8
B
% H-2K^b-SIINFEKL (lung)
60
40
20
0
****
*
aDEC205-empty/PBS
aDEC205-OVA/PBS
aDEC205-OVA/aDEC205-OVA
aDEC205-OVA/MG1-OVA
C
H-2K^b-SIINFEKL-specific CD8+ T cells(lung)
5000000
4500000
4000000
3500000
3000000
2500000
250000
200000
150000
100000
50000
0
****
aDEC205-empty/PBS
aDEC205-OVA/PBS
aDEC205-OVA/aDEC205-OVA
aDEC205-OVA/MG1-OVA

Figure 2-7. Induction of potent cellular OVA-specific CD8+ T cells in the lungs of mice immunized with aDEC205-OVA prime and MG1-OVA boost. C57BL/6 mice (n=10/group) were immunized i.v with 10µg of aDEC205-OVA or aDEC205-empty+50µg poly:IC+50µg anti-CD40 at day 0 (D0). Fourteen days later, mice were immunized with a boosting dose of either, PBS, 10µg aDEC205-OVA i.v +50µg poly:IC+ 50µg anti-CD40 or 10^8 pfu of MG1-OVA. Lungs were harvested 7 days following boost to evaluate cellular immune response to prime-boost regimens. **A, B.** The percentage and **C.** total number of SIINFEKL-specific $CD8^+$ T cells was determined by H2-K^b-SIINFEKL pentamer staining. *, $p<0.05$; **** $p<0.0001$ (one-way ANOVA).

2.2.6 Heterologous prime-boost vaccine with aDEC205-OVA and rhabdovirus encoding OVA confers a survival advantage in tumor bearing mice

We next evaluated the therapeutic efficacy of the aDEC205-OVA / MG1-OVA prime-boost vaccine in an experimental model of lung metastasis. Briefly, $3x10^5$ B16-OVA cells were injected i.v. in C57BL/6 mice and different primes were administered 5 days post B16-OVA tumor implantation (Figure 2-8A). Generation of SIINFEKL-specific T-cell responses was evaluated by H-2Kb-SIINFEKL pentamer staining of blood 7 days after boost. The heterologous prime-boost combination employing aDEC205-OVA or rAd-OVA as a prime generated the greatest percentage of circulating antigen specific T-cells. Interestingly, whereas different routes of administration of the aDEC205-OVA prime (i.v. vs i.p.) did not significantly impact priming responses (Figure 2-3), there was a trend for a higher magnitude of SIINFEKL-specific CD8+ T-cell response generated after prime with aDEC205-OVA administered i.v. compared to aDEC205-OVA prime administered i.p (Figure 2-8B, D). In general, all OVA-targeted heterologous prime-boost regimens led to improved survival of tumor bearing mice, with rAd-OVA/MG1-OVA and aDEC205-OVA/MG1-OVA regimens being the most effective (30% complete remission). Administering a prime-boost of aDEC205-OVA/VSV-OVA also resulted in the generation of greater SIINFEKL specific CD8+ T cells, similar antibody titers to aDEC205-OVA / MG1-OVA and improved survival of tumor bearing mice (Figure 2-9). Cured mice were re-challenged with a subcutaneous injection of $2x10^6$ B16-OVA cells (data not shown); no mice previously cured by any prime-boost regimen developed tumors thus confirming that anti-SIINFEKL responses were long lasting and conferred protection against recurrent tumors.

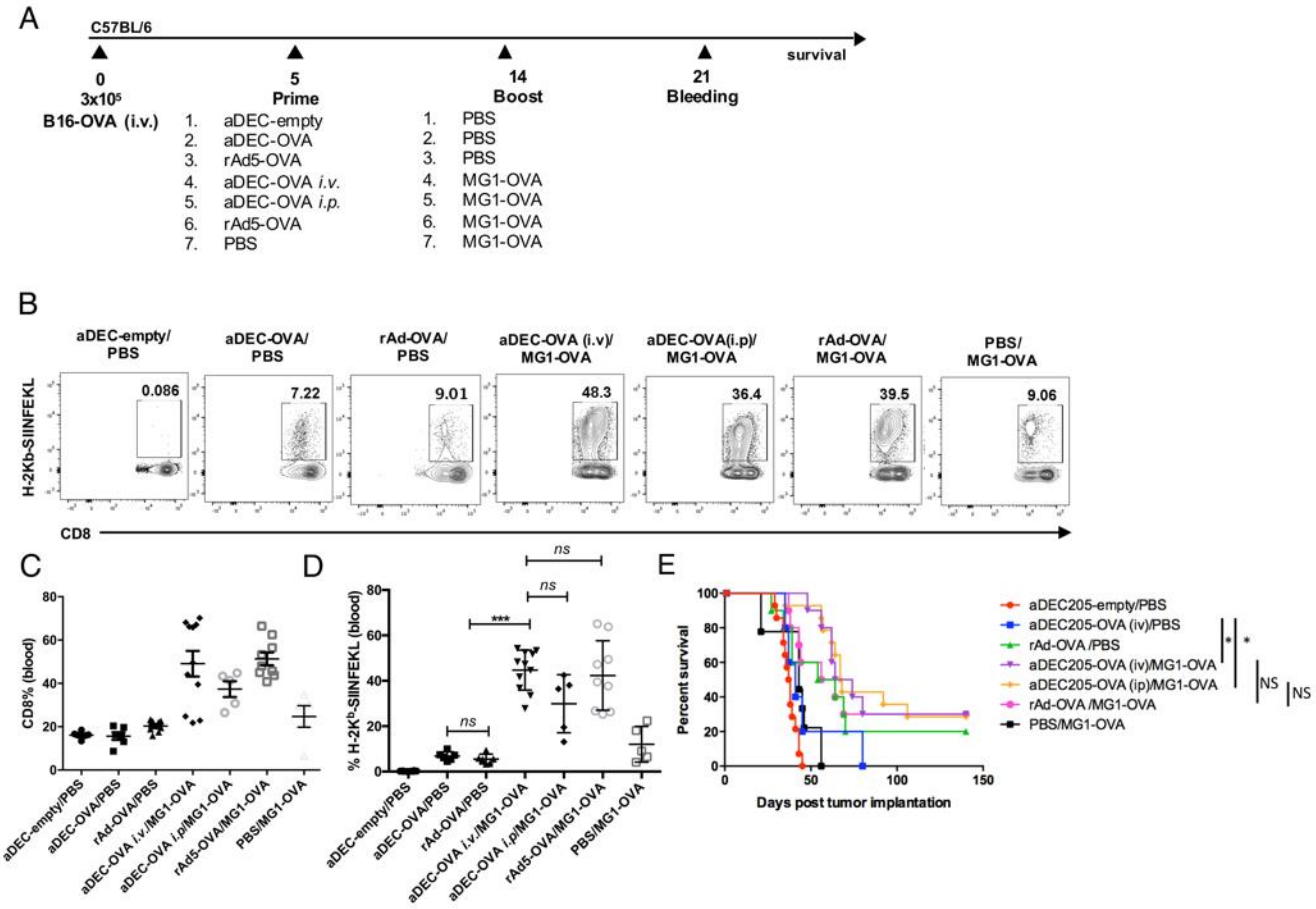
A
C57BL/6
survival
0
3x10^5
B16-OVA (i.v.)
5
Prime
1. aDEC-empty
2. aDEC-OVA
3. rAd5-OVA
4. aDEC-OVA i.v.
5. aDEC-OVA i.p.
6. rAd5-OVA
7. PBS
14
Boost
1. PBS
2. PBS
3. PBS
4. MG1-OVA
5. MG1-OVA
6. MG1-OVA
7. MG1-OVA
21
Bleeding
B
aDEC-empty/ PBS
aDEC-OVA/ PBS
rAd-OVA/ PBS
aDEC-OVA (i.v)/ MG1-OVA
aDEC-OVA(i.p)/ MG1-OVA
rAd-OVA/ MG1-OVA
PBS/ MG1-OVA
H-2Kb-SIINFEKL
0.086
7.22
9.01
48.3
36.4
39.5
9.06
CD8
C
CD8% (blood)
D
% H-2K^b-SIINFEKL (blood)
ns
***
E
Percent survival
Days post tumor implantation
aDEC205-empty/PBS
aDEC205-OVA (iv)/PBS
rAd-OVA /PBS
aDEC205-OVA (iv)/MG1-OVA
aDEC205-OVA (ip)/MG1-OVA
rAd-OVA /MG1-OVA
PBS/MG1-OVA
NS

Figure 2-8. Therapeutic efficacy of aDEC205/OVA prime-boost vaccine. A. Schematic representation of immunization schedule. Briefly, C57BL/6 mice received $3x10^5$ B16-OVA cells i.v.. At D5 mice were immunized i.v. or i.p. with either 10μg of aDEC205-OVA or aDEC205-empty+ 50μg poly:IC+50μg anti-CD40, 10^8 recombinant adenovirus expressing the SIINFEKL transgene (rAd-SIINFEKL) or PBS. At day 14 mice were immunized with a boosting dose of either PBS or 10^8 MG1-OVA. **B, C, D.** At day 21 saph bleeds were performed to assess the percentage of bulk circulating $CD8^+$ T cells and SIINFEKL-specific $CD8^+$ T cells, the latter determined by H-2Kb-SIINFEKL pentamer staining. *P*-value considered nonsignificant (NS) when >0.05; ***, p<0.001 (one-way ANOVA). **E.** Mice were monitored for survival 140 days post B16-OVA implantation. Data from three independent survival experiments are pooled. *P*-value considered nonsignificant (NS) when >0.05; * p <0.05 (Log-Rank Mantel Cox).

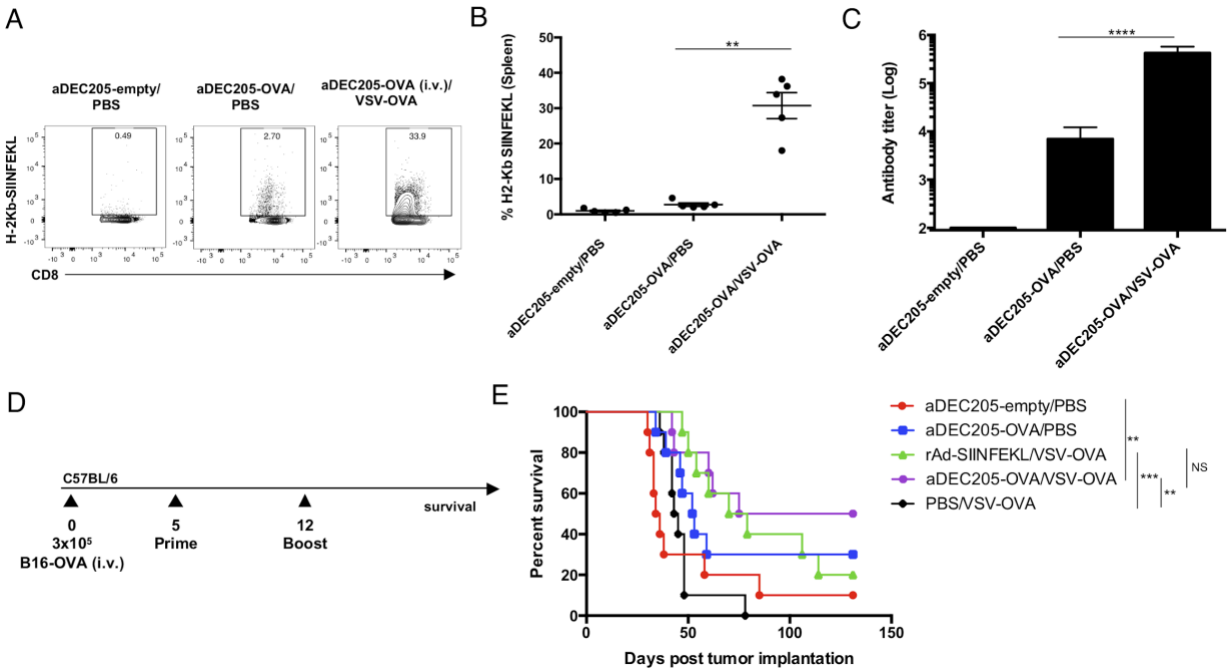
A
aDEC205-empty/ PBS
aDEC205-OVA/ PBS
aDEC205-OVA (i.v.)/ VSV-OVA
0.49
2.70
33.9
H-2Kb-SIINFEKL
CD8
B
% H2-Kb SIINFEKL (Spleen)
**
aDEC205-empty/PBS
aDEC205-OVA/PBS
aDEC205-OVA/VSV-OVA
C
Antibody titer (Log)
****
aDEC205-empty/PBS
aDEC205-OVA/PBS
aDEC205-OVA/VSV-OVA
D
C57BL/6
survival
0
3x10⁵
B16-OVA (i.v.)
5
Prime
12
Boost
E
Percent survival
Days post tumor implantation
aDEC205-empty/PBS
aDEC205-OVA/PBS
rAd-SIINFEKL/VSV-OVA
aDEC205-OVA/VSV-OVA
PBS/VSV-OVA
**
***
**
NS

Figure 2-9. Evaluating the boosting capacity of VSV-OVA and survival in tumour bearing mice. A, B. C57BL/6 mice were immunized i.v with 10μg of aDEC205-OVA or aDEC205-empty+ 50μg poly:IC+50μg anti-CD40 at D0. At day 14 mice received a boosting dose of 10E8 VSV-OVA or PBS. Spleens were harvested on day 21 and assessed for the percentage of OVA-specific CD8+ T cells determined by H-2K^{b}-SIINFEKL pentamer staining. **C.** The titers of anti-OVA antibodies in the sera of mice were determined by ELISA to evaluate the humoral immune response to aDEC205-OVA prime-boost regimen day 7. **D.** C57BL/6 mice were given i.v. injections of 3x10^{5} B16-OVA tumour cells. After 5 days, mice were given i.m. injection of rAd5 or i.v. injections of aDEC205-OVA or aDEC205-empty. 7 days post prime, all mice were injected VSV-OVA i.v.. **E.** Mice were monitored for survival 140 days post B16-OVA implantation. ** $p < 0.005$, **** $p<0.0005$.

2.3 Discussion

Cancer immunotherapy has emerged as a promising alternative to conventional cancer treatments. Therapeutic strategies that actively stimulate the immune system to reject tumors have grown to include diverse platforms including immune modulating antibodies, small molecules, as well as genetically engineered bacteria, cells, and viruses.[130,193–197] OVs are attracting increasing interest as multi-mechanistic platforms for immunotherapy, owing in part to the recent approval of Imlygic® for the treatment of melanoma and to the possibility of combining OVs with antibodies targeting immune checkpoints.[192] Indeed, it is increasingly recognized that OVs have significant potential as part of combination therapy regimens.[198]

In this study we have further explored one such combination strategy consisting of a heterologous prime-boost, where the priming and boosting vectors share a similar tumor antigen, and where the boosting vector is an oncolytic rhabdovirus.[199] This is a strategy that is now under phase I/II clinical evaluation using a non-replicating Ad5 as a priming vector, and oncolytic MG-1 as a boosting vector. In contrast with repeat dosing with the same vector (homologous vaccination), this heterologous prime-boost approach has been shown to skew the immune response from antiviral to anti-tumor, promoting long lasting anti-tumor immunity.[112,200] The secondary immunization with rhabdovirus, which preferentially infects tumors, not only induces oncolysis but also boosts the primary anti-tumor adaptive immune response and breaks immune tolerance.[131]

Although non-replicating Ad5 is an effective and well-validated vector for vaccination, pre-existing immunity to Ad5 resulting from prior exposure to wild-type adenoviruses in humans can potentially limit its effectiveness in clinical trials.[139,182] Indeed, we found that administration of rAd-SIINFEKL in pre-immunized mice led to both significantly lower percentages of

SIINFEKL-specific CD8+ T-cells (Figure 2-1C, D), and a reduction in their functionality (Figure 2-1E, F).

As an alternative to Ad5, we demonstrate here, in line with other studies, that i.p. or i.v. administration of aDEC205-OVA generates antigen specific and functionally robust anti-SIINFEKL T cells as well as humoral immunity towards OVA.[187,190,201] However, as a standalone vaccination agent, we observed that aDEC205-OVA did not perform as well as rAd-SIINFEKL in terms of controlling B16-OVA tumors (Figure 2-8E) and generating activated (IFNγ+, TNFα+) SIINFEKL-specific CD8+ T-cells, even though the numbers of SIINFEKL-specific T-cells was similar with both primes (Figure 2-8B). This difference could relate to dosing inequivalence between aDEC205 relative to Ad5; however, something which is difficult to establish owing to differences in how immune responses are initiated with the two vaccination methods. However, the dose of aDE205-OVA used in this study is within the range of the human equivalent dose of what is being evaluated in clinical trials employing aDEC205 (NCT01834248, NCT01127464).[202,203] In comparison, Ad5 was administered at a higher human equivalent dose than what is administered in current clinical trials; further illustrating the potential of aDEC205 over Ad5. Additionally, pre-existing immunity to wtAd5, as evidenced by the presence of adenovirus neutralizing antibodies (Figure 2-1B), strongly decreased the ability of rAd-SIINFEKL to produce an immune response against SIINFEKL antigen, but predictably bore no impact on the ability of aDEC205-OVA to generate functional anti-SIINFEKL CD8+ T cells.

Consistent with other studies, we found that heterologous boosting with an oncolytic rhabdovirus such as MG1-OVA amplifies antigen specific immunity in the spleen at days 7 and 14 to a higher extent than homologous boosting, for example with aDEC205-OVA (Figure 2-6, 2-7).[138,198] All heterologous regimens tested conferred a survival advantage in B16-OVA bearing

mice (Figure 2-8) and in this regard, primes using chimeric aDEC205 or Ad5 were essentially equivalent. This suggests that aDEC205 chimeric antibodies are a feasible alternative to Ad5 in the context of heterologous prime-boost with an oncolytic rhabdovirus. In addition to overcoming pre-existing immunity, which may be a barrier when using certain viral priming vectors, chimeric aDEC205 antibodies can provide additional practical advantages, including but not limited to, ease of manufacturing, storage, and the possibility of repeat dosing. This last point is a notable limitation for viral vectors encoding antigens which generally induce an anti-viral immune response after the first dose.

Vaccines employing DCs loaded *ex vivo* with tumor lysate or MHC I peptides for re-administration to patients have been studied for decades and have been shown to generate robust memory CD8+ T cell responses.[204] Following research in the nineties on antigen loaded DC vaccines, many clinical trials carried out to this end have been unable to achieve significant clinical responses.[205,206] Objective response rates for a range of DC vaccines loaded with antigens such as tyrosinase, gp100, MART-1, MAGE-3 and autologous peptides in melanoma patients did not exceed 5-10%.[207] Considering limitations and logistical challenges in producing DC vaccines, DC-targeting using chimeric antibodies like aDEC205 may be more feasible for treating a diverse population of patients.[208] However, as observed in this study (Figure 6E), chimeric aDEC205 antibodies may be insufficient as standalone anticancer vaccines.

One key feature of chimeric aDEC205 antibodies is that they deliver a specific antigen directly to DCs, which in turn present antigen and activate CD4+ T cells as well as cross-present antigen to CD8+ T cells. However, this approach is also not without limitations. For example, there can be antibody/protein engineering challenges restricting the choice of antigen, and how

many antigens can be fused to a given aDEC205 antibody. This can be somewhat addressed by using more restricted epitopes in tandem or using multiple different chimeric antibodies.

Another consideration for use of chimeric aDEC205 antibodies is the requirement for an adjuvant.[107] In our study, we found that aDEC205-OVA administered with polyI:C and anti-CD40 adjuvants was effective in generating anti-OVA responses in mice; however, while anti-CD40 antibodies (that target the co-stimulatory receptor CD40 on DCs to induce their maturation), are highly effective in mice, they have displayed severe toxicity in human cancer immunotherapy trials.[209,210] Although this regimen was selected for modeling purposes in mice, we expect adjuvants that are amenable to human use and that have been used in clinical trials (e.g. poly ICLC Hiltonol®) to be similarly effective in combination with aDEC205.[202] Indeed, many human-compatible adjuvants are known and available, and routinely used in the context of cancer vaccines. These include but are not limited to, alum, polyI:C, CpG, LPS, Th1 specific cytokines, and growth factors like Flt3L important for the development of classical DCs.[211–213] These adjuvants, cytokines and growth factors may be further combined. For example, CDX-301, a soluble rhuFlt3L, has been used in combination with poly ICLC in the context of a phase II human trial testing an aDEC205-NY-ESO-1 melanoma vaccination strategy.[214]

Altogether, our study indicates that a vaccine consisting of an aDEC205-OVA prime followed by a rhabdovirus boost is a promising alternative to the current heterologous prime-boost that employs Ad5-OVA as a priming agent. To our knowledge, this study is the first of its kind to showcase a combination of the well-studied aDEC205 antibody in combination with an OV. Additional studies in other tumor models and antigenic targets will be necessary to assess the applicability of this novel approach to a broad range of disease models.

2.3 Methods

2.3.1 Cell Lines

Human embryonic kidney cells (HEK) 293T cells, kindly donated by the Oncolytic Virus Manufacturing Facility (OVMF, Ottawa, Canada) for antibody production and purification were cultured in HyQ high-glucose Dulbecco's modified Eagle's medium (Hyclone) supplemented with 10% ultra-low IgG fetal bovine serum (Gibco), 5% penicillin/streptomycin (Gibco), and 5% L-glutamine (Gibco). B16-F10-OVA cells, kindly gifted by Dr. Yonghong Wan (McMaster University) and were cultured in Roswell Park Memorial Institute (Hyclone) supplemented with 10% fetal bovine serum, penicillin/streptomycin, 1M HEPES buffer, and 50ug/mL geneticin sulfate (G148 sulfate) (Gibco). All cell lines were incubated at 37 °C in a 5% CO_2 humidified incubator. All cells were tested by PCR and Hoecht's staining to ensure they are free of mycoplasma contamination.

2.3.2 Mice

Six to eight week-old female C57BL/6J mice were obtained from Charles River Laboratories. All animals were handled in strict accordance with good animal practice, and approved by appropriate committee in collaboration with the Office of Animal Ethics and Compliance.

2.3.3 Antibody Production and Purification

The pcDNA plasmids expressing the heavy chain anti-DEC205; anti-DEC205-OVA and anti-DEC205-empty, and the light chain DEC-kappa sequences were generated by Dr. Silvia Boscardin (University of Sao Paulo). The plasmid DNA were individually transformed in competent DH5-α

and DNA were purified using the Qiagen Plasmid Maxi Kit (Cat. 12165). Transfection of 90% confluent human embryonic kidney cells (HEK) 293T cells in 150 mm tissue culture-dishes, collection of antibody from culture supernatant and antibody purification were performed as previously described.[213]

2.3.4 Peptides

Peptides corresponding to the immunodominant epitope of ovalbumin (SIINFEKL) that binds to H-2K^b were synthesized by New England Peptide (Lot No. 3001-1/48-21) and have >95% purity.

2.3.5 Tissue Processing

SIINFEKL-specific T-cell responses were measured in blood, spleen and lung. Briefly, saphenous bleeds of mice from hind limb were performed and blood (70-100uL) was collected in sterile heparin tubes. Red blood cells were lysed using ACK lysis buffer. Spleens were excised from sacrificed mice and filtered through a 100um plastic cell strainer (Fisherbrand™ 352360, 22-363-549) for cell collection. The cell viability of the resulting white blood cells was determined using Trypan blue staining. Lungs were also excised from sacrificed mice after lung perfusion, and dissociated using the Lung Dissociation Kit-Mouse (Miltenyi Biotech. 130-095-927), according to the manufacturer's instructions. Upon resuspension in R10 buffer (RPMI, 10% FBS), the cells from blood, spleen and lung were counted and 1x10^6 cells per condition were stained for flow cytometry.

2.3.6 Immunoblotting

After aDEC205-OVA antibody quantification by NanoDrop ND1000 Spectrometer, 1 ug of antibody was run on NuPAGE Novex 4-12% Bis-Tris precast gels (Thermo Fisher Scientific) under reducing conditions using the XCell SureLock Mini-Cell System (Thermo Fisher Scientific) and transferred to nitrocellulose membranes (Hybond-C, Bio-Rad). Blots were blocked with 2% milk and probed with a goat anti-mouse peroxidase-conjugated antibody (1:2000) (Jackson ImmunoResearch Laboratories). Bands were visualized using the SuperSignal West Pico Chemiluminescent substrate (Thermo Fisher Scientific).

2.3.7 ELISA

Murine serum was collected from blood for detection of OVA specific antibodies. Briefly, blood (500uL) from immunized mice was collected in sterile 1.5 mL eppendorf tubes. Collected blood was centrifuged for 10 mins at 2000g and the resulting serum in the supernatant, was collected and frozen at -20 degrees Celsius for downstream use. Murine serum samples were evaluated for presence of OVA specific antibodies by ELISA for all groups. 96 well EIA/RIA assay microplates (Corning, Cat. CLS3590) were coated with albumin (Sigma-Aldrich, A5503-1G), at a concentration of 2ng/uL in PBS and incubated overnight at 4°C. Plates were washed twice with PBS-Tween20 0.02% and blocked with blocking buffer (PBS-Tween20 0.02%, 5% non-fat milk and 1% BSA) for 1 hour at room temperature. Blocking buffer was removed and serum dilutions (1:500-1:1000000 dilution in PBS-Tween20 0.02%, 5% non-fat milk and 0.25% BSA) were added to wells and incubated for 2 hours at room temperature. Plates were washed three times with PBS-Tween20 0.02%, and HRP-AffiniPure goat anti-mouse IgG (Jackson ImmunoResearch) diluted 1:4000 was added to wells and incubated for 1 hour at room temperature. Plates were washed six

times with PBS-Tween 20 0.02%, developed with substrate solution (R&D systems, Cat. DY99) and incubated for 20 minutes in the dark (RT), development was stopped by addition of 2N sulfuric acid and absorbance was read at 510 nm on a Multiskan Ascent plate reader (Thermo LabSystems).

2.3.8 Neutralization assay

A neutralization assay was performed to quantify the amount neutralizing antibodies against wtAd5 present in serum samples of pre-immunized murine, and is based on the ability of serum antibodies to block adenovirus infection of A549 cells. Adenovirus used carries the firefly luciferase (Fluc) reporter gene, E1 deletion and CMV promoter. 2-fold serum dilutions (1:100, 1:200, 1:400, 1:800, 1:1600, 1:3200 1:6400 1:12800, 1:25600, 1:51200, 1:102400) were tested. In 96-well flat-bottom plates, Ad-Fluc virus (MOI 100) was combined with different serum dilutions and incubated for 1 hour at 37°C. Contents of this plate were transferred to a 96-well flat-bottom plate previously seeded with $2x10^5$ A549 cells per well washed 3x with PBS, and incubated for 48h at 37°C. To read plate, luciferin was added at a final concentration of 2mg/mL luciferin per well, and imaged/read by Biotek Synergy Mx Microplate Reader. The antibody neutralizing unit (NU) was defined as the minimum serum dilution required to achieve at least an 80% reduction in luciferase activity, which was assumed to correlate directly to an inhibition of vector infection.

2.3.9 Mouse Tumor Model and Injections

B16-OVA lung tumors were established in 8-week-old female C57BL/6 mice by intravenous injection of $3x10^5$ cells in 100 uL phosphate-buffered saline (PBS). For adenovirus injections, mice were anesthetized with 5% isoflourane. Wild type adenovirus serotype 5 (wtAd5, 10^{10} pfu) and recombinant adenovirus-SIINFEKL (rAd5-SIINFEKL, 10^8 pfu) were administered

intramuscularly in 50 uL phosphate-buffered saline. For aDEC205 injections a solution containing 10ug of aDEC205, 50ug polyI:C and 50ug anti-CD40L in 150 uL of phosphate-buffered saline was administered either i.v. or i.p.. Oncolytic rhabdoviruses (MG-1-OVA and VSVΔ51-OVA) were administered i.v. in 100 uL of PBS.

2.3.10 Detection of antigen-specific T cell responses

OVA-specific T-cell responses were measured 7 days and 14 days post-boost in blood, spleen and lung. Splenocytes and lung-resident lymphocytes were isolated and stained for presence of SIINFEKL specific T cells using a H-2K^{b}-SIINFEKL pentamer. For SIINFEKL-specific CD8+ T cell *in vitro* re-stimulation, 1x10^{6} splenocytes and lung-resident lymphocytes were incubated in RPMI medium supplemented with 10% fetal bovine serum and 5% pen-strep containing 5uM of SIINFEKL peptide and brefeldin A (Golgi plug) for 4 hours. Intracellular cytokine staining was performed as described below.

2.3.11 Virus Preparation

The adenoviruses were made using standard techniques.[214] The Indiana serotype of VSV (VSVΔ51 or VSVΔ51-OVA) and the Brazilian maraba virus (MG-1 or MG1-OVA) were used throughout this study and were propagated in Vero cells. VSVΔ51-expressing and MG-1-expressing OVA are recombinant derivatives of VSVΔ51 and MG1 described previously.[215] All viruses were propagated on Vero cells and purified on 5–50% Optiprep (Sigma) gradient and all virus titers were quantified by the standard plaque assay on Vero cells as previously described.[216]

2.3.12 Antibody binding assay

A flow cytometry based binding assay was performed for evaluation of aDEC205-OVA and aDEC205-empty binding specificity to the target DEC205 receptor on dendritic cells. Bulk splenocytes were isolated from spleens of naïve C57BL/6J mice. Red blood cells were lysed, and $5x10^6$ bulk splenocytes were incubated with graded concentrations of antibody (0.1 ug/uL, 1 ug/uL and 10 ug/uL) in a 96 well plate for 45 minutes (4°C). After incubation, cells were stained for flow cytometry.

2.3.13 Flow Cytometry

After processing the tissues as described above, cells were then stained with the FVS780 viability dye (BD Biosciences, San Jose, CA) PBS for 15 min at room temperature. Following washes, cells were incubated with anti-CD16/32 in 0.5% BSA/PBS at 4°C to block nonspecific antibody (Ab) interaction with Fc receptors. Subsequently, the following protocols were used for staining:

Staining for antibody binding assay: anti-CD11c-PE-Cy7, anti-MHC-I-PE, anti-CD8-PE-CF594, anti-IgG-APC, anti-CD3-FITC, and anti-CD19-FITC antibodies were added to cells and incubated for 30 minutes (4°C).

Staining for ICS: First, $1x10^6$ cells were incubated with antibodies targeting T-cell surface markers CD3-AF700 and CD8-PE-CF594 for 30 minutes (4°C). Cells were washed twice with FACS buffer. Next, the mouse Cytofix, Cytoperm Plus (BD Bioscience) was used for permeabilization and intracellular cytokine staining. Cells were incubated with cytofix for 20 minutes to permeabilize cells for intracellular cytokine staining (4°C). Cells were washed twice with PermWash and incubated with anti-IFNγ-BV650 and anti-TNFα-AF647 diluted in PermWash 30 minutes (4°C).

Staining for OVA specific T-cells/pentamer staining: Cells were washed with FACs buffer. In a 96 well plate, 3uL of H-2K^{b}-SIINFEKL pentamer-APC (Proimmune) in 50 uL of FACs buffer was added per well and incubated for 10 minutes (RT) in the dark. Cells were washed twice with FACs buffer and stained with fixable viability stain for 30 minutes (4°C). Subsequently, the cells were washed with FACS buffer and incubated with anti-CD16/32 in FACS buffer for 5 minutes (4°C). Next, cells were stained with anti-CD8-PE-CF594 and anti-CD3-AF700 for 30 minutes (4°C)

After staining, cells were washed with FACs buffer and fixed in 1% paraformaldehyde. Cells were acquired on BD flow cytometry (Fortessa) and analyses were performed using FlowJo software v9.

2.3.14 VSV-OVA cloning and rescue

pBSSK-VSVΔ51, plasmid containing viral genome, was used to construct VSVΔ51-OVA. In brief, OVA gene was PCR amplified from pcDNA expressing aDEC-205-OVA using the following primers, Forward: AATTCTCGAGATGGGCTCCATCG and Reverse: CATCGCTAGCTCACTACAGATCCTC. PCR amplicon was digested by XhoI and NheI and cloned into the multiple cloning site (MCS) of PBSSK-VSVd51 between G and L ORFs. Positive clones were screened by restriction digestion mapping and verified by sequencing.

2.3.15 Statistics

Statistical significance was calculated using Student's t test or one-way or two-way ANOVA test, using Tukey's multiple comparison test, as indicated in the figure legends. The log rank (Mantel-Cox) test was used to determine significant differences in plots for survival studies. Error bars

represent standard error of the mean. Significance is based on a P value <0.05. Statistical analyses were performed using GraphPad Prism 6.0 and Excel.

Chapter 3 - Development of a novel methodology for the discovery of tumor antigens

3.1 Introduction

Methodologies employed for discovery of tumor specific antigens are complex, costly and inefficient. For example, the reverse immunology approach is based on *in silico* screening of a variety of protein sequences with anchor-motif residues that are most likely to bind onto MHC. The disadvantage of this approach is that the screening method cannot predict receptor binding affinity, post-translational modification of these MHC ligands or indicate immunogenicity of the identified peptide.[163–165] The immunoaffinity chromatography method is currently a gold-standard in the discovery of MHC I specific antigens and is based on the isolation of pMHC complexes from lysed tumour tissue using MHC specific mAb. The large amount of mAbs needed for isolation is one limitation. Furthermore, the method is complex and is unable to distinguish between intracellular and extracellular pMHC, of which only the latter is expressed and likely to be immunogenic. Therefore, immunogenicity is uncertain but it may be ascertained with further downstream *ex vivo* antigen screening.[166–168]

The CTL based approach relies on the existence of tumor specific effector or memory T cells which are used to generate CTL clones in order to screen target cells *in vitro*. Target cells are cell lines transfected with a cDNA library deriving from the tumour of interest. Screening is performed with pools of target cells and the identification of the appropriate transfected target cell by a CTL clone is based on detection of cytokine production by the CTL.[159] Sequential limiting dilutions are necessary to isolate the desired target from the selected pools. An advantage of this method is that immunogenic antigens that elicit a CTL response can be isolated. However, one major challenge is the complexity of generating T cell clones, which themselves may not necessarily represent the full repertoire of tumour specific CTLs present in the patient. This

limitation is further exacerbated by the necessity to subclone the selected pools of target cells, which requires a second step of sequential limiting dilutions. However, the ability to discern CTL-target cell interactions makes this an attractive method to build upon.

CTLs are a component of the adaptive immune system that target infected or malignant cells. Following T cell priming by dendritic cells, antigen specific CTLs cells recognize and target host cells expressing cognate pMHC.[31] CTLs induce apoptosis of infected or malignant cells by secretion of perforin and granzyme or through Fas mediated cell death. Perforin and granzyme are stored within vesicles in the cytoplasm of CTLs. Upon formation of the cytotoxic synapse, these vesicles fuse with the cell membrane in a process called degranulation. This leads to the directed release of granules towards the target cell.[38,39] CD107a, or LAMP-1, is one of the most abundant lysosomal associated membrane glycoproteins found on the vesicle surface.[217,218] Thus, upon fusion of these vesicles with the cell membrane, CD107a is transiently expressed on the cell surface.[219] The transient expression of CD107a can be tagged by a fluorochrome conjugated antibody and used as a marker of target cell specific CTL activation.[220,221]

We therefore wished to expand on the CTL based antigen identification approach to streamline the process of antigen discovery and evaluation of corresponding immunogenicity in the context of cognate antigen specific CTLs. As such, we set out to develop a method for building on the immunological probing of target cells expressing a cDNA library representing the transcriptional landscape of a tissue sample of interest by corresponding CTLs. We hypothesized that assessment of CD107a expression can be used for identification and isolation of activated CTLs and their cognate fluorescently-tagged antigen-expressing target cells in a co-culture setting. We further hypothesized that, following co-culture of target cells and T cells for an allotted time, a fixation step could maintain the target cell-CD8+ T cell association (the cytotoxic/immunological

synapse). The resulting "doublet" cells should be detected by flow cytometry based on the size parameters of cell area vs. height (A vs H) shifts, since doublet cells have a greater area: height ratio.[222] Moreover, staining for CTL activation markers (e.g. CD8, CD107a) would further isolate doublets containing both target and activated T cells. Thus, doublets that are positive for T cell activation and the fluorescent target cell marker (e.g. GFP or RFP) can be enriched for by cell sorting. The sorted doublet cells can be subsequently unfixed and the target cells subjected to next generation sequencing (NGS) of poly-adenylated mRNA to uncover the full breadth of recognized antigens.

The feasibility of this methodology and optimization of the technique was tested with B16 melanoma cells or COS7 monkey kidney fibroblasts target cells expressing ovalbumin (OVA) and GFP. The OVA protein is considered a model antigen and has been widely studied as a T cell dependent antigen in mouse models. OVA's associated MHC I and II epitopes have been well described in literature. The most commonly studied epitope in the C57BL/6 mouse model is SIINFEKL, at amino-acid position 257-264, of the OVA protein and binds to the H-2Kb MHC I haplotype.[223,224] CTLs derived from the transgenic mouse model, OT-1, encode TCRs specific for the MHC-I restricted SIINFEKL epitope and are a vital tool in the study of T cell and antigen interactions.[225]

As a framework to study the proposed methodology, OT-1 CTLs (herein referred to as OT-1 T cells) were initially chosen as a model for SIINFEKL epitope recognition in OVA expressing target cells. OT-1 cells were co-cultured with B16-OVA-GFP or COS7-OVA-GFP cells, either of which can serve as the antigen expressing target cell. The target cell-CTL synapses (doublet cells) were fixed by paraformaldehyde (4% PFA) then stained for CD107a and CD8 and assessed by flow cytometry (Figure 3-1). In this framework, the parameters such as co-culture and flow

cytometry conditions could be optimized and evaluated based on the expectation that the antigen of interest, in this case the coding sequence of SIINFEKL, would be enriched within the GFP+(target) /CD8+(CTL) doublet sequence pool following PCR amplification (Figure 3-1). Success within this framework, meaning relative enrichment in PCR amplification of SIINFEKL in isolated GFP+CD8+ doublets, was considered as a key metric to gauge the feasibility of adapting this method to identify antigens in a disease model, specifically for the identification of antigen in a pre-clinical model of RMS.

A number of key steps of our proposed methodology required optimization and included: 1) determination of the activation state of CTL (activated vs memory) that leads to a higher specific target cell binding; 2) establishment of the optimal condition for *in vitro* T cell expansion (anti-CD3/CD28, cytokines, antigen stimulation expansion); 3) identification of the optimal target to effector cell ratio; 4) determination of the optimal timing (2h vs 4h vs 24h) for co-culture of target-effector; 5) establishment of fixation conditions; 6) establishment of the minimal number of "real" target cell (in this case, B16-OVA) in a pool of other targets (here, B16-GFP) necessary to be identified by a CTL (mixing B16-OVA with B16-GFP at different ratios: 1:10, 1:100, 1:1000, 1:10000); 7) similarly, identify the minimal number of specific CTLs necessary to identify a target cell (mixing CD8+ T cells from OT-I with CD8+ T cells purified from a naïve C57BL/6 mice at different ratios) and 8) the appropriate target cell for antigen expression.

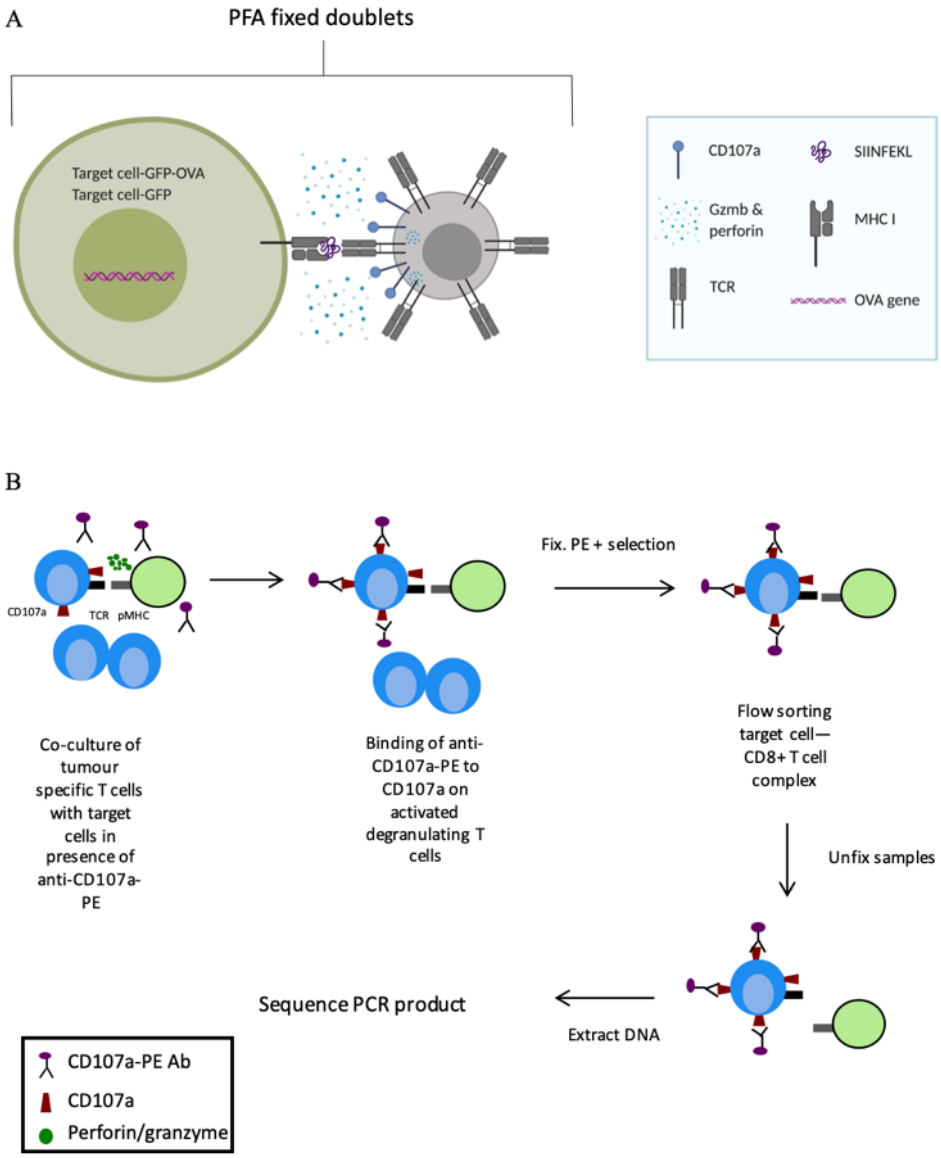
A
PFA fixed doublets
Target cell-GFP-OVA
Target cell-GFP
CD107a
SIINFEKL
Gzmb & perforin
MHC I
TCR
OVA gene
B
CD107a
TCR
pMHC
Co-culture of tumour specific T cells with target cells in presence of anti-CD107a-PE
Binding of anti-CD107a-PE to CD107a on activated degranulating T cells
Fix. PE + selection
Flow sorting target cell—CD8+ T cell complex
Unfix samples
Extract DNA
Sequence PCR product
CD107a-PE Ab
CD107a
Perforin/granzyme

Figure 3-1. Schematic summary of CTL and target cell co-cultures. A. Formation of the immunological synapse (doublet cells) upon OT-1 TCR recognition of cognate pMHC presenting SIINFEKL ($OVA_{257-264}$) and release of cytotoxic granules granzyme B (Gzmb) and perforin leading to transient expression of lysosomal associated glycoprotein CD107a on the OT-1 T cell surface. **B.** OT-1 cells are co-cultured with target cells expressing SIINFEKL and GFP in the presence of anti-CD107a fluorochorome conjugated antibody which leads to tagging of functionally degranulating OT-1 T cells. The immunological synapse is fixed with 4% PFA and stained for extracellular CD8 receptor. Doublet cells triple positive for CD8, CD107a and GFP are sorted through the MoFlo Astrio Cell Sorter. The purified cells are unfixed through heat application. DNA extracted from target cells is subject to poly-A sequencing of mRNA.

3.2 Results

3.2.1 Generation of GFP expressing B16-OVA target cell

Firstly, we designed an appropriate target cell line for probing with CTLs. To do this, B16F10-OVA (B16-OVA) and B16F10 (B16) cells were transduced with a lentivirus encoding GFP and a puromycin resistance gene. The positively transduced cells were selected for by treatment with puromycin to generate stable cell lines expressing the GFP fluorescent marker. After two weeks of *in vitro* culture in the presence of puromycin, ~90% of B16-OVA and ~70% of B16 cells displayed positive GFP signal as quantified by flow cytometry and fluorescence EVOS microscopy (Figure 3-2A).

Target cells in the context of an immunological co-culture assay are required to present MHC to display antigens on its surface. At a baseline, B16F10 cells express low levels of MHC and require induction.[226] IFN-γ treatment of B16 cells leads to the upregulation of surface MHC I.[227] Therefore, B16 cells were treated with varying concentrations of IFN-γ for 24 or 48 hours and probed for surface MHC by staining with α H-2Kb-PE. Untreated B16-OVA-GFP and B16-GFP expressed a low level of H-2Kb. When treated with 100ng/mL or 250ng/mL of IFN-γ for 24-48 hours, both cell lines displayed higher median fluorescence intensity (MFI) of staining, indicative of median H-2Kb expression, than untreated cells (~8000-10,000 vs. 10, respectively) (Figure 3-2 B). For all subsequent experiments, B16 target cells were pre-treated with 100ng/mL IFN-γ prior to co-culture with CTLs.

A

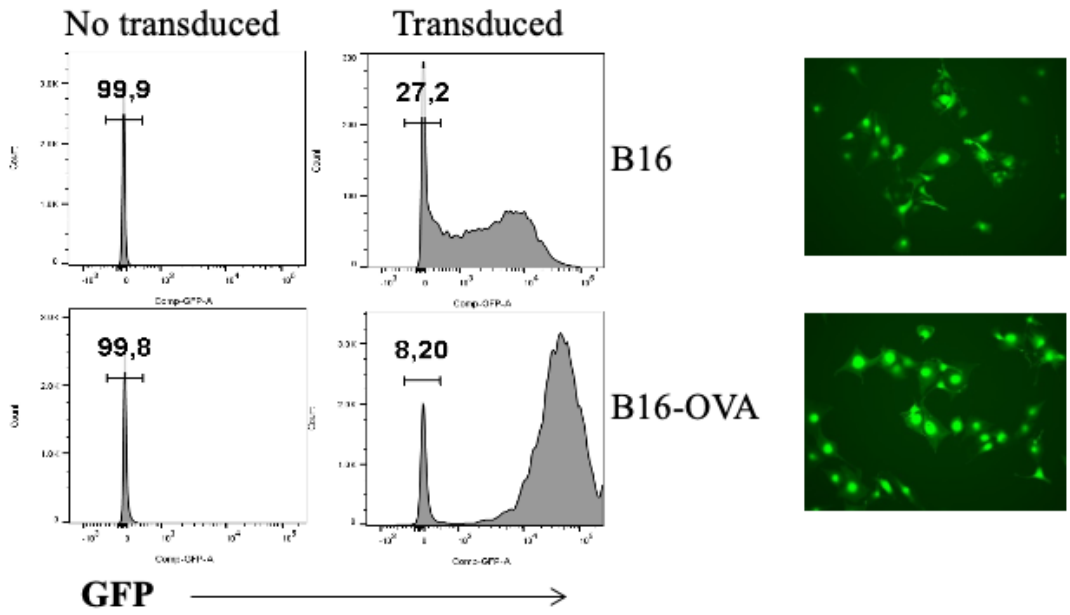
No transduced
Transduced
99,9
27,2
B16
99,8
8,20
B16-OVA
GFP

B

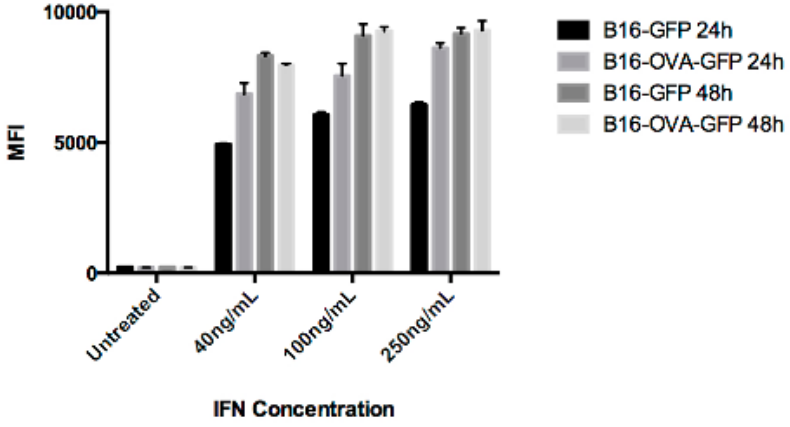
10000
5000
0
MFI
Untreated
40ng/mL
100ng/mL
250ng/mL
IFN Concentration
B16-GFP 24h
B16-OVA-GFP 24h
B16-GFP 48h
B16-OVA-GFP 48h

Figure 3-2. Generation of MHC expressing stable cell lines through transduction of target cells with pLenti-GFP. A. B16F10 and B16F10-OVA cells at a sub-confluent density were transduced with pLenti-GFP virus for 24 hours in the presence of polybrene. 48 hours later, transduced cells were selected for with puromycin. *Left,* 1E6 cells were harvested in FACS buffer (0.5% BSA in PBS) and assessed for GFP expression. *Right,* cells were also imaged by the EVOS microscope. **B.** B16-GFP and B16-OVA-GFP cells were treated with 40ng/mL, 100ng/mL or 250ng/mL of recombinant murine IFN-gamma (rmIFN-γ) for 24 or 48 hours, harvested, then stained with α-H-2Kb-APC antibody and analyzed by flow cytometry for the median fluorescence intensity (MFI) of APC.

3.2.2 First co-culture with naïve OT-1 T cells to establish baseline target and effector cell marker characteristics

The initial optimization of culture conditions involved co-culture of B16-OVA-GFP or B16-GFP cells with naïve OT-1 CD8+ T cells at two different target:effector (T:E) ratios (1:1 and 1:2) for either 4 or 24 hours. The αCD107a antibody was added during the entire duration of co-culture with the Golgi stop monensin. This combination is described in literature to effectively probe for degranulating cells that rapidly recycle vesicles to and from the cell surface.[220] After the allotted time, cells were fixed with 4% PFA, stained with α-CD8-APC-Cy7 and acquired by flow cytometry to assess the percentage of doublet cells expressing GFP, CD8 and CD107a (gating strategy described in Appendix Figure 3). We observed that approximately ~1% and 3.5% of cells were GFP+CD8+CD107a+ doublets for all conditions after 4 and 24 hours of co-culture, respectively. This lack of significant differential expression of CD107a indicated that target cells were unable to activate OT-1 CD8+T cells (Figure 3-3).

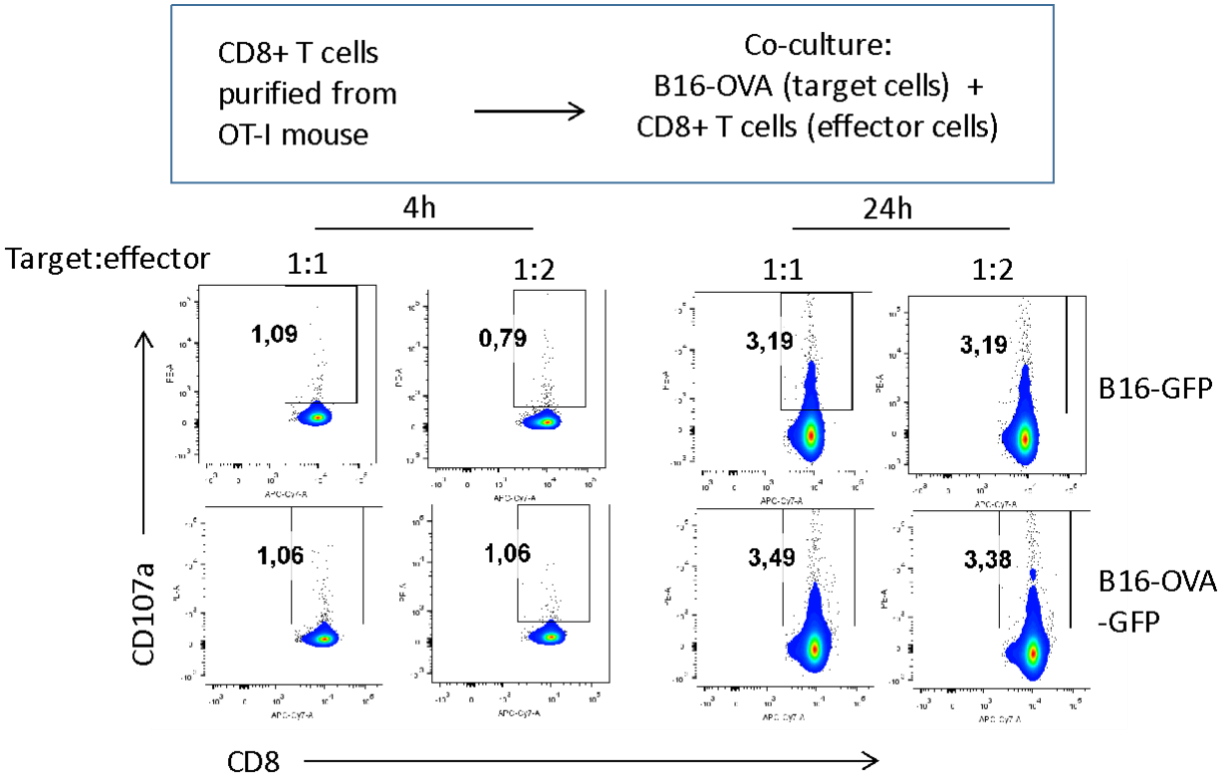
CD8+ T cells purified from OT-I mouse
Co-culture: B16-OVA (target cells) + CD8+ T cells (effector cells)
4h
24h
Target:effector
1:1
1:2
1:1
1:2
1,09
0,79
3,19
3,19
1,06
1,06
3,49
3,38
B16-GFP
B16-OVA -GFP
CD107a
CD8

Figure 3-3. First test of OT-1 purified CD8+ T cells in co-culture with B16-OVA-GFP and B16-GFP indicates no differential expression of CD107a. CD8+ T cells were purified from the spleens of OT-1 transgenic mice by negative selection. Naïve T cells were plated with $1x10^4$ B16-OVA-GFP and B16-GFP target cells at a 1:1 or 2:1 E:T ratio in the presence of anti-CD107a-PE antibody and the Golgi stop monensin. The co-culture proceeded for 4 or 24 hours after which cells were fixed with 4% PFA, harvested and stained with anti-CD8-APC-Cy7. The percentage of GFP+ doublet cells expressing CD107a and CD8 were evaluated.

3.2.3 OT-1 T cells pre-activated with SIINFEKL peptide and rmIL-2 have upregulated and sustained CD107a expression

To overcome the lack of activation of naïve OT-1 T cells when in co-culture with B16-OVA-GFP, OT-1 T cells were instead pre-activated, or primed, prior to co-culture. As such, purified splenocytes from OT-1 mice were incubated *in vitro* with SIINFEKL peptide for 24h. After 24 hours, CD8+ T cells were purified from the splenocyte pool, using a negative selection kit based on magnetic bead sorting, from the splenocyte pool. Purified OT-1 T cells were then maintained in 20 ng/mL recombinant murine IL-2 (rmIL-2) for 48 hours prior to co-culture and assessed for CD107a expression. A majority (83%) of OT-I CD8+ T cells expressed CD107a (Figure 3-4A). However, high CD107a expression at a baseline was indeed a limitation as differences in antigen induced OT-1 activation could not be discerned upon co-culture with OVA expressing or control B16-GFP cells. Therefore, we could not use CD107a to identify specific binding. However, encouragingly, there was a greater proportion of GFP+CD8+ doublets in co-cultures of activated OT-1 CTLs with B16-OVA-GFP than in those with B16-GFP, suggesting preferential interaction between OT-1 CTLs and B16 presenting OVA. There was also an increasing percentage of GFP+CD8+ doublets with increasing effectors in relation to targets (Figure 3-4B).

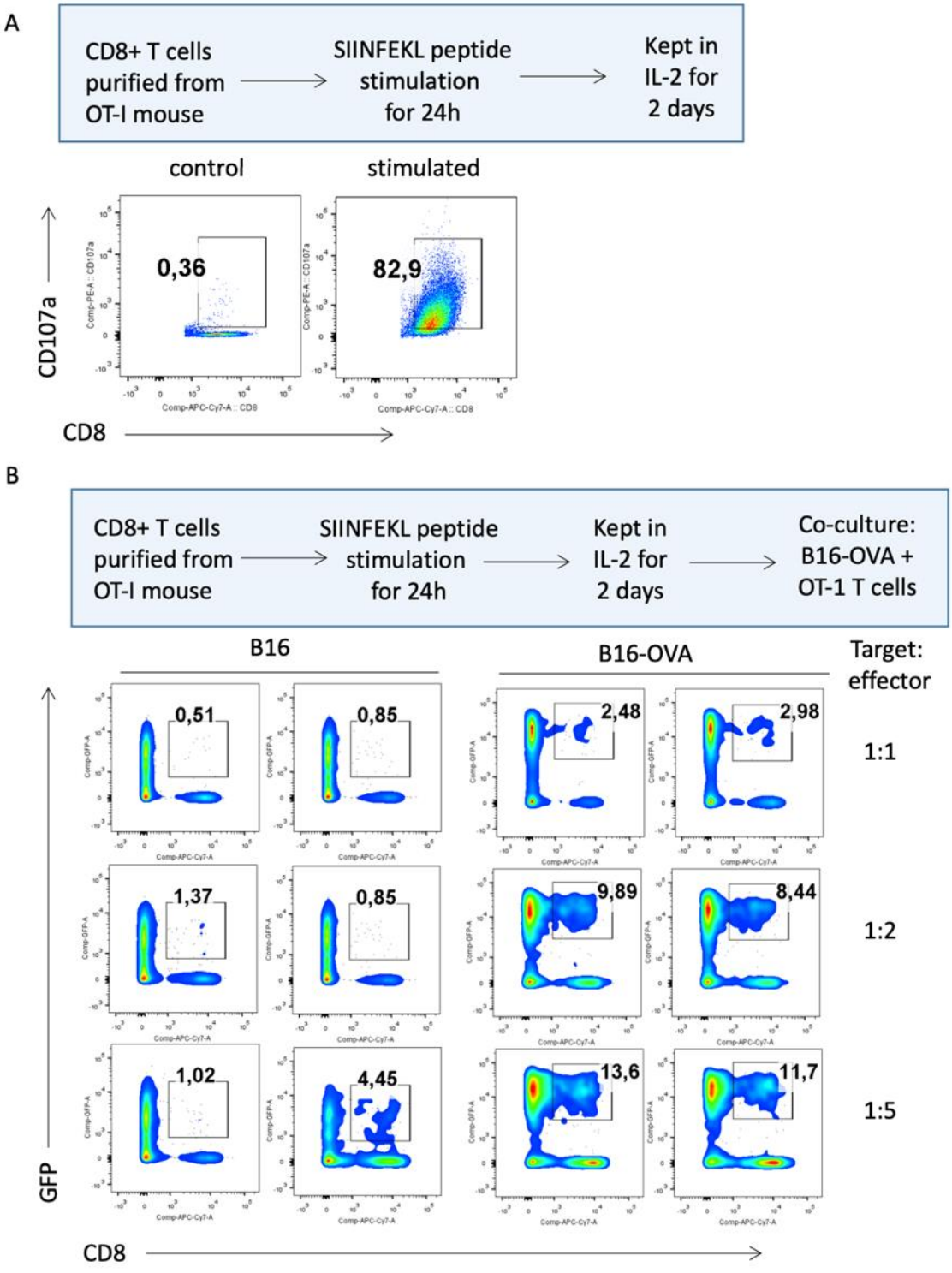
A
CD8+ T cells purified from OT-I mouse
SIINFEKL peptide stimulation for 24h
Kept in IL-2 for 2 days
control
stimulated
0,36
82,9
CD107a
CD8
B
CD8+ T cells purified from OT-I mouse
SIINFEKL peptide stimulation for 24h
Kept in IL-2 for 2 days
Co-culture: B16-OVA + OT-1 T cells
B16
B16-OVA
Target: effector
1:1
1:2
1:5
0,51
0,85
2,48
2,98
1,37
0,85
9,89
8,44
1,02
4,45
13,6
11,7
GFP
CD8

Figure 3-4. Increased GFP+CD8+ doublets in co-cultures of SIINFEKL activated OT-1 CTL target cells with B16-OVA-GFP as compared to B16-GFP. A. Naïve OT-1 T cells were stimulated with 10uM of SIINFEKL peptide for 24 hours. After 24 hours, cells were washed and supplemented with fresh media containing and 20ng/mL of murine recombinant IL-2 (mrIL-2) for 48 hours. After 48 hours, cells were fixed with 4% PFA, harvested and stained with aCD107a-PE and aCD8-APC-Cy7 antibodies. The percentage of cells expressing CD107a were assessed. **B.** OT-1 T cells pre-activated with SIINFEKL peptide and rmIL-2 were co-cultured with $1x10^4$ B16-OVA-GFP and B16-GFP cells in the presence of aCD107a-PE, Golgi stop monensin at varying E:T ratios for 4 hrs. Cells were then harvested and stained with aCD8-APC-Cy7. The percentage of GFP+CD8+ doublet cells were assessed.

3.2.4 Alternative activation of OT-1 T cells with mitogenic factors PMA/iono and maintaining in IL-7 and IL-15 for 4 days

In order to ensure that expression of CD107a correlates to specific binding of CTLs with their cognate targets, it is necessary to strike a balance between T cell priming and appropriate re-activation with target cells that would accurately reflect surface CD107a expression changes. We considered that this may be possible by allowing activated CTLs to enter the contraction phase following antigen priming. Carrio et al. (2004) observed that *in vitro* activated T cells re-cultured in either IL-7 or IL-15 had reduced levels of the activation markers CD69 and CD25 and increased expression of memory and homing marker CD62L as early as 3 days post re-culture and deemed these cells as "memory-like" T cells.[228] This is because IL-7 and IL-15 are complimentary cytokines imperative for the regulation, generation, and maintenance of memory CTLs.[229] Therefore, to reduce the expression of baseline CD107a, OT-1 CTLs at were cultured with IL-7 and IL-15 for 4 days following activation with the mitogenic factor PMA and the calcium ionophore ionomycin. Then the "memory-like" OT-1 CTLs were co-cultured with target cells at varying target-to-effectors ratios for 4 hours and doublet cells were assessed by flow cytometry (Figure 3-5). Again, the percentage of GFP+CD8+CD107a+ doublets was greater in co-cultures with B16-OVA-GFP than with B16-GFP, however the percentage observed in B16-GFP was unexpectedly high, suggesting antigen-nonspecific binding. As observed before, an increase in the percentage of GFP+CD8+CD107a+ doublets correlated with increasing effector cells in proportion to target cells in co-culture for both B16-OVA-GFP and B16-GFP conditions (Figure 3-5).

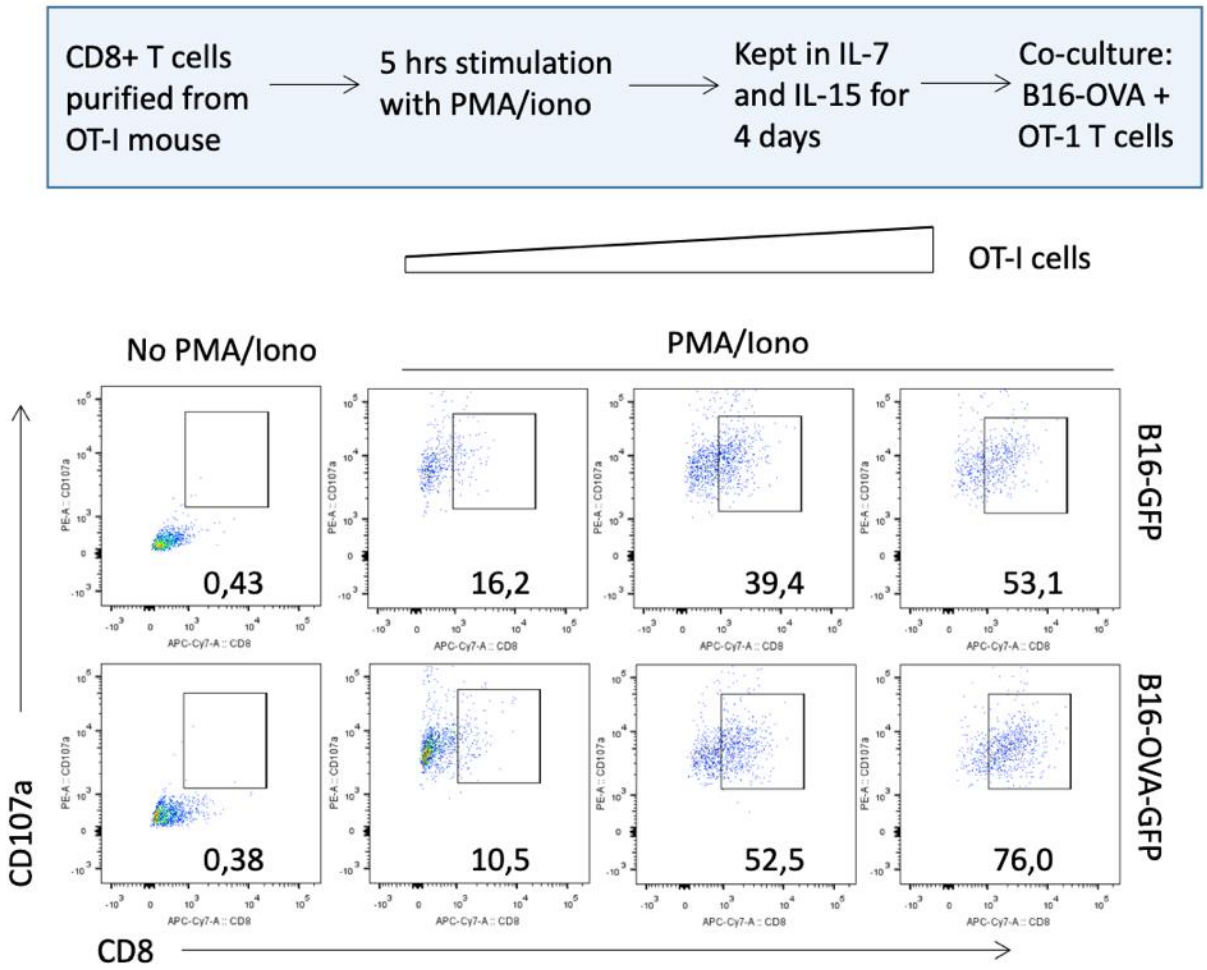
CD8+ T cells purified from OT-I mouse
5 hrs stimulation with PMA/iono
Kept in IL-7 and IL-15 for 4 days
Co-culture: B16-OVA + OT-1 T cells
OT-I cells
No PMA/Iono
PMA/Iono
B16-GFP
B16-OVA-GFP
CD107a
CD8
0,43
16,2
39,4
53,1
0,38
10,5
52,5
76,0

Figure 3-5. Increased GFP+CD8+CD107a+ doublets observed with increasing effectors-to-targets in co-culture of B16-OVA-GFP and B16-GFP with pre-activated OT-1 CTLs. Naïve OT-1 T cells were stimulated with PMA and ionomycin (PMA/iono) for 5 hours. After 5 hours, cells were washed and supplemented with fresh media containing and 15ng/mL of murine recombinant IL-7 and IL-15 (mrIL-7, rmIL-15) for 4 days. After 4 days, OT-1 T cells were placed in co-culture with $1x10^4$ B16 target cells in the presence of aCD107a-PE and Golgi stop monensin. Cells were then fixed with 4% PFA, harvested and stained with aCD8-APC-Cy7. The percentage of GFP+CD8+CD107a+ doublet cells were assessed.

3.2.5 Optimization of target-to-effector ratio in co-culture conditions

Next, we sought to determine the optimal target-to-effector ratio needed to observe differences in GFP+CD8+CD107a+ doublets between the B16-OVA-GFP and B16-GFP co-cultures as well as the minimum ratio required to make compelling conclusions about the activity of CTLs between conditions. Typically, optimal ratios between target and effector cells in a co-culture assay need to be determined as CTL killing may vary depending on the target.[230,231] As such, target-to-effector ratios were varied from 8:1 to 1:5. No significant differences in the percentage of GFP+CD8+CD107a+ doublets was detected upon adding more target cells in relation to effector cells. However, increasing the proportion of effector cells in relation to target cells resulted in increased percentage of GFP+CD8+CD107a+ doublets in both B16-OVA-GFP and B16-GFP conditions. At a target-to-effector ratio of 1:2 and 1:5, there were more doublets found to be GFP+CD8+CD107a+ in the B16-OVA-GFP co-culture (12.4% and 21.9%, respectively) than in the B16-GFP co-culture (5.63% and 12.4%, respectively) (Figure 3-6). Although a correlation of increasing degranulating OT-1 CTLs with an increasing E:T ratio was observed when in co-culture with antigen expressing B16 cells, the target-to-effector ratio of 1:2 provided lower unspecific binding (5.63%) than the 1:5 ratio (12.4%) as evidenced by the control B16 cells. (Figure 3-6).

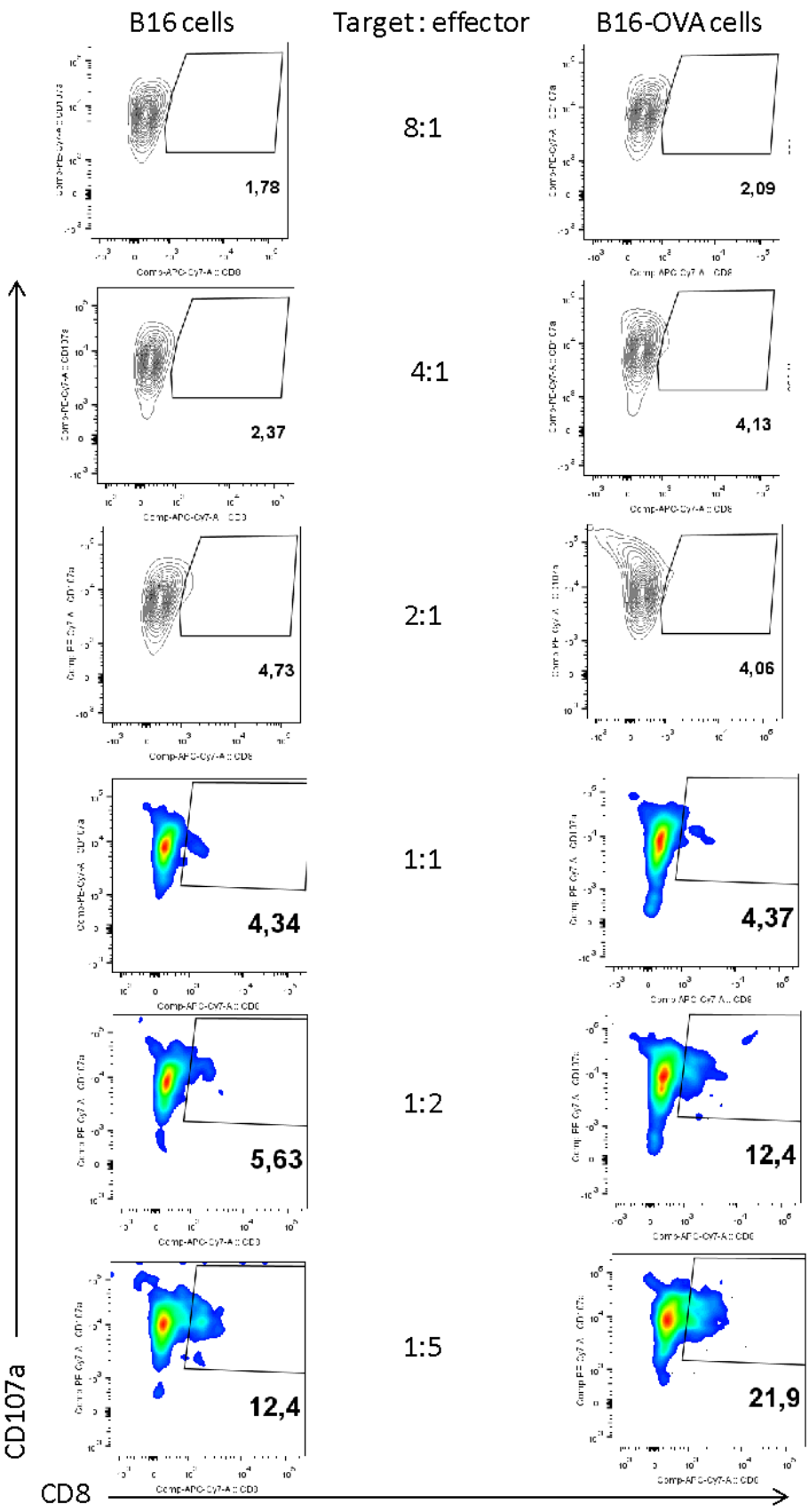
B16 cells
Target : effector
B16-OVA cells
8:1
1,78
2,09
4:1
2,37
4,13
2:1
4,73
4,06
1:1
4,34
4,37
1:2
5,63
12,4
1:5
12,4
21,9
CD107a
CD8

Figure 3-6. Increased percentage of GFP+CD8+CD107a+ doublets in co-cultures of B16-OVA-GFP with higher relative CTLs numbers. Naïve OT-1 T cells were stimulated with PMA and ionomycin (PMA/iono) for 5 hours. After 5 hours, cells were washed and supplemented with fresh media containing and 15ng/mL of murine recombinant IL-7 and IL-15 (mrIL-7, rmIL-15) for 4 days. After 4 days, OT-1 T cells were placed in co-culture with aCD107a-PE and Golgi stop monensin at varying target-to-effector ratios for up to 5 hours. Cells were then fixed with 4% PFA, harvested and stained with aCD8-APC-Cy7. The percentage of GFP+CD8+CD107a+ doublet cells were assessed.

3.2.6 An alternate CTL activation strategy with CD3 and CD28 agonistic antibodies

Consistently, the total number of T cells available for co-culture was a limiting step. To overcome this problem, we tested different T cell activating conditions and assessed up-regulation of activation markers CD69 and CD25 as well as degree of T cell expansion by flow cytometry. Two different concentrations of plate-bound antibodies (2ug/ml of αCD3 plus 2ug/ml of αCD28 or 5ug/ml αCD3 plus 2ug/ml of αCD28) with 20U/ml of IL-2 were used to stimulate CD8+ T cells for 24, 48 or 72h in a 96 or 24 well plate format. We observed the highest proportion of activated CTLs cultured in 24 well plates in which cells were stimulated with 2ug/mL each αCD3+αCD28+ 20U/mL IL2 for 24 hours (33.3% positive) (Figure 3-7A). In comparison, 27.6% of CTLs exhibited activation when stimulated with the same condition but in a 96 well plate (Figure 3-7B). Furthermore, passaging T cells every 48 hours in the presence of IL-2 for 6 days led to expansion of T cells from $2x10^7$ to up to a total of $1x10^8$ cells (~ 5-fold increase, data not shown). This optimized protocol for T cell activation and expansion increased the viability and number of CTLs (Figure 3-7).

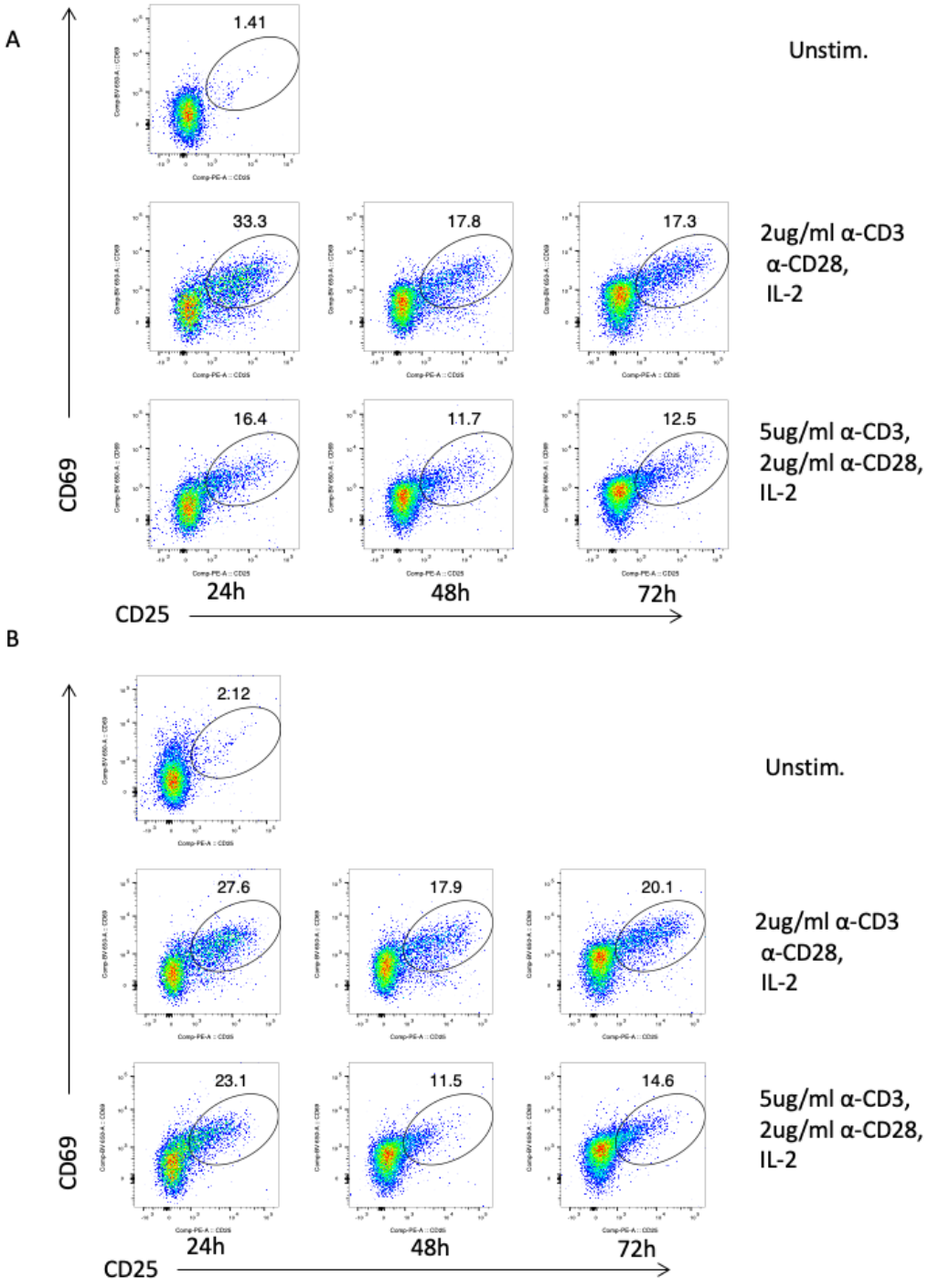
A
1.41
Unstim.
33.3
17.8
17.3
2ug/ml α-CD3
α-CD28,
IL-2
16.4
11.7
12.5
5ug/ml α-CD3,
2ug/ml α-CD28,
IL-2
CD69
24h
48h
72h
CD25
B
2.12
Unstim.
27.6
17.9
20.1
2ug/ml α-CD3
α-CD28,
IL-2
23.1
11.5
14.6
5ug/ml α-CD3,
2ug/ml α-CD28,
IL-2
CD69
24h
48h
72h
CD25

Figure 3-7. Stimulation of OT-1 CTLs for 24 hours with αCD3+αCD28 and IL-2 induces T cell activation and long term cell viability. Naïve OT-1 T cells were stimulated with the following plate-bound antibodies 2ug/mL of aCD3 and 2ug/mL aCD28 or 5ug/mL of αCD3 and 2ug/mL of αCD28 for 24 hours, 48 or 72 hours in a **A.** 24-well or **B**. 96-well plate. After the allotted time, cells were washed and supplemented with fresh media containing 20ng/mL of murine recombinant IL-2 and cultured for an additional 7 days with cell passaging steps every 3 days. After 7 days in IL-2 containing media, OT-1 T cells were harvested and stained for surface expression of CD69 and CD25. The percentage of CD25+CD69+ cells were assessed.

3.2.7 Assay sensitivity evaluated by diluting the pure OT-1 effector cell population with spiked in BL/6 T cells

The next step of optimization was to evaluate the sensitivity of the assay. We wanted to determine the minimum number of antigen-specific CTLs necessary to identify target cells. We hypothesized that if there is a decreased proportion of antigen specific CD8+ T cells, in a pool of effectors, in the co-culture, there would be a relative reduction in the percentage of GFP+CD8+CD107a+ doublets observed. Our approach to evaluate the necessary proportion of antigen-specific CTLs was to spike the co-culture conditions with unspecific CTLs from naïve C57BL/6 mice. Initially, varying ratios of OT-I and BL/6 CTLs were added to the co-culture conditions but maintaining the target to effector ratio of 1:2 (Table 1). There was a greater percentage of doublets observed in the B16-OVA-GFP condition than the B16-GFP condition for all OT-1 and C57BL/6 spiking ratios (Figure 3-8A). Interestingly, there was no difference in the percentage of doublets observed in the conditions that contained either 100% or 12.5% of OT-1 T cells. However, there were no differences observed in the percentage of GFP+ CD8+CD107a+ doublets between B16-OVA-GFP and B16-GFP (Figure 3-8B), suggesting non-specific background in these conditions compared to what was previously observed (Figure 3-6). Nevertheless, the total number of GFP+CD8+CD107a+ doublets from the B16-OVA-GFP co-culture was higher than those from B16-GFP co-culture, an observation consistent with previous experiments (Figure 3-6).

Table 1. OT-1 effector cell spiking with C57BL/6 derived T cells in varying proportions from 100% to 12.5% antigen specific cells relative to targets (the target:effector ratio was maintained at 1:2)

# Target Cells	# OT-1 T cells	# C57BL/6 T cells
50,000	100,000 (100%)	0
50,000	50,000 (50%)	50,000 (50%)
50,000	25,000 (25%)	75,000 (75%)
50,000	12,500 (12.5%)	87,500 (87.5%)

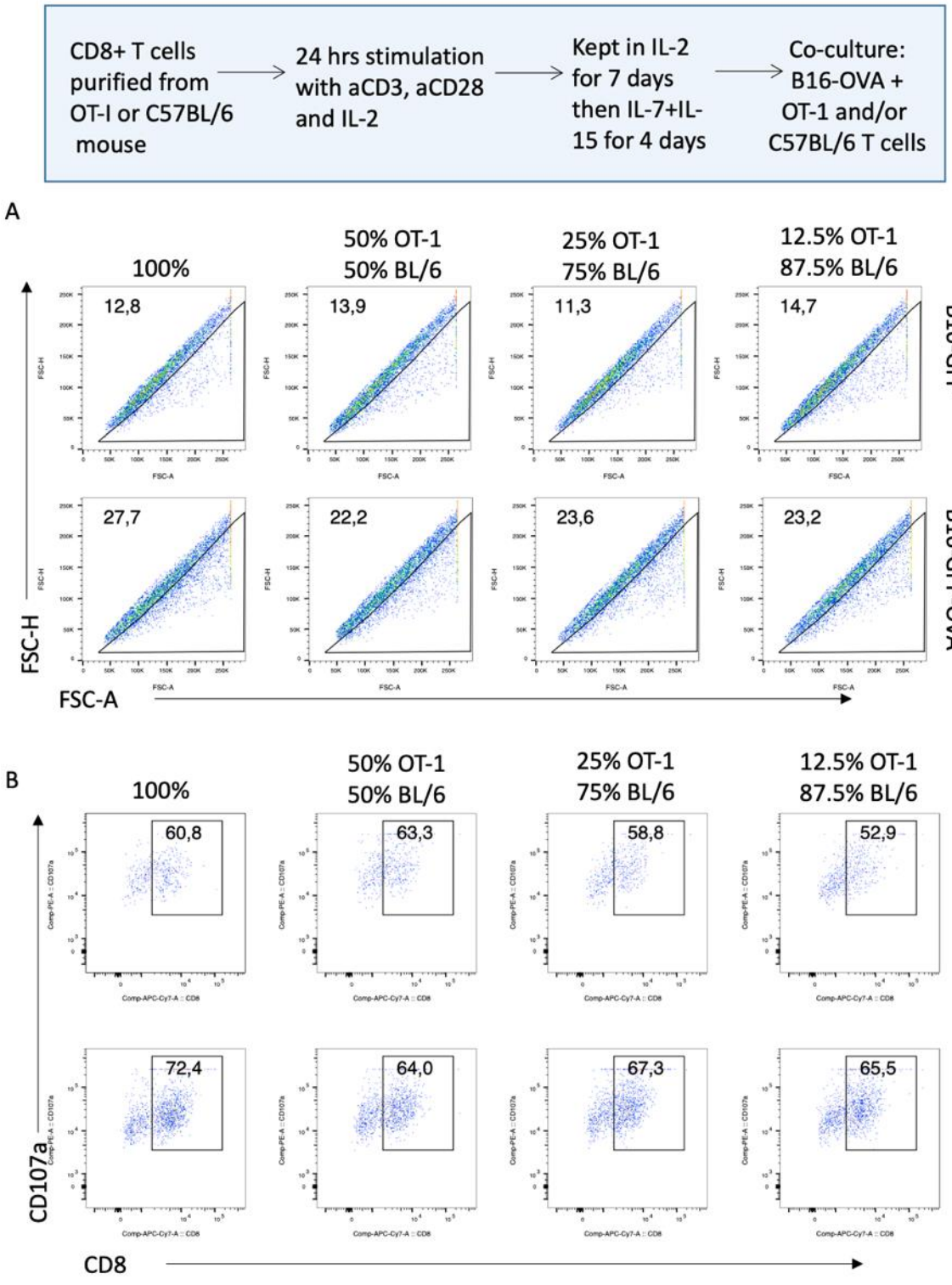
CD8+ T cells purified from OT-I or C57BL/6 mouse
24 hrs stimulation with aCD3, aCD28 and IL-2
Kept in IL-2 for 7 days then IL-7+IL-15 for 4 days
Co-culture: B16-OVA + OT-1 and/or C57BL/6 T cells
A
100%
50% OT-1 50% BL/6
25% OT-1 75% BL/6
12.5% OT-1 87.5% BL/6
12,8
13,9
11,3
14,7
27,7
22,2
23,6
23,2
B16-GFP
B16-GFP-OVA
FSC-H
FSC-A
B
100%
50% OT-1 50% BL/6
25% OT-1 75% BL/6
12.5% OT-1 87.5% BL/6
60,8
63,3
58,8
52,9
72,4
64,0
67,3
65,5
B16-GFP
B16-GFP-OVA
CD107a
CD8

Figure 3-8. No differences in the percentage of GFP+CD8+CD107a+ doublets acquired with increasingly diluted OT-1 target cells for both B16-OVA-GFP and B16-GFP conditions. Naïve OT-1 or C57BL/6 T cells were stimulated with plate-bound 2ug/mL of αCD3 and 2ug/mL αCD28 for 24 hours. After 24 hours, cells were washed and supplemented with fresh media containing 20ng/mL of murine recombinant IL-2 and cultured for an additional 7 days with cell splitting steps every 3 days. After 7 days in IL-2 containing media, T cells were maintained in media containing 15ng/mL of murine recombinant IL-7 and IL-15 for up to 4 days. After 4 days, OT-1 and C57BL/6 T cells were placed in co-culture with αCD107a-PE and Golgi stop monensin at varying target-to-effector ratios for up to 5 hours. Cells were then fixed with 4% PFA, harvested and stained with αCD8-APC-Cy7. The percentage of **A.** doublets that are **B.** GFP+CD8+CD107a+ were assessed.

3.2.8 Reducing background staining in spiking conditions by co-culture with flow sorted OT-1 CD8+ T cells

To enhance the amount of GFP+CD8+CD107a+ doublets obtained and to reduce background, we flow sorted CTLs that were CD25+CD69+ after activation and expansion, and prior to IL-7/IL-15 culture. This was done to ensure that all T cells in the co-culture were previously activated. This is based on the observation that upon stimulation, ~ 35% of CTLs show the typical activation signature 24h post-stimulation (Figure 3-7). Ultimately, the addition of a CD25+CD69+ sorting step contributed to a reduction of doublets from 12.8% to 7% in the B16-GFP condition when in co-culture with 100% OT-1 CTLs (Figure 3-8, 3-9). A greater proportion of doublet cells in the B16-OVA-GFP condition (20%) compared to the B16-GFP condition (6%-9%) was observed. However, of those doublets, the percentage that was GFP+CD8+CD107a+ was the same between both groups. The sorting step, unfortunately, resulted in a reduction in the number of effector cells available which therefore, limited the amount of cells that could be used for downstream experimentation. In this context a 1:2 target-to-effector ratio was used however, additional ratios that included more E:T (e.g. 5:1 or 10:1 as evidenced by Figure 3-6) would help to confirm whether valid differences between the B16-OVA-GFP and B16-GFP co-cultures are valid (Figure 3-9). Additionally, background positive events in the B16-GFP co-culture continued to be observed.

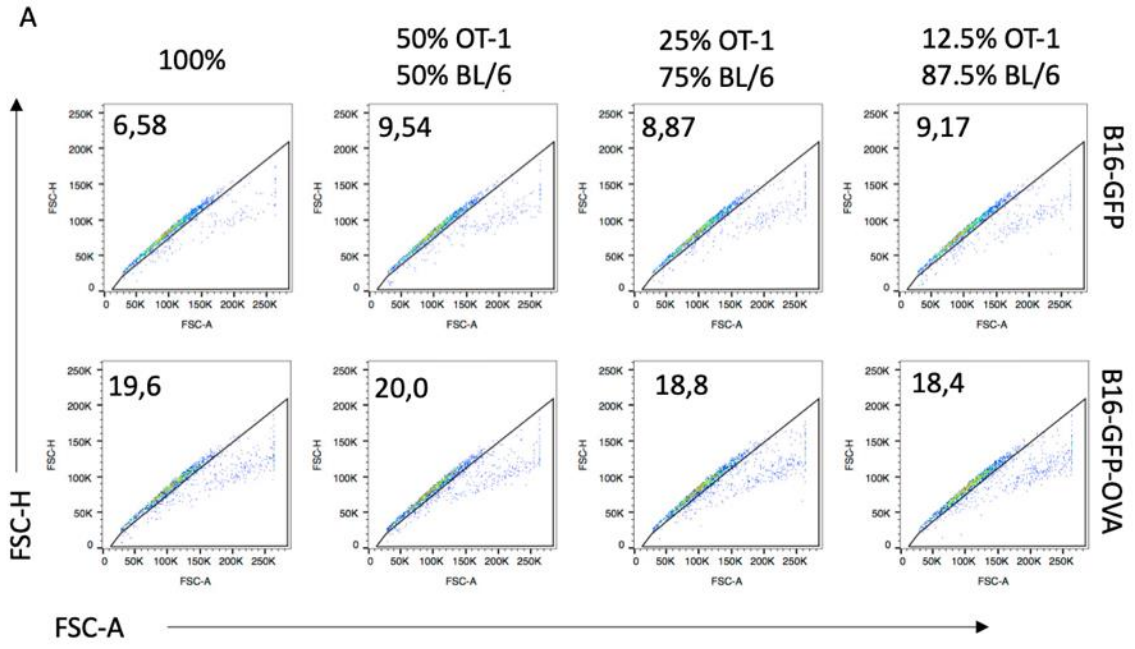
A
100%
50% OT-1
50% BL/6
25% OT-1
75% BL/6
12.5% OT-1
87.5% BL/6
6,58
9,54
8,87
9,17
19,6
20,0
18,8
18,4
B16-GFP
B16-GFP-OVA
FSC-H
FSC-A

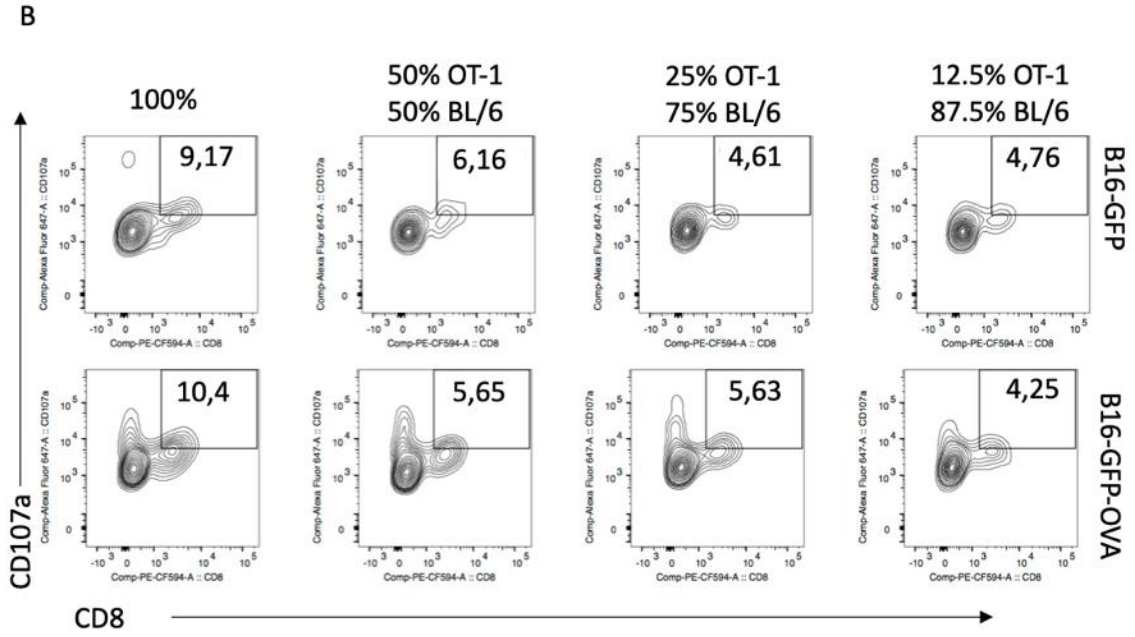
B
100%
50% OT-1
50% BL/6
25% OT-1
75% BL/6
12.5% OT-1
87.5% BL/6
9,17
6,16
4,61
4,76
10,4
5,65
5,63
4,25
B16-GFP
B16-GFP-OVA
CD107a
CD8

Figure 3-9. Co-culture of purified, sorted T cells, diluted with naive CD8+ T cells, with target cells B16-OVA-GFP and B16-GFP again revealed no differences in the acquisition of GFP+CD8+CD107a+ doublets. Naïve OT-1 or C57BL/6 T cells were stimulated with plate-bound 2ug/mL of aCD3 and 2ug/mL aCD28 for 24 hours. After 24 hours, cells were washed and supplemented with fresh media containing 20ng/mL of murine recombinant IL-2 and cultured for an additional 7 days with cell splitting steps every 3 days. After 7 days in IL-2 containing media, OT-1 and C57BL/6 T cells were harvested and stained for surface expression of CD69 and CD25. Cells that were CD25+CD69+ were sorted using the MoFlo Astrios Cell Sorter. Sorted cells were maintained in media containing 15ng/mL of murine recombinant IL-7 and IL-15 for up to 4 days. After 4 days, OT-1 and C57BL/6 T cells were placed in co-culture with αCD107a-PE and Golgi stop monensin at varying target-to-effector ratios for up to 5 hours. Cells were then fixed with 4% PFA, harvested and stained with aCD8-APC-Cy7. The percentage of **A.** doublets that were **B.** GFP+CD8+CD107a+ were assessed.

3.2.9 Generation of a new cell line with low expression of CD107a

Throughout the co-culture experiments, an intriguing observation was made relating to the unexpected expression of CD107a on CD8- cells. Initially, we supposed this may be associated with unspecific binding of the αCD107a-PE flow antibody, . To address this possibility, we probed B16-OVA-GFP cells for surface CD107a expression. Indeed, we observed that ~30% B16-OVA-GFP target cells were positive for surface CD107a (Figure 3-10A). A review of previous studies revealed that CD107a may indeed be expressed on highly metastatic and aggressive tumour cell lines.[232] In particular, B16-F10 has been previously cited to express CD107a.[233] This finding may explain the false positive and background doublets observed in all co-culture experiments. In light of this, we sought to evaluate the use of other target cell lines to be used for future co-cultures in order to reduce the background percentage of GFP+CD8+CD107a+ cells. As such, we screened various cell lines for CD107a expression: 1) 3 tumor cell lines from C57BL/6 background, Pan02, MC38 and CT2A, 2) the dendritic cell line Jaws-II and, 3) the fibroblast cell line COS7 which is typically used in CTL assays (as described in Chapter 1). Among the cell lines selected for testing, Pan02, CT2A and JawsII cells all expressed baseline surface CD107a (Figure 3-10B) thus, would not serve as appropriate targets for our methodology. However, MC38 and COS7 did not express surface CD107a and the former had high expression of H-2Kb (Figure 3-10B). Ultimately, COS7 cells were chosen for further exploration owing its historical use, its' negligible CD107a expression and the ease of transfectability and transducibility with cDNA libraries and a range of MHC molecules.[234–236]

As per the generation of GFP expressing target cells described previously, COS7 cells were transduced with lentivirus expressing GFP (Figure 3-12C). We used two COS7 cell lines: parental COS7 that do not express any murine MHC (termed COS7) and COS7 that functionally expressed

the MHC I allotype from C57BL/6 mice, H-2Kb (termed COS7-kb). Neither COS7 line expressed the OVA protein and thus did not express SIINFEKL in the context of MHC I. Therefore, for co-culture with OT-1, OVA-expressing COS7 cells were generated. As a first method chosen to express OVA, COS7 cells were transduced with an *OVA* expressing lentivirus. To begin, cDNA from B16-OVA cells was generated and rtPCR was performed amplify the *OVA* gene with primers containing BamHI and XbaI flanking sites. The PCR product was then ligated into the pLenti-PGK-V5-Fluc vector between the BamHI and XbaI restriction sites. Predicted positive clones from *E. coli* transformed colonies were evaluated for incorporation of the *OVA* transgene by restriction enzyme digest. The OVA DNA fragment of predicted size of ~1200kb was observed indicating its integration into the pLenti vector (Appendix Figure 7). We then proceeded to produce and rescue mature lentiviral particles by *in vitro* transfection in 293T host cells transfected with pLenti-PGK-OVA and the lentivirus structural components pLP1, pLP2 and VSV G (Appendix Figure 7). To confirm the production of mature pLenti-OVA, the harvested virus was used to transduce 293T cells and probed with an αOVA antibody and then assessed by immunoblot. B16-OVA cells and transfected 293T cells, used as positive controls, showed expression of the OVA protein at 42kDa. However, none of the transduced 293T cells showed expression of the OVA protein (Appendix Figure 7).

As an alternative to present SIINFEKL epitope on MHC-I in target cells, COS7-kb cells were peptide pulsed with SIINFEKL peptide. In this experiment, COS7-kb-GFP cells, which express a functional MHC I, and COS7-GFP cells that do not express MHC I (therefore cannot present any antigen) were both peptide pulsed with 5uM of SIINFEKL peptide for 45 mins and stained with αSIINFEKL/H-2kb-PE. Peptide pulsed COS7-Kb-GFP, but not pulsed COS7-GFP cells, displayed strong GFP signal indicative of antigen presentation (Figure 3-10D).

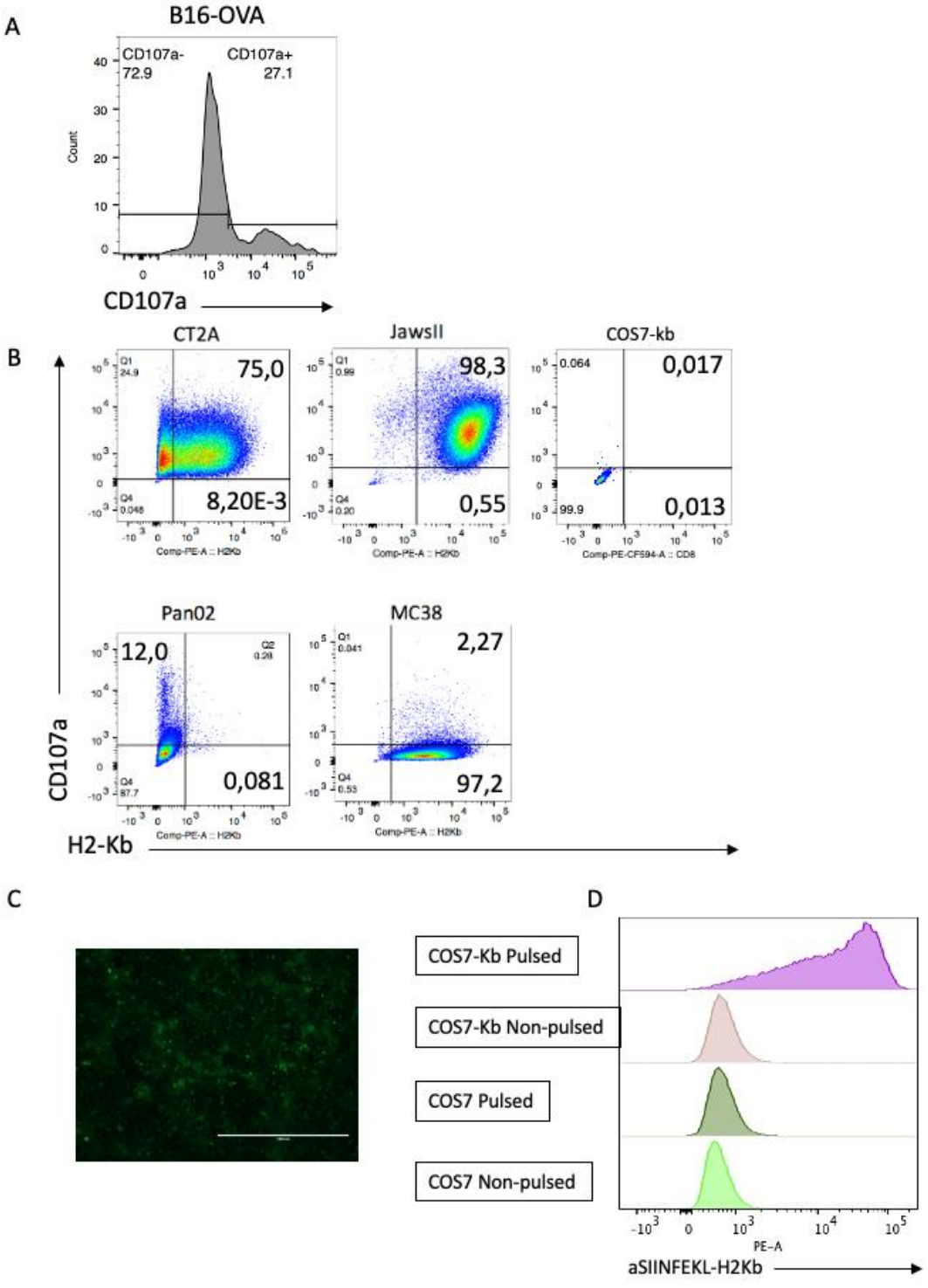
A
B16-OVA
CD107a-
72.9
CD107a+
27.1
Count
CD107a
B
CT2A
75,0
8,20E-3
JawsII
98,3
0,55
COS7-kb
0,017
0,013
Pan02
12,0
0,081
MC38
2,27
97,2
CD107a
H2-Kb
C
D
COS7-Kb Pulsed
COS7-Kb Non-pulsed
COS7 Pulsed
COS7 Non-pulsed
PE-A
aSIINFEKL-H2Kb

Figure 3-10. B16 target cells express basal, extracellular CD107a prompting the evaluation of other target cells including CT2A, JawsII, COS7, Pan02, and MC38. A. $1x10^6$ B16-OVA cells were harvested and stained with aCD107a-AF647. A histogram displaying the percentage and level of expression of CD107a on the surface of B16-OVA cells was assessed. **B.** $1x10^6$ CT2A, JawsII, Pan02, MC38 and COS7 were harvested and stained with aH2-Kb-PE and aCD107a-AF647. The percentage of singlet cells that are CD107a+H2Kb+ was assessed. **C.** COS7kb were transduced with pLenti-GFP virus for 24 hours in the presence of polybrene. 48 hours later, transduced cells were cells were selected for with puromycin to grow surviving population of cells. 1E6 COS7-kb cells were harvested in FACS buffer (0.5% BSA in PBS) and assessed for GFP expression. **D)**. 5E6 COS7-Kb and COS7 cells were incubated with 5uM of SIINFEKL peptide for 45 mins, washed, stained for anti-SIINFEKL/H2-kb-PE. All samples were acquired by flow cytometry and assessed for expression of aSIINFEKL-H2Kb.

3.2.10 Co-culture of OT-1 CD8+ T cells with new COS7 target cells and synapse evaluation by microscopy

Based on the results described above, COS7-kb-GFP and COS7-GFP cells were both peptide pulsed with 5uM of SIINFEKL peptide for 45 mins, washed and added in culture with previously expanded OT-1 T cells. Following 4 hours of co-culture, cells were imaged by microscopy to visually evaluate differences in the presence of cytotoxic synapses, and also assessed by flow cytometry. Brightfield microscopy images (Figure 3-11A) show more cell synapse formation (as evidenced by white arrows) in the co-culture condition in which target cells express SIINFEKL than in the negative control target cells. However, there were no differences in the capture of GFP+CD8+CD107a+ doublets by flow cytometry in co-cultures with COS7-kb-GFP-OVA (45%) and COS7-GFP-OVA (43.3%) (Figure 3-11B).

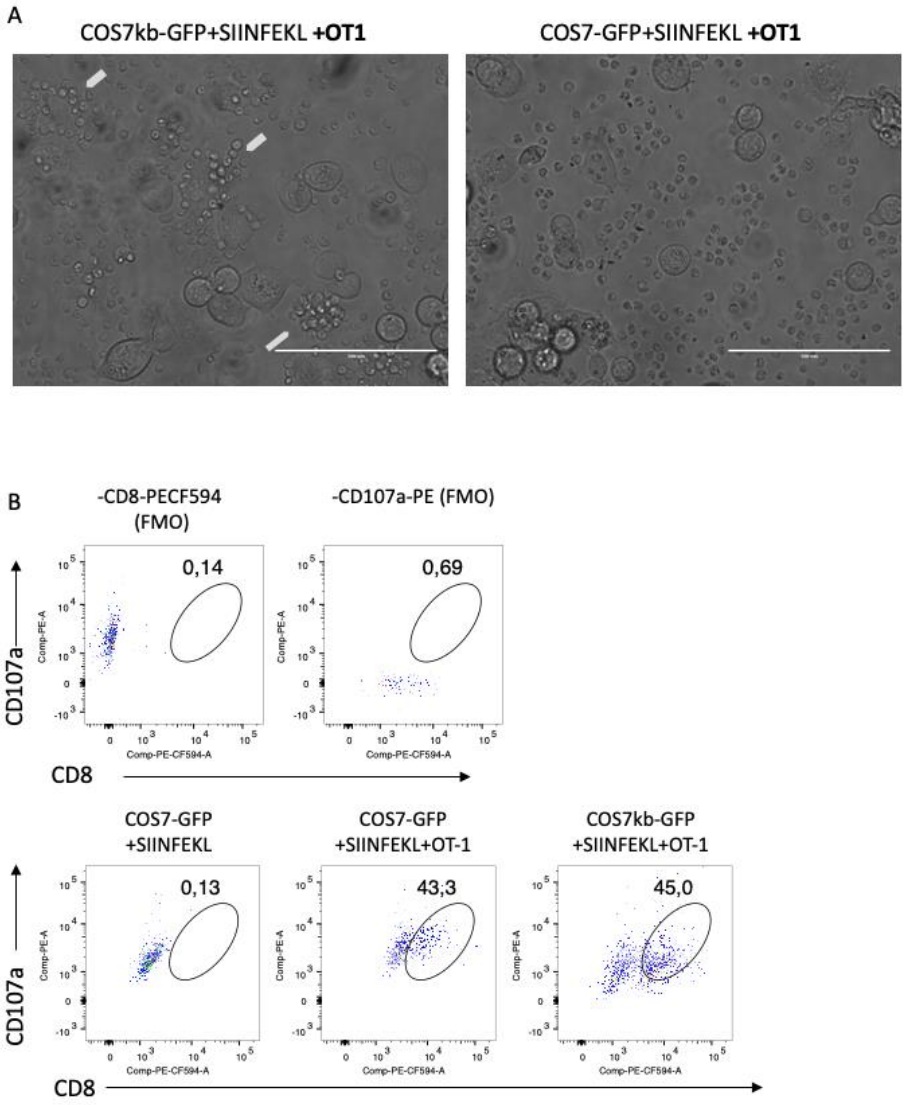
A
COS7kb-GFP+SIINFEKL +OT1
COS7-GFP+SIINFEKL +OT1
B
-CD8-PECF594
(FMO)
-CD107a-PE (FMO)
0,14
0,69
CD107a
CD8
COS7-GFP
+SIINFEKL
COS7-GFP
+SIINFEKL+OT-1
COS7kb-GFP
+SIINFEKL+OT-1
0,13
43,3
45,0
Comp-PE-A
Comp-PE-CF594-A

Figure 3-11. Co-culture of OT-1 T cells with SIINFEKL pulsed COS7kb-GFP and COS7-GFP target cells reveal multiplets observable by microscopy but not sensitive acquisition by flow cytometry. Naïve OT-1 T cells were stimulated with plate-bound 2ug/mL of aCD3 and 2ug/mL aCD28 for 24 hours. After 24 hours, cells were washed and supplemented with fresh media containing 20ng/mL of murine recombinant IL-2 and cultured for an additional 7 days with cell splitting steps every 3 days. Cells were harvested and maintained in media containing 15ng/mL of murine recombinant IL-7 and IL-15 for up to 4 days After 4 days, OT-1 and T cells were placed in co-culture with peptide pulsed COS7kb-GFP and COS7-GFP target cells in the presence of Golgi stop (monensin) and aCD107a-AF647 for 5 hours. Cells were then fixed with 4% PFA, harvested and stained with aCD8-PECF594. The percentage of GFP+CD8+CD107a+ doublet cells were assessed by **A.** brightfield microscopy; white arrows depict multi-cell synapses and **B.** flow cytometry.

3.4 Discussion

In this chapter, we presented a series of experiments designed to assess the feasibility of developing a flow cytometry-based approach for isolating CTL-target cell doublets formed by the anchorage of cognate TCR-peptide MHC complexes. We sought to establish the optimal conditions for the methodology, necessary for the identification of antigen driven cytotoxic synapses that may encompass and allow to decode simultaneously an immunogenic antigen and its associated responsive TCR. In this pursuit, we established a strategy for the preparation of mature effector CD8+ T cells and antigen expressing target cells. Firstly naïve OT-1 CD8+ T cells were found to be ill suited for cognate pMHC recognition, with ultimately little effect on cytotoxic granule mobilization and thus an inability to capture cells using CD107a. On the opposite spectrum, stimulation with SIINFEKL peptide and rmIL-2 greatly induced cytotoxic granule release followed by upregulation and maintained expression of CD107a, rendering nuanced deviations of CD107a expression immeasurable as a result. However, sufficient activation with CD3+CD28 receptor agonists and the addition of IL-7+IL-15 to long term CD8+ T cell culture generated transitional T cells that encountered sufficient priming but retained capacity for pMHC recognition and response. This method of CD8+ T cell activation would allow for the preparation of a breadth of primary effector CD8+ T cells isolated from human PBMCs as it does not rely on antigen-specific priming, a feat difficult to achieve when probing with a multitude of TCRs downstream. Secondly, the co-culture incubation period is an important consideration in this methodology. An incubation period of less than 2 hours yielded no differences in the detection of GFP+CD8+CD107a+ doublets between the antigen expressing and non-expressing targets, perhaps owing to insufficient scanning of targets by CTLs and thus reducing the capture of rare events. Indeed, Gourdain et al. (2013) and Barber et al. (2003) describe the detection of CTL

cytotoxicity between 2-4 hours in co-cultures by ^{51}chromimium-based killing assays and target cell caspase probing.[237,238] Conversely, an incubation of greater than 8 hours was too long and the cytotoxic effects of cognate CTLs killed target cells; indeed CTLs may program antigen-specific targets towards apoptosis within minutes of binding but true apoptosis is evidenced after several hours.[239] Thus, the detection of CD107a falls in line with previous evidence. Finally, as evidenced in co-culture studies, the choice of effector-to-target ratios is vital to the detection of cytotoxic synapses and CTL functional activity. A reasonable E:T ratio would enlist greater effectors to target, but to a threshold that would ensure the survival of targets after 4 hours for flow cytometric capture.[240–242] As such, differences were observed in the proportion of GFP+CD8+CD107a+ doublets between the antigen expressing and non-expressing target cell conditions at an E:T ratio >2:1 indicating this to be the limit of specific detection.

During the development of this methodology, a number of key challenges were uncovered that impeded the identification of short-lived and rare cytotoxic synapses. Although differential CTL-target cell "multiplets", rather than doublets, were identified by microscopy, there was a lack of translation when attempting to identify such multiplet events by flow cytometry. In its essence, the use of flow cytometry to sensitively capture specific doublets requires further optimization for a number of reasons. Most importantly, probing for extracellular CD107a is not ideal, as evidenced by the high baseline GFP+CD8+CD107a+ doublet populations seen in both B16-OVA and B16 co-culture conditions, indicating a lack of sensitivity of this marker. While, in the context of B16 target cells, the background events seen were partially explained by the expression of CD107a on B16 cells themselves, the problem however, persisted even with COS7 target cells. Although puzzling, evidence of a phenomenon called trogocytosis may offer some explanation of these observations. Trogocytosis is a process by which lymphocytes ingest the products of a target cell's

plasma membrane following the formation of an immunological synapse and may be intended to function as a form of intercellular communication, aid in the selection of high-affinity CTLs, or contribute to 'fratricide' (self CTL killing).[243,244] Intriguingly, the transfer of plasma membrane proteins is bidirectional and T cell membrane proteins can be trogocytosed by bound target cells. As a result of trogocytosis, target COS7-kb-OVA cells with no baseline CD107a expression may present this CTL activation marker after co-culture, thus precluding its use as a CTL specific marker in our technology. Li and Bethune et al. (2019) exploited the functions of trogocytosis to develop a TCR discovery technology whereby CTL "labelled" target cells are isolated and the cognate TCR ligand is sequenced.[245]

Another limitation of our proposed methodology is the inability to capture antigen specific cytotoxic synapse events throughout the duration of co-culture. Antigen recognition by CTLs is a transient and dynamic process that initiates target cell apoptosis in the process. Indeed, the nature of our methodology evaluates synapses formed at a singular moment of time and provides only a high level overview of this biological process, thus short-lived synapses occurring prior to fixation are not captured. A solution to this problem would involve a process by which target cells may be labelled following each antigen-specific interaction with cognate CTLs. In fact, Sharma et al. (2019) developed an elegant FRET based granzyme B (GZMB) reporter strategy to circumvent this issue and to capture all antigen recognition events. Essentially, target cells are engineered to express a GZMB-cleavable FRET reporter protein, in tandem with an epitope encoding minigene library. Upon recognition of cognate pMHC by antigen specific CTLs, GZMB within target cells initiates its protease functions including cleavage of the reporter protein causing a fluorescence emission shift visualized by flow cytometry.[246] Thus, all target cells recognized by CTLs throughout the duration of a co-culture may be tagged in this way and is not limited by the time of

detection. Furthermore, target cells in which the apoptotic pathways have initiated, can also be captured. The use of both trogocytosis associated markers and fluorescent markers for the discovery of CTL-target cell interactions are robust technologies with great potential and implications in the discovery of tumour antigens.

Ultimately, due to the reasons described above, we conclude that the identification of cytotoxic synapses by fixation and probing of extracellular markers using the presented methodology is insufficiently sensitive or specific to be useful for novel antigen discovery. Consequently, in Chapter 4 we used another strategy for the discovery of RMS antigens employing instead MHC-I pulldown and LC-MS/MS for the identification of MHC bound peptides.

3.5 Materials and Methods

3.5.1 Cell Culture

B16-F10-OVA cells were kindly gifted by Dr. Yonghong Wan (McMaster University). B16-OVA-GFP, B16-GFP and Pan02 cells were cultured in Roswell Park Memorial Institute (Hyclone) supplemented with 10% fetal bovine serum, 100 U/mL penicillin/streptomycin, 1M HEPES buffer, and 50ug/mL geneticin sulfate (G148 sulfate) (Gibco). Primary T cells were maintained in the same RPMI-1640 media and supplemented additionally with 50uM of β-mercaptoethanol. MC38, CT2A and COS-7 cells were maintained in DMEM supplemented with 2mM GlutaMAXCulture 1mM sodium pyruvate, 100 U/mL PS and 10% FBS. JawsII cells were maintained in Alpha-MEM supplemented with 4mM GlutaMAX, 1mM sodium pyruvate, 20% heat-inactivated FBS and 5ng/mL GM-CSF. All media and supplements were purchased from Gibco. Cells were maintained at 37°C and an atmosphere of 5% CO_2. All cells were tested by PCR and Hoecht's staining to ensure they are free of mycoplasmas contamination.

3.5.2 Mice

Six to eight week-old female C57BL/6J mice were obtained from Charles River Laboratories. OT-1 mice were acquired from the lab of Dr. Subash Sad (University of Ottawa). All animals were handled in strict accordance with good animal practice, and approved by appropriate committee in collaboration with the Office of Animal Ethics and Compliance.

3.5.3 Peptides

Peptides corresponding to the immunodominant epitope of ovalbumin (SIINFEKL) that binds to H-2Kb were synthesized by New England Peptide (Lot No. 3001-1/48-21) and have >95% purity.

3.5.4 Spleen Processing

Spleens from C57BL/6 and OT-1 mice were excised from sacrificed mice and filtered through a 100um plastic cell strainer (Fisherbrand ™ 352360, 22-363-549) for cell collection. Red blood cells were lysed using ACK lysis buffer and cell viability of the resulting leukocytes was determined using Trypan blue staining. Cells were then resuspended in R10 buffer at the appropriate dilution.

3.5.5 CTL isolation and activation

CD8+ T cells (CTLs) were isolated by negative selection using the EasySep™ Mouse CD8+ T cell Isolation Kit (Stemcell, Cat. 19853) following the manufacturer's protocol. The cell preparations contained >95% pure CTLs.

Activation with SIINFEKL peptide

$1x10^6$ purified CTLs were seeded into U-bottom 96 well plates in RPMI+10% media and stimulated with 10ug/mL SIINFEKL peptide for 24 hours. After 24 hours, cells were harvested and washed 2x in RPMI+10% then seeded into a new U-bottom 96 well plate at a concentration of $2x10^6$ cells in the presence of 20ng/mL recombinant murine IL-2 (Peprotech, Cat. 212-12) for 48 hours. After 48 hours, CTLs were harvested and counted for downstream use.

Activation with PMA/ionomycin

$5x10^5$ purified CTLs were seeded into U-bottom 96 well plates in RPMI+10% media and stimulated with an activation cocktail consisting of 1ug/mL PMA and 1ug/mL ionomycin for 5 hours. After 5 hours, the cells were collected and washed 2x in RPMI+10% then

seeded into a new U-bottom 96 well plate at a concentration of $1x10^6$ cells. To this, 15ng/mL of recombinant murine IL-7 (Peprotech, Cat. 217-17) and 15ng/mL of recombinant murine IL-15 (Peprotech, Cat. 210-15) was added for 96 hours after which CTLs were harvested and counted for downstream use.

Activation with αCD3, αCD28 and rmIL-2

$2x10^6$ cells were seeded onto a flat bottom 24-well plate that had been pre-coated overnight in a solution of PBS containing 2ug/mL or 5ug/mL hamster α-mouse CD3 (clone 145-2C11; BD Bioscience Cat. 550275), 2ug/mL hamster α-mouse CD28 (clone 37.51; BD Bioscience Cat. 553295) and 20ng/mL IL-2. Coated wells were washed 2x with PBS prior to the addition of cells. After 24, 48 or 72 hours, splenocytes were either harvested for flow staining or removed and diluted 1:2 in fresh media and seeded into a new flat bottom 24-well plate. In addition, 20ng/mL of recombinant mouse IL-2 was added to the media. T cell expansion was maintained by splitting cells in this fashion every 3 days for 7 days. On day 7 post stimulation and expansion, CTLs were again harvested, washed and maintained in media containing IL-7 and IL-15 for an addition 4 days. After 4 day, CTLs were used for downstream application.

3.5.6 CTL and target cell co-cultures

Target cells (either B16-OVA-GFP, B16-GFP, COS7, COS7-GFP) were harvested and plated onto flat bottom 96-well plates at the appropriate concentration in 100uL of R10%. The 96 well plates were pre-coated with 30-50uL of 20mg/mL polyhema and washed 2x with PBS prior to addition of cells. Previously activated and expanded CTLs were harvested and counted using Trypan blue staining by hemocytometer resuspended and 100uL added to target cells. The target to effector

ratio ranged from 1:1 up to 1:10. Golgi stop (Monensin, BD Bioscience, Cat. 554724) was added to the co-culture at a concentration of 0.5ng/mL as well as αCD107a-PE or αCD107a-AF647 antibody diluted 1:100. The co-cultures were incubated for the allotted time (upwards of 24 hours) in 37℃ and 5% CO_2 atmosphere.

3.5.7 Transduction

B16-OVA, COS7-Kb and COS7 were seeded into either 6-well plates or 10cm dishes 24 hours prior to infection with GFP expressing lentivirus (LV-GFP). When cells reached 40-60%, confluency, they were transduced with 200uL of LV-GFP in the presence of polybrene for 24 hours. After 24 hours, the culture medium was replaced with fresh media containing puromycin. Cells were cultured continuously in the presence of puromycin until a largely uniform population of GFP+ cells remained. Viable GFP+ cells were sorted using the Mo Flo AstriosEQ to obtain a single homogenous population then cultured for downstream use.

3.5.8 Immunoblotting

Cells were lysed on ice for 10 minutes in protein extraction buffer (50mM Hepes, 150mM NaCl, 10mM EDTA, 10mM Na4P2O7, 1% NP-40 pH 7.4) containing 1M NaF, 200mM Na_3VO_4 and protease inhibitor cocktail (Roche, Mississauga, Ontario, Canada). Lysates were centrifuged at 16,000xg for 10 minutes at 4℃. Protein concentrations were determined by Bradford assay (Protein Assay Solution, BioRad) and 20-50μg of protein extracts were prepared in NuPAGE 4X LDS sample buffer (Invitrogen) containing dithiothreitol (DTT). Lysates were separated by SDS-PAGE using 4-12% Bis-Tris precast gradient gels (Thermo Fisher Scientific) in the XCell SureLock Mini-cell system (Thermo Fisher Scientific), and then transferred onto nitrocellulose

membranes (GE Healthcare). Membranes were blocked with 5% bovine serum albumin (BSA) or 5% non-fat dry milk in 0.1% TBS-Tween-20 for 1 hour at room temperature and then incubated overnight at 4°C with rabbit anti-ovalbumin antibody (AB Science, Cat. ab181688). The membranes were then probed with horseradish-peroxidase conjugated anti-rabbit (1:2000, Jackson Immunoresearch Labs) secondary antibodies for 1 hour at RT. Bands were imaged using ClarityTM Western ECL blotting substrates (Bio-Rad) on HyBlotCL autoradiography films (Denville Scientific).

3.5.9 Peptide Pulsing

$5x10^6$ COS7-Kb-GFP or COS7-GFP cells were harvested and washed 2x with warm complete DMEM media. Cells were placed in 15mL falcon tubes in a volume of 5mL complete DMEM containing 10uM SIINFEKL peptide. The cells were incubated at 37°C for 45 minutes, ensuring mixing of the cells every 15 minutes. After 45 minutes, the cells were centrifuged, counted by hemocytomer and used for co-culture.

3.5.10 Construction of lentivirus plasmid

pLenti-PGK-V5-Luc plasmid was used to construct the pLenti-PGK-V5-OVA plasmid. In brief, the OVA gene was PCR amplified from pcDNA expressing aDEC205-OVA using the following primers, Forward: CCCTTGGATCCATGATGGGCTCCATCGGCGCAG and Reverse: TCACTACAGATCCTCTTAGATCTTTTCCC. PCR amplicon was digested by BamHI and NheI and cloned into the cognate digested site in pLenti-PGK-V5. Positive clones were screened by restriction digest mapping and verified by sequencing.

3.5.11 Flow Cytometry

Single cell suspension and doublet cells were processed in different ways prior to flow staining. Single cell suspensions were harvested and washed 2x with PBS. Cells were then stained with the FVS780 viability dye (BD Biosciences, Cat. 565388) in PBS for 15 min at room temperature. Following washes, cells were incubated with anti-CD16/32 in 0.5% BSA/PBS at 4°C to block nonspecific antibody (Ab) interaction with Fc receptors. Subsequently, αCD8-PE-CF594, αCD3-FITC, αCD69-BV650, αCD25-PE, αCD107a-AF647 antibodies were added to cells and incubated for 30 minutes (4°C). Conversely, samples containing co-culture were carefully removed from the incubator and up to 190uL of media was slowly removed and discarded from each well using a multichannel P200 pipette. To fix the cytotoxic synapse (i.e. doublets) 100uL of 1% paraformaldehyde (PFA) was dispensed slowly onto the sides of each well and incubated for 10 minutes at RT. Then, 100uL of 0.5% BSA/PBS (FACS buffer) was added to each sample, mixed and dispensed into 5ml FACS tubes for staining. Doublet samples were washed 2x in FACS buffer. Following washes, cells were incubated with anti-CD16/32 in FACS buffer at 4°C to block nonspecific antibody (Ab) interaction with Fc receptors. Subsequently, αCD8-PE-CF594 and either αCD107a-AF647 or αCD107a-PE antibodies were added to cells and incubated for 30 minutes (4°C). After staining, cells were washed with FACs buffer and fixed in 1% paraformaldehyde. Cells were acquired on BD flow cytometry (Fortessa) and analyses were performed using FlowJo software v9.

Chapter 4 - Identification of novel rhabdomyosarcoma antigens using proteomics and evaluation of prime-boost vaccination

4.1 Introduction

The immunopeptidome is the tabulated representation of all MHC I and II presented peptides. The categorization of these peptides is based on its structure, length, antigen processing machinery and corresponding T cell activity.[247] An array representing these peptides, which are presented in the context of disease and pathology, is a tremendous tool for the study of, and therapeutic interventions necessary for, autoimmunity, infectious disease and cancer. As such, effective and efficient technologies employing mass spectrometry for the detection and analysis of context specific peptide/antigen landscapes have made impressive progress since their conception in the 1990s by Donald Hunt.[248] A comprehensive analysis of proteins and peptides is achieved by proteomics approaches. The gold standard method of proteomics characterization is mass spectrometry (MS). Many MS methodologies exist such as electrospray ionization-MS (ESI-MS) or matrix-assisted laser desorption ionization (MALDI-MS) coupled with capillary liquid chromatography tandem MS (LC-MS/MS).[248,249,250] In order to detect MHC-associated antigens using MS-based approaches, it is often desirable to isolate MHC-loaded peptides. For example, MHC-antigen complexes can be immunoaffinity-purified (IP) and the peptides can be further isolated by acid elution. The heterogeneous mixture is further separated by several iterations of HPLC, facilitating the identification of unique peptides. Mass spectrum data (wherein MS is employed for a second time, also called MS/MS) is used to correlate and delineate sequence specific information. The peptide sequence data can be further deconvoluted/characterized by shotgun or targeted database searches from a reference proteome to identify peptide/protein sequences. While helpful to identify multiple potential MHC-presented antigens, one disadvantage

of this methodology is that the immunogenic potential of identified peptides must be verified by bioassays measuring the responsiveness of CTLs or CD4+ T cells to the peptides. This generally requires immunization with the putative antigens.[251]

Considerable progress in the field of MS and immunopeptidome screening methodologies have led to improved resolution, specificity, sensitivity, and advanced *in silico* database/search software.[252] As the identification of TSAs of murine origin is relatively simpler than in humans, due to less allelic diversity of murine MHC, this approach is instrumental in the identification of murine tumour antigens. Well-characterized, and widely used, MHC allotype specific antibodies are used for IP of the two major MHC I variants: H-2Kb (antibody Y3) and H-2Db (antibody B22.249) molecules from tissues of C57BL/6 mouse origin. The resulting MS/MS (MS2) spectral data from tissue can be searched against an existing protein database to identify spectral matches i.e. the extent to which a predicted peptide's mass matches the observed peptide mass in the output MS2 data. Typically, the prediction of peptide binding affinity to an MHC allotype is performed after the consolidation of matched peptide sequences to determine the extent to which identified peptides are likely to be immunogenic.[253] An approach by Gujar et al. (2017) limits the peptide database search to an *a priori* generated library of peptides predicted to effectively bind MHC-I by employing the NetMHC prediction software to an input of FASTA protein databases.[254] This targeted database search approach leads to a reduction in the false discovery rate (FDR) and improved peptide identification (almost 2 fold) compared to the traditional methods.[254]

Through a collaborative effort with the Gujar group, our team sought to identify novel MHC I epitopes from a pre-clinical model of RMS utilizing the 76-9 syngeneic tumour model. The goal was to employ discovered antigens in the aDEC205-ORV prime boost vaccine strategy discussed in chapter 2 to explore the applicability of active immunotherapies for RMS. We

proposed the use of LC-MS/MS and the targeted database approach (outlined by Gujar et al., 2017) to pulldown and verify MHC I associated peptides from 76-9 tumours and tumour bearing mouse spleens. We hypothesized that the murine RMS tumour ligandome, when compared to naïve tissue ligandome, would yield differentially expressed peptides/antigens with the potential to prime and activate tumour antigen-specific CTL responses. The immunogenicity of the differentially expressed 76-9 peptides would be further validated by *in vitro* functional activation of pre-existing CTLs collected following mouse immunization, by assessing IFN-γ induction (Figure 4-1). The results from this ligandome screen intended to serve two purposes: 1) corroborate antigen/peptide sequences from LC-MS/MS method with the antigens potentially discovered from the flow cytometry method outlined in chapter two and 2) provide an alternative means for antigen discovery if the flow cytometry method be deemed unsuccessful. In this final chapter the IP-MHC coupled with LC-MS/MS methodology was used to identify MHC I epitopes enriched in murine 76-9 RMS tumours (Figure 4-1). We further set out to validate the immunogenicity of the candidate antigens, and design and construct an aDEC205/ORV vaccine and investigate its therapeutic efficacy in a 76-9 bearing mouse model.

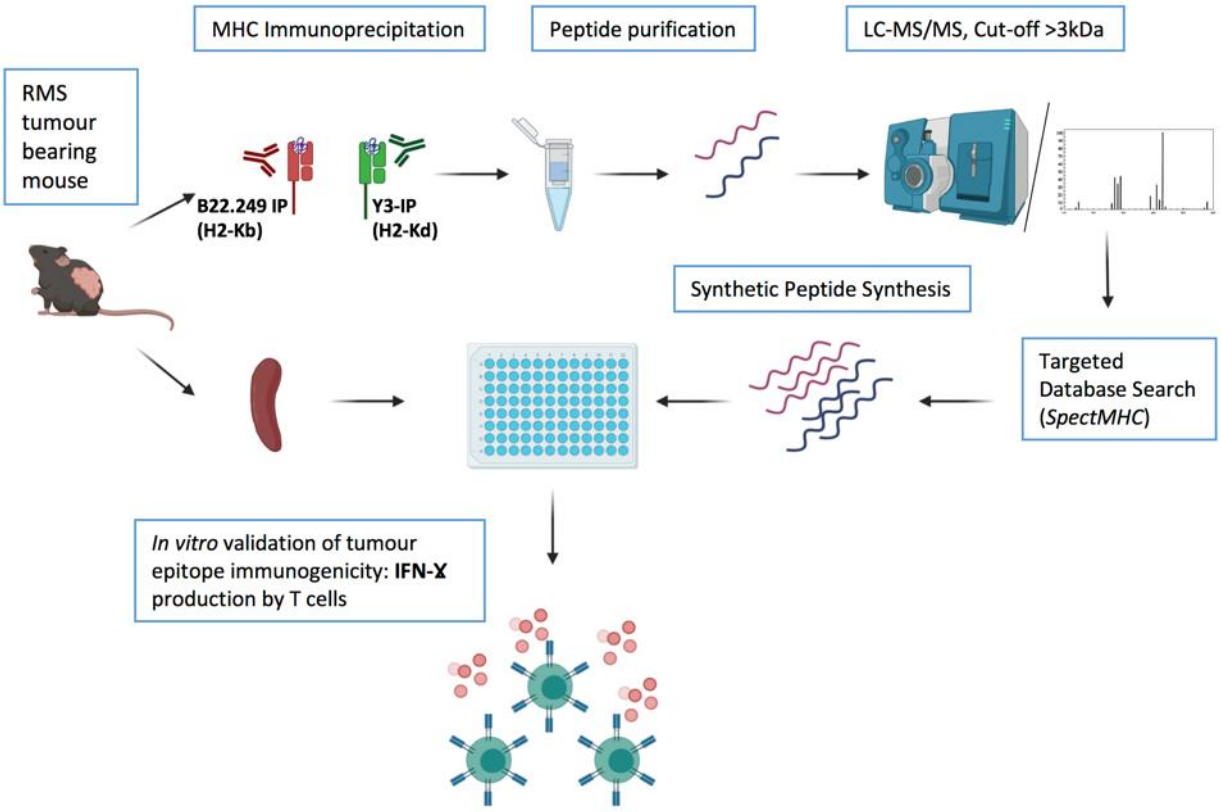
MHC Immunoprecipitation
Peptide purification
LC-MS/MS, Cut-off >3kDa
RMS tumour bearing mouse
B22.249 IP (H2-Kb)
Y3-IP (H2-Kd)
Synthetic Peptide Synthesis
Targeted Database Search (SpectMHC)
In vitro validation of tumour epitope immunogenicity: IFN-γ production by T cells

Figure 4-1. Schematic summary of peptide elution and characterization of MHC I presented murine RMS (76-9) ligands. Flash frozen tumour and spleen tissue is harvested from a 76-9 tumour-bearing mouse and lysed. H-2Kb and H-2Kd MHC molecules are precipitated using MHC allele specific antibodies B22.249 and Y3, respectively. Peptides are eluted, purified and characterized by mass spectrometry. The library of eluted peptides is subjected to a targeted *in silico* database search using SpectMHC software to identify and predict the most likely antigen candidates. The promising peptides are synthesized and validated for *in vitro* immunogenicity by stimulating T cells from immunized or tumour bearing 76-9 mouse with the peptides and assessed T cell functionality by way of IFN-ɣ production.

4.2 Results

4.2.1 MHC I ligand discovery using mass spectrometry and NetMHC targeted database search

To identify immunogenic tumour associated antigens in a murine model of RMS (76-9 derived implanted tumour), we immunoprecipitated peptides from MHC class I molecules (H-2Kd and H-2Kb allotypes), derived from the spleen and tumor of 76-9 bearing and naive C57BL/6. The eluted peptides were subject to LC/MS-MS to identify the amino acid sequence. The resulting MHC I ligands were then subjected to a targeted database search comprising of an *in silico* generated library of murine peptides from the FASTA database predicted to bind MHC I by NetMHC (Figure 4-1).[254] The primary pulldown from 76-9 tumour bearing mice resulted in the identification of 3056 peptides. When accounting for peptide sequences present in naïve spleen and eliminating common peptides between both groups, 107 MHC I-associated peptides were found to be uniquely present in the tumour and spleen of 76-9 tumour bearing mice (Table 2 and 3). A greater number of peptides were H-2Kb than H-2Db associated (Figure Appendix). Typical output MS data of peptides consists of the following key parameters: a peptide-spectral match score (PSM), binding affinity to the cognate MHC I allotype (expressed as a concentration in nM) and the % rank of that binding affinity (<0.5 rank is considered a strong binder and <2 is considered a weak or non-binder). PSM is an assigned scoring function to determine the matching quality between a theoretical peptide sequence and the MS/MS spectra; a higher PSM instills greater confidence in the peptide match.[255] The binding affinity, or the strength of peptide binding with MHC, is similar to the dissociation constant (Kd); a higher concentration in nM is indicative of weaker binding.[256] The binding affinity is further correlated with the % rank in that higher concentration.[257]

Table 2. The list of unique H-2Kb MHC I associated peptides identified in 76-9 tumours and their associated PSM #, MHC binding affinity (nM) and rank

Sequence	Master Uniprot Accession	# PSMs	H-2 Kb Rank	H-2-Kb nM
TAFVFPRL	Q8BK62	38	0.01	3.2
VNFPFLVKL	P05132	21	0.05	15.1
VMYRVIQV	E0CYP7	19	0.1	34.4
SSLLFVKL	F6WF94	18	0.015	5.6
VVFIFRVL	Q02738	17	0.01	5
VVFVFRVL	P28231	16	0.01	4.3
FNLVYENL	Q8R4V1	16	0.05	15.8
VILEYFTRL	Q9CR08	15	0.01	4.6
IIPMFSNL	G3UWL2	15	0.01	2.6
TNYKFFML	Q5Y5T1	14	0.01	2.9
SQYVFTEM	Q5SYH2	14	0.02	7.8
SILELFPKL	Q4ZGD9	14	0.175	58
SVLQFLGL	Q99JZ4	13	0.025	8.6
AIFAFRWV	Q64364	13	0.25	82.8
SIYDAFPKV	Q9QXZ0	12	0.15	48.5
ATYTFIQQL	Q9R0N0	11	0.02	7.6
HSYDFNQL	Q8JZY1	10	0.03	11
SIYEKLIQF	Q02614	10	0.25	89.8
VVYDLSIRGF	Q62348	10	1.3	641.5
VNVEFVRV	D3YVQ9	10	0.05	17.9
VAYLMQKL	Q9DBB1	10	0.03	9.4
ETPVYANL	P15066	10	0.125	42.8
ATFQFSNL	A2A8V7	9	0.01	2.5
TNPSFDGRL	Q6PA06	9	0.25	88.6
ATQQFQQL	P11370	9	0.2	67.6
SAMVFSAM	P63082	9	0.025	8.4
VNDIFERI	Q9D2U9	9	2	1171.7
SAMVFSAM	P63082	9	0.025	8.4
SILKFFEI	P34152	8	0.3	108
TIFNFIITV	Q5SYH2	8	0.2	68
VNYQFTQI	O08665	8	0.01	3.5
SNPEFSSV	P26039	8	0.15	44.6
VQYTFDLQL	H3BJJ4	8	0.06	21
ALLQYINL	A0A0G2	8	0.15	46.5
ASYRYTGV	P01633	8	0.01	3
VAIRFDSGL	Q9ERU3	7	0.03	9.5
VGIQHSLV	F6VR84	7	0.5	182.1
SSVKFNPV	Q6PAC3	7	0.04	12.2
VNYEFGIAL	Q8BHN7	7	0.025	8.2
ISFEFRSLL	G5E8J7	7	0.01	4.3
ASYEFTTL	Q9QXB9	7	0.01	2.6
SAPTFINF	A2ADH1	7	0.2	67.5
GSYQFSMV	Q03347	7	0.03	10.8
TSVVFNKL	Q791N7	7	0.05	16.7

VIFEMTNL	Q60751	7	0.015	5.9
INFDFNTI	Q8CDD8	7	0.06	19.8
VVYGGFSRL	Q7TPQ8	7	0.03	10.1
VMYRVIQV	E0CYP7	7	0.1	34.4
VALDFEQEM	P60710	7	0.25	87.5
VMYKFLTV	Q9WVC3	6	0.015	6.1
KNQGFGKL	F6RBL8	6	1.5	795.9
RNVRYVHI	Q8QZX5	6	0.4	116.5
TNYSFLQAV	Q91ZD1	6	0.03	9.4
SQYVFTEM	Q5SYH2	6	0.02	7.8
SVYQPAQL	B2RVL6	6	0.04	13.6
KNFTKKIQL	Q9JK92	6	0.5	172.6
SNFNFRQL	Q91WT7	6	0.01	3.5
TTYVTKEL	Q8WURO	6	1.2	572.6
QNYTYSSL	Q810S1	6	0.01	3.9
VLYVWAQL	Q99J56	6	0.015	6.4
VIQDFVKM	Q8BHG9	6	0.5	189.8
VVILFHFL	Q9D0Z3	6	0.025	9.4
SLVIFMQL	Q9R049	6	0.15	46.8
RAYEFAERC	Q68FD5	6	1.2	587.5
QQYSFINQM	D3YUV5	6	0.2	65.7
VALDFEQEM	P60710	6	0.25	87.5
SGFQAKTQM	Q8R2U2	5	2.5	1372.1
KVQEFQRL	Q62172	5	0.175	59.9
HTYVHATL	Q9EQJ0	5	0.05	15
TAVEFANHL	F6QAV8	5	0.15	47.1
SNYAFMQAL	Q07104	5	0.01	3.9
TNVDFPSL	Q9Z179	5	0.25	90.7
IMYNVTEL	Q3TIR1	5	0.06	21
RGVEFVHV	Q3TW96	5	0.6	247.2
ANVVFTQL	F8VQE9	5	0.04	13.4
TIIVFHSL	Q8C9D0	5	0.04	14.4
SILAMINNM	Q9D8X5	5	0.8	361.5
ESYSFEARM	Q9CQG3	5	0.06	18.5
ASNNDLASL	P61092	5	6	4275.8
TWLSSLPRL	Q5F2D4	5	0.6	234.2
ASLRFVFL	Q3TJY1	5	0.02	7.3
IDYSFPSL	Q91VE6	5	0.07	21.7
SNLQYSLL	Q9R1X5	5	0.015	5.7
SALIYSNL	O55013	5	0.01	3.4
TNYKFFML	Q5Y5T1	5	0.01	2.9
AICIFREL	A2AW05	5	0.4	158.9
AVCTFIHL	A2AC29	5	0.2	64.7

Table 3. The list of unique H-2Db MHC I associated peptides identified in 76-9 tumours and their associated PSM #, MHC binding affinity (nM) and rank

Sequence	Master Uniprot Accession	# PSMs	H-2 Db Rank	H-2-Db nM
SQPKNLDPA	A2AEB6	10	0.02	27.8
TAPVNIAVI	Q99JF5	9	0.01	4.6
STISNDVFI	Q80U12	7	0.01	7.7
AGHRNREVL	E9Q6T6	7	0.025	33.2
SAVTSQDLL	J3QPN1	6	0.06	88.9
VATVNKAGSEL	Q9QXZ0	6	0.6	2003.1
YAVGNHDFI	Q8BFV2	6	0.01	3.2
SQPKNLDPAL	A2AEB6	5	0.025	32.5
SGIHLTIEM	G5E829	5	0.6	2060.8
SVLKNRPLSVM	A0A0R4	5	0.6	1991.8
SATSNQDIL	O70494	5	0.015	19.1
SAGPSHVAAM	Q9EPU0	5	0.6	2005.9
RSVPNSRGDYM	P35569	5	0.125	216.7
TAATNTTIM	A0A067	5	0.015	25.6
KSLENILTL	Q8K2I9	5	0.01	11.4
TAATNTTIM	A0A067	5	0.015	25.6
SSPNNASEL	A0A0J9	5	0.01	15.4
SGIHLTIEM	G5E829	5	0.6	2060.8
ITPLNKDHI	Q99P88	5	0.1	180.4
SGPINFTVF	P97457	5	0.025	37.2

4.2.2. A prophylactic 76-9 infected cell vaccine leads to a delay in tumour progression

The next step was to determine the immunogenicity of the isolated 76-9 tumour peptides with anti-tumour CD8+ T cells. Firstly, it was imperative to determine if strong adaptive immune responses could be generated against the entire landscape of 76-9 antigens *in vivo.* To this end, a prime-boost prophylactic vaccine approach was employed using an infected cell vaccine (ICV). An ICV consists of vaccinating with irradiated and infected whole tumour cells, for example with an oncolytic rhabdovirus such as MG-1 or VSV. It has been previously shown that the ICV method, in some pre-clinical contexts, can mount long lasting CTL responses to a broad spectrum of cell specific antigens. Furthermore, a boosting dose of irradiated cells infected with an OV, which functions as a potent immune stimulator, leads to enhanced CTL responses, delays tumour growth and prolongs survival.[258,259] To determine whether an immune response can be established in the 76-9 model, the ICV preparation was first optimized. Irradiation and ICV preparation for 76-9 cells were found to be comparable to the previously optimized CT26-WT cell line as both 60gy and 90gy irradiation showed >90% cell viability and sufficient MG1-GFP infection indicated by GFP positivity (Appendix Figure 8). Following optimization, mice were given a prophylactic immunization consisting of a priming dose of irradiated 76-9 cells followed 7 days later with a boosting dose of 76-9 ICV cells infected with MG1-GFP OV. A further 7 days post boost, mice were challenged with a subcutaneous implant of 1E6 76-9 cells and followed for the development of tumours. Mice that received the prophylactic 76-9 ICV displayed a delay in tumour growth 40 days post implantation indicating the generation of an adaptive immune response to a potentially broad spectrum of 76-9 antigens (Figure 4-2).

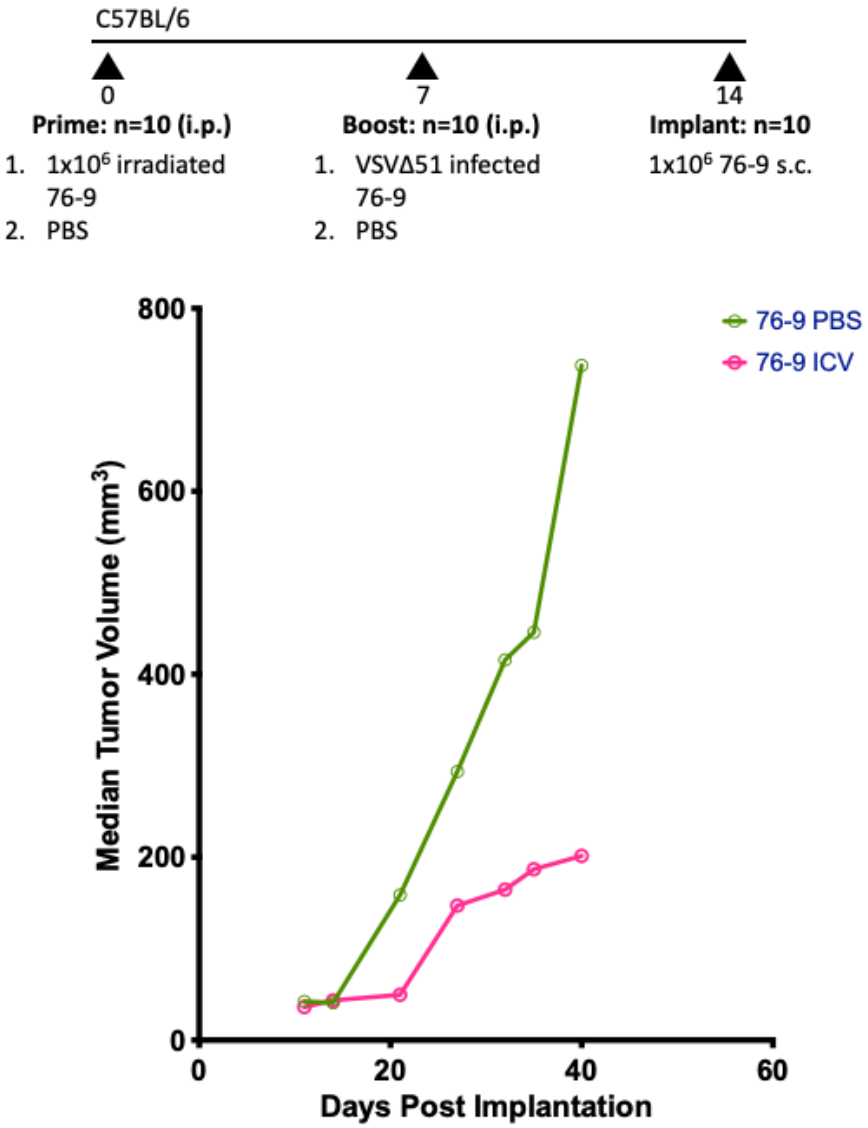
C57BL/6
0
7
14
Prime: n=10 (i.p.)
1. 1x10^6 irradiated 76-9
2. PBS
Boost: n=10 (i.p.)
1. VSVΔ51 infected 76-9
2. PBS
Implant: n=10
1x10^6 76-9 s.c.
76-9 PBS
76-9 ICV
Median Tumor Volume (mm^3)
800
600
400
200
0
0
20
40
60
Days Post Implantation

Figure 4-2. Delayed tumour progression, up to 40 days, of mice immunized with prophylactic 76-9 ICV prime boost vaccination. On day 0 Naïve C57BL/6 mice were administered i.p. priming doses of either irradiated 76-9 cells or PBS. Seven days post prime, animals were administered a boosting i.p. dose of either irradiated+VSVΔ51 infected 76-9 cells or PBS. A further 7 days post boost, all animals were implanted s.c. with $1x10^6$ 76-9 cells and monitored for tumour progression until day 40 at which time the first animal in the experiment reached endpoint (day 40).

4.3.3. In vitro stimulation of splenocytes from ICV immunized mice with the predicted peptide library leads to IFNγ production by lymphocytes

To assess the immunogenicity of the MHC I 76-9 specific ligandome, lymphocytes from 76-9 ICV immunized mice were stimulated *in vitro* with the peptide library. Briefly, splenocytes from 76-9 ICV immunized mice and naive mice were harvested on day 12 (5 days after administration of boosting dose) and stimulated *in vitro* with 10ug/mL of each peptide from the predicted MHC I ligand library. After 48 hours of stimulation with the peptides, IFN-γ production was assessed by cytokine ELISA. Of the 107 peptide stimulants, 24 peptides showed 2-fold or higher IFN-γ production in stimulated splenocytes compared to mock treated control (with DMSO alone); there were negligible concentrations of IFN-γ detected in naïve splenocytes (Appendix Figure 9). When comparing fold-change as a function of PSM, a majority of the 24 peptides were within a scoring range of 5-10. Peptide 58 had the highest PSM score of 38 but only induced a 1.7 fold change of IFN-γ compared to mock and was not deemed to be a potential candidate (Figure 4-3). Fold change was also assessed as a function of peptide binding affinity to H-2Kb and H-2Db. There was no clear pattern of binding affinity as a function of fold change and the top 24 hits were heterogeneous in their distribution (Figure 4-4). Following unblinding, the peptide sequence and its parent protein were identified.

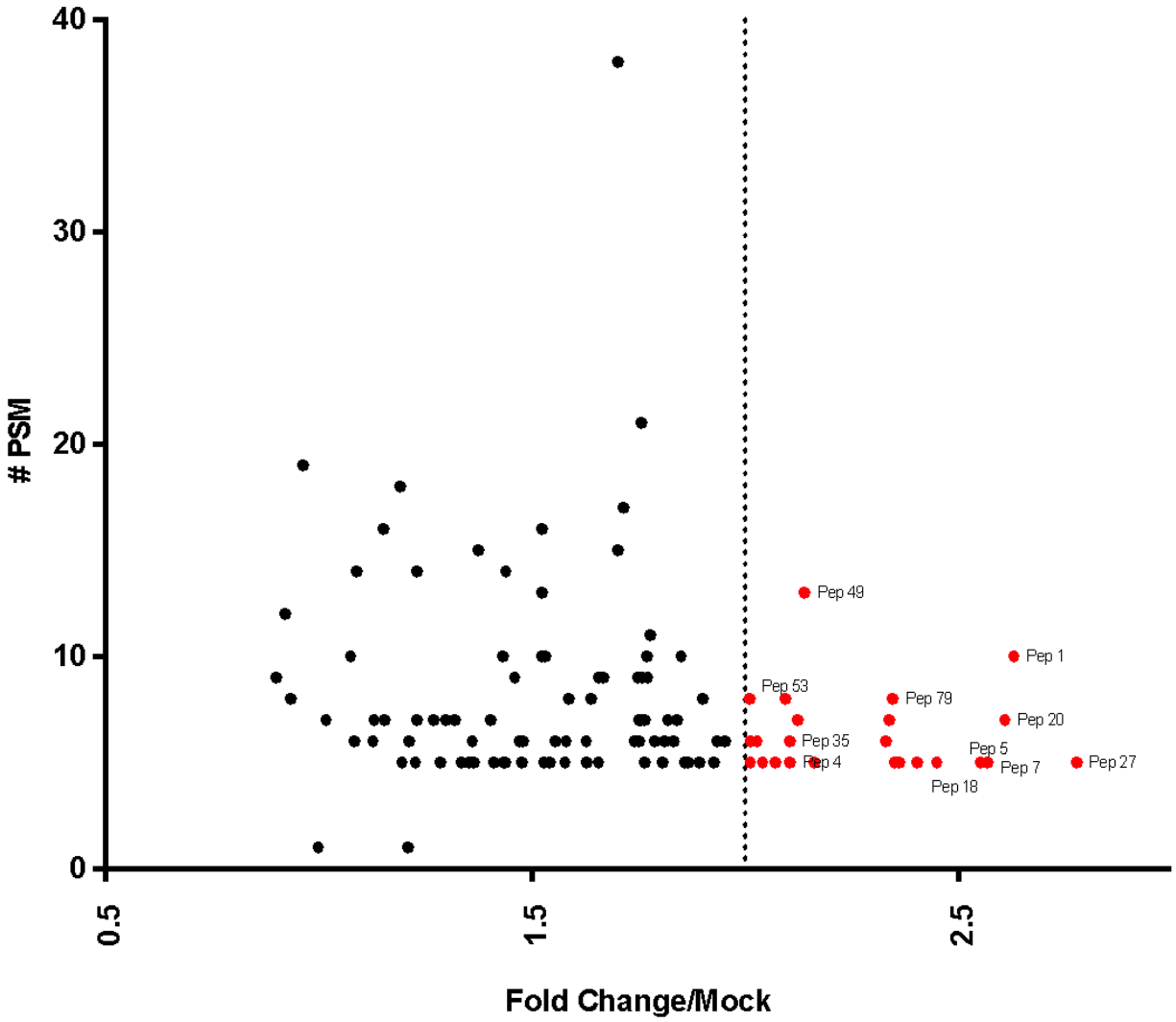
40
30
20
10
0
PSM
0.5
1.5
2.5
Fold Change/Mock
Pep 49
Pep 1
Pep 53
Pep 79
Pep 20
Pep 35
Pep 5
Pep 4
Pep 7
Pep 27
Pep 18

Figure 4-3. ELISA for IFNγ production by splenocytes following *ex vivo* stimulation with 76-9 peptides compared to #PSM of each peptide. Graph depicts a volcano plot of IFN-**γ** fold change/mock vs. # PSM (peptide-spectral match score) of all 107 peptides, an average of biological duplicates. Red dots depict the top 24 hits and black dots depict all other peptides.

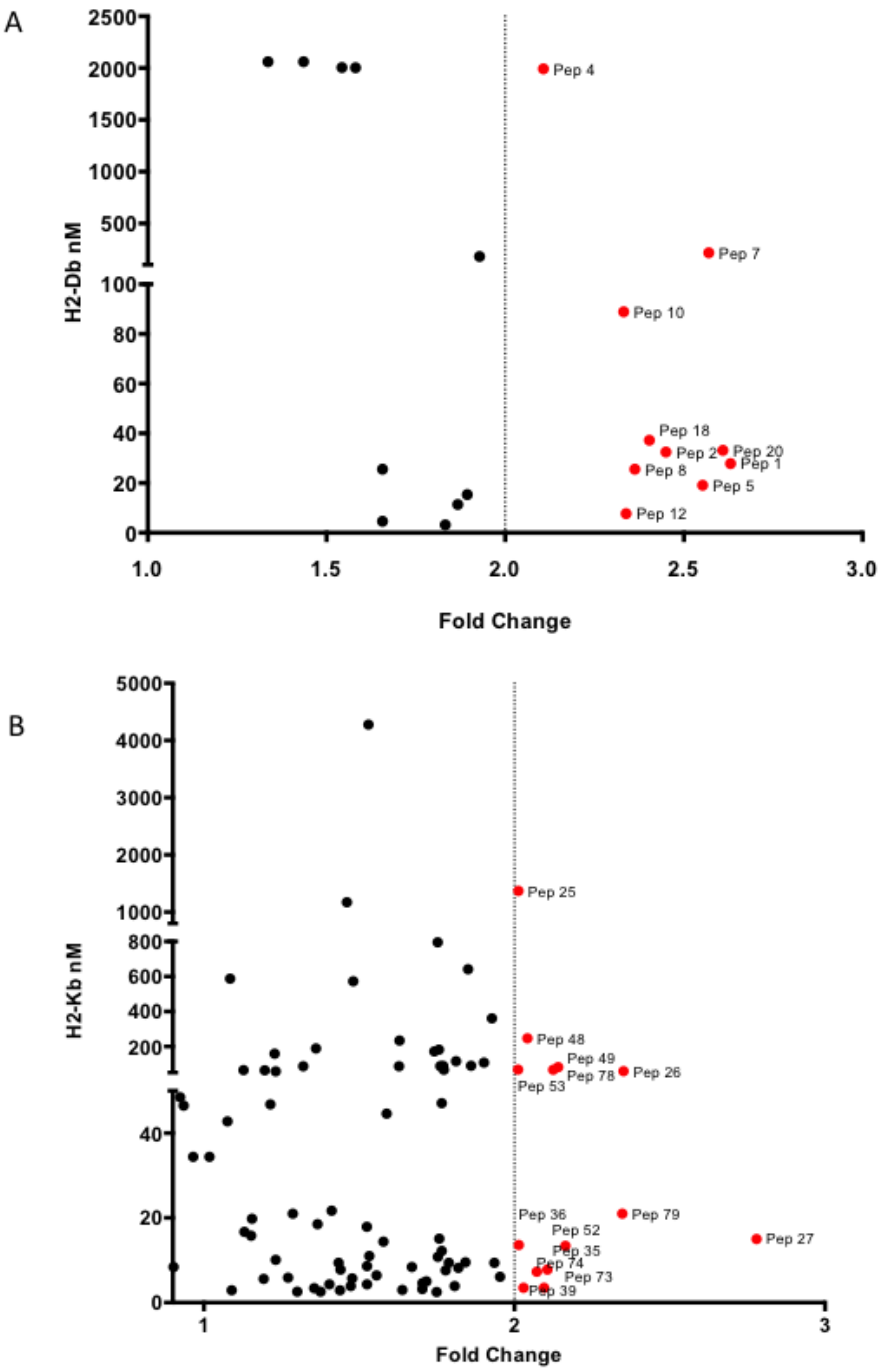
A
H2-Db nM
2500
2000
1500
1000
500
100
80
60
40
20
0
Pep 4
Pep 7
Pep 10
Pep 18
Pep 2
Pep 20
Pep 1
Pep 8
Pep 5
Pep 12
1.0
1.5
2.0
2.5
3.0
Fold Change
B
H2-Kb nM
5000
4000
3000
2000
1000
800
600
400
200
40
20
0
Pep 25
Pep 48
Pep 49
Pep 78
Pep 26
Pep 53
Pep 36
Pep 79
Pep 52
Pep 27
Pep 35
Pep 74
Pep 73
Pep 39
1
2
3
Fold Change

Figure 4-4. ELISA for IFNγ production by splenocytes following *ex vivo* stimulation with 76-9 peptides compared to peptide binding affinity for the 24 hits identified. Graph depicts a volcano plot of IFN-γ/mock fold change vs. **A.** H-2Db nM binding affinity and **B.** H-2Kb nM binding affinity, an average of biological duplicates. Red dots depict the top 24 hits and black dots depict all other peptides.

4.3.4. Selected peptide hits originate from a variety of proteins and cellular pathways

The *ex vivo* splenocyte stimulation screen was conducted in a blinded fashion. Thus, the peptide sequence and parent protein identity was revealed after ascertaining the hits that generate an adequate CTL cytokine response. Unblinding revealed that the 24 chosen peptides originated from a variety of genes coding for proteins belonging to various cellular pathways (Table 3). 10 peptide candidates were chosen for evaluation in the prime-boost vaccine, based on IFN-γ induction capacity, implications in other cancers, and MHC binding affinity. Of note, two peptide sequences, peptides 1, 2 and peptides 53, 35, were identified from each of the respective proteins, mortality factor 4-like protein 2 (*Morf4I2*) and transmembrane protein 199 (*Tmem199*), which I hypothesize indicates a high likelihood of these proteins to be antigenic and be presented by 76-9 tumours. The peptides 1 and 2, originating from the mortality factor 4-like protein 2, were identical in sequence barring the presence of leucine on the C-terminus of peptide 2. However, peptide 1 showed a lower nM binding affinity to H-2Db than peptide 2 (27.8nM vs. 32.5nM). Thus, peptides 1, 35, and 53 were selected for the vaccine study. Furthermore, the overexpression of genes *Tpcn1, Irs1, Tdrd3, Tdg and Sp3* have been associated with other cancer subtypes such as breast, colorectal, lung, prostate and melanoma, thus meeting our inclusion criteria for the vaccine study of the peptides originating from these genes (Table 3).[260–264] Finally, peptides 18 and 49 displayed higher of IFN-γ and PSM score, respectively, and were selected as the final 2 peptides for a total of 10 to be encoded into the aDEC205 and VSVΔ51 vectors.

Table 4. Detailed information of the 24 peptide candidates including: gene, protein identity and associated biological process

Peptide #	Gene	Peptide	Protein	Biological Process (GO)
Pep 27	Tpcn1	HTYVHATL	Two pore calcium channel protein 1	Ion transport, cation transport
Pep 1	Morf4l2	SQPKNLDPA	Mortality factor 4-like protein 2	Histone H2A acetylation, Histone acetylation, regulation of growth
Pep 20	Tdrd3	AGHRNREVL	Tudor domain containing protein 3	
Pep 7	Irs1	RSVPNSRGDYM	Insulin receptor substrate 1	Regulation of glucose import, cellular response to peptide hormone stimulus
Pep 5	Sp3	SATSNQDIL	Transcription factor Sp3	Regulation of RNA metabolic process
Pep 2	Morf4l2	SQPKNLDPAL	Mortality factor 4-like protein 2	
Pep 18	Mylpf	SGPINFTVF	Myosin regulatory light chain 2	Muscle system process, muscle contraction, muscle development
Pep 8	aadA2	TAATNTTIM	Streptomycin 3"-adenylyltransferance	No information
Pep 26	Ralbp1	KVQEFQRL	RaIA-binding protein 1	Small GTPase mediated signal transduction, Ras protein signal transduction, cytoskeleton organization
Pep 79	Tdg	VQYTFDLQL	G/T mismatch-specific thymine DNA glycosylase	DNA methylation, DNA metabolic process
Pep 12	Sgsm2	STISNDVFI	Small G protein signaling modulator 2	Regulation of vesicle fusion, activation of GTPase activity, protein transport
Pep 10	Dlgap5	SAVTSQDLL	Disks large-associated protein 5	Cell division, cell cycle, mitotic cell cycle process. May play role in carcinogenesis of cancer cells
Pep 52	Agap3	ANVVFTQL	Arf-GAP with GTPase, ANK repeat and PH domain-containing protein 2	GTPase activator activity

Peptide #	Gene	Peptide	Protein	Biological Process (GO)
Pep 49	Cdkn2a	AIFAFRWV	Tumor suppressor ARF	Negative regulation of cell cycle, regulation of mitotic cell cycle. Acts as a tumor suppressor
Pep 78	Magt1	SAPTFINF	Magnesium transporter protein 1	Protein N-linked glycosylation, glycoprotein metabolic process
Pep 4	Cytb	SVLKNRPLSVM	Cytochrome b	Electron transport chain, mitochondrial ATP synthesis coupled electron transport, ATP metabolic process
Pep 35	Tmem 199	SQYVFTEM	Transmembrane protein 199	Vacuolar acidification, AT hydrolysis coupled ion transmembrane transport
Pep 73	Sema3a	VNYQFTQI	Semaphorin-3A	Regulation of axon extension, regulation of neuron projection development
Pep 74	Mcrs1	ASLRFVFL	Microspherule protein 1	Histone H4-K16 acetylation, histone H4-K8 acetylation, Histone H4-K5 acetylation
Pep 48	Uap1l1	RGVEFVHV	UDP-N-acetylhexosamine pyrophosphorylase-like protein 1	Amino sugar biosynthetic process,
Pep 39	Akr1c14	SNFNFRQL	3-alpha-hydroxysteroid dehydrogenase type 1	Cellular hormone metabolic process, lipid metabolic process
Pep 36	Zcchc24	SVYQPAQL	Zinc finger CCHC domain-containing protein 24	No information
Pep 25	Nepro	SGFQAKTQM	Nucleolus and neural progenitor protein	tRNA-5’ leader removal, may play role in cortex development as part of Notch signaling pathway
Pep 53	Tmem 199	TIFNFIITV	Transmembrane protein 199	

4.3.5 Evaluation of the biological relevancy of syngeneic 76-9 tumours

Several studies have reported on the transcriptional and genetic landscape of clinical and pre-clinical RMS with the general consensus that PAX3-FOXO1 and PAX7-FOXO1 fusion proteins are oncogenic drivers that uniquely target downstream proteins.[265–267]The immunological landscape however is much less, if at all, characterized for pre-clinical RMS models. To perform a comprehensive study of our novel cancer vaccine, it was relevant to examine the immunological context of the vaccine of choice to determine dosing, vaccine regimen, and if the therapy may benefit with the addition of immune checkpoint inhibitors (ICI). Thus, an immune profiling experiment was undertaken to determine the immune cell populations that traffic into the 76-9 TME overtime. The percentage of polarized CD4+Th1 cells, Tregs, CD8+ T cells, NK cells, DCs, B cells and macrophages in the 76-9 TME were evaluated at various time points of tumour growth. With increasing 76-9 tumour volume, the trafficking of polarized CD4+ Th1 cells, B cells and macrophages did not change. However, we observed a trend of significantly increasing infiltration of Tregs, CD8+ T cells and DCs into the TME with increasing tumour growth. The infiltration of NK cells significantly decreased with increasing tumour growth (Figure 4-5A). The expression of PD-L1 was also evaluated on the surface of tumour cells at tumour volumes $100mm^3$ and $500mm^3$. PD-L1 expression was significantly upregulated in larger tumours as compared to small tumours (Figure 4-5B). These trends highlight a number of key considerations for the study of future therapeutics in the 76-9 pre-clinical model, including our aDEC205/ORV prime-boost strategy. Notably this suggests that checkpoint inhibitors, namely aCTLA-4 and aPD-L1 may be promising additions to our strategy to counteract the activity of increased Tregs infiltration and upregulated PD-L1 expression on 76-9 tumours.[268,269] Finally, as the principal complication of high grade RMS is the development of pulmonary metastasis,[270] we assessed whether a mouse model of lung

metastasis that could be explored as another pre-clinical model, in addition or alternatively to subcutaneous implantation. To establish a lung metastasis model, naïve C57BL/6 mice were given i.v. injections, through tail vein, of $2.5x10^5$ or $5x10^5$ single-cell 76-9 suspensions on day 0. On days 12, 19 and 26, lungs from mice were extracted and assessed for the presence of metastasis. Indeed, the injection of $5x10^5$ 76-9 cells led to the establishment of a greater number of pulmonary metastases as compared to $2.5x10^5$ cells. Furthermore, there were a significantly greater number of pulmonary metastases found in mouse lungs on day 26 as compared to day 12 in mice implanted with $5x10^5$ tumour cells (Figure 4-5C). At day 26, the mice had detectable metastases but did not yet show signs of distress or breathing difficulty and this timepoint was used as the upper limit of treatment administration for this model. We considered that a reduction in the number, and size, of pulmonary lesions in the 76-9 model would be a good indicator of the effectiveness of the proposed immunotherapeutic regiment utilizing aDEC205/ORV encoding 76-9 antigens. .

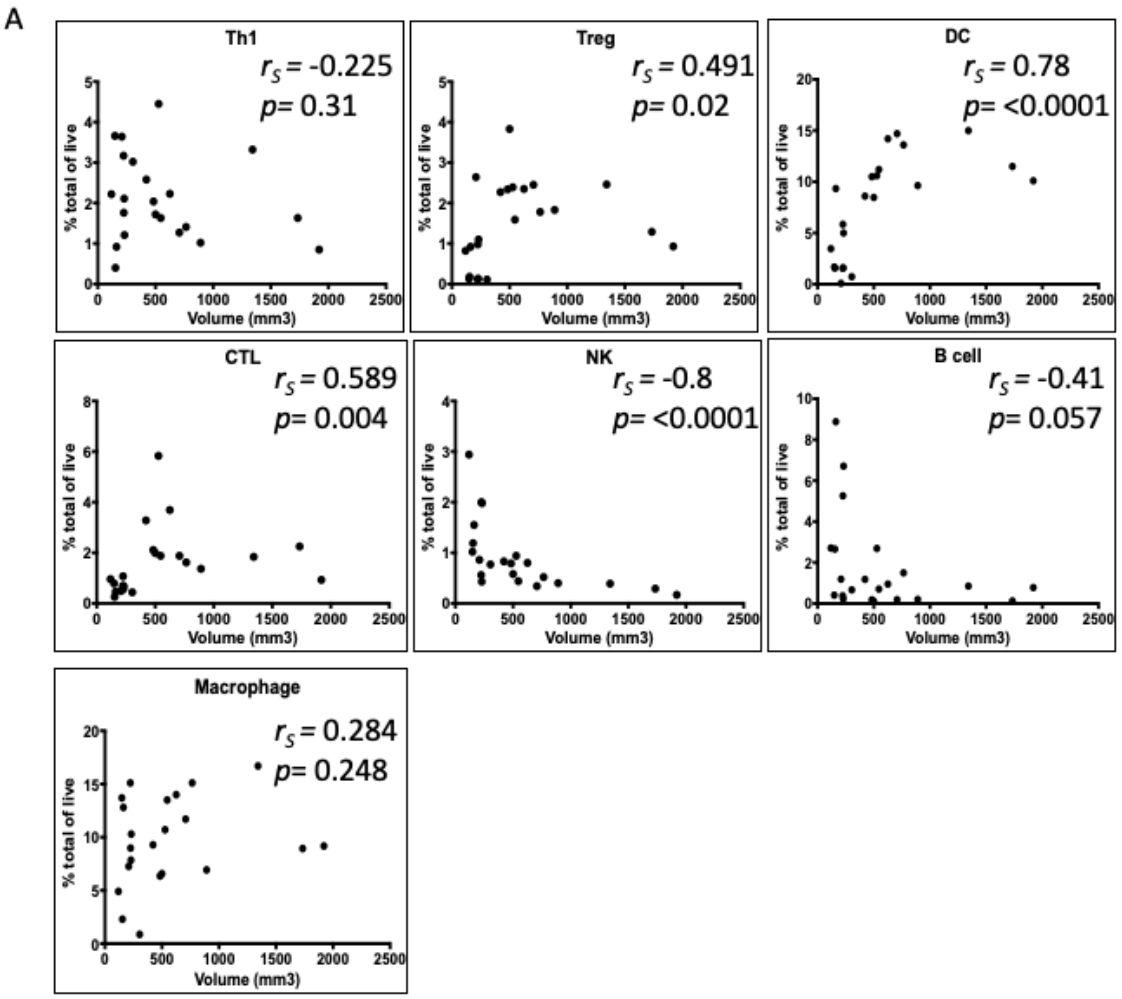
A
Th1
r_S = -0.225
p= 0.31
Treg
r_S = 0.491
p= 0.02
DC
r_S = 0.78
p= <0.0001
CTL
r_S = 0.589
p= 0.004
NK
r_S = -0.8
p= <0.0001
B cell
r_S = -0.41
p= 0.057
Macrophage
r_S = 0.284
p= 0.248
% total of live
Volume (mm3)
B
CD45-PDL1+
MFI
****
100
500
C
Number of Mets
2.5E5
5E5
*
Day 12
Day 19
Day 26

Figure 4-5. Immune profiling of tumour infiltrating lymphocytes and DCs, NK cells, and macrophages and PD-L1 expression of subcutaneously implanted 76-9 tumours. Pulmonary lesions are detected following 76-9 implantation through tail vein. A. Correlation between tumour growth over time and % of CD4+, Treg, CD8+ T cells (CTL), NK, dendritic cells (DC), B cells, and macrophages in all live, CD45+ infiltrating cells. Spearman-correlation coefficient. **B.** Median-fluorescence intensity (MFI) of PDL1 expressed on CD45- tumour cells, n=5. Bars show the mean ± SEM of 5 biological replicates; ****$p<0.0001$, two-tailed, unpaired, student's t-test. **C.** Naïve C57BL/6 mice were injected through tail vein with $2.5x10^5$ or $5x10^5$ 76-9 tumour cells and sacrificed on days 12, 19 and 26 to detect the presence of pulmonary metastasis (mets) by India ink staining, n=3 per time point. Bars show mean ± SEM of biological triplicates; *$p<0.05$; comparing day 26 to day 12; two-way ANOVA.

4.3.6 Design, construction and production of a therapeutic aDEC205 antibody fused to a synthetic polypeptide of tandem 76-9 epitopes

A synthetic polypeptide was designed to include the 10 peptides/epitopes selected from the screen described in section 4.2.1 with its respective codon optimized sequences depicted in Table 5. The aDEC205 fusion antibody will herein be termed aDEC205-769. A pcDNA expression vector encoding aDEC205-769 was designed to include the CH1, CH2, hinge and CH3 regions of the aDEC205 heavy chain and bound to the 76-9 polypeptide by an antibody linker (Figure 4-6A). Each peptide is connected with a glycine-proline (GPGPG) linker known to facilitate immune cell processing and used in the design and construction of polypeptide vaccines for infectious disease (sequence found in Appendix III).[271–273] The recombinant aDEC205-769 was produced by transient transfection in 293T cells and purification by Protein G resin affinity and column purification.[274] Eluted antibodies were characterized by immunoblotting for the recombinant heavy chain and kappa light chain. The expected protein size of the aDEC205-769 heavy chain is 70kDa which accounts for the 50kDa heavy chain plus an approximately 10-20kDa of the polypeptide containing 450 base pairs. Figure 4-7B shows that the heavy and light chains of the purified recombinant antibodies had the expected size for both the fused aDEC205-769 (~70kDa and 25kDa, respectively) and the control antibody aDEC205-empty (50kDa and 25kDa, respectively). Furthermore, the capacity of recombinant aDEC205-769 and aDEC205-OVA antibodies to bind to the DEC205 receptor on JawsII dendritic cells was assessed using a standard binding assay and probed for mouse IgG1. Incubation of JawsII cells with 5ug of both recombinant antibodies showed similar binding capacity (Figure 4-7C).

A small pilot experiment was conducted with the purified aDEC205-769 to assess the prophylactic response to a homologous prime-boost immunization. Naïve C57BL/6 mice were

immunized on day 0 and day 14 with 5ug aDEC205-769, 1ug of aDEC205-769 or PBS. On day 19, mice were implanted subcutaneously with 76-9 tumour cells and the tumour volume was monitored (Figure 4-6D). The administration of two doses of 5ug or 1ug of aDEC205-769 delayed tumour progression compared to PBS. Interestingly, the lower dose vaccine showed a significant delay in tumour progression whereas the 5ug dose did not (Figure 4-6D). This pilot study warranted further *in vivo* exploration to assess various dosing regimens and additional groups. This required the production of more aDEC205-769 and aDEC205-empty antibodies.

Table 5. Selected immunogenic peptides from initial peptide library. Summary of the 10 predicted immunogenic peptides from 76-9 tumours depicting gene identity, amino acid sequence and DNA sequence

Peptide #	Gene	Peptide amino acid sequence	DNA sequence
27	*Tpcn1*	HTYVHATL	CATACCTACGTTCATGCCACCCTG
1	*Morf4l2*	SQPKNLDPA	AGCCAACCCAAGAATCTCGACCCCGCG
7	*Irs1*	RSVPNSRGDYM	CGCTCAGTACCCAACTCTAGGGGCGACTATATG
20	*Tdrd3*	AGHRNREVL	GCGGGGCATCGAAACCGAGAGGTGCTG
5	*Sp3*	SATSNQDIL	AGCGCTACCAGTAACCAGGATATACTG
35	*Tmem199*	SQYVFTEM	AGCCAATACGTTTTCACCGAAATG
53	*Tmem199*	TIFNFIITV	ACCATCTTCAACTTTATAATCACCGTG
79	*Tdg*	VQYTFDLQL	GTGCAATATACTTTCGATCTTCAACTG
18	*Mylpf*	SGPINFTVF	AGCGGTCCAATCAATTTTACTGTGTTT
49	*Cdkn2a*	AIFAFRWV	GCGATCTTCGCCTTCCGCTGGGTG

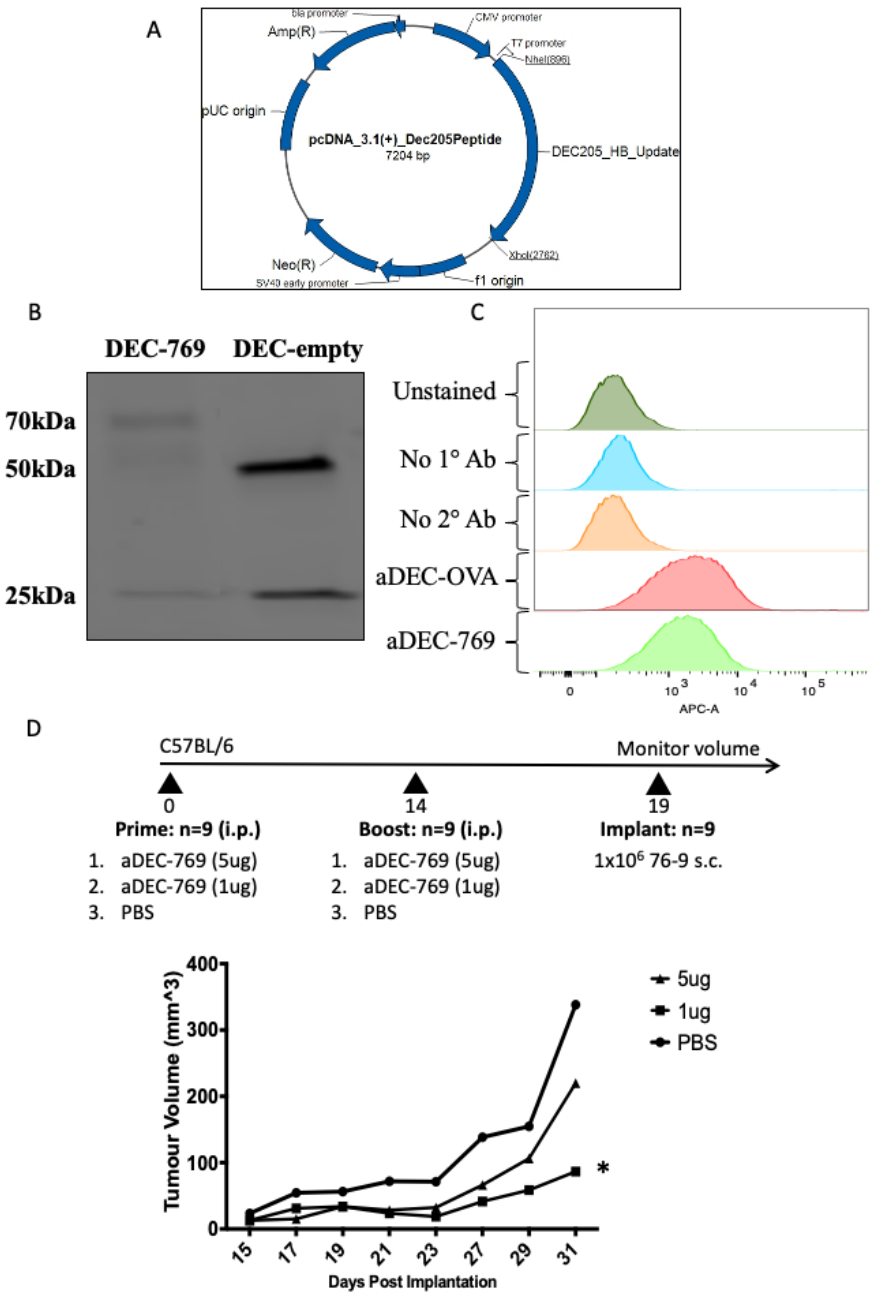
A
bla promoter
Amp(R)
CMV promoter
T7 promoter
NheI(896)
pUC origin
pcDNA_3.1(+)_Dec205Peptide
7204 bp
DEC205_HB_Update
XbaI(2782)
Neo(R)
SV40 early promoter
f1 origin
B
DEC-769
DEC-empty
70kDa
50kDa
25kDa
C
Unstained
No 1° Ab
No 2° Ab
aDEC-OVA
aDEC-769
APC-A
D
C57BL/6
Monitor volume
0
14
19
Prime: n=9 (i.p.)
1. aDEC-769 (5ug)
2. aDEC-769 (1ug)
3. PBS
Boost: n=9 (i.p.)
1. aDEC-769 (5ug)
2. aDEC-769 (1ug)
3. PBS
Implant: n=9
1x10^6 76-9 s.c.
Tumour Volume (mm^3)
Days Post Implantation
5ug
1ug
PBS
*

Figure 4-6. Design, production and characterization of aDEC205-769. A. pcDNA3.1+ vector map containing full length aDEC205-769 sequence flanked by NheI and XhoI restriction digestion sites. **B.** The final antibody product was reduced by β-mercaptoethanol and verified by immunoblotting for the heavy and light chains. aDEC205-empty shows a heavy chain at 50kDa and a light chain at 25kDa. aDEC205-769 shows the heavy chain linked with the 76-9 polypeptide at 70kDa; and a light chain at 25kDa. **C.** A binding assay was performed to verify effective binding of 5ug of aDEC205-769 to the DEC205 receptor on JawsII cells, compared to the binding capacity of aDEC205-OVA. aDEC205 was probed with an anti-IgG1-APC antibody and detected by flow cytometry. **D.** *Top,* Schematic representation of the immunization schedule. *Bottom,* Tumour volume was monitored for 30 days post implant. Data is expressed as mean volume of n=3 mice/group; *$p<0.05$ comparing 1ug to PBS; two-way ANOVA.

4.3.7 The production of aDEC205 fusion antibodies is inefficient, variable and a limitation in our study

A recurring and persistent problem with our in-house antibody production was low, and often, variable yield. aDEC205 antibodies are produced by transient transfection of 293T cells and collecting output from supernatant, which would contain the full length fusion antibody, for downstream protein G Sepharose bead column purification. Although this method is sufficient for the production of aDEC205-OVA, it was inefficient for aDEC205-769. To determine why this may be the case, and to optimize the methodology, various steps of production were evaluated. A quantitative RT-PCR was performed to quantify the degree of plasmid translation, by amplifying the OVA and 76-9 polypeptide regions, following transfection of 293T with pcDNA-aDEC-OVA and pcDNA-aDEC-769. Twenty-four and 48 hours after transfection, there were no significant differences in the amplification of either OVA or 76-9 polypeptide (figure 4-7A). Western blot for folded full length aDEC205 antibody revealed no discernable differences of protein production and folding between cells transfected with aDEC-OVA, aDEC-empty and aDEC-769 after 24 and 48 hours. However, protein content in the supernatant showed an absence of the aDEC205-769 heavy chain, the segment fused to the 76-9 polypeptide, after 24 and 48 hours whereas aDEC205-OVA and aDEC205-empty heavy chain and light chains were effectively secreted (Figure 4-7B). Indeed, immunofluorescence staining and imaging revealed that the aDEC205-769 antibody is retained in vesicles and forms large protein aggregates, an effect that is less pronounced in aDEC205-OVA, indicating that aDEC205-769 may be misfolded and unable to be secreted into the supernatant (Figure 4-7C). As a result, antibody production scale-up was ultimately outsourced to Proteogenix who have an optimized platform allowing for the effective production of a variety of recombinant antibody products. While generating sufficient antibody for our studies, it should

be noted that productivity using the Proteogenix platform was nevertheless much less efficient for aDEC205-769 as compared to aDEC205-OVA, altogether suggesting that the fusion antigen can significantly affect yield.

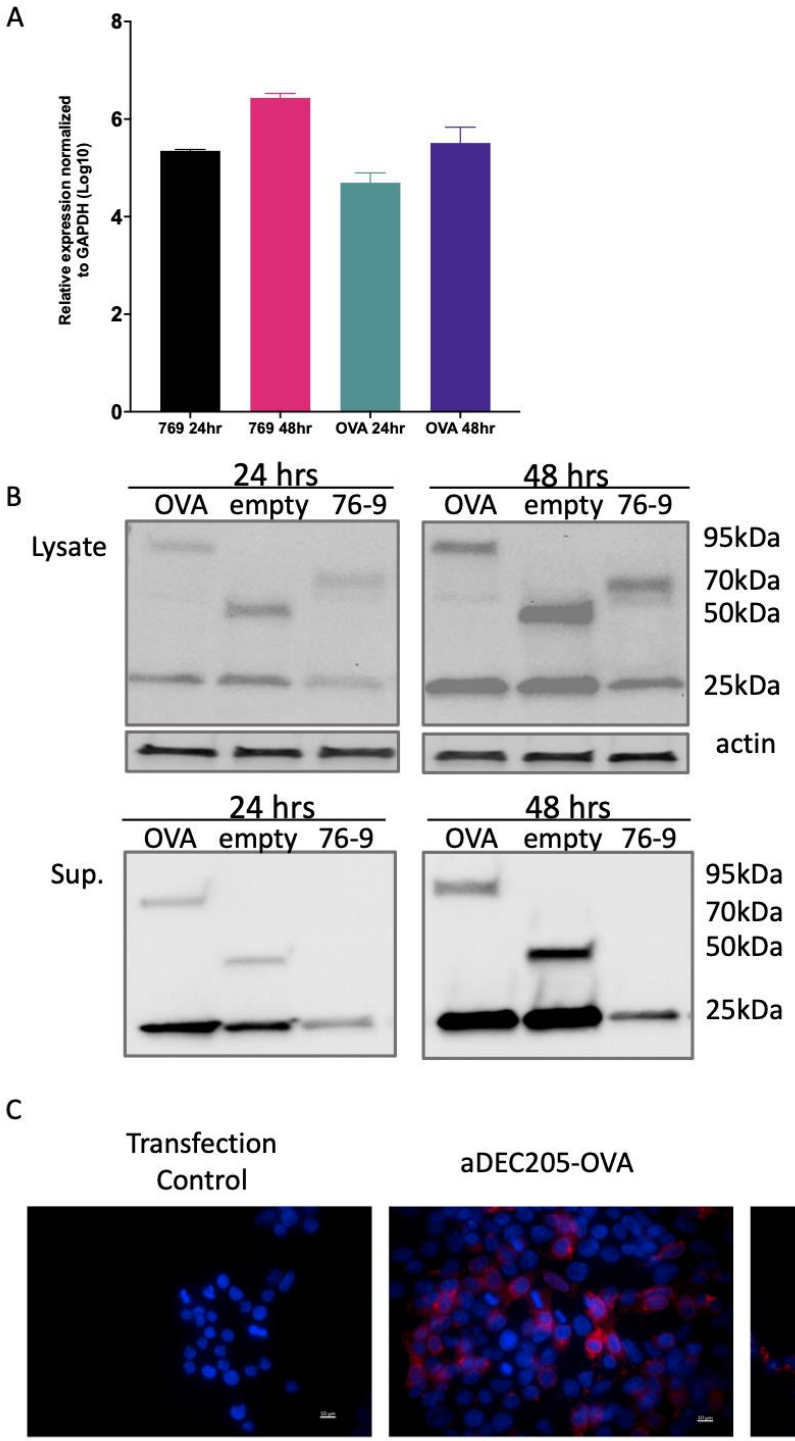
A
Relative expression normalized to GAPDH (Log10)
8
6
4
2
0
769 24hr
769 48hr
OVA 24hr
OVA 48hr
B
24 hrs
48 hrs
OVA empty 76-9
OVA empty 76-9
Lysate
95kDa
70kDa
50kDa
25kDa
actin
24 hrs
48 hrs
OVA empty 76-9
OVA empty 76-9
Sup.
95kDa
70kDa
50kDa
25kDa
C
Transfection Control
aDEC205-OVA
aDEC205-76-9

Figure 4-7. Amplification of fusion antigens at 24 and 48 hours is similar in 293T cells transfected with pcDNA-aDEC205-OVA and pcDNA-aDEC205-769 but the latter antibody shows intracellular protein aggregates and no extracellular secretion. A. Relative gene expression of *OVA* and *76-9 polypeptide* from transfected 293T cells, normalized to GAPDH. Bars show mean±SEM of 3 biological replicates. **B.** Cell lysate and supernatant from transfected cells was reduced by β-mercaptoethanol and probed for the heavy and light chains. aDEC205-empty shows a heavy chain at 50kDa and a light chain at 25kDa. aDEC205-OVA shows the heavy chain linked with OVA at 95kDa; and a light chain at 25kDa. aDEC205-769 shows the heavy chain linked with the 76-9 polypeptide at 70kDa; and a light chain at 25kDa. **C.** 293T cells were seeded on coverslips and transfected with 0.5ug of pcDNA-aDEC205-OVA and pcDNA-aDEC205-769 for 48 hours then cells were fixed with 2% PFA, permeabilized and labelled with anti-IgG secondary antibody (red) and Hoechst counterstain for nuclei (blue); white arrows depict protein aggregates.

4.3.8 Generation of an oncolytic VSVΔ51 expressing the 76-9 synthetic polypeptide

The recombinant ORV VSVΔ51 was engineered to express the 76-9 tandem repeat peptides (polypeptide) between the *G* and *L* genes flanked by XhoI and NheI restriction enzyme sites (Figure 4-8A). Restriction enzyme digest confirmed the presence of a 450bp insertion in the pVSVΔ51-769 backbone indicative of the 76-9 synthetic polypeptide, the amplified PCR product was confirmed by sequencing (Figure 4-8B). pVSVΔ51 and packaging plasmids encoding for VSV N, L and P were used for viral rescue by plaque purification on Vero cells, described previously.[216,275] Rescued virus was subsequently purified by OptiPrep gradient. RT-PCR was performed from cDNA extracted from 786-0 cells infected with VSVΔ51-769 and sequenced, which confirmed the insertion and transcription of the 76-9 synthetic polypeptide in the rescued VSVΔ51-769. Furthermore, qRT-PCR probing for the 76-9 synthetic polypeptide transgene and the VSV M gene showed amplification of VSV M from both VSVΔ51-769 and VSVΔ51-GFP infected cells but amplification of the transgene only in the former (Figure 4-8C). Finally, the viral growth kinetics of VSVΔ51-769 was tested by performing multi-step growth curves and was found to be similar to the parental VSVΔ51-GFP virus (Figure 4-8D).

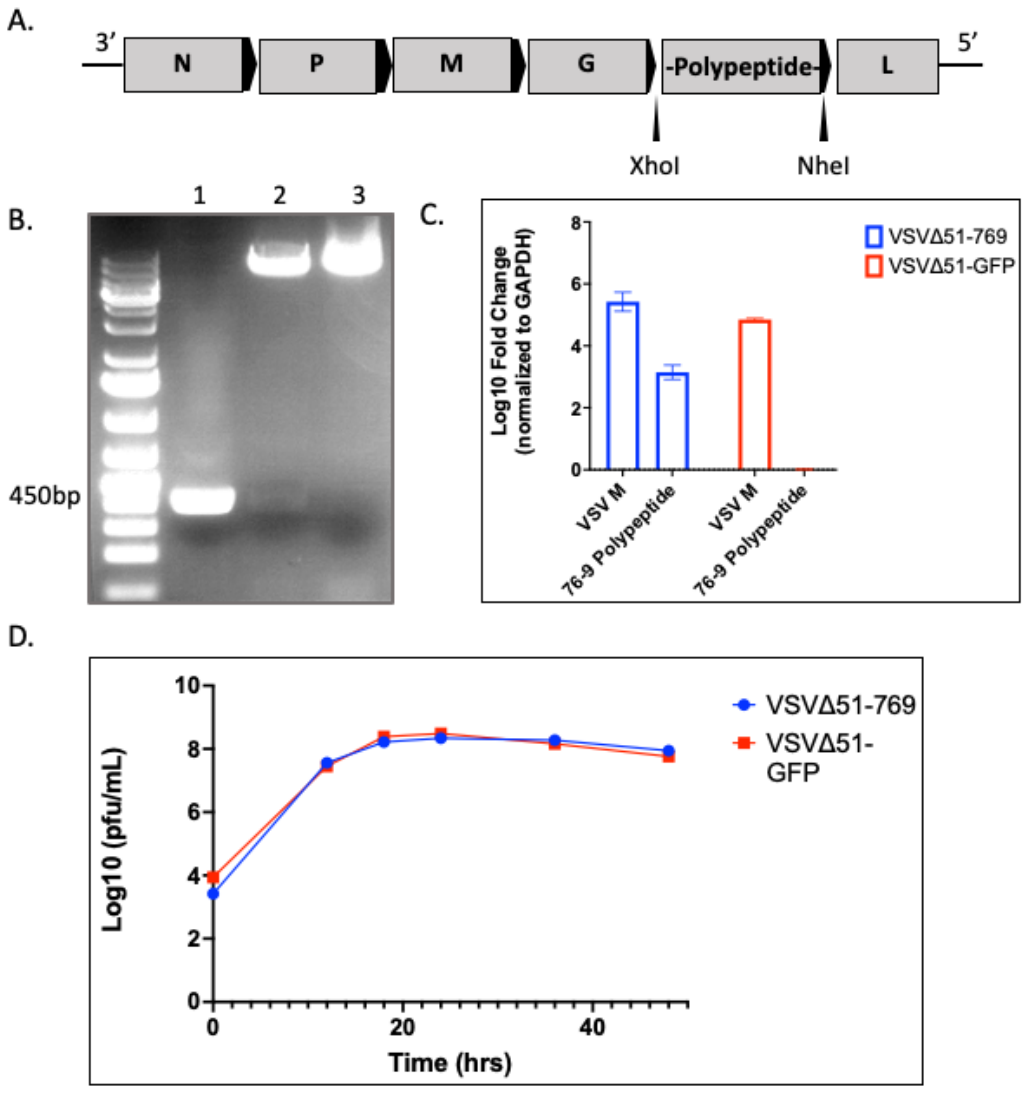
A.
3'
N
P
M
G
-Polypeptide-
L
5'
XhoI
NheI
B.
1
2
3
450bp
C.
Log10 Fold Change (normalized to GAPDH)
VSVΔ51-769
VSVΔ51-GFP
VSV M
76-9 Polypeptide
VSV M
76-9 Polypeptide
D.
Log10 (pfu/mL)
Time (hrs)
VSVΔ51-769
VSVΔ51-GFP

Figure 4-8. Design and construction of VSVΔ51-769. A. VSVΔ51 expressing the 76-9 polypeptide was made by inserting the transgene between the *G* and *L* genes of the recombinant VSVΔ51 genome. **B.** Agarose gel electrophoresis image of the PCR product (769 transgene) of 450bp size in lane 1, XhoI and NheI digested product also of 450bp and undigested plasmid in lane 3. **C.** Fold change (over mock) in gene expression of 76-9 polypeptide gene and VSVM gene of 786-0 cells infected with VSVΔ51-769 or VSV-GFP; normalized to GAPDH. **D.** Veros were infected with MOI 0.01 (multi-step) of VSVΔ51-769 or VSVΔ51-GFP. Supernatant were collected and titered by plaque assay. Accurate insertion and mRNA expression of VSVΔ51-769 was also confirmed by DNA sequencing.

4.3.9 Immunization with aDEC205-769 and VSVΔ51-769 to assess the epitope-specific response after prime or boost

With the availability of both vaccine vectors for the study, aDEC205-769 and VSVΔ51-769, the next key experiment was to assess if an antigen specific immune response following immunization can be generated. Naïve C57BL/6 mice were administered an i.p. priming dose of either 1ug aDEC205-empty or 1ug aDEC205-769 (plus adjuvants aCD40 and polyI:C) or PBS. Fourteen days post prime, they were administered an i.v. boosting dose of $1x10^8$ pfu VSVΔ51-769 or PBS (Figure 4-9A). Lymphocytes harvested from the spleen seven days post prime and seven days post boost were stimulated *ex vivo* with a 76-9 peptide pool or VSV N peptide. The antigen specific immune response was evaluated by ELISPOT and ICS assays probing for the production of IFNγ. There were no observable differences in the production of IFNγ from total lymphocytes or CD8+ T cells between all groups both after prime and after boost (Figure 4-9B-I). However, significantly high IFNγ production was observed in response to VSV N stimulation in groups given aDEC205-empty or aDEC205-769 (Figure 4-9B-I). This indicates that an immune response was established, albeit not primarily to the viral antigens.

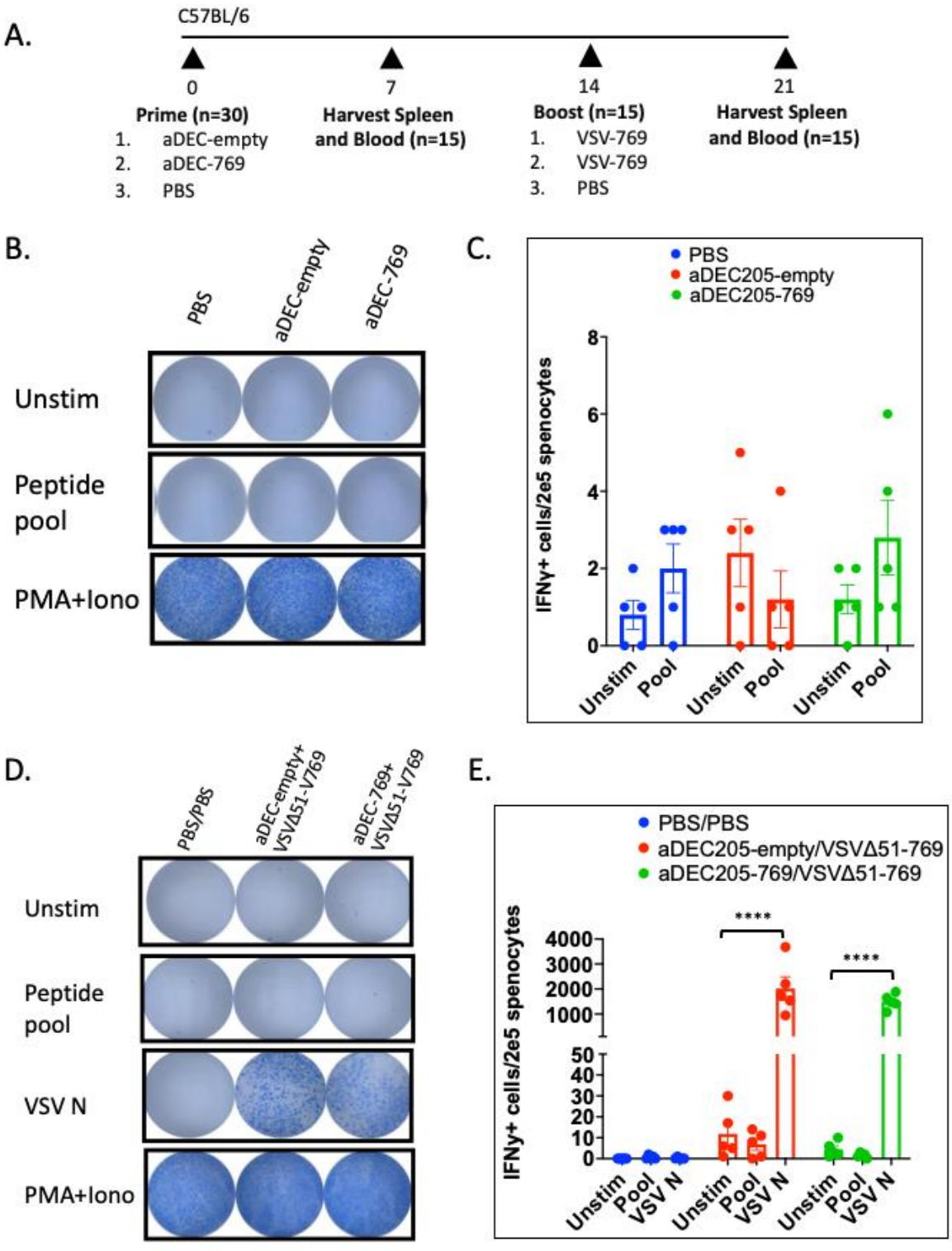
A.
C57BL/6
0
7
14
21
Prime (n=30)
1. aDEC-empty
2. aDEC-769
3. PBS
Harvest Spleen and Blood (n=15)
Boost (n=15)
1. VSV-769
2. VSV-769
3. PBS
Harvest Spleen and Blood (n=15)
B.
PBS
aDEC-empty
aDEC-769
Unstim
Peptide pool
PMA+Iono
C.
PBS
aDEC205-empty
aDEC205-769
IFNγ+ cells/2e5 spenocytes
Unstim
Pool
D.
PBS/PBS
aDEC-empty+ VSVΔ51-V769
aDEC-769+ VSVΔ51-V769
Unstim
Peptide pool
VSV N
PMA+Iono
E.
PBS/PBS
aDEC205-empty/VSVΔ51-769
aDEC205-769/VSVΔ51-769
IFNγ+ cells/2e5 spenocytes
****
Unstim
Pool
VSV N

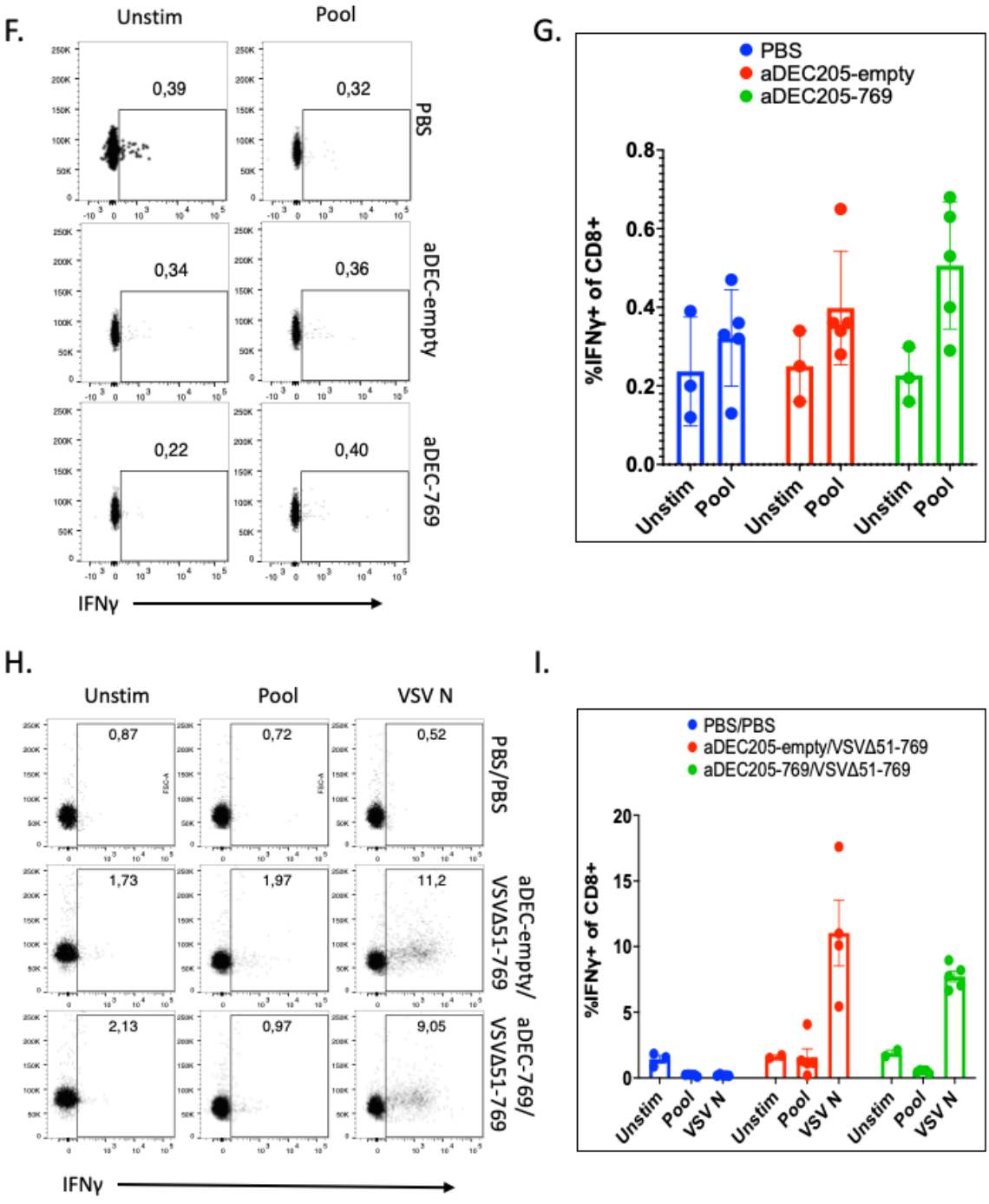
F.
Unstim
Pool
0,39
0,32
PBS
0,34
0,36
aDEC-empty
0,22
0,40
aDEC-769
IFNγ
G.
PBS
aDEC205-empty
aDEC205-769
%IFNγ+ of CD8+
0.0
0.2
0.4
0.6
0.8
Unstim
Pool
H.
Unstim
Pool
VSV N
0,87
0,72
0,52
PBS/PBS
1,73
1,97
11,2
aDEC-empty/ VSVΔ51-769
2,13
0,97
9,05
aDEC-769/ VSVΔ51-769
IFNγ
I.
PBS/PBS
aDEC205-empty/VSVΔ51-769
aDEC205-769/VSVΔ51-769
%IFNγ+ of CD8+
0
5
10
15
20
Unstim
Pool
VSV N

Figure 4-9. Measurement of antigen specific T cell responses by ELISPOT and ICS. A. Naïve C57BL/6 mice were primed with 1ug of aDEC205-769+ 50ug polyI:C + 50ug of aCD40 or 1ug aDEC205-empty + 50ug polyI:C + 50ug of aCD40 OR PBS i.p. Fourteen days post prime, mice were administered $1x10^8$ pfu i.v. of VSVΔ51-769 or PBS. Interferon gamma (IFN**γ**) ELISPOT assay was performed to quantify antigen specific responses **B,C.** 7 days post prime and **D, E.** 7 days post boost. Briefly, $2.5x10^5$ splenocytes were cultured for 24 hours in the presence DMSO (unstimulated control), PMA/ionomycin (positive control), VSV N peptide (8ug/mL) or a peptide pool (2ug/mL per peptide). IFN**γ** positive spots were quantified and imaged using an automatic plate-scanner. ICS assay was performed to quantify antigen specific CD8+ T cell responses **F,G.** 7 days post prime and **H,I.** 7) days post boost. Briefly, $1x10^6$ splenocytes were stimulated for 12 hours with a peptide pool (2ug/mL per peptide), DMSO (unstimulated control), VSV N (8ug/mL) or PMA/iono (pos control). The percentage of antigen-specific CD8+ T cells producing IFN**γ** was evaluated by flow cytometry. Bars depict mean ± SEM of 5 biological replicates; *p<0.05, ****p<0.0001, two-way ANOVA.

4.3.10 Evaluating the cellular and humoral immune milieu of blood from aDEC205-769+VSVΔ51-769 vaccinated mice

In immunization investigations, it may be beneficial to study how changes in the milieu of circulating immune cells following vaccination can serve as key biomarkers to predict vaccine efficacy. For example, a transient decrease of peripheral myeloid DCs, as a consequence of DC trafficking to local draining lymph nodes, is indicative of an induction of serum antibodies. Additionally, increases in the absolute number of CD8+ T cells in peripheral blood, and in particular decreases in CD4/CD8 T cell ratios, is associated with a favourable response to some vaccine regimens.[276,277] An analysis of circulating immune cells in the blood, namely CD4+ T cells, CD8+ T cells and CD11c+ dendritic cells (DCs), revealed no differences in their proportions between all vaccination groups after prime (Figure 4-10). However, there was a marked reduction in circulating CD4+ T cells (from 46% in PBS to 34% in aDEC-empty and 38% in aDEC205-769) compared to PBS. The CD4:CD8 T cell ratios also decreased after boost but only in the aDEC205-empty group from 2 to 1.3. The reduction in circulating CD4 and in the CD4:CD8 ratio is likely attributed to an immune response against virus and not the vaccination (Figure 4-10 C, D). Finally, to assess the production, and degree, of antibody specific responses to 76-9 antigens, serum from the blood of vaccinated animals was diluted 1:100 and incubated with $5x10^5$ 76-9 cells. Bound antibody was detected using secondary antibodies against IgG or IgM and assessed by flow cytometry. Again, there were no differences in the proportion of 76-9 cells with bound IgG or IgM between the 3 vaccination groups post prime and post boost (Figure 4-11).

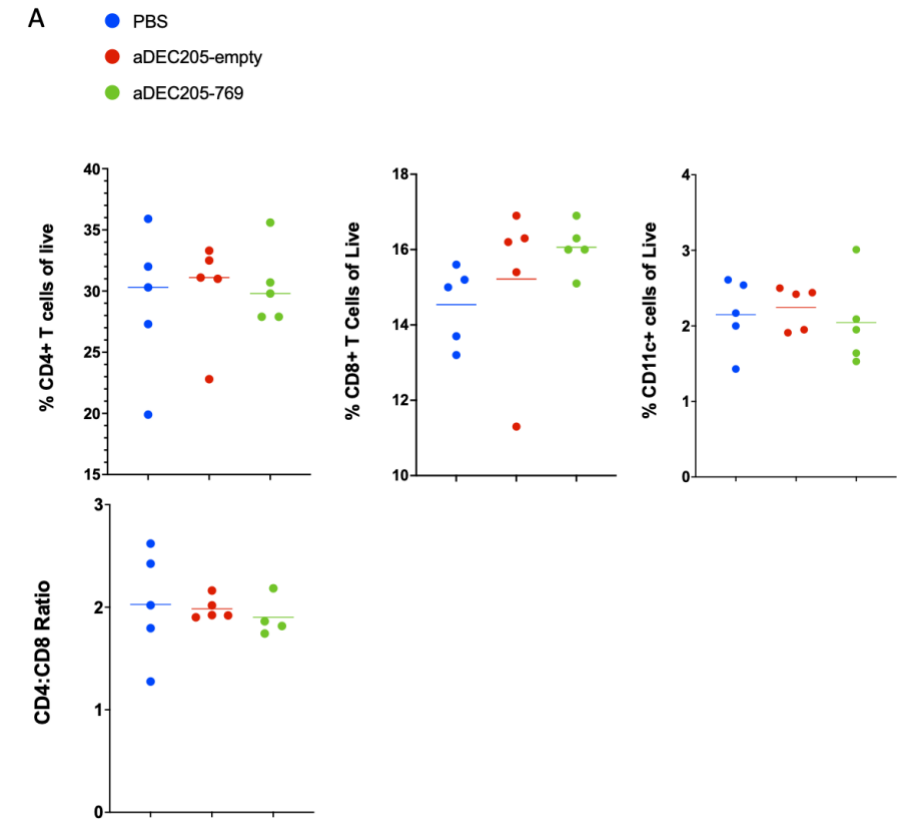
A
PBS
aDEC205-empty
aDEC205-769
% CD4+ T cells of live
% CD8+ T Cells of Live
% CD11c+ cells of Live
CD4:CD8 Ratio

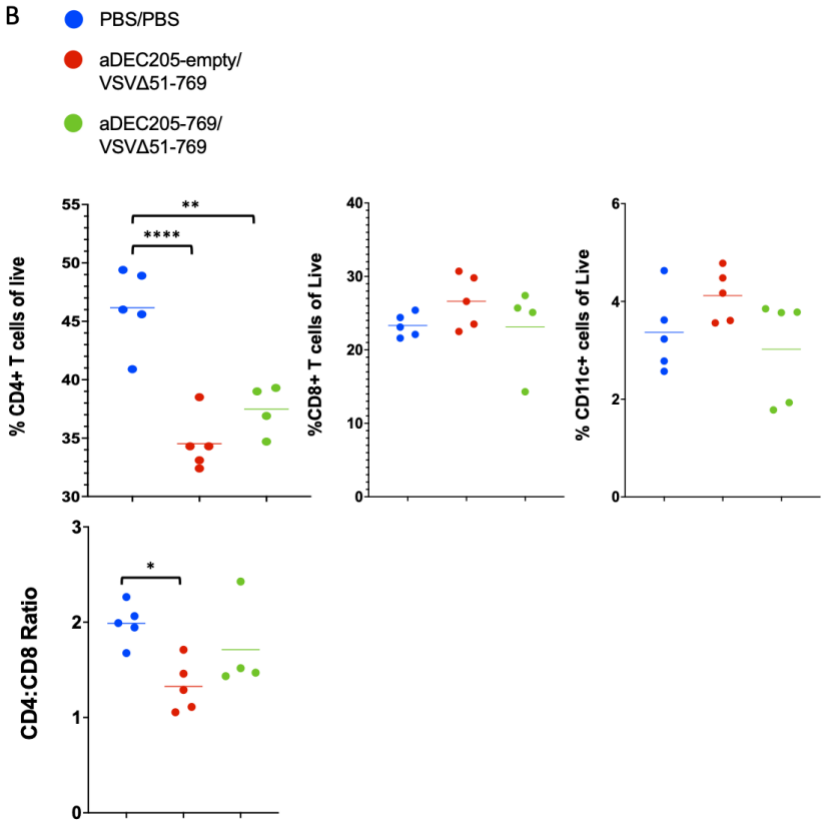
B
PBS/PBS
aDEC205-empty/
VSVΔ51-769
aDEC205-769/
VSVΔ51-769
% CD4+ T cells of live
%CD8+ T cells of Live
% CD11c+ cells of Live
CD4:CD8 Ratio
**
****
*

Figure 4-10. Quantification of immune populations in the blood of immunized mice. A. circulating CD4+, CD8+, CD11c+ and CD4:CD8 ratio 7 days after prime. **B.** circulating CD4+, CD8+, CD11c+ and CD4:CD8 ratio 7 days after boost. Scatter plot depicts mean ± SEM of 5 biological replicates per group; *$p<0.05$, **$p=0.016$, ****$p<0.0001$, ordinary one-way ANOVA.

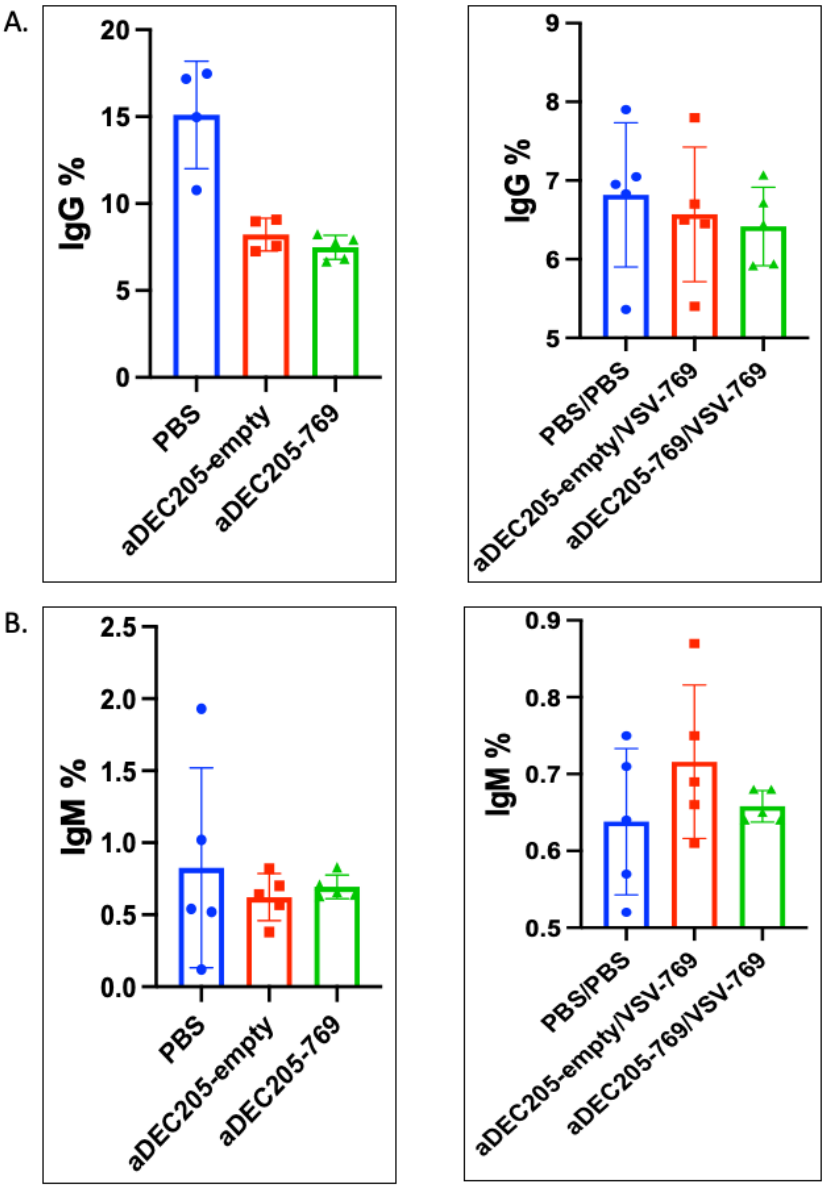
A.
IgG %
20
15
10
5
0
PBS
aDEC205-empty
aDEC205-769
IgG %
9
8
7
6
5
PBS/PBS
aDEC205-empty/VSV-769
aDEC205-769/VSV-769
B.
IgM %
2.5
2.0
1.5
1.0
0.5
0.0
PBS
aDEC205-empty
aDEC205-769
IgM %
0.9
0.8
0.7
0.6
0.5
PBS/PBS
aDEC205-empty/VSV-769
aDEC205-769/VSV-769

Figure 4-11. Serum antibody binding to 76-9 cells A. 7 days post prime and B. 7 days post boost (right). $5x10^5$ 76-9 cells were incubated in the presence of serum from vaccinated and PBS control mice (dilute 1:100) for 45-60 minutes. Bound IgG (left) and IgM (right) were detected with secondary detection antibodies.

4.3.11 The aDEC205-769+VSVΔ51-769 prime boost vaccine effect on tumour progression and survival of tumour bearing mice

Finally, we wanted to determine if the aDEC205-769+VSVΔ51-769 prime-boost would confer therapeutic benefit in tumour bearing mice. Naïve C57BL/6 mice were implanted subcutaneously with $1x10^6$ 76-9 cells. When tumour sizes reached $100mm^3$, approximately 12-14 days post implant, mice were given an i.p. priming dose of 1ug aDEC-empty or 1ug aDEC-769 (plus adjuvants aCD40 and polyI:C), with or without immune checkpoint inhibitors (ICI) aCTLA4 or aPD-L1, or PBS. Seven days post prime, ICI groups were given a boosting dose of aCTLA4 or aPD-L1. A further 7 days post ICI boost (14 days post prime), all mice were administered the vaccination boost i.v. of $1x10^8$ pfu VSVΔ51-769 or VSVΔ51-GFP or PBS. Animals were monitored for tumour progression and survival (Figure 4-12A). There was a significant delay of tumour progression observed in the prime-boost aDEC-769+VSVΔ51-769+aCTLA4 and aCTLA4 alone mice compared to aDEC-769+VSVΔ51-769, aDEC-empty+VSVΔ51-769, aDEC-empty+VSVΔ51-GFP and PBS+PBS groups (Figure 4-12B). We observed an overall survival rate of 80% in the aDEC-769+VSVΔ51-769+aCTLA4 (4 cures) and aCTLA4 alone animals (4 cures) which was significantly greater than all other groups (Figure 4-12C). Altogether, aDEC205-769+ VSVΔ51-769 prime-boost did not significantly prolong the survival of tumour bearing mice.

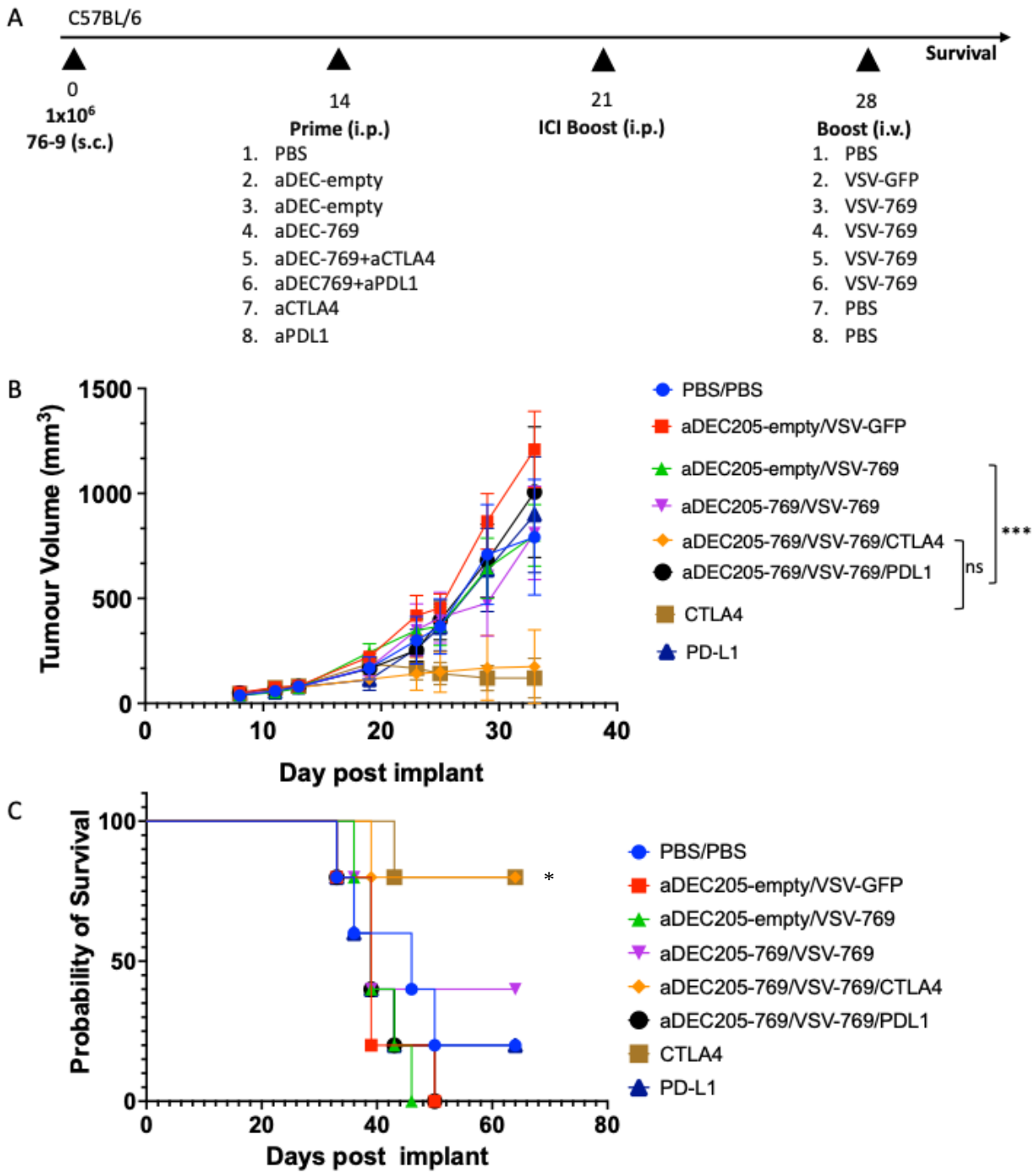
A
C57BL/6
Survival
0
1x10^6
76-9 (s.c.)
14
Prime (i.p.)
1. PBS
2. aDEC-empty
3. aDEC-empty
4. aDEC-769
5. aDEC-769+aCTLA4
6. aDEC769+aPDL1
7. aCTLA4
8. aPDL1
21
ICI Boost (i.p.)
28
Boost (i.v.)
1. PBS
2. VSV-GFP
3. VSV-769
4. VSV-769
5. VSV-769
6. VSV-769
7. PBS
8. PBS
B
Tumour Volume (mm3)
Day post implant
PBS/PBS
aDEC205-empty/VSV-GFP
aDEC205-empty/VSV-769
aDEC205-769/VSV-769
aDEC205-769/VSV-769/CTLA4
aDEC205-769/VSV-769/PDL1
CTLA4
PD-L1
ns
***
C
Probability of Survival
Days post implant
*
PBS/PBS
aDEC205-empty/VSV-GFP
aDEC205-empty/VSV-769
aDEC205-769/VSV-769
aDEC205-769/VSV-769/CTLA4
aDEC205-769/VSV-769/PDL1
CTLA4
PD-L1

Figure 4-12. Tumour progression of 76-9 tumour bearing mice treated with heterologous prime-boost vaccination. A. Naïve C57BL/6 mice were implanted subcutaneously (s.c.) with $1x10^6$ 76-9 cells on day 0. When tumours grew to $100mm^3$ (14 days post implant), mice were administered 1ug of aDEC205-769 + 50ug polyI:C + 50ug of aCD40 or aDEC205-empty + 50ug polyI:C + 50ug of aCD40 either alone or in combination with 200ug aCTLA-4 or 250ug aPD-L1 intraperitoneally (i.p.); control mice were administered PBS i.p. Seven days post prime, selected groups were administered another dose of aCTLA-4 or aPD-L1. Fourteen days post prime, mice were administered $1x10^8$ pfu i.v. of VSVΔ51-769, VSVΔ51-GFP or PBS. **B.** Tumour volume was monitored for 40 days post implant. **C.** Mice were monitored for survival 140 days post 76-9 implantation. Data is expressed as mean volume of n=5 mice/group. Data depicts mean ± SEM of 5 biological replicates per group; *$p<0.05$, ***$p<0.0005$, ns=$p>0.05$; two-way ANOVA and Log-Rank Mantel Cox.

4.4 Discussion

In this chapter, I have demonstrated an end-to-end approach for the discovery and validation of cancer antigens for integration in a therapeutic vaccine regimen. This was done by first successfully identifying 107 differentially expressed antigens from the murine syngeneic RMS model 76-9, employing CTL assays in order to select immunogenic antigens for inclusion into the prime-boost vaccine strategy described in Chapter 2, and finally assessing its immunogenicity and therapeutic capacity. Overall, this study for the first time, characterized new immunogenic murine 76-9 RMS-associated antigens that may be used to model and test active immune therapy modalities for the treatment of RMS tumours. This study highlights the need for better models to carry out pre-clinical studies of immunotherapeutics' development for RMS and the necessity to further define antigens, characterize the immune profile of associated tumours and generate novel vaccination tools. Finally, this study teaches on the challenges associated with the derivation of immunotherapies based on "personalized" antigens generally.

Research into developing personalized immunotherapies for RMS, in particular, has significantly lagged behind those for other sarcomas. Indeed, many ongoing clinical trials are evaluating adoptive cell transfer, CAR T cells, vaccines, adoptive NK cells, ICI and combination therapies in a plethora of STS types including synovial sarcoma, myxoid/round cell liposarcoma, osteosarcoma and Ewing's sarcoma.[87] Trials with broad enrollment criteria often include a heterogeneous population of STS patients, which include only small subsets of those with RMS. Davis et al. conducted a phase 1-2 trial (NCT02304458) in 2020 evaluating the safety and efficacy of nivolumab in pediatric STS which enrolled only 12 with RMS.[278] Similarly, a phase 1 trial in 2016 by Merchant et al. evaluating ipilimumab only included 2 RMS patients.[279] Both studies alluded to anti-PD-L1 inhibitors as being promising therapies for RMS but a lack of appropriate

sample size limits the interpretation and usefulness of immune checkpoints inhibitors. Furthermore, the only vaccine modality tested in clinical trials used autologous DCs pulsed with known sarcoma antigens MAGE and NY-ESO-1 but again in a general STS patient population and not specifically in RMS.[280,281] Additionally, no study has described novel MHC I or MHC II antigens from RMS. Only the cell surface antigens GD2, insulin-like growth factor receptor (IGF1R) and tyrosine kinase-like orphan receptor 1 (ROR1) has been described and targeted by CAR T cells or monoclonal antibodies.[282,283] No study, pre-clinical or clinical, has attempted to define MHC presented RMS antigens and employ them in a standalone prime-boost vaccine or in combination with ICI.

We have shown a model of how such an endeavor may be undertaken for understudied cancers. Firstly, I showed a comprehensive immune profile of a biologically relevant and syngeneic RMS model and showed how a pseudo-metastatic disease can be established. The results of this study corroborate other studies that suggest that immune checkpoint receptors, in particular CTLA4, may be promising targets for RMS presenting with immune profiles similar to 76-9. Indeed, the increased infiltration of Tregs and upregulated expression of PD-L1 with progressing 76-9 tumours supported the use of ICI against CTLA4 and PD-L1, albeit CTLA4 proved more effective in this context.

While 76-9 ICV regimens could lead to detectable responses against the antigens described in this study, when employed in the aDEC205-769+ VSVΔ51-769 vaccine in naïve C57BL/6 mice, there were no significant differences in the generation of antigen specific immune responses (Figure 4-9). There was also no therapeutic advantage (tumour progression or survival) of the aDEC-769+VSVΔ51-769 prime-boost vaccine. There was, however, a significant delay of tumour progression and increased survival in animals who received aCTLA-4 ICI, irrespective of the

addition of aDEC-769+VSVΔ51-769, indicating that therapeutic benefit arose from the ICI treatment alone (Figure 4-13). This may be attributed to the increased infiltration of Tregs in the tumour microenvironment, which is correlated with progressing 76-9 tumours (Figure 4-6).

The lack of generation of an immune response to the 10 selected 76-9 peptides encoded by aDEC205-769+ VSVΔ51-769, as discovered by LC-MS/MS, may be attributed to several factors. Firstly, our novel prime-boost vaccine encodes only CD8+ T cell epitopes, which may not be sufficient to prime optimal antigen specific responses without CD4+ T cell help.[284] We saw the induction of epitope specific responses following the 76-9 ICV vaccine platform, but this is likely due to the addition of the whole antigen, which provides both CD4+ and CD8+ T cell epitopes. Furthermore, the aDEC205+ORV vaccine described in Chapter 2 employed the full ovalbumin protein which provides MHC I (immunodominant SIINFEKL) and MHC II (immunodominant ISQAVHAAHAEINEAGR) peptides. Thereby, CD8+ and CD4+ T cell activation are more robust and comprehensive as demonstrated by the generation of functional CD8+ T cells in response to *ex vivo* stimulation and the generation of humoural responses. To elicit CD4+ T cell help in the aDEC/ORV context for 76-9 tumours, it may be necessary to encode whole proteins from which the discovered peptides arose. Theoretically, a number of aDEC205 fusion constructs could be engineered expressing a plethora of proteins and administered as an antibody cocktail to induce diverse responses. However, a major drawback of this approach, and a key limitation of this technology, is the difficulty in producing sufficient aDEC205 antibodies. As demonstrated here the aDEC205-769 produced very low yield compared to aDEC205-OVA or aDEC205-empty. Indeed, large clusters of protein/antibody aggregates were seen in transfected cells that impeded secretion and thus, purification. This unexpected technical problem could not have been predicted prior to actually attempting to produce the antibody as no effective technology was available that

can envisage biological protein folding and structure. *In silico* technologies are only now being explored to accurately predict 3D protein structures from an amino-acid sequence with the advent and application of artificial intelligence tools. AlphaFold, an algorithm developed by Google's artificial intelligence firm DeepMind, is making incredible progress on this necessary feature of predicting protein structures.[285–287] This technology will be vital for the prediction of novel aDEC205 fusion constructs to determine its downstream constraints and redirect design early (at the cloning step) to make production more efficient. In the interim, there may be value in combining the 76-9 ICV with the aDEC-769+VSVΔ51-769 to elucidate the role of CD4+ T cell help as an ICV delivers all proteins/peptides from irradiated tumours.

Secondly, the choice of adjuvant in a vaccine is an important consideration. Some multi-epitope constructs encode adjuvants in addition to epitopes, such as β-defensin, that increase their immunogenic potential, durability and peptide processing in the cell.[288] Although the adjuvants aCD40 and polyI:C were administered with aDEC205-769, their immunogenic effect may be insufficient in driving appropriate processing of the 76-9 synthetic polypeptide and thus would benefit from the addition of a β-defensin adjuvant.

Finally, multi-epitope polypeptides are joined in tandem by linkers that serve various functions. Most importantly is the ability of delivered epitopes to be cleaved, processed and presented effectively on MHC I by dendritic cells The epitopes in our 76-9 synthetic peptide are linked together by the GPGPG linker which enable immune processing, prevent the formation of junctional epitopes and provide stability.[289] However, a number of other linkers, such as GGGS and AAY, have also been used previously to adjoin epitopes in a multiepitope vaccine.[290,291] It is entirely possible that inappropriate linkers were encoded in our construct thereby precluding appropriate epitope processing and presentation. A study incorporating other linkers to adjoin the

76-9 epitopes is warranted to study their effect on synthetic peptide stability, antigen processing and presentation.

4.3 Materials and Methods

4.3.1 Cell Lines

Human embryonic kidney cells (HEK) 293T cells, kindly donated by the Oncolytic Virus Manufacturing Facility (OVMF, Ottawa, Canada) for antibody production and purification were cultured in HyQ high-glucose Dulbecco's modified Eagle's medium (Hyclone) supplemented with 10% ultra-low IgG fetal bovine serum (FBS) (Gibco), 5% penicillin/streptomycin (Gibco), and 5% L-glutamine (Gibco). 293T cells and CT26WT were cultured in DMEM supplemented with 10% FBS, 5% penicillin/streptomycin, and 5% L-glutamine. 76-9 cells were kindly gifted by Dr. Martin Holcik (University of Ottawa) and were cultured in Roswell Park Memorial Institute (Hyclone) supplemented with 15% fetal bovine serum, penicillin/streptomycin, 1M HEPES buffer, and 50uM β-mercaptoethanol. JawsII cells (ATCC Cat No. CRL-11904) were cultured in minimal essential medium (Alpha MEM, Hyclone) supplemented with 20% heat-shocked FBS, 5% penicillin/streptomycin (Gibco), 5% L-glutamine (Gibco) and 20ng/mL GM-CSF (Peprotech, Cat. 315-03). All cell lines were incubated at 37 °C in a 5% CO_2 humidified incubator. All cells were tested by PCR and Hoecht's staining to ensure they are free of mycoplasma contamination.

4.3.2 Mice

Six to eight week-old female C57BL/6J mice were obtained from Charles River Laboratories. All animals were handled in strict accordance with good animal practice, and approved by appropriate committee in collaboration with the Office of Animal Ethics and Compliance.

4.3.3 Mass Spectrometry

Immunoprecipitation of peptides from MHC I deriving from 76-9 tumour tissue and spleen was conducted by the lab of Dr. Shashi Gujar and are outlined in the following publications: 1) Murphy J.P., et al. et al Therapy-Induced MHC I Ligands Shape Neo-Antitumor CD8 T Cell Responses during Oncolytic Virus-Based Cancer Immunotherapy. *J. Proteome Res.* 2019;18: 2666-2675. doi: 10.1021/acs.jproteome.9b00173 and 2) Murphy, J.P., et al. Multiplexed Relative Quantitation with Isobaric Tagging Mass. *Analytical. Chem.* 2019;91(8): 5106-5115. doi: 10.1021/acs.analchem.8b05616.

4.3.4 Peptides

All peptides were custom synthesized by JPT Peptide Technologies (PepTrack Peptide Library) and have >80% purity.

4.3.5 ELISA

An ELISA was performed to quantify the degree of IFNγ production by splenocytes stimulated with a library of 76-9 derived peptides. Spleen from ICV vaccinated and PBS control mice was processed as described below (4.3.13) and $1x10^6$ lymphocytes were incubated with 10ug/mL of each peptide+1ug/mL anti-CD28 (clone 37.51; BD Bioscience Cat. 553295) in R10% (RPMI+10% heat shocked FBS). Control conditions included: splenocytes only, mock stimulation (no anti-CD28) and positive control with PMA/iono. The cells were incubated for 48 hours at 37℃, 5% CO_2. After 48 hours, supernatants were collected and stored at -80℃. The ELISA was performed using the R&D Mouse IFN-gamma DuoSet ELISA kit (R&D, Cat. DY485) using Nunc

Maxisorop Immuno Plate (ThermoFisher Cat. 12565136). The absorbance was read at 510 nm on a Multiskan Ascent plate reader (Thermo LabSystems).

4.3.6 Antibody Production and Purification

The pcDNA plasmids expressing the heavy chain anti-DEC205-empty, and the light chain DEC-kappa sequences were generated by Dr. Silvia Boscardin (University of Sao Paulo). The pcDNA plasmid expressing the heavy chain anti-DEC205-769 was provided by ThermoFisher. The plasmid DNA were individually transformed in competent DH5-α and DNA were purified using the Qiagen Plasmid Maxi Kit (Cat. 12165). Transfection of 90% confluent human embryonic kidney cells (HEK) 293T cells in 150 mm tissue culture-dishes, collection of antibody from culture supernatant and antibody purification were performed as previously described.[213]

4.3.7 Immunoblotting

After aDEC205-769 antibody quantification by NanoDrop ND1000 Spectrometer, 1 ug of antibody was run on NuPAGE Novex 4-12% Bis-Tris precast gels (Thermo Fisher Scientific) under reducing conditions using the XCell SureLock Mini-Cell System (Thermo Fisher Scientific) and transferred to nitrocellulose membranes (Hybond-C, Bio-Rad). Blots were blocked with 2% milk and probed with a goat anti-mouse peroxidase-conjugated antibody (1:2000) (Jackson ImmunoResearch Laboratories). Bands were visualized using the SuperSignal West Pico Chemiluminescent substrate (Thermo Fisher Scientific).

4.3.8 Antibody binding assay

A flow cytometry based binding assay was performed for evaluation of aDEC205-769 and aDEC205-empty binding specificity to the target DEC205 receptor on JawsII cells. $1x10^6$ JawsII

cells were harvested and incubated with 1ug of antibody in a U-bottom 96 well plate for 45 minutes (4°C). After incubation, cells were stained with anti-IgG-APC and acquired by flow cytometry.

4.3.9 Cloning of Oncolytic VSVΔ51-769

The 76-9 polypeptide region was PCR amplified from pcDNA expressing aDEC-205-OVA using the following primers, forward primer: CAG TAG TTG GAA AAG CTC TAT TGC, reverse primer: GGT CTC AAA ATC GTG GAC TTC CAT. The PCR amplicon was digested by XhoI and NheI and cloned into the multiple cloning site (MCS) of pBSSK-VSVΔ51-GFP after removing GFP. Positive clones were screened by restriction digestion mapping and verified by sequencing.

4.3.10 Oncolytic Virus Rescue and Plaque Purification

The recombinant VSVΔ51-769 was rescued and purified using standard procedures.[292]In summary, 50-70% confluent 293T cells were infected with an MOI 0.05 T7 vaccinia virus in serum free DMEM and incubated at 37℃ for 1.5 hours. After incubation, the cells were supplemented with fresh media and transfected in optimem and lipofectatime 2000, following manufacturer's instruction, (ThermoFisher Scientific, Cat. 11668027) and the following plasmid constructs: 1ug VSV N, 0.25ug VSV L, 1.25ug VSV P and 2ug VSVΔ51-769 then incubated at 37℃ for 48 hours. After 2 days, supernatant was collected, filtered through 0.2uM filter unit (now called rescue 1, R1) and used to infect Vero cells. Infected Vero cells were monitored for cytopathic effect (CPE) and, once observed, supernatant was collected and filtered through 0.2uM filter unit (now called rescue 2 R2). Veros were infected with diluted R2 (1:10, 1:100 and 1:100) and incubated for 1 hour then overlayed with 1% agarose in DMEM+10% FBS and incubated overnight. After 24 hours, plaques were picked, diluted and used to infect veros as described above. VSVΔ51-769 was plaque purified this way for 5 rounds. The final plaque purified virus was propagated on Vero cells

and purified on 5–50% Optiprep (Sigma) gradient. Virus titer was quantified by the standard plaque assay on Vero cells as previously described.[216]

4.3.11 Quantitative real-time PCR

Total RNA from infected or mock-infected 786-0 cells was extracted using the RNeasy Mini Kit as per manufacturer's instruction (Qiagen, Cat. 74104). One microgram of RNA was converted to cDNA using the RevertAid First Strand cDNA Synthesis Kit (ThermoFisher Scientific, Cat. K1621). The real-time PCR reactions were performed with 40ng of cDNA using the PowerUp ™ SYBR ™ Green Master Mix (ThermoFisher Scientific, Cat. A25776) on the 7500 Fast Real-Time PCR system (Applied Biosystems). Gene expression was normalized to GAPDH and fold change was calculated relative to the mock treated samples for each gene using the Pfaffle method. Primers used to amplify the sequence coding for 76-9 polypeptide were forward-CACAGAAATAGAGAAGTG and reverse-GACTGTGATGATGAAGTTGAA. Primers used to amplify GAPDH were forward-ACAGTCAGCCGCATCTTCTT and reverse-GTTAAAAGCAGCCCTGGTGA. Primers used to amplify VSV M were forward-GAGCTCAATCGTTCCCTTGT and VSV M reverse-CGGTATTGGCAGATCAAGGT

4.3.12 Mouse Tumor Model and Injections

76-9 tumors were established in 8-week-old female C57BL/6 mice by subcutaneous injection of $1x10^6$ cells in 100 uL phosphate-buffered saline (PBS). Animals were administered various therapeutics as described below:

aDEC205: for aDEC205 injections a solution containing 1ug of aDEC205-769 (Proteogenix, France) or 1ug of aDEC205-empty (Protegenix, France), 50ug polyI:C (InVivoGen, Cat. tlrl-pic)

and 50ug anti-CD40L (Leinco, clone FGK45, Cat. F1195) in 100 uL of phosphate-buffered saline was administered i.p.

Viruses: a total of $1x10^8$ pfu of oncolytic VSVΔ51-769 or VSVΔ51-GFP was administered i.v. in 50 uL of PBS.

Immune checkpoint inhibitors: The following ICIs were administered i.p. in 50uL of PBS: 200ug aCTLA4 (Lienco, clone 9H10; Cat. C1614) and 250ug aPD-L1 (Leinco, clone 10F.9G2; Cat. P363).

Irradiated and/or infected cell vaccine: 76-9 and CT26WT cells were harvested and aliquoted into Eppendorf tubes at a concentration of $3x10^7$ cells/300uL in PBS. The cells were γ-irradiated for 60Gy or 90Gy and topped with one volume of PBS. For the irradiated priming dose, 100uL of this preparation was injected i.p., thus administering $5x10^6$ irradiated cells total. For the ICV preparation, irradiated cells were infected with an MOI 10 of VSVΔ51-GFP in one volume of PBS and incubated, while rotating, for 2 hours at 37℃. This preparation was injected i.p., thus administering $5x10^6$ cells and $5x10^7$ viral particles.

4.3.13 Tissue Processing

Peptide-specific T-cell responses were measured in the spleen. Briefly, spleens were excised from sacrificed mice and filtered through a 100um plastic cell strainer (Fisherbrand™ 352360, 22-363-549) for cell collection. Red blood cells were lysed using ACK lysis buffer. The cell viability and count of the resulting white blood cells was determined using Trypan blue staining and resuspended in R10 buffer (RPMI, 10% FBS) and $1x10^6$ cells per condition were stimulated with either individual peptides or a peptide pool. 76-9 tumours were evaluated for the measurement of infiltrating TILs. Tumours were excised from sacrificed mice and dissociated using the Tumour Dissociation Kit-mouse (Miltenyi Biotech, Cat. 130-096-730) according to the manufacturer's

instructions. Circulating immune cells and serum antibody concentrations were evaluated in the blood of vaccinated mice. Terminal blood was collected in BD Microtainer ™ tubes (Fisher Scientific, Cat. BD 365967). Tubes were centrifuged for 20 minutes at 14,000 RPM. The separated serum was collected into Eppendorf tubes at stored at -80°C. The blood was subjected to 2 or more rounds of ACK lysis to remove red blood cells. The resulting white blood cells were stained for flow cytometry.

4.3.14 Detection of antigen-specific T cell responses

Antigen-specific T-cell responses were measured 7 days post-prime and boost in the spleen. For measurement by ICS, $1x10^6$ splenocytes were incubated in R10 media (RPMI+10% heat shocked FBS) in a U-bottom 96 well plate with either: 1) a peptide pool containing 2ug/mL of each peptide (for 10 peptides, the pooled stimulation was with a total of 20ug), 2) 8uM of VSV N peptide, RGYVYQGL (MBL International Corporation, Cat. TS-M529-P), 3) 1:500 cell activation cocktail (Biolegend, 423301) or 4) mock/unstimulated control. The cells were incubated for 12 hours at 37°C, 5% CO_2. After 12 hours, 0.2uL per sample of GolgiPlug ™ Brefeldin A (BD Bioscience, Cat. 555028) was added and the cells were incubated for a further 4 hours. After 4 hours, they were stained for flow cytometry. For measurement by ELISPOT, $2x10^5$ splenocytes were cultured with peptide pool, VSV N peptide, cell activation cock or mock/unstimulated conditions, as described above, in CTL-Test ™ media from the Mouse IFN-γ Single-Color ELISPOT kit (ImmunoSpot, Cat. mIFNgp-2M/2) for up to 26 hours.

4.3.15 ELISPOT

An ELISPOT assay was performed to probe for IFN-γ using the Mouse IFN-γ Single-Color ELISPOT kit (ImmunoSpot, Cat. mIFNgp-2M/2) as per manufacturer's instruction. IFN**γ** positive spots were quantified and imaged using an automatic plate-scanner.

4.3.16 Flow Cytometry

After processing the tissues as described above, cells were then stained with the FVS780 viability dye (BD Biosciences, Cat. 565388) in PBS for 15 min at room temperature. Following washes, cells were incubated with anti-CD16/32 (BD Biosciences, Cat. 553142) in 0.5% BSA/PBS at 4°C to block nonspecific antibody (Ab) interaction with Fc receptors. Subsequently, the following protocols were used for staining:

Staining for antibody binding assay: an anti-IgG-APC antibody (BD Biosciences, clone A85-1) was added to cells and incubated for 30 minutes (4°C).

Staining for ICS: First, $1x10^6$ cells were incubated with antibodies targeting T-cell surface markers anti-CD3-AF700 (BD Bioscience, clone 500A2) and anti-CD8-PerCPCy5.5 (BD Bioscience, clone 53-6.7) for 30 minutes (4°C). Cells were washed twice with FACS buffer. Next, the mouse Cytofix, Cytoperm Plus (BD Bioscience) was used for permeabilization and intracellular cytokine staining. Cells were incubated with cytofix for 20 minutes to permeabilize cells for intracellular cytokine staining (4°C). Cells were washed twice with PermWash and incubated with anti-IFNγ-BV421 (BD Bioscience, clone XMG1.2) and anti-TNFα-AF647 (BD Bioscience, clone MP6-XT22) diluted in PermWash 30 minutes (4°C).

Staining for TILs in TME: cells were stained with CD45-BV786 (BD Bioscience, clone 30-F11), anti-CD3-AF700 (BD Bioscience, clone 500A2), anti-CD4-V450 (BD Bioscience, clone RM4-5),

anti-CD8-PerCPCy5.5 (BD Bioscience, clone 53-6.7), anti-CD25-PE (eBioscience, clone PC61.5), anti-CD69-BV605 (BD Bioscience, clone H1.2F3, anti-PD-L1-APCCy7 (10F.9G2), anti-CD127-PECy7 (BD Bioscienc, clone SB/199), anti-CD49b-FITC (BD Bioscience, clone DX5) for 30 minutes (4°C).

Staining for dendritic cells, B cells and macrophages in TME: cells were stained with CD45-BV786 (BD Bioscience, clone 30-F11), anti-CD11b-APC (BD Bioscience, clone M1/70), anti-CD11c-PE (BD Bioscience, clone HL3), anti-F4/80-APCCy7 (Biolegend, clone BM8), anti-CD86-APCR700 (BD Bioscience, clone GL1), anti-IA/IE (MHC II)-BV605 (BD Bioscience, clone M5/114.15.2) and anti-CD19-FITC (clone 145-2C11).

Staining for TILs in blood: anti-CD3-AF700 (BD Bioscience, clone 500A2), anti-CD4-V450 (BD Bioscience, clone RM4-5), anti-CD8-PerCPCy5.5 (BD Bioscience, clone 53-6.7), and CD11c-PE (BD Bioscience, clone HL3).

Staining for serum binding assay: anti-IgG-PE (Biolegend, clone poly4053) and anti-IgM-PerCp/Cy5.5 (Biolegend, clone RMM-1).

After staining, cells were washed with FACs buffer and fixed in 1% paraformaldehyde. Cells were acquired on BD flow cytometry (Fortessa) and analyses were performed using FlowJo software v9.

4.3.17 Statistics

Statistical significance was calculated using Student's t test or one-way or two-way ANOVA test, using Tukey's multiple comparison test, as indicated in the figure legends. The log rank (Mantel-Cox) test was used to determine significant differences in plots for survival studies. Error bars represent standard error of the mean. Significance is based on a P value <0.05. Statistical analyses were performed using GraphPad Prism 6.0 and Excel.

Chapter 5 – General Discussion

In Canada, rhabdomyosarcoma is an incredibly rare and, if detected too late, deadly cancer that largely afflicts children under 9 years of age. The global incidence rate is about 4.5 per 1 million individuals under the age of 21.[293,294] Complicating matters further, RMS can present in two major etiologically distinct subtypes, alveolar (ARMS) and embryonal (ERMS), that are driven by separate molecular mechanisms.[295] A further two even rarer subtypes are recognized by the World Health Organization: pleomorphic RMS which occurs in adults and a spindle cell/sclerosing variant in children associated with poor clinical outcome.[296] Advances in chemotherapy and radiation have improved survival of RMS patients with low-to-mid grade disease but the chances are grim for patients with metastatic or recurrent disease.[169] Greater scientific development is required to improve clinical outcomes for patients with high grade RMS considering that novel therapies are yet to be introduced.

Research into this disease would benefit from advancement in two important areas 1) understanding disease origins, pathology and progression and 2) identifying promising therapeutic targets. The advent of next generation sequencing, molecular diagnostic tools, and the collaboration of multi-institutional groups such as the European paediatric soft tissue sarcoma study group (EpSSG), COG Soft Tissue Sarcoma Committee, and the Cooperative Weichteilsarkom Studiengruppe der GPOH (CWS) play an important role in leading RMS research.[297] In the last 3 decades, the molecular understanding of RMS has improved greatly and is a contributing factor for the application of more precise multifaceted therapies like ionizing radiation, surgery and chemotherapy combinations VAC (vincristine, actinomycin D and cyclophosphamide) and IVA (ifosfamide, vincristine and actinomycin D).[298,299] However, chemotherapy and radiation causes great toxicity, adverse events and generally poor quality of

life.[300] Furthermore, high grade patients, despite undergoing chemo/radiation, still have poor survival and high likelihood of relapse.[301] An investigation of the immunological landscape, such as the TME, tumour stroma and neoantigens, is still understudied for RMS. Despite growing evidence supporting the use of immunotherapies in other sarcoma subtypes, its application in RMS is severely lacking. This study demonstrates a framework for the study of cancer immunotherapy in RMS, in particular, the application of CD8+ T cell targeting cancer vaccines.

Chapter 2 describes a novel prime-boost strategy that employs dendritic cell targeting antigen-fusion antibodies (aDEC205) combined with antigen matched oncolytic viruses (VSVΔ51). Our proof-of-concept study showed that robust antigen specific cellular and humoral immune responses are generated, on par with current adenovirus coupled heterologous vaccines, the latter of which has limited use in a large proportion of the population with seroprevalence of anti-Ad5 antibodies.[184] Furthermore, our prime-boost strategy provides therapeutic benefit, delayed tumour progression and increased survival of animals, in a metastatic melanoma model.

In an effort to employ the aDEC205+VSVΔ51 vaccine in a model of RMS and study vaccine efficacy in the context of endogenous cancer antigens, we sought to first uncover MHC I epitopes from a pre-clinical RMS model, 76-9. As such, two different methodologies were evaluated to identify MHC I antigens: 1) a CTL screening of tumour exome library-expressing target cells, which couples epitope discovery with T-cell functionality, and 2) the gold standard IP-MS approach. Ultimately, only the second approach led to the discovery 76-9 tumour associated antigens.

Considering the lack of adequate technologies that decipher both cognate TCR and MHCI antigens, the first objective was to develop a methodology that builds upon the CTL antigen discovery platform. We developed a number of tools that, with greater optimization, could provide

a formidable strategy for high-throughput screening of antigen libraries with TCR. This strategy involves the use of flow cytometry and a cell surface probing system to detect rare CTL-target cell pairs. Although a number of key features were successfully developed, such as optimal CTL activation, effector:target ratios, and method of doublet gating, a number of other features require further optimization. As described previously, the chosen aCD107a marker was inherently unspecific due to its expression on the selected target cells, B16. The phenomenon of trogocytosis, the process by which cells, upon forming synapses, exchange plasma membrane material, precludes the specific detection of cell surface markers for both targets and effectors.[243,244] Furthermore, counter to our hypothesis, evaluation of doublets by flow cytometry was not sensitive enough to capture the fixed cytotoxic synapses visible by microscopy. For these reasons, this methodology was not explored for the discovery of RMS antigens.

Chapter 4 described the undertaking of a second approach for antigen discovery by instead focusing on using the gold-standard immunoprecipitation and mass spectrometry method to decipher RMS antigens. This method uncovered 107 differentially expressed MHC I bound peptides from 76-9 tumour and spleen tissue of tumour bearing C57BL/6 mice when compared to naïve mouse tissue. *Ex vivo* stimulation with each of the 107 peptides, revealed that 24 peptides induced a re-activation of CTLs from previously immunized mice. Ten of the 24 peptides were incorporated, as a tandem synthetic polypeptide, in the aDEC205+VSVΔ51 vaccine and evaluated for immunogenicity and therapeutic response. Unfortunately, the aDEC205-769+VSVΔ51-769 did not induce cellular or humoral immune responses against the chosen peptides nor did the therapeutic delivery of the vaccine delay tumour progression or increase survival in 76-9 tumour bearing mice.

This final chapter discusses the relevant applications of the study presented in this thesis as well as opportunities to further optimize and develop the antigen discovery technology and improve the immunogenicity of aDEC205-769+VSVΔ51-769. I will delve deeper into the current exploration of cancer vaccines and antigen discovery platforms, its associated outstanding problems and an understanding of immunity in the context of RMS.

5.1 The limitations of therapeutic cancer vaccines

Immunotherapy for cancer is widely hailed as the next health care revolution with promise to shrink tumours, extend survival and long-term remission. In fact, we are already at the beginning stages of many scientific breakthroughs in immunology that have progressed to regulatory approval such as the approval of ICI, ipilimumab that target CTLA-4, by the FDA in 2011.[302] In reality, few patients truly benefit from ICI treatment for reasons such as: irreversible T cell exhaustion, an immune 'desert' phenotype characterized by lack of immune cells in the TME and when inflammation is induced, a hostile TME that precludes T cell infiltration.[303] Investigating predictive biomarkers like checkpoint receptor expression levels, characterizing immune cell infiltration, and uncovering the mutational landscape would greatly benefit the identification of patients that may benefit the most from ICI therapies.

The same challenges apply to cancer vaccines, which have seen a revival in the last 10 years. The premise of therapeutic cancer vaccines is to supply high quality, and highly tumour-specific, antigens to professional antigen presenting cells, namely DCs, which then train CD8+ and CD4+ T cells to eradicate the tumour. However, a number of components are needed for a vaccine to be conducive to success including: 1) delivering appropriate antigens, 2) efficiently targeting DCs, 3) inducing strong and sustainable adaptive responses and 4) a TME that allows for

infiltration of tumour targeting T cells.[122,304] But typically, not all of these necessary components are met. Firstly, several tumour associated antigens have been described and employed in cancer vaccine platforms, such as MAGE family (MAGE-A1, MAGE-A3), NY-ESO-1, Her2, and PAP, but the discovery of neoantigens is greatly disadvantaged.[158,305–309] This is owning, in part, to the cumbersome process of identifying neoantigens that are sufficiently immunogenic. Secondly, there are many antigen delivery vehicles with varying degrees of success that are further dependent on choice of adjuvant, dose, site of injection, and how effectively they reach DCs. Furthermore, even when appropriate antigens are delivered in an effective vehicle, tumours can develop resistance (such as changing antigen processing, downregulating antigens and reducing HLA expression) that limits the sustainability of T cell responses.[310] Finally, as is the case of ICIs, an unfavourable TME poses an additional barrier to vaccine efficacy. Therefore, the investigation of therapeutic cancer vaccines must address these described limitations.

5.2 Next generation antigen screening platforms

The identification of antigens is the most important step for the development of therapeutic cancer vaccines. However, a lack of technologies that can effectively characterize the antigenic landscape of cancer, autoimmunity and even infectious disease alike, are a significant hindrance. TCR repertoire sequencing is an incredibly powerful tool in the biomedical field because profiling of TCRs provide insight into disease diagnosis and prognosis.[311] Furthermore, adoptive cell therapies are particularly advantaged if a patient's TCR repertoire can be deciphered to extract and expand *ex vivo* the appropriate T cells for infusion.[312] In fact, deep TCR-seq experiments can recover up to 1 million unique TCR clonotypes from a single individual and many online repositories including CIG-DB, VDJdb and TCRdb contain millions more TCR sequence

databases of known antigen specificity.[311] Unfortunately, epitope scanning approaches do not match that of TCRs; the Immune Epitope Database (IEDB) describes only $2.6x10^5$ B cell and T cell antigens and the SYFPEITHI database contains 7000 MHC ligands.[313–316] Although epitope prediction tools, such as NetMHC, and whole exome sequencing of patient tissues can reveal potential tumour neoantigens, they cannot predict peptide immunogenicity. A considerable knowledge gap exists in accurately coupling TCRs with peptide-MHC molecules.[317] Some existing approaches that assess T cell functionality (by ELISA and ^{15}chromium release assays) in response to cognate epitopes is low-throughput, requires iterative serial dilutions and large amount of CD8+ T cells for epitope scanning, making the process cumbersome.[318] The work presented in this thesis proposed a solution to this problem by isolating immunological synapses of TCR/pMHC complexes by flow cytometry and characterizing each component, the TCR sequence and the epitope sequence, to accurately couple information about both aspects of the antigen response. Theoretically, an exome library from a tumour of interest would be expressed in target cells for scanning by expanded polyclonal T cells. Upon flow sorting of doublets (TCR/pMHC complexes) the epitope encoding gene library would be deciphered downstream and matched with TCR-seq data. The proof-of-concept study described in chapter 2 that employed the known TCR, OT-1, for scanning of SIINFEKL expressing target cells, revealed poor sensitivity and specificity of this assay. However, future improvements, such as the selection of appropriate markers and a more effective method for teasing apart complexes, may render this technology valuable for high-throughput tumour antigen discovery. Indeed, strategies that can more accurately and efficiently characterize immunogenic antigens, such as those in development will be the key to developing tools for antigen discovery.[246,319]

5.3 Effective antigen delivery to dendritic cells

The next critical element in the development of an effective response to cancer vaccines is ensuring the delivery of high-quality antigens to professional dendritic cells. Dendritic cells are the key drivers for the development of coordinated and sophisticated responses to cancer antigens. Delivery vehicle, antigen concentration, injection route and choice of adjuvants are all factors involved in the introduction of antigens to T and B cells.[320] DNA and RNA vaccines encoding neoantigens, which also contain built-in adjuvants, are relatively easy to produce and have shown promising efficacy in clinical trials but require DCs' transcriptional and translational machinery. A DNA vaccine encoding HPV-16/HPV-18 E6 and E7 oncogenes showed clinical efficacy in high-grade cervical neoplasia patients in a phase2b trial.[321] Furthermore, an RNA vaccine encoding personalized neoantigens was evaluated for its safety and efficacy in a phase 1 trial in melanoma patients and showed the induction of robust anti-tumour immune responses and reduced metastases.[322] Peptide vaccines do not rely on transcription and translation by DCs and are given with adjuvants such as CpG or incomplete Freund's adjuvant. Although the clinical data from using peptide formulations are less encouraging, the next generation of peptide delivery in the form of synthetic long peptides holds more promise as SLPs have been shown to have improved antigen processing and presentation.[104] Indeed, a phase I trial was conducted in which stage III/IV melanoma patients were vaccinated with a synthetic long peptide encoding NY-ESO-1 epitopes and CpG and given in conjunction with adjuvant Montanide ISA-51.[323] This trial showed that robust CD8+ and CD4+ T cell responses were generated in response to vaccine. Finally, direct loading of DCs with peptides *ex vivo* is a method that ensures delivery of the chosen antigens but has been met with poor clinical outcomes in cancer patients. Furthermore, methods for DC isolation, culturing, antigen loading, co-stimulatory factors, the choice of DC subtypes and the

method of delivery still require extensive optimization to truly harness the full potential of this vaccination method.[324]

In this study, the aim was to delivery payloads to DCs more efficiently *in vivo* by targeting the DEC205 endocytic receptor, found on immature DCs, with fusion antibodies bound to, theoretically, any kind of antigenic protein or tandem peptides.[325] Several phase I and phase II trials are evaluating the anti-DEC205+NY-ESO-1 fusion antibody (CDX-1401) in combination with chemotherapy in melanoma and acute myeloid leukemia patients (NCT01834248, NCT03358719, NCT02129075).[212,326]

Our combination consists of aDEC205 fusions with antigen matched oncolytic viruses. We hypothesized that the addition of an antigen-matched oncolytic virus as a boosting agent could provide a strong secondary antigen stimulation, increases inflammation in the TME and elicits oncolysis with the added advantage of releasing even more endogenous antigens to draining DCs. Our study in chapter 2 evaluated an aDEC205-OVA+ORV-OVA (either MG1-OVA or VSVΔ51OVA) which indeed elicited robust CD8+ T cell and humoural responses and increased survival of mice with B16-OVA pulmonary lesions. When employing this strategy for the targeting of endogenous antigens for 76-9 in the form of an aDEC205 fused to a synthetic long peptide, the result was less promising. In the context of personalized neoantigen fusions with aDEC205, further optimization is needed to determine the limits of antigen processing, effective adjuvant combinations and dosing in the human context. There is considerable progression in understanding the aDEC205 antigen delivery vehicle and the results of the aforementioned clinical trials will provide meaningful data on its clinical relevance.

5.4 Combinations of ICI, OVs and other platforms

The future success of immunotherapy relies on employing strategies that combine agents to facilitate immune activation that, in essence, can be personalized for each cancer subtype or even for each patient. Monotherapies fail to address the myriad of components necessary for holistically inducing robust immune responses that target primary disease but also induce immune memory to avert relapse. A study by Ott et al (2017) investigated a personalized neoantigen peptide vaccine monotherapy encoding 20 epitopes in melanoma patients with resectable disease.[327] Although a majority of patients (4/6) with stage IIIB/C disease responded favourably and had no tumour recurrence 25 months post treatment, 2 patients with stage IVM1b disease upon trial initiation, did experience recurrence within 25 months.[327]

Thus, an immunotherapy must not target just one cell type or one antigen or just one type of response: it must harness the biology of a system that is conducive to curative therapeutic success. The 2 melanoma patients described above with recurrent disease following peptide vaccine monotherapy were given an additional anti-PD-L1 therapy. The addition of anti-PD-L1 did not only lead to tumour regression, it also induced the expansion of neoepitope specific T cells.[327] Fundamentally, a guiding principle of combinations must be established based on the immunological landscape of the respective malignancy. In the immediate, vaccines, agonistic antibodies, CAR T cells, and adoptive therapies benefit from the addition of ICIs that 'release the brakes' of tumour immunity and drive T and B cell functionality forward. Consistently, evidence has shown a favourable response to ICI in tumours with a high mutational burden. But tumours with low mutational burden may benefit from a combination treatment of vaccines that facilitate the delivery of antigens coupled with ICIs that antagonize inhibitory receptors. Oncolytic viruses selectively target and kill tumours with the added benefit of unshielding antigens to prime T cells

that further accelerate tumour cytolysis in local and distant sites.[328] There are also a multitude of OV vectors in study including: adenovirus, vaccinia, poxvirus, measles, reovirus, NDV, HSV and rhabdoviruses, each with unique features that enable multiple functionalities. Vaccinia OVs, for example, are slow replicating and are well suited for prolonged transgene expression making them ideal vector for encoding chemokines and cytokines including CCL5, GM-CSF, and IL-2.[329,330] Whereas, rhabdoviruses like VSV and Maraba are pro-inflammatory and induce an immunogenic environment in the TME but also disseminate to secondary lymphoid organs making them ideally suited for antigen delivery.[331] However, all OV monotherapies face two critical challenges: 1) viral clearance of the OV and 2) poor infectivity of tumours, indicating that OV combination therapies are the key to overcoming these challenges. Numerous studies are evaluating ICI combinations with either standalone OVs, or vectors that encode chemokines, cytokines and antigens.[328] Notably, a combination comprising of T-VEC encoding GM-CSF and ipilimumab (aCTLA) significantly improved objective response rates of patients with unresectable melanoma, compared to either treatment alone.[332] It should be noted however, that this combination ultimately failed to meet its primary objective in a larger Phase 3 trial indicating a need to explore various combinations. OV combinations with cancer vaccines is another promising avenue of research. As it currently stands, scientists are not armed with the necessary tools (few MHC I and even fewer MHC II epitopes are known) to develop specific cancer vaccines with appropriate antigens. However, the added benefit of oncolysis and adjuvanticity provided by an OV combination with tumour-antigen targeting DNA/RNA/peptide vaccines, drives the further release of endogenous MHC I and MHC II antigens in an inflamed environment for uptake by draining DCs and antigen cross-presentation.[333]

In our heterologous prime-boost model, antigen specific CD8+ T cell responses are significantly greater in the aDEC205-OVA+ORV-OVA combination than in a homologous aDEC205-OVA+aDEC205-OVA immunization (Figure 2-6, 2-7). Furthermore, tumour bearing animals exhibit greater survival following therapeutic immunization which owes credence to our hypothesis that a combination of vaccine with ORV leads to better responses than aDEC205 or ORV alone (Figure 2-8, 2-9). One of the limitations of the study presented in Chapter 2 was that a triple combination with ICI was not evaluated. B16-F10 is a highly aggressive and treatment resistant tumour model but does response to aPD-L1 blockade therapy.[334,335] In fact, CD8+ T cells and NK cells are critical for the antitumour neoepitope response seen in the B16 model after aPD-L1 monotherapy. But treatment efficacy is augmented following a Trp2 peptide vaccine combination with aPD-L1, as evidenced by improved tumour control and stronger anti-Trp2 CD8+ T cell responses generated by the re-activation of these cells with ICI.[334] Future studies involving aDEC205+ORV prime boost should include combinations with tumour targeting ICI such as anti-PDL1 and aCTLA-4 or TIL targeting anti-PD-1 and anti-LAG3 (evidenced to be co-expressed in B16 TME) to discern its therapeutic efficacy.[334,336,337]

5.5 Spearheading development of tools for RMS treatment

Selecting the most appropriate and efficacious combinatorial agents for cancer immunotherapy will be one of the biggest challenges that biomedical science will face in the future. Cancer is a heterogenous disease and so, therapeutics must address the unique challenges of each malignancy. The study conducted in chapter 3 aimed to immunologically profile the 76-9 tumour model, discover antigens and employ them in a combination vaccine that addressed the challenges of the 76-9 model. Based on the promising results of chapter 2, in which an aDEC205-OVA+ORV-OVA vaccine was evaluated, a similar vaccine regimen was employed to generate CD8+ T cell responses against endogenous 76-9 peptides, that were identified as being tumour associated antigens. The same heterologous prime-boost vaccine however, did not generate any antigen responses or significantly prolong survival. The triple agent combination therapy of aDEC205-769+VSVΔ51-769+aCTLA4 offered significantly better survival and delayed tumour progression than the double agent therapy, but this efficacy was also seen in the aCTLA4 monotherapy group, indicating that the vaccine did not contribute to the effect observed. Even in pre-clinical mouse models, a therapeutic intervention that may produce promising results in one model, may not translate to another as seen by our study. Many avenues could be explored to optimize the priming of CD8+ T cells against the synthetic 76-9 polypeptide described above including: 1) assess various aDEC205 doses 2) varying the timing of prime and boost doses (5, 7, 14, 21 day intervals), 3) employing other priming vectors such as vaccinia that provide more prolonged transgene expression, and 4) re-constructing the synthetic polypeptide aDEC205 fusion with different linkers such as AAY or GGGS or different ordering of epitopes.

Although the overarching goal of chapter 4 was well conceived, the results of our vaccine ultimately did not support the proposed hypotheses. However, the tools we developed are

meaningful and useful for further study of RMS. The tumour associated antigens described above and insight from the immunological profiling study creates opportunities for the exploration of many vaccine strategies, and in particular, for the improvement of OV therapeutic efficacy in a pre-clinical model. The 76-9 cell line and *ex vivo* tumour cores from syngeneic implantation are not only susceptible to rhabdovirus infection, but infectivity can be greatly increased with the addition of viral sensitizers.[138] Rhabdoviruses have also been combined with inhibitor of apoptosis (IAP) compounds LCL161 and showed bystander killing of RMS cell lines *in vitro* and in particular, inhibited 76-9 tumour growth in implanted mice.[338] In another study, mice implanted with 76-9 tumours showed modest increase in survival following treatment with the oncolytic, attenuated form of HSV.[339] The combination of these studies, including the one presented in this thesis, paves the path for developing multiple tools to study the applicability of cancer immunotherapy for RMS.

5.6 Concluding thoughts

The renewed interest in cancer immunotherapy has sparked the advent of remarkable multi-modal strategies that, in the next era, have the potential to triumph over the mainstay cytotoxic drugs and radiation treatments. The cancer vaccine field, in particular, is entering a new phase of development in which combination approaches with OVs, adjuvants and ICI are reaching greater efficacy than as monotherapy. With the increasing quality and quantity of research, there is greater conviction in the success of vaccines for the treatment of heterogeneous malignancies. The investigation presented here operates as a logical framework for vaccine development, specifically to explore immunotherapy for RMS. This study underscores how immunotherapy must holistically engage several key features to elicit anti-tumour immunity including DCs, CD8+ T cells, CD4+ T cells, innate inflammation, and immune checkpoint receptors. Till present, this work has focused on building immunization tools to study the application of heterologous prime-boost vaccination with DC targeting antibodies combined with OVs. Future work should continue to explore our described vaccine modality in various tumour models, adapt the framework for RMS, optimize the immunization technique and explore further combinations. Overall, this work has been a strong contribution to the field of RMS research and has helped to grow the limited library of its therapeutic targets, which will ultimately facilitate research for this rare disease.

References

1. Zinkernagel RM, Doherty PC. The discovery of MHC restriction. *Immunol Today*. 1997;18(1):14-17. doi:10.1016/s0167-5699(97)80008-4
2. Mosmann TR, Coffman RL. TH1 and TH2 cells: different patterns of lymphokine secretion lead to different functional properties. *Annu Rev Immunol*. 1989;7:145-173. doi:10.1146/annurev.iy.07.040189.001045
3. Masopust D, Vezys V, Wherry EJ, Ahmed R. A brief history of CD8 T cells. *Eur J Immunol*. 2007;37(S1):S103-S110. doi:10.1002/eji.200737584
4. Rock KL, Reits E, Neefjes J. Present Yourself! By MHC Class I and MHC Class II Molecules. *Trends Immunol*. 2016;37(11):724-737. doi:10.1016/j.it.2016.08.010
5. Barral DC, Brenner MB. CD1 antigen presentation: how it works. *Nat Rev Immunol*. 2007;7(12):929-941. doi:10.1038/nri2191
6. Robinson J, Halliwell JA, Hayhurst JD, Flicek P, Parham P, Marsh SGE. The IPD and IMGT/HLA database: allele variant databases. *Nucleic Acids Res*. 2015;43(D1):D423-D431. doi:10.1093/nar/gku1161
7. Anderson MS, Miller J. Invariant chain can function as a chaperone protein for class II major histocompatibility complex molecules. *Proc Natl Acad Sci*. 1992;89(6):2282-2286. doi:10.1073/pnas.89.6.2282
8. Natarajan SK, Assadi M, Sadegh-Nasseri S. Stable peptide binding to MHC class II molecule is rapid and is determined by a receptive conformation shaped by prior association with low affinity peptides. *J Immunol*. 1999;162(7):4030-4036.
9. Chou C-L, Sadegh-Nasseri S. Hla-Dm Recognizes the Flexible Conformation of Major Histocompatibility Complex Class II. *J Exp Med*. 2000;192(12):1697-1706. doi:10.1084/jem.192.12.1697
10. Ortmann B, Androlewicz MJ, Cresswell P. MHC class l/β2-microglobulin complexes associate with TAP transporters before peptide binding. *Nature*. 1994;368(6474):864-867. doi:10.1038/368864a0
11. Ortmann B, Copeman J, Lehner PJ, et al. A Critical Role for Tapasin in the Assembly and Function of Multimeric MHC Class I-TAP Complexes. *Science*. 1997;277(5330):1306-1309. doi:10.1126/science.277.5330.1306
12. Kovacsovics-Bankowski M, Rock KL. A Phagosome-to-Cytosol Pathway for Exogenous Antigens Presented on MHC Class I Molecules. *Science*. 1995;267(5195):243-246. doi:10.1126/science.7809629
13. Yanagi Y, Yoshikai Y, Leggett K, Clark SP, Aleksander I, Mak TW. A human T cell-specific cDNA clone encodes a protein having extensive homology to immunoglobulin chains. *Nature*. 1984;308(5955):145-149. doi:10.1038/308145a0
14. Willioms AF. The T -lymphocyte antigen receptor - elusive no more. *Nature*. 1983;961(1979):1983-1984.
15. Reinherz EL. Revisiting the Discovery of the TCR Complex and Its Co-Receptors. *Front Immunol*. 2014;5. doi:10.3389/fimmu.2014.00583
16. Alcover A, Alarcón B, Di Bartolo V. Cell Biology of T Cell Receptor Expression and Regulation. *Annu Rev Immunol*. 2018;36(1):103-125. doi:10.1146/annurev-immunol-042617-053429
17. Bassing CH, Swat W, Alt FW. The Mechanism and Regulation of Chromosomal V(D)J Recombination. *Cell*. 2002;109(2):S45-S55. doi:10.1016/S0092-8674(02)00675-X

18. Jung D, Alt FW. Unraveling V(D)J Recombination. *Cell*. 2004;116(2):299-311. doi:10.1016/S0092-8674(04)00039-X
19. Davis M, Chien Y. T-cell antigen receptors. In: Paul W, ed. *Fundamental Immunology*. 7th ed. Lippincot Williams Wilkins; 2013:279-310.
20. Krogsgaard M, Li Q, Sumen C, Huppa JB, Huse M, Davis MM. Agonist/endogenous peptide–MHC heterodimers drive T cell activation and sensitivity. *Nature*. 2005;434(7030):238-243. doi:10.1038/nature03391
21. Chien Y, Jores R, Crowley MP. Recognition by γ/δ T Cells. *Annu Rev Immunol*. 1996;14(1):511-532. doi:10.1146/annurev.immunol.14.1.511
22. Xing Y, Hogquist KA. T-Cell Tolerance: Central and Peripheral. *Cold Spring Harb Perspect Biol*. 2012;4(6):a006957-a006957. doi:10.1101/cshperspect.a006957
23. Derbinski J, Gäbler J, Brors B, et al. Promiscuous gene expression in thymic epithelial cells is regulated at multiple levels. *J Exp Med*. 2005;202(1):33-45. doi:10.1084/jem.20050471
24. Laydon DJ, Bangham CRM, Asquith B. Estimating T-cell repertoire diversity: limitations of classical estimators and a new approach. *Philos Trans R Soc B Biol Sci*. 2015;370(1675):20140291. doi:10.1098/rstb.2014.0291
25. Klein L, Kyewski B, Allen PM, Hogquist KA. Positive and negative selection of the T cell repertoire: what thymocytes see (and don't see). *Nat Rev Immunol*. 2014;14(6):377-391. doi:10.1038/nri3667
26. Dhamne C, Chung Y, Alousi AM, Cooper LJN, Tran DQ. Peripheral and Thymic Foxp3+ Regulatory T Cells in Search of Origin, Distinction, and Function. *Front Immunol*. 2013;4. doi:10.3389/fimmu.2013.00253
27. Martinez-Sanchez ME, Huerta L, Alvarez-Buylla ER, Villarreal Luján C. Role of Cytokine Combinations on CD4+ T Cell Differentiation, Partial Polarization, and Plasticity: Continuous Network Modeling Approach. *Front Physiol*. 2018;9:877. doi:10.3389/fphys.2018.00877
28. Kalia V, Sarkar S. Regulation of Effector and Memory CD8 T Cell Differentiation by IL-2-A Balancing Act. *Front Immunol*. 2018;9:2987. doi:10.3389/fimmu.2018.02987
29. Mak TW, Saunders ME. 14-T Cell Activation. In: *The Immune Response*. Elsevier; 2006:373-401. doi:10.1016/B978-012088451-3.50016-8
30. Parry R V., Chemnitz JM, Frauwirth KA, et al. CTLA-4 and PD-1 Receptors Inhibit T-Cell Activation by Distinct Mechanisms. *Mol Cell Biol*. 2005;25(21):9543-9553. doi:10.1128/MCB.25.21.9543-9553.2005
31. Dustin ML, Long EO. Cytotoxic immunological synapses. *Immunol Rev*. 2010;235(1):24-34. doi:10.1111/j.0105-2896.2010.00904.x
32. Varma R, Campi G, Yokosuka T, Saito T, Dustin ML. T cell receptor-proximal signals are sustained in peripheral microclusters and terminated in the central supramolecular activation cluster. *Immunity*. 2006;25(1):117-127. doi:10.1016/j.immuni.2006.04.010
33. Onnis A, Baldari CT. Orchestration of Immunological Synapse Assembly by Vesicular Trafficking. *Front Cell Dev Biol*. 2019;7:110. doi:10.3389/FCELL.2019.00110/BIBTEX
34. Zhang Y, Wang H. Integrin signalling and function in immune cells. *Immunology*. 2012;135(4):268-275. doi:10.1111/j.1365-2567.2011.03549.x
35. Freiberg BA, Kupfer H, Maslanik W, et al. Staging and resetting T cell activation in SMACs. *Nat Immunol*. 2002;3(10):911-917. doi:10.1038/ni836
36. Samelson LE, Patel MD, Weissman AM, Harford JB, Klausner RD. Antigen activation of

murine T cells induces tyrosine phosphorylation of a polypeptide associated with the T cell antigen receptor. *Cell*. 1986;46(7):1083-1090. doi:10.1016/0092-8674(86)90708-7
37. Romeo C, Amiot M, Seed B. Sequence requirements for induction of cytolysis by the T cell antigenFc receptor ζ chain. *Cell*. 1992;68(5):889-897. doi:10.1016/0092-8674(92)90032-8
38. Koretzky GA, Boerth NJ. The role of adapter proteins in T cell activation. *Cell Mol Life Sci*. 1999;56(11-12):1048-1060. doi:10.1007/s000180050492
39. Smith-Garvin JE, Koretzky GA, Jordan MS. T Cell Activation. *Annu Rev Immunol*. 2009;27(1):591-619. doi:10.1146/annurev.immunol.021908.132706
40. Vaeth M, Kahlfuss S, Feske S. CRAC Channels and Calcium Signaling in T Cell-Mediated Immunity. *Trends Immunol*. 2020;41(10):878-901. doi:10.1016/j.it.2020.06.012
41. Porciello N, Tuosto L. CD28 costimulatory signals in T lymphocyte activation: Emerging functions beyond a qualitative and quantitative support to TCR signalling. *Cytokine Growth Factor Rev*. 2016;28:11-19. doi:10.1016/j.cytogfr.2016.02.004
42. London CA, Lodge MP, Abbas AK. Functional Responses and Costimulator Dependence of Memory CD4 + T Cells. *J Immunol*. 2000;164(1):265-272. doi:10.4049/jimmunol.164.1.265
43. Borowski AB, Boesteanu AC, Mueller YM, et al. Memory CD8 + T Cells Require CD28 Costimulation. *J Immunol*. 2007;179(10):6494-6503. doi:10.4049/jimmunol.179.10.6494
44. Fuse S, Zhang W, Usherwood EJ. Control of Memory CD8 + T Cell Differentiation by CD80/CD86-CD28 Costimulation and Restoration by IL-2 during the Recall Response. *J Immunol*. 2008;180(2):1148-1157. doi:10.4049/jimmunol.180.2.1148
45. Takeuchi A, Saito T. CD4 CTL, a Cytotoxic Subset of CD4+ T Cells, Their Differentiation and Function. *Front Immunol*. 2017;8. doi:10.3389/fimmu.2017.00194
46. Castiglioni P, Gerloni M, Cortez-Gonzalez X, Zanetti M. CD8 T cell priming by B lymphocytes is CD4 help dependent. *Eur J Immunol*. 2005;35(5):1360-1370. doi:10.1002/eji.200425530
47. Elgueta R, Benson MJ, de Vries VC, Wasiuk A, Guo Y, Noelle RJ. Molecular mechanism and function of CD40/CD40L engagement in the immune system. *Immunol Rev*. 2009;229(1):152-172. doi:10.1111/j.1600-065X.2009.00782.x
48. Schoenberger SP, Toes REM, van der Voort EIH, Offringa R, Melief CJM. T-cell help for cytotoxic T lymphocytes is mediated by CD40–CD40L interactions. *Nature*. 1998;393(6684):480-483. doi:10.1038/31002
49. Curtsinger JM, Schmidt CS, Mondino A, et al. Inflammatory cytokines provide a third signal for activation of naive CD4+ and CD8+ T cells. *J Immunol*. 1999;162(6):3256-3262. http://www.ncbi.nlm.nih.gov/pubmed/10092777
50. Blott EJ, Griffiths GM. Secretory lysosomes. *Nat Rev Mol Cell Biol*. 2002;3(2):122-131. doi:10.1038/nrm732
51. Trapani JA, Smyth MJ. Functional significance of the perforin/granzyme cell death pathway. *Nat Rev Immunol*. 2002;2(10):735-747. doi:10.1038/nri911
52. Nagata S. Fas-Mediated Apoptosis. In: *Advances in Experimental Medicine and Biology*. Vol 406. Adv Exp Med Biol; 1996:119-124. doi:10.1007/978-1-4899-0274-0_12
53. Leist TP, Eppler M, Zinkernagel RM. Enhanced virus replication and inhibition of lymphocytic choriomeningitis virus disease in anti-gamma interferon-treated mice. *J Virol*. 1989;63(6):2813-2819. doi:10.1128/jvi.63.6.2813-2819.1989
54. A to Z List of Cancer Types - National Cancer Institute. Accessed June 12, 2020.

https://www.cancer.gov/types
55. Hanahan D, Weinberg RA. Hallmarks of Cancer: The Next Generation. *Cell*. 2011;144(5):646-674. doi:10.1016/j.cell.2011.02.013
56. Canadian Cancer Statistics 2017 Special topic: Pancreatic cancer. Published 2017. Accessed June 12, 2020. https://publications.gc.ca/collections/collection_2017/statcan/CS2-37-2017-eng.pdf
57. Cancer Classification | SEER Training. Accessed July 15, 2021. https://training.seer.cancer.gov/disease/categories/classification.html
58. Burningham Z, Hashibe M, Spector L, Schiffman JD. The Epidemiology of Sarcoma. *Clin Sarcoma Res*. 2012;2(1):14. doi:10.1186/2045-3329-2-14
59. Katz D, Palmerini E, Pollack SM. More Than 50 Subtypes of Soft Tissue Sarcoma: Paving the Path for Histology-Driven Treatments. *Am Soc Clin Oncol Educ B*. 2018;38(38):925-938. doi:10.1200/EDBK_205423
60. Ferguson JL, Turner SP. Bone Cancer: Diagnosis and Treatment Principles. *Am Fam Physician*. 2018;98(4):205-213. Accessed July 15, 2021. www.aafp.org/afp
61. Skapek SX, Ferrari A, Gupta AA, et al. Rhabdomyosarcoma. *Nat Rev Dis Prim*. 2019;5(1):1. doi:10.1038/s41572-018-0051-2
62. Huh WW, Skapek SX. Childhood Rhabdomyosarcoma: New Insight on Biology and Treatment. *Curr Oncol Rep*. 2010;12(6):402-410. doi:10.1007/s11912-010-0130-3
63. Huh W, Egas Bejar D. Rhabdomyosarcoma in adolescent and young adult patients: current perspectives. *Adolesc Health Med Ther*. 2014;5:115-125. doi:10.2147/AHMT.S44582
64. Sorensen PHB, Lynch JC, Qualman SJ, et al. PAX3-FKHR and PAX7-FKHR Gene Fusions Are Prognostic Indicators in Alveolar Rhabdomyosarcoma: A Report From the Children's Oncology Group. *J Clin Oncol*. 2002;20(11):2672-2679. doi:10.1200/JCO.2002.03.137
65. Gabbiani G. The myofibroblast in wound healing and fibrocontractive diseases. *J Pathol*. 2003;200(4):500-503. doi:10.1002/path.1427
66. Räsänen K, Vaheri A. Activation of fibroblasts in cancer stroma. *Exp Cell Res*. Published online 2010. doi:10.1016/j.yexcr.2010.04.032
67. Liao Z, Tan ZW, Zhu P, Tan NS. Cancer-associated fibroblasts in tumor microenvironment – Accomplices in tumor malignancy. *Cell Immunol*. 2019;343:103729. doi:10.1016/j.cellimm.2017.12.003
68. Clayton A, Evans RA, Pettit E, Hallett M, Williams JD, Steadman R. Cellular activation through the ligation of intercellular adhesion molecule-1. *J Cell Sci*. 1998;111 (Pt 4:443-453. http://www.ncbi.nlm.nih.gov/pubmed/9443894
69. Nishida N, Yano H, Nishida T, Kamura T, Kojiro M. Angiogenesis in cancer. *Vasc Health Risk Manag*. 2006;2(3):213-219. doi:10.2147/vhrm.2006.2.3.213
70. Sahai E, Astsaturov I, Cukierman E, et al. A framework for advancing our understanding of cancer-associated fibroblasts. *Nat Rev Cancer*. 2020;20(3):174-186. doi:10.1038/s41568-019-0238-1
71. Orimo A, Gupta PB, Sgroi DC, et al. Stromal Fibroblasts Present in Invasive Human Breast Carcinomas Promote Tumor Growth and Angiogenesis through Elevated SDF-1/CXCL12 Secretion. *Cell*. 2005;121(3):335-348. doi:10.1016/j.cell.2005.02.034
72. Carmeliet P, Jain RK. Molecular mechanisms and clinical applications of angiogenesis. *Nature*. 2011;473(7347):298-307. doi:10.1038/nature10144

73. Eble JA, Niland S. The extracellular matrix in tumor progression and metastasis. *Clin Exp Metastasis*. 2019;36(3):171-198. doi:10.1007/s10585-019-09966-1
74. WILLIS AL, SABEH F, LI X-Y, WEISS SJ. Extracellular matrix determinants and the regulation of cancer cell invasion stratagems. *J Microsc*. 2013;251(3):250-260. doi:10.1111/jmi.12064
75. Aras S, Zaidi MR. TAMeless traitors: macrophages in cancer progression and metastasis. *Br J Cancer*. 2017;117(11):1583-1591. doi:10.1038/bjc.2017.356
76. Anani W, Shurin MR. Targeting Myeloid-Derived Suppressor Cells in Cancer. In: *Advances in Experimental Medicine and Biology*. Vol 1036. Springer New York LLC; 2017:105-128. doi:10.1007/978-3-319-67577-0_8
77. Balkwill FR, Capasso M, Hagemann T. The tumor microenvironment at a glance. *J Cell Sci*. 2012;125(23):5591-5596. doi:10.1242/jcs.116392
78. Ellyard JI, Simson L, Parish CR. Th2-mediated anti-tumour immunity: friend or foe? *Tissue Antigens*. 2007;70(1):1-11. doi:10.1111/j.1399-0039.2007.00869.x
79. Guo FF, Cui JW. The Role of Tumor-Infiltrating B Cells in Tumor Immunity. *J Oncol*. 2019;2019:1-9. doi:10.1155/2019/2592419
80. Wang M, Zhao J, Zhang L, et al. Role of tumor microenvironment in tumorigenesis. *J Cancer*. 2017;8(5):761-773. doi:10.7150/jca.17648
81. Chimal-Ramírez GK, Espinoza-Sánchez NA, Fuentes-Pananá EM. Protumor Activities of the Immune Response: Insights in the Mechanisms of Immunological Shift, Oncotraining, and Oncopromotion. *J Oncol*. 2013;2013:1-16. doi:10.1155/2013/835956
82. Mapara MY, Sykes M. Tolerance and Cancer: Mechanisms of Tumor Evasion and Strategies for Breaking Tolerance. *J Clin Oncol*. 2004;22(6):1136-1151. doi:10.1200/JCO.2004.10.041
83. Dunn GP, Old LJ, Schreiber RD. The Three Es of Cancer Immunoediting. *Annu Rev Immunol*. 2004;22(1):329-360. doi:10.1146/annurev.immunol.22.012703.104803
84. Roberts SS, Chou AJ, Cheung N-K V. Immunotherapy of Childhood Sarcomas. *Front Oncol*. 2015;5:181. doi:10.3389/fonc.2015.00181
85. Schuster M, Nechansky A, Kircheis R. Cancer immunotherapy. *Biotechnol J*. 2006;1(2):138-147. doi:10.1002/biot.200500044
86. Makkouk A, Weiner GJ. Cancer Immunotherapy and Breaking Immune Tolerance: New Approaches to an Old Challenge. *Cancer Res*. 2015;75(1):5-10. doi:10.1158/0008-5472.CAN-14-2538
87. Birdi HK, Jirovec A, Cortés-Kaplan S, et al. Immunotherapy for sarcomas: New frontiers and unveiled opportunities. *J Immunother Cancer*. 2021;9(2):1580. doi:10.1136/jitc-2020-001580
88. Silverstein A. *A History of Immunology*. Elsevier; 2009. doi:10.1016/B978-0-12-370586-0.X0001-7
89. Clem A. Fundamentals of vaccine immunology. *J Glob Infect Dis*. 2011;3(1):73. doi:10.4103/0974-777X.77299
90. Lu S. Heterologous prime-boost vaccination. *Curr Opin Immunol*. Published online 2009. doi:10.1016/j.coi.2009.05.016
91. Covián C, Fernández-Fierro A, Retamal-Díaz A, et al. BCG-Induced Cross-Protection and Development of Trained Immunity: Implication for Vaccine Design. *Front Immunol*. 2019;0:2806. doi:10.3389/FIMMU.2019.02806
92. Netea MG, Domínguez-Andrés J, Barreiro LB, et al. Defining trained immunity and its

role in health and disease. *Nat Rev Immunol*. 2020;20(6):375-388. doi:10.1038/s41577-020-0285-6
93. Kim S-B, Ahn J-H, Kim J, Jung KH. A phase 1 study of a heterologous prime-boost vaccination involving a truncated HER2 sequence in patients with HER2-expressing breast cancer. *Mol Ther - Methods Clin Dev*. 2015;2:15031. doi:10.1038/mtm.2015.31
94. Roden RBS, Stern PL. Opportunities and challenges for human papillomavirus vaccination in cancer. *Nat Rev Cancer*. 2018;18(4):240-254. doi:10.1038/nrc.2018.13
95. Hollingsworth RE, Jansen K. Turning the corner on therapeutic cancer vaccines. *npj Vaccines*. 2019;4(1):7. doi:10.1038/s41541-019-0103-y
96. Redelman-Sidi G, Glickman MS, Bochner BH. The mechanism of action of BCG therapy for bladder cancer—a current perspective. *Nat Rev Urol*. 2014;11(3):153-162. doi:10.1038/nrurol.2014.15
97. Nemunaitis J. Vaccines in cancer: GVAX®, a GM-CSF gene vaccine. *Expert Rev Vaccines*. 2005;4(3):259-274. doi:10.1586/14760584.4.3.259
98. Hege KM, Jooss K, Pardoll D. GM-CSF Gene-Modifed Cancer Cell Immunotherapies: Of Mice and Men. *Int Rev Immunol*. 2006;25(5-6):321-352. doi:10.1080/08830180600992498
99. Santos PM, Butterfield LH. Dendritic Cell–Based Cancer Vaccines. *J Immunol*. 2018;200(2):443-449. doi:10.4049/jimmunol.1701024
100. Kantoff PW, Higano CS, Shore ND, et al. Sipuleucel-T Immunotherapy for Castration-Resistant Prostate Cancer. *N Engl J Med*. 2010;363(5):411-422. doi:10.1056/NEJMoa1001294
101. Butterfield LH, Comin-Anduix B, Vujanovic L, et al. Adenovirus MART-1–engineered Autologous Dendritic Cell Vaccine for Metastatic Melanoma. *J Immunother*. 2008;31(3):294-309. doi:10.1097/CJI.0b013e31816a8910
102. Bijker MS, van den Eeden SJF, Franken KL, Melief CJM, van der Burg SH, Offringa R. Superior induction of anti-tumor CTL immunity by extended peptide vaccines involves prolonged, DC-focused antigen presentation. *Eur J Immunol*. 2008;38(4):1033-1042. doi:10.1002/eji.200737995
103. Toes REM, Offringa R, Blom RJJ, Melief CJM, Kast WM. Peptide vaccination can lead to enhanced tumor growth through specific T-cell tolerance induction. *Proc Natl Acad Sci*. 1996;93(15):7855-7860. doi:10.1073/pnas.93.15.7855
104. Rosalia RA, Quakkelaar ED, Redeker A, et al. Dendritic cells process synthetic long peptides better than whole protein, improving antigen presentation and T-cell activation. *Eur J Immunol*. 2013;43(10):2554-2565. doi:10.1002/eji.201343324
105. Burgdorf S, Kurts C. Endocytosis mechanisms and the cell biology of antigen presentation. *Curr Opin Immunol*. 2008;20(1):89-95. doi:10.1016/j.coi.2007.12.002
106. Villadangos JA, Ploegh HL. Proteolysis in MHC Class II Antigen Presentation. *Immunity*. 2000;12(3):233-239. doi:10.1016/S1074-7613(00)80176-4
107. Kato M, McDonald KJ, Khan S, et al. Expression of human DEC-205 (CD205) multilectin receptor on leukocytes. *Int Immunol*. 2006;18(6):857-869. doi:10.1093/intimm/dxl022
108. Cao L, Chang H, Shi X, Peng C, He Y. Keratin mediates the recognition of apoptotic and necrotic cells through dendritic cell receptor DEC205/CD205. *Proc Natl Acad Sci*. 2016;113(47):13438-13443. doi:10.1073/pnas.1609331113
109. Lahoud MH, Ahmet F, Zhang J-G, et al. DEC-205 is a cell surface receptor for CpG

oligonucleotides. *Proc Natl Acad Sci*. 2012;109(40):16270-16275. doi:10.1073/pnas.1208796109
110. Bonifacino JS, Dell'Angelica EC. Molecular Bases for the Recognition of Tyrosine-based Sorting Signals. *J Cell Biol*. 1999;145(5):923-926. doi:10.1083/jcb.145.5.923
111. Kato M, Neil TK, Fearnley DB, McLellan AD, Vuckovic S, Hart DNJ. Expression of multilectin receptors and comparative FITC–dextran uptake by human dendritic cells. *Int Immunol*. 2000;12(11):1511-1519. doi:10.1093/intimm/12.11.1511
112. Mahnke K, Guo M, Lee S, et al. The Dendritic Cell Receptor for Endocytosis, Dec-205, Can Recycle and Enhance Antigen Presentation via Major Histocompatibility Complex Class II–Positive Lysosomal Compartments. *J Cell Biol*. 2000;151(3):673-684. doi:10.1083/jcb.151.3.673
113. Hossain M, Wall K. Use of Dendritic Cell Receptors as Targets for Enhancing Anti-Cancer Immune Responses. *Cancers (Basel)*. 2019;11(3):418. doi:10.3390/cancers11030418
114. Bonifaz LC, Bonnyay DP, Charalambous A, et al. In Vivo Targeting of Antigens to Maturing Dendritic Cells via the DEC-205 Receptor Improves T Cell Vaccination. *J Exp Med*. 2004;199(6):815-824. doi:10.1084/jem.20032220
115. Birkholz K, Schwenkert M, Kellner C, et al. Targeting of DEC-205 on human dendritic cells results in efficient MHC class II–restricted antigen presentation. *Blood*. 2010;116(13):2277-2285. doi:10.1182/blood-2010-02-268425
116. Wang B, Zaidi N, He L-Z, et al. Targeting of the non-mutated tumor antigen HER2/neu to mature dendritic cells induces an integrated immune response that protects against breast cancer in mice. *Breast Cancer Res*. 2012;14(2):R39. doi:10.1186/bcr3135
117. Dudziak D, Kamphorst AO, Heidkamp GF, et al. Differential Antigen Processing by Dendritic Cell Subsets in Vivo. *Science (80-)*. 2007;315(5808):107-111. doi:10.1126/science.1136080
118. Apostólico J de S, Lunardelli VAS, Yamamoto MM, Cunha-Neto E, Boscardin SB, Rosa DS. Poly(I:C) Potentiates T Cell Immunity to a Dendritic Cell Targeted HIV-Multiepitope Vaccine. *Front Immunol*. 2019;10:843. doi:10.3389/fimmu.2019.00843
119. Price PJR, Torres-Domínguez LE, Brandmüller C, Sutter G, Lehmann MH. Modified Vaccinia virus Ankara: Innate immune activation and induction of cellular signalling. *Vaccine*. 2013;31(39):4231-4234. doi:10.1016/j.vaccine.2013.03.017
120. Ura T, Okuda K, Shimada M. Developments in Viral Vector-Based Vaccines. *Vaccines*. 2014;2(3):624-641. doi:10.3390/vaccines2030624
121. Melief CJM, van Hall T, Arens R, Ossendorp F, van der Burg SH. Therapeutic cancer vaccines. *J Clin Invest*. 2015;125(9):3401-3412. doi:10.1172/JCI80009
122. Saxena M, van der Burg SH, Melief CJM, Bhardwaj N. Therapeutic cancer vaccines. *Nat Rev Cancer*. 2021;21(6):360-378. doi:10.1038/s41568-021-00346-0
123. Harrop R. Viral Vectors for Cancer Immunotherapy. *Front Biosci*. 2006;11(1):804. doi:10.2741/1838
124. Rosenberg SA, Zhai Y, Yang JC, et al. Immunizing Patients With Metastatic Melanoma Using Recombinant Adenoviruses Encoding MART-1 or gp100 Melanoma Antigens. *JNCI J Natl Cancer Inst*. 1998;90(24):1870-1872. doi:10.1093/jnci/90.24.1894
125. Daemen T, Regts J, Holtrop M, Wilschut J. Immunization strategy against cervical cancer involving an alphavirus vector expressing high levels of a stable fusion protein of human papillomavirus 16 E6 and E7. *Gene Ther*. 2002;9(2):85-94. doi:10.1038/sj.gt.3301627

126. Scherwitzl I, Hurtado A, Pierce CM, Vogt S, Pampeno C, Meruelo D. Systemically Administered Sindbis Virus in Combination with Immune Checkpoint Blockade Induces Curative Anti-tumor Immunity. *Mol Ther - Oncolytics*. 2018;9:51-63. doi:10.1016/j.omto.2018.04.004
127. Shen Y, Nemunaitis J. Herpes simplex virus 1 (HSV-1) for cancer treatment. *Cancer Gene Ther*. 2006;13(11):975-992. doi:10.1038/sj.cgt.7700946
128. DiPaola R, Plante M, Kaufman H, et al. A Phase I Trial of Pox PSA vaccines (PROSTVAC®-VF) with B7-1, ICAM-1, and LFA-3 co-stimulatory molecules (TRICOM^{TM}) in Patients with Prostate Cancer. *J Transl Med*. 2006;4(1):1. doi:10.1186/1479-5876-4-1
129. Ilkow CS, Swift SL, Bell JC, Diallo J-S. From Scourge to Cure: Tumour-Selective Viral Pathogenesis as a New Strategy against Cancer. Hobman TC, ed. *PLoS Pathog*. 2014;10(1):e1003836. doi:10.1371/journal.ppat.1003836
130. Chiocca EA, Rabkin SD. Oncolytic Viruses and Their Application to Cancer Immunotherapy. *Cancer Immunol Res*. 2014;2(4):295-300. doi:10.1158/2326-6066.CIR-14-0015
131. Brun J, McManus D, Lefebvre C, et al. Identification of Genetically Modified Maraba Virus as an Oncolytic Rhabdovirus. *Mol Ther*. 2010;18(8):1440-1449. doi:10.1038/mt.2010.103
132. Ciechonska M, Duncan R. Reovirus FAST proteins: virus-encoded cellular fusogens. *Trends Microbiol*. 2014;22(12):715-724. doi:10.1016/j.tim.2014.08.005
133. Le Boeuf F, Gebremeskel S, McMullen N, et al. Reovirus FAST Protein Enhances Vesicular Stomatitis Virus Oncolytic Virotherapy in Primary and Metastatic Tumor Models. *Mol Ther - Oncolytics*. 2017;6:80-89. doi:10.1016/j.omto.2017.08.001
134. Rehman H, Silk AW, Kane MP, Kaufman HL. Into the clinic: Talimogene laherparepvec (T-VEC), a first-in-class intratumoral oncolytic viral therapy. *J Immunother Cancer*. 2016;4(1):53. doi:10.1186/s40425-016-0158-5
135. Lichty BD, Breitbach CJ, Stojdl DF, Bell JC. Going viral with cancer immunotherapy. *Nat Rev Cancer*. 2014;14(8):559-567. doi:10.1038/nrc3770
136. Lemay CG, Rintoul JL, Kus A, et al. Harnessing Oncolytic Virus-mediated Antitumor Immunity in an Infected Cell Vaccine. *Mol Ther*. 2012;20(9):1791-1799. doi:10.1038/mt.2012.128
137. Bridle BW, Boudreau JE, Lichty BD, et al. Vesicular Stomatitis Virus as a Novel Cancer Vaccine Vector to Prime Antitumor Immunity Amenable to Rapid Boosting With Adenovirus. *Mol Ther*. 2009;17(10):1814-1821. doi:10.1038/mt.2009.154
138. Le Boeuf F, Selman M, Son HH, et al. Oncolytic Maraba Virus MG1 as a Treatment for Sarcoma. *Int J Cancer*. Published online 2017. doi:10.1002/ijc.30813
139. Bridle BW, Nguyen A, Salem O, et al. Privileged Antigen Presentation in Splenic B Cell Follicles Maximizes T Cell Responses in Prime-Boost Vaccination. *J Immunol*. Published online 2016. doi:10.4049/jimmunol.1600106
140. Barouch DH, Korber B. HIV-1 Vaccine Development After STEP. *Annu Rev Med*. 2010;61(1):153-167. doi:10.1146/annurev.med.042508.093728
141. Yu B, Wang Z, Dong J, et al. A serological survey of human adenovirus serotype 2 and 5 circulating pediatric populations in Changchun, China, 2011. *Virol J*. 2012;9(1):287. doi:10.1186/1743-422X-9-287
142. Kaur D, Patiyal S, Sharma N, Usmani SS, Raghava GPS. PRRDB 2.0: a comprehensive

database of pattern-recognition receptors and their ligands. *Database*. 2019;2019(1):76. doi:10.1093/database/baz076
143. Roh JS, Sohn DH. Damage-Associated Molecular Patterns in Inflammatory Diseases. *Immune Netw*. 2018;18(4). doi:10.4110/in.2018.18.e27
144. Hernandez C, Huebener P, Schwabe RF. Damage-associated molecular patterns in cancer: a double-edged sword. *Oncogene*. 2016;35(46):5931-5941. doi:10.1038/onc.2016.104
145. Nüssing S, Trapani JA, Parish IA. Revisiting T Cell Tolerance as a Checkpoint Target for Cancer Immunotherapy. *Front Immunol*. 2020;11:2461. doi:10.3389/fimmu.2020.589641
146. O'Donnell JS, Teng MWL, Smyth MJ. Cancer immunoediting and resistance to T cell-based immunotherapy. *Nat Rev Clin Oncol*. 2019;16(3):151-167. doi:10.1038/s41571-018-0142-8
147. Akers SN, Odunsi K, Karpf AR. Regulation of cancer germline antigen gene expression: implications for cancer immunotherapy. *Futur Oncol*. 2010;6(5):717-732. doi:10.2217/fon.10.36
148. Haas GG, D'Cruz OJ, De Bault LE. Distribution of Human Leukocyte Antigen-ABC and -D/DR Antigens in the Unfixed Human Testis. *Am J Reprod Immunol Microbiol*. 1988;18(2):47-51. doi:10.1111/j.1600-0897.1988.tb00234.x
149. Finnigan JP, Rubinsteyn A, Hammerbacher J, Bhardwaj N. Mutation-Derived Tumor Antigens: Novel Targets in Cancer Immunotherapy. *Oncology (Williston Park)*. 2015;29(12):970-972, 974-975. http://www.ncbi.nlm.nih.gov/pubmed/26676902
150. Jiang T, Shi T, Zhang H, et al. Tumor neoantigens: from basic research to clinical applications. *J Hematol Oncol*. 2019;12(1):93. doi:10.1186/s13045-019-0787-5
151. Iacovides D, Michael S, Achilleos C, Strati K. Shared mechanisms in stemness and carcinogenesis: lessons from oncogenic viruses. *Front Cell Infect Microbiol*. 2013;3. doi:10.3389/fcimb.2013.00066
152. Welters MJP, Kenter GG, Piersma SJ, et al. Induction of Tumor-Specific CD4+ and CD8+ T-Cell Immunity in Cervical Cancer Patients by a Human Papillomavirus Type 16 E6 and E7 Long Peptides Vaccine. *Clin Cancer Res*. 2008;14(1):178-187. doi:10.1158/1078-0432.CCR-07-1880
153. Bright RK, Bright JD, Byrne JA. Overexpressed oncogenic tumor-self antigens. *Hum Vaccin Immunother*. 2014;10(11):3297-3305. doi:10.4161/hv.29475
154. Pitcovski J, Shahar E, Aizenshtein E, Gorodetsky R. Melanoma antigens and related immunological markers. *Crit Rev Oncol Hematol*. 2017;115:36-49. doi:10.1016/j.critrevonc.2017.05.001
155. Guevara-Patiño JA, Turk MJ, Wolchok JD, Houghton AN. Immunity to Cancer Through Immune Recognition of Altered Self: Studies with Melanoma. In: *Advances in Cancer Research*. ; 2003:157-177. doi:10.1016/S0065-230X(03)90005-4
156. Van den Eynde BJ, Boon T. Tumor antigens recognized by T lymphocytes. *Int J Clin Lab Res*. 1997;27(2-4):81-86. doi:10.1007/BF02912440
157. Wang R-F, Rosenberg SA. Human tumor antigens for cancer vaccine development. *Immunol Rev*. 1999;170(1):85-100. doi:10.1111/j.1600-065X.1999.tb01331.x
158. van der Bruggen P, Traversari C, Chomez P, et al. A Gene Encoding an Antigen Recognized by Cytolytic T Lymphocytes on a Human Melanoma. *Science (80-)*. 1991;254(5038):1643-1647. doi:10.1126/science.1840703
159. Laheru DA, Pardoll DM, Jaffee EM. Genes to vaccines for immunotherapy: how the molecular biology revolution has influenced cancer immunology. *Mol Cancer Ther*.

2005;4(11):1645-1652. doi:10.1158/1535-7163.MCT-05-0151
160. Zhou S, Yi T, Zhang B, et al. Mapping the High Throughput SEREX Technology Screening for Novel Tumor Antigens. *Comb Chem High Throughput Screen*. 2012;15(3):202-215. doi:10.2174/138620712799218572
161. Nakatsura T, Senju S, Ito M, Nishimura Y, Itoh K. Cellular and humoral immune responses to a human pancreatic cancer antigen, coactosin-like protein, originally defined by the SEREX method. *Eur J Immunol*. 2002;32(3):826. doi:10.1002/1521-4141(200203)32:3<826::AID-IMMU826>3.0.CO;2-Y
162. Viatte S, Alves PM, Romero P. Reverse immunology approach for the identification of CD8 T-cell-defined antigens: Advantages and hurdles. *Immunol Cell Biol*. 2006;84(3):318-330. doi:10.1111/j.1440-1711.2006.01447.x
163. Thomas AM, Santarsiero LM, Lutz ER, et al. Mesothelin-specific CD8+ T Cell Responses Provide Evidence of In Vivo Cross-Priming by Antigen-Presenting Cells in Vaccinated Pancreatic Cancer Patients. *J Exp Med*. 2004;200(3):297-306. doi:10.1084/jem.20031435
164. Müller L, McArdle S, Derhovanessian E, et al. Current Strategies for the Identification of Immunogenic Epitopes of Tumor Antigens. In: *Immunotherapy of Cancer*. Humana Press; 2006:21-44. doi:10.1385/1-59745-011-1:021
165. Parham P, Barnstable CJ, Bodmer WF. Use of a monoclonal antibody (W6/32) in structural studies of HLA-A,B,C, antigens. *J Immunol*. 1979;123(1):342-349. Accessed June 12, 2020. http://www.ncbi.nlm.nih.gov/pubmed/87477
166. Shackelford DA, Lampson LA, Strominger JL. Separation of three class II antigens from a homozygous human B cell line. *J Immunol*. 1983;130(1):289-296. https://www.jimmunol.org/content/130/1/289
167. Coulie PG, Van den Eynde BJ, van der Bruggen P, Boon T. Tumour antigens recognized by T lymphocytes: at the core of cancer immunotherapy. *Nat Rev Cancer*. 2014;14(2):135-146. doi:10.1038/nrc3670
168. Number and rates of new cases of primary cancer, by cancer type, age group and sex. Accessed June 12, 2020. https://www150.statcan.gc.ca/t1/tbl1/en/tv.action?pid=1310011101
169. Okcu F, Hicks J, Horowitz M. Rhabdomyosarcoma in childhood and adolescence: Epidemiology, pathology, and molecular pathogenesis. *UpToDate*. Published online 2016. https://www.uptodate.com/contents/rhabdomyosarcoma-in-childhood-and-adolescence-epidemiology-pathology-and-molecular-pathogenesis
170. Chen C, Dorado Garcia H, Scheer M, Henssen AG. Current and Future Treatment Strategies for Rhabdomyosarcoma. *Front Oncol*. 2019;9. doi:10.3389/fonc.2019.01458
171. D'Angelo SP, Tap WD, Schwartz GK, Carvajal RD. Sarcoma Immunotherapy: Past Approaches and Future Directions. *Sarcoma*. 2014;2014:1-13. doi:10.1155/2014/391967
172. Saraf AJ, Dickman PS, Hingorani P. Disialoganglioside GD2 Expression in Pediatric Rhabdomyosarcoma: A Case Series and Review of the Literature. *J Pediatr Hematol Oncol*. 2019;41(2):118-120. doi:10.1097/MPH.0000000000001311
173. Bertolini G, Bergamaschi L, Ferrari A, et al. PD-L1 assessment in pediatric rhabdomyosarcoma: a pilot study. *BMC Cancer*. 2018;18(1):652. doi:10.1186/s12885-018-4554-8
174. Strausberg RL. Tumor microenvironments, the immune system and cancer survival. *Genome Biol*. 2005;6(3):211. doi:10.1186/gb-2005-6-3-211
175. Russell SJ, Peng K-W, Bell JC. Oncolytic virotherapy. *Nat Biotechnol*. 2012;30(7):658-

670. doi:10.1038/nbt.2287
176. Gujar S, Bell J, Diallo JS. SnapShot: Cancer Immunotherapy with Oncolytic Viruses. *Cell*. Published online 2019. doi:10.1016/j.cell.2019.01.051
177. Russell SJ, Peng KW. Measles virus for cancer therapy. *Curr Top Microbiol Immunol*. Published online 2009. doi:10.1007/978-3-540-70617-5_11
178. Miyamoto S, Inoue H, Nakamura T, et al. Coxsackievirus B3 Is an Oncolytic Virus with Immunostimulatory Properties That Is Active against Lung Adenocarcinoma. *Cancer Res*. 2012;72(10):2609-2621. doi:10.1158/0008-5472.CAN-11-3185
179. Zamarin D, Ricca JM, Sadekova S, et al. PD-L1 in tumor microenvironment mediates resistance to oncolytic immunotherapy. *J Clin Invest*. 2018;128(4):1413-1428. doi:10.1172/JCI98047
180. Selman M, Rousso C, Bergeron A, et al. Multi-modal Potentiation of Oncolytic Virotherapy by Vanadium Compounds. *Mol Ther*. 2018;26(1):56-69. doi:10.1016/j.ymthe.2017.10.014
181. Pol JG, Zhang L, Bridle BW, et al. Maraba Virus as a Potent Oncolytic Vaccine Vector. *Mol Ther*. 2014;22(2):420-429. doi:10.1038/mt.2013.249
182. Sekaly R-P. The failed HIV Merck vaccine study: a step back or a launching point for future vaccine development? *J Exp Med*. 2008;205(1):7-12. doi:10.1084/jem.20072681
183. Barnes E, Folgori A, Capone S, et al. Novel Adenovirus-Based Vaccines Induce Broad and Sustained T Cell Responses to HCV in Man. *Sci Transl Med*. 2012;4(115). doi:10.1126/scitranslmed.3003155
184. Mast TC, Kierstead L, Gupta SB, et al. International epidemiology of human pre-existing adenovirus (Ad) type-5, type-6, type-26 and type-36 neutralizing antibodies: Correlates of high Ad5 titers and implications for potential HIV vaccine trials. *Vaccine*. 2010;28(4):950-957. doi:10.1016/j.vaccine.2009.10.145
185. Nwanegbo E, Vardas E, Gao W, et al. Prevalence of Neutralizing Antibodies to Adenoviral Serotypes 5 and 35 in the Adult Populations of The Gambia, South Africa, and the United States. *Clin Vaccine Immunol*. 2004;11(2):351-357. doi:10.1128/CDLI.11.2.351-357.2004
186. Saxena M, Van TTH, Baird FJ, Coloe PJ, Smooker PM. Pre-existing immunity against vaccine vectors – friend or foe? *Microbiology*. 2013;159(Pt_1):1-11. doi:10.1099/mic.0.049601-0
187. Trombetta ES, Mellman I. Cell biology of antigen processing in vitro and in vivo. *Annu Rev Immunol*. 2005;23(1):975-1028. doi:10.1146/annurev.immunol.22.012703.104538
188. Bonifaz L, Bonnyay D, Mahnke K, Rivera M, Nussenzweig MC, Steinman RM. Efficient Targeting of Protein Antigen to the Dendritic Cell Receptor DEC-205 in the Steady State Leads to Antigen Presentation on Major Histocompatibility Complex Class I Products and Peripheral CD8+ T Cell Tolerance. *J Exp Med*. 2002;196(12):1627-1638. doi:10.1084/jem.20021598
189. Moriya K, Wakabayashi A, Shimizu M, Tamura H, Dan K, Takahashi H. Induction of tumor-specific acquired immunity against already established tumors by selective stimulation of innate DEC-205+ dendritic cells. *Cancer Immunol Immunother*. 2010;59(7):1083-1095. doi:10.1007/s00262-010-0835-z
190. Yang TC, Dayball K, Wan YH, Bramson J. DetailedAnalysis of the CD8 + T-Cell Response followingAdenovirusVaccination. *J Virol*. 2003;77(24):13407-13411. doi:10.1128/JVI.77.24.13407-13411.2003

191. Mukherjee G, Geliebter A, Babad J, et al. DEC-205-mediated antigen targeting to steady-state dendritic cells induces deletion of diabetogenic CD8+ T cells independently of PD-1 and PD-L1. *Int Immunol*. 2013;25(11):651-660. doi:10.1093/intimm/dxt031
192. Zamarin D, Holmgaard RB, Subudhi SK, et al. Localized Oncolytic Virotherapy Overcomes Systemic Tumor Resistance to Immune Checkpoint Blockade Immunotherapy. *Sci Transl Med*. 2014;6(226). doi:10.1126/scitranslmed.3008095
193. Scott AM, Allison JP, Wolchok JD. Monoclonal antibodies in cancer therapy. *Cancer Immun*. 2012;12:14. Accessed July 19, 2021. /pmc/articles/PMC3380347/
194. Liu M, Wang X, Wang L, et al. Targeting the IDO1 pathway in cancer: from bench to bedside. *J Hematol Oncol*. 2018;11(1):100. doi:10.1186/s13045-018-0644-y
195. Zhao Y, Adjei AA. The clinical development of MEK inhibitors. *Nat Rev Clin Oncol*. 2014;11(7):385-400. doi:10.1038/nrclinonc.2014.83
196. Liang K, Liu Q, Li P, Luo H, Wang H, Kong Q. Genetically engineered Salmonella Typhimurium: Recent advances in cancer therapy. *Cancer Lett*. 2019;448:168-181. doi:10.1016/j.canlet.2019.01.037
197. Miliotou AN, Papadopoulou LC. CAR T-cell Therapy: A New Era in Cancer Immunotherapy. *Curr Pharm Biotechnol*. 2018;19(1):5-18. doi:10.2174/1389201019666180418095526
198. Phan M, Watson MF, Alain T, Diallo JS. Oncolytic Viruses on Drugs: Achieving Higher Therapeutic Efficacy. *ACS Infect Dis*. 2018;4(10):1448-1467. doi:10.1021/acsinfecdis.8b00144
199. Bridle BW, Stephenson KB, Boudreau JE, et al. Potentiating Cancer Immunotherapy Using an Oncolytic Virus. *Mol Ther*. 2010;18(8):1430-1439. doi:10.1038/mt.2010.98
200. JG P, SA A, B Y, et al. Preclinical evaluation of a MAGE-A3 vaccination utilizing the oncolytic Maraba virus currently in first-in-human trials. *Oncoimmunology*. 2018;8(1). doi:10.1080/2162402X.2018.1512329
201. Miller G, Pillarisetty VG, Shah AB, Lahrs S, DeMatteo RP. Murine Flt3 Ligand Expands Distinct Dendritic Cells with Both Tolerogenic and Immunogenic Properties. *J Immunol*. 2003;170(7):3554-3564. doi:10.4049/jimmunol.170.7.3554
202. Bowen WS, Svrivastava AK, Batra L, Barsoumian H, Shirwan H. Current challenges for cancer vaccine adjuvant development. *Expert Rev Vaccines*. 2018;17(3):207-215. doi:10.1080/14760584.2018.1434000
203. Nair A, Jacob S. A simple practice guide for dose conversion between animals and human. *J Basic Clin Pharm*. 2016;7(2):27. doi:10.4103/0976-0105.177703
204. Tacken PJ, de Vries IJM, Torensma R, Figdor CG. Dendritic-cell immunotherapy: from ex vivo loading to in vivo targeting. *Nat Rev Immunol*. 2007;7(10):790-802. doi:10.1038/nri2173
205. Nestle FO, Alijagic S, Gilliet M, et al. Vaccination of melanoma patients with peptide- or tumorlysate-pulsed dendritic cells. *Nat Med*. 1998;4(3):328-332. doi:10.1038/nm0398-328
206. Hsu FJ, Benike C, Fagnoni F, et al. Vaccination of patients with B–cell lymphoma using autologous antigen–pulsed dendritic cells. *Nat Med*. 1996;2(1):52-58. doi:10.1038/nm0196-52
207. Lesterhuis WJ, Aarntzen EHJG, De Vries IJM, et al. Dendritic cell vaccines in melanoma: From promise to proof? *Crit Rev Oncol Hematol*. 2008;66(2):118-134. doi:10.1016/j.critrevonc.2007.12.007
208. Caminschi I, Maraskovsky E, Heath WR. Targeting Dendritic Cells in vivo for Cancer

Therapy. *Front Immunol*. 2012;3(FEB). doi:10.3389/fimmu.2012.00013
209. Wen PY, Reardon DA, Armstrong TS, et al. A Randomized Double-Blind Placebo-Controlled Phase II Trial of Dendritic Cell Vaccine ICT-107 in Newly Diagnosed Patients with Glioblastoma. *Clin Cancer Res*. 2019;25(19):5799-5807. doi:10.1158/1078-0432.CCR-19-0261
210. Vonderheide RH, Flaherty KT, Khalil M, et al. Clinical Activity and Immune Modulation in Cancer Patients Treated With CP-870,893, a Novel CD40 Agonist Monoclonal Antibody. *J Clin Oncol*. 2007;25(7):876-883. doi:10.1200/JCO.2006.08.3311
211. Anandasabapathy N, Feder R, Mollah S, et al. Classical Flt3L-dependent dendritic cells control immunity to protein vaccine. *J Exp Med*. 2014;211(9):1875-1891. doi:10.1084/jem.20131397
212. Bhardwaj N, Pavlick AC, Ernstoff MS, et al. A Phase II Randomized Study of CDX-1401, a Dendritic Cell Targeting NY-ESO-1 Vaccine, in Patients with Malignant Melanoma Pre-Treated with Recombinant CDX-301, a Recombinant Human Flt3 Ligand. *J Clin Oncol*. 2016;34(15_suppl):9589-9589. doi:10.1200/JCO.2016.34.15_suppl.9589
213. Henriques HR, Rampazo E V., Gonçalves AJS, et al. Targeting the Non-structural Protein 1 from Dengue Virus to a Dendritic Cell Population Confers Protective Immunity to Lethal Virus Challenge. McDowell MA, ed. *PLoS Negl Trop Dis*. 2013;7(7):e2330. doi:10.1371/journal.pntd.0002330
214. Ross PJ, Parks RJ. Construction and Characterization of Adenovirus Vectors. *Cold Spring Harb Protoc*. 2009;2009(5):pdb.prot5011. doi:10.1101/pdb.prot5011
215. Stojdl DF, Lichty BD, TenOever BR, et al. VSV strains with defects in their ability to shutdown innate immunity are potent systemic anti-cancer agents. *Cancer Cell*. 2003;4(4):263-275. doi:10.1016/S1535-6108(03)00241-1
216. Diallo J-S, Vähä-Koskela M, Le Boeuf F, Bell J. Propagation, Purification, and In Vivo Testing of Oncolytic Vesicular Stomatitis Virus Strains. In: *Methods in Molecular Biology (Clifton, N.J.)*. Vol 797. Methods Mol Biol; 2012:127-140. doi:10.1007/978-1-61779-340-0_10
217. Fukuda M. Lysosomal membrane glycoproteins. Structure, biosynthesis, and intracellular trafficking. *J Biol Chem*. 1991;266(32):21327-21330. http://www.ncbi.nlm.nih.gov/pubmed/1939168
218. Chang M, Karageorgos L, Meikle P. CD107a (LAMP-1) and CD107b (LAMP-2). *Bio Regul Homeost Agents*. 2002;16(2):147-151.
219. Aktas E, Kucuksezer UC, Bilgic S, Erten G, Deniz G. Relationship between CD107a expression and cytotoxic activity. *Cell Immunol*. 2009;254(2):149-154. doi:10.1016/j.cellimm.2008.08.007
220. Betts MR, Brenchley JM, Price DA, et al. Sensitive and viable identification of antigen-specific CD8+ T cells by a flow cytometric assay for degranulation. *J Immunol Methods*. 2003;281(1-2):65-78. doi:10.1016/S0022-1759(03)00265-5
221. Rubio V, Stuge TB, Singh N, et al. Ex vivo identification, isolation and analysis of tumor-cytolytic T cells. *Nat Med*. 2003;9(11):1377-1382. doi:10.1038/nm942
222. Wersto RP, Chrest FJ, Leary JF, Morris C, Stetler-Stevenson M, Gabrielson E. Doublet discrimination in DNA cell-cycle analysis. *Cytometry*. 2001;46(5):296-306. doi:10.1002/cyto.1171
223. Klein J. The Major Histocompatibility Complex of the Mouse. *Science (80-)*. 1979;203(4380):516-521. doi:10.1126/science.104386

224. Karandikar SH, Sidney J, Sette A, Selby MJ, Korman AJ, Srivastava PK. Identification of epitopes in ovalbumin that provide insights for cancer neoepitopes. *JCI Insight*. 2019;4(8). doi:10.1172/jci.insight.127882
225. Clarke SRm, Barnden M, Kurts C, Carbone FR, Miller JF, Heath WR. Characterization of the ovalbumin-specific TCR transgenic line OT-I: MHC elements for positive and negative selection. *Immunol Cell Biol*. 2000;78(2):110-117. doi:10.1046/j.1440-1711.2000.00889.x
226. Merritt RE, Yamada RE, Crystal RG, Korst RJ. Augmenting major histocompatibility complex class I expression by murine tumors in vivo enhances antitumor immunity induced by an active immunotherapy strategy. *J Thorac Cardiovasc Surg*. 2004;127(2):355-364. doi:10.1016/j.jtcvs.2003.09.007
227. Cho CH, Lee BK, Kwak SM, Kim JD. Monophosphoryl lipid A (MPL) upregulates major histocompatibility complex (MHC) class I expression by increasing interferon-gamma (IFN-γ). *Yonsei Med J*. 1999;40(1):20. doi:10.3349/ymj.1999.40.1.20
228. Carrio R, Bathe OF, Malek TR. Initial Antigen Encounter Programs CD8 + T Cells Competent to Develop into Memory Cells That Are Activated in an Antigen-Free, IL-7- and IL-15-Rich Environment. *J Immunol*. 2004;172(12):7315-7323. doi:10.4049/jimmunol.172.12.7315
229. Rubinstein MP, Lind NA, Purton JF, et al. IL-7 and IL-15 differentially regulate CD8+ T-cell subsets during contraction of the immune response. *Blood*. 2008;112(9):3704-3712. doi:10.1182/blood-2008-06-160945
230. Miller FR, Blazkovec AA. Cytolytic Activity in Vitro of Lymph Node Cells After Exposure in Vivo to Tumor Cells Suspended in Blocking Sera. *Immunol Commun*. 1979;8(2):193-202. doi:10.3109/08820137909048683
231. Lövgren T, Baumgaertner P, Wieckowski S, et al. Enhanced cytotoxicity and decreased CD8 dependence of human cancer-specific cytotoxic T lymphocytes after vaccination with low peptide dose. *Cancer Immunol Immunother*. 2012;61(6):817-826. doi:10.1007/s00262-011-1140-1
232. Sarafian V, Jadot M, Foidart J-M, et al. Expression of Lamp-1 and Lamp-2 and their interactions with galectin-3 in human tumor cells. *Int J Cancer*. 1998;75(1):105-111. doi:10.1002/(SICI)1097-0215(19980105)75:1<105::AID-IJC16>3.0.CO;2-F
233. Agarwal AK, Srinivasan N, Godbole R, et al. Role of tumor cell surface lysosome-associated membrane protein-1 (LAMP1) and its associated carbohydrates in lung metastasis. *J Cancer Res Clin Oncol*. 2015;141(9):1563-1574. doi:10.1007/s00432-015-1917-2
234. Osawa R, Tsunoda T, Yoshimura S, et al. Identification of HLA-A24-Restricted Novel T Cell Epitope Peptides Derived from P-Cadherin and Kinesin Family Member 20A. *J Biomed Biotechnol*. 2012;2012:1-10. doi:10.1155/2012/848042
235. Graff-Dubois S, Faure O, Gross D-A, et al. Generation of CTL Recognizing an HLA-A*0201-Restricted Epitope Shared by MAGE-A1, -A2, -A3, -A4, -A6, -A10, and -A12 Tumor Antigens: Implication in a Broad-Spectrum Tumor Immunotherapy. *J Immunol*. 2002;169(1):575-580. doi:10.4049/jimmunol.169.1.575
236. Nozaki M, Haraguchi S, Miyazaki T, et al. Expression of steroidogenic enzymes and metabolism of steroids in COS-7 cells known as non-steroidogenic cells. *Sci Rep*. 2018;8(1):2167. doi:10.1038/s41598-018-20226-2
237. Gourdain P, Boucau J, Kourjian G, Lai NY, Duong E, Le Gall S. A real-time killing assay

to follow viral epitope presentation to CD8 T cells. *J Immunol Methods*. 2013;398-399(1):60-67. doi:10.1016/j.jim.2013.09.009
238. Barber DL, Wherry EJ, Ahmed R. Cutting Edge: Rapid In Vivo Killing by Memory CD8 T Cells. *J Immunol*. 2003;171(1):27-31. doi:10.4049/jimmunol.171.1.27
239. Charles A Janeway J, Travers P, Walport M, Shlomchik MJ. T cell-mediated cytotoxicity. In: *Immunobiology: The Immune System in Health and Disease. 5th Edition.* 5th ed. Garland Science; 2001. Accessed July 24, 2021. https://www.ncbi.nlm.nih.gov/books/NBK27101/
240. Jiang X, Chen X, Carpenter TJ, et al. Development of a Target cell-Biologics-Effector cell (TBE) complex-based cell killing model to characterize target cell depletion by T cell redirecting bispecific agents. *MAbs*. 2018;10(6):876-889. doi:10.1080/19420862.2018.1480299
241. Dolnikov A, Klamer G, Chitranjan A, et al. Identifying the Factors Modulating the Efficacy of CAR-T Cell Therapy. *Blood*. 2014;124(21):5813-5813. doi:10.1182/blood.V124.21.5813.5813
242. Li G, Boucher JC, Kotani H, et al. 4-1BB enhancement of CAR T function requires NF-κB and TRAFs. *JCI Insight*. 2018;3(18). doi:10.1172/jci.insight.121322
243. Joly E, Hudrisier D. What is trogocytosis and what is its purpose? *Nat Immunol*. 2003;4(9):815-815. doi:10.1038/ni0903-815
244. Dance A. Core Concept: Cells nibble one another via the under-appreciated process of trogocytosis. *Proc Natl Acad Sci*. 2019;116(36):17608-17610. doi:10.1073/pnas.1912252116
245. Li G, Bethune MT, Wong S, et al. T cell antigen discovery via trogocytosis. *Nat Methods*. 2019;16(2):183-190. doi:10.1038/s41592-018-0305-7
246. Sharma G, Rive CM, Holt RA. Rapid selection and identification of functional CD8+ T cell epitopes from large peptide-coding libraries. *Nat Commun*. 2019;10(1):4553. doi:10.1038/s41467-019-12444-7
247. Caron E, Vincent K, Fortier M, et al. The MHC I immunopeptidome conveys to the cell surface an integrative view of cellular regulation. *Mol Syst Biol*. 2011;7(1):533. doi:10.1038/msb.2011.68
248. Hunt DF, Henderson RA, Shabanowitz J, et al. Characterization of Peptides Bound to the Class I MHC Molecule HLA-A2.1 by Mass Spectrometry. *Science (80-)*. 1992;255(5049):1261-1263. doi:10.1126/science.1546328
249. Woods AS, Huang AYC, Cotter RJ, Pasternack GR, Pardoll DM, Jaffee EM. Simplified High-Sensitivity Sequencing of a Major Histocompatibility Complex Class I-Associated Immunoreactive Peptide Using Matrix-Assisted Laser Desorption/Ionization Mass Spectrometry. *Anal Biochem*. 1995;226(1):15-25. doi:10.1006/abio.1995.1185
250. Cox AL, Skipper J, Chen Y, et al. Identification of a Peptide Recognized by Five Melanoma-Specific Human Cytotoxic T Cell Lines. *Science (80-)*. 1994;264(5159):716-719. doi:10.1126/science.7513441
251. Hofmann S, Glückmann M, Kausche S, et al. Rapid and Sensitive Identification of Major Histocompatibility Complex Class I-associated Tumor Peptides by Nano-LC MALDI MS/MS. *Mol Cell Proteomics*. 2005;4(12):1888-1897. doi:10.1074/mcp.M500076-MCP200
252. Iwamoto N, Shimada T. Recent advances in mass spectrometry-based approaches for proteomics and biologics: Great contribution for developing therapeutic antibodies.

Pharmacol Ther. 2018;185:147-154. doi:10.1016/j.pharmthera.2017.12.007
253. Freudenmann LK, Marcu A, Stevanović S. Mapping the tumour human leukocyte antigen (HLA) ligandome by mass spectrometry. *Immunology*. 2018;154(3):331-345. doi:10.1111/imm.12936
254. Murphy JP, Konda P, Kowalewski DJ, et al. MHC-I Ligand Discovery Using Targeted Database Searches of Mass Spectrometry Data: Implications for T-Cell Immunotherapies. *J Proteome Res*. 2017;16(4):1806-1816. doi:10.1021/acs.jproteome.6b00971
255. Frank AM. A Ranking-Based Scoring Function for Peptide−Spectrum Matches. *J Proteome Res*. 2009;8(5):2241-2252. doi:10.1021/pr800678b
256. Paul S, Weiskopf D, Angelo MA, Sidney J, Peters B, Sette A. HLA Class I Alleles Are Associated with Peptide-Binding Repertoires of Different Size, Affinity, and Immunogenicity. *J Immunol*. 2013;191(12):5831-5839. doi:10.4049/jimmunol.1302101
257. Nielsen M, Andreatta M. NetMHCpan-3.0; improved prediction of binding to MHC class I molecules integrating information from multiple receptor and peptide length datasets. *Genome Med*. 2016;8(1):33. doi:10.1186/s13073-016-0288-x
258. Lemay CG, Rintoul JL, Kus A, et al. Harnessing Oncolytic Virus-mediated Antitumor Immunity in an Infected Cell Vaccine. *Mol Ther*. 2012;20(9):1791-1799. doi:10.1038/mt.2012.128
259. Niavarani S-R, Lawson C, Boudaud M, Simard C, Tai L-H. Oncolytic vesicular stomatitis virus–based cellular vaccine improves triple-negative breast cancer outcome by enhancing natural killer and CD8 + T-cell functionality. *J Immunother Cancer*. 2020;8(1):e000465. doi:10.1136/jitc-2019-000465
260. Nguyen ONP, Grimm C, Schneider LS, et al. Two-Pore Channel Function Is Crucial for the Migration of Invasive Cancer Cells. *Cancer Res*. 2017;77(6):1427-1438. doi:10.1158/0008-5472.CAN-16-0852
261. Morettin A, Paris G, Bouzid Y, et al. Tudor Domain Containing Protein 3 Promotes Tumorigenesis and Invasive Capacity of Breast Cancer Cells. *Sci Rep*. 2017;7(1):5153. doi:10.1038/s41598-017-04955-4
262. Mancuso P, Tricarico R, Bhattacharjee V, et al. Thymine DNA glycosylase as a novel target for melanoma. *Oncogene*. 2019;38(19):3710-3728. doi:10.1038/s41388-018-0640-2
263. Hedrick E, Cheng Y, Jin U-H, Kim K, Safe S. Specificity protein (Sp) transcription factors Sp1, Sp3 and Sp4 are non-oncogene addiction genes in cancer cells. *Oncotarget*. 2016;7(16):22245-22256. doi:10.18632/oncotarget.7925
264. Porter HA, Perry A, Kingsley C, Tran NL, Keegan AD. IRS1 is highly expressed in localized breast tumors and regulates the sensitivity of breast cancer cells to chemotherapy, while IRS2 is highly expressed in invasive breast tumors. *Cancer Lett*. 2013;338(2):239-248. doi:10.1016/j.canlet.2013.03.030
265. Gartrell J, Pappo A. Recent advances in understanding and managing pediatric rhabdomyosarcoma. *F1000Research*. 2020;9:685. doi:10.12688/f1000research.22451.1
266. Milewski D, Pradhan A, Wang X, et al. FoxF1 and FoxF2 transcription factors synergistically promote rhabdomyosarcoma carcinogenesis by repressing transcription of p21Cip1 CDK inhibitor. *Oncogene*. 2017;36(6):850-862. doi:10.1038/onc.2016.254
267. Milewski D, Shukla S, Gryder BE, et al. FOXF1 is required for the oncogenic properties of PAX3-FOXO1 in rhabdomyosarcoma. *Oncogene*. 2021;40(12):2182-2199. doi:10.1038/s41388-021-01694-9
268. Swart M, Verbrugge I, Beltman JB. Combination Approaches with Immune-Checkpoint

Blockade in Cancer Therapy. *Front Oncol*. 2016;6:1. doi:10.3389/fonc.2016.00233
269. Mangsbo SM, Sandin LC, Anger K, Korman AJ, Loskog A, Tötterman TH. Enhanced Tumor Eradication by Combining CTLA-4 or PD-1 Blockade With CpG Therapy. *J Immunother*. 2010;33(3):225-235. doi:10.1097/CJI.0b013e3181c01fcb
270. Rodeberg D, Arndt C, Breneman J, et al. Characteristics and outcomes of rhabdomyosarcoma patients with isolated lung metastases from IRS-IV. *J Pediatr Surg*. 2005;40(1):256-262. doi:10.1016/j.jpedsurg.2004.09.045
271. Meza B, Ascencio F, Sierra-Beltrán AP, Torres J, Angulo C. A novel design of a multi-antigenic, multistage and multi-epitope vaccine against Helicobacter pylori: An in silico approach. *Infect Genet Evol*. 2017;49:309-317. doi:10.1016/j.meegid.2017.02.007
272. Nezafat N, Karimi Z, Eslami M, Mohkam M, Zandian S, Ghasemi Y. Designing an efficient multi-epitope peptide vaccine against Vibrio cholerae via combined immunoinformatics and protein interaction based approaches. *Comput Biol Chem*. 2016;62:82-95. doi:10.1016/j.compbiolchem.2016.04.006
273. Saadi M, Karkhah A, Nouri HR. Development of a multi-epitope peptide vaccine inducing robust T cell responses against brucellosis using immunoinformatics based approaches. *Infect Genet Evol*. 2017;51:227-234. doi:10.1016/j.meegid.2017.04.009
274. Tzelepis F, Birdi HK, Jirovec A, et al. Oncolytic Rhabdovirus Vaccine Boosts Chimeric Anti-DEC205 Priming for Effective Cancer Immunotherapy. *Mol Ther - Oncolytics*. 2020;19:240-252. doi:10.1016/j.omto.2020.10.007
275. Garcia V, Krishnan R, Davis C, et al. High-throughput Titration of Luciferase-expressing Recombinant Viruses. *J Vis Exp*. 2014;(91):e51890. doi:10.3791/51890
276. Kobie JJ, Treanor JJ, Ritchlin CT. Transient decrease in human peripheral blood myeloid dendritic cells following influenza vaccination correlates with induction of serum antibody. *Immunol Invest*. 2014;43(6):606-615. doi:10.3109/08820139.2013.871555
277. Waki K, Kawano K, Tsuda N, Komatsu N, Yamada A. CD4/CD8 ratio is a prognostic factor in IgG nonresponders among peptide vaccine-treated ovarian cancer patients. *Cancer Sci*. 2020;111(4):1124-1131. doi:10.1111/cas.14349
278. Davis KL, Fox E, Merchant MS, et al. Nivolumab in children and young adults with relapsed or refractory solid tumours or lymphoma (ADVL1412): a multicentre, open-label, single-arm, phase 1–2 trial. *Lancet Oncol*. 2020;21(4):541-550. doi:10.1016/S1470-2045(20)30023-1
279. Merchant MS, Wright M, Baird K, et al. Phase I Clinical Trial of Ipilimumab in Pediatric Patients with Advanced Solid Tumors. *Clin Cancer Res*. 2016;22(6):1364-1370. doi:10.1158/1078-0432.CCR-15-0491
280. Merchant MS, Bernstein D, Amoako M, et al. Adjuvant Immunotherapy to Improve Outcome in High-Risk Pediatric Sarcomas. *Clin Cancer Res*. 2016;22(13):3182-3191. doi:10.1158/1078-0432.CCR-15-2550
281. Krishnadas DK, Shusterman S, Bai F, et al. A phase I trial combining decitabine/dendritic cell vaccine targeting MAGE-A1, MAGE-A3 and NY-ESO-1 for children with relapsed or therapy-refractory neuroblastoma and sarcoma. *Cancer Immunol Immunother*. 2015;64(10):1251-1260. doi:10.1007/s00262-015-1731-3
282. Huang X, Park H, Greene J, et al. IGF1R- and ROR1-Specific CAR T Cells as a Potential Therapy for High Risk Sarcomas. Castresana JS, ed. *PLoS One*. 2015;10(7):e0133152. doi:10.1371/journal.pone.0133152
283. Dobrenkov K, Ostrovnaya I, Gu J, Cheung IY, Cheung N-K V. Oncotargets GD2 and

GD3 are highly expressed in sarcomas of children, adolescents, and young adults. *Pediatr Blood Cancer*. 2016;63(10):1780-1785. doi:10.1002/pbc.26097
284. Ghaffari-Nazari H, Tavakkol-Afshari J, Jaafari MR, Tahaghoghi-Hajghorbani S, Masoumi E, Jalali SA. Improving Multi-Epitope Long Peptide Vaccine Potency by Using a Strategy that Enhances CD4+ T Help in BALB/c Mice. Khodarahmi R, ed. *PLoS One*. 2015;10(11):e0142563. doi:10.1371/journal.pone.0142563
285. Callaway E. 'It will change everything': DeepMind's AI makes gigantic leap in solving protein structures. *Nature*. 2020;588(7837):203-204. doi:10.1038/d41586-020-03348-4
286. Yang J, Anishchenko I, Park H, Peng Z, Ovchinnikov S, Baker D. Improved protein structure prediction using predicted interresidue orientations. *Proc Natl Acad Sci*. 2020;117(3):1496-1503. doi:10.1073/pnas.1914677117
287. Hutson M. AI protein-folding algorithms solve structures faster than ever. *Nature*. Published online July 22, 2019. doi:10.1038/d41586-019-01357-6
288. Ashfaq UA, Saleem S, Masoud MS, et al. Rational design of multi epitope-based subunit vaccine by exploring MERS-COV proteome: Reverse vaccinology and molecular docking approach. Barozai MYK, ed. *PLoS One*. 2021;16(2):e0245072. doi:10.1371/journal.pone.0245072
289. Kar T, Narsaria U, Basak S, et al. A candidate multi-epitope vaccine against SARS-CoV-2. *Sci Rep*. 2020;10(1):10895. doi:10.1038/s41598-020-67749-1
290. Sanches RCO, Tiwari S, Ferreira LCG, et al. Immunoinformatics Design of Multi-Epitope Peptide-Based Vaccine Against Schistosoma mansoni Using Transmembrane Proteins as a Target. *Front Immunol*. 2021;12:490. doi:10.3389/fimmu.2021.621706
291. Pandey RK, Ojha R, Aathmanathan VS, Krishnan M, Prajapati VK. Immunoinformatics approaches to design a novel multi-epitope subunit vaccine against HIV infection. *Vaccine*. 2018;36(17):2262-2272. doi:10.1016/j.vaccine.2018.03.042
292. Lawson ND, Stillman EA, Whitt MA, Rose JK. Recombinant vesicular stomatitis viruses from DNA. *Proc Natl Acad Sci*. 1995;92(10):4477-4481. doi:10.1073/pnas.92.10.4477
293. Ognjanovic S, Linabery AM, Charbonneau B, Ross JA. Trends in childhood rhabdomyosarcoma incidence and survival in the United States, 1975-2005. *Cancer*. 2009;115(18):4218-4226. doi:10.1002/cncr.24465
294. Amer KM, Thomson JE, Congiusta D, et al. Epidemiology, Incidence, and Survival of Rhabdomyosarcoma Subtypes: SEER and ICES Database Analysis. *J Orthop Res*. 2019;37(10):2226-2230. doi:10.1002/jor.24387
295. Rubin BP, Nishijo K, Chen H-IH, et al. Evidence for an Unanticipated Relationship between Undifferentiated Pleomorphic Sarcoma and Embryonal Rhabdomyosarcoma. *Cancer Cell*. 2011;19(2):177-191. doi:10.1016/j.ccr.2010.12.023
296. Rudzinski ER, Anderson JR, Hawkins DS, Skapek SX, Parham DM, Teot LA. The World Health Organization Classification of Skeletal Muscle Tumors in Pediatric Rhabdomyosarcoma: A Report From the Children's Oncology Group. *Arch Pathol Lab Med*. 2015;139(10):1281-1287. doi:10.5858/arpa.2014-0475-OA
297. Malempati S, Hawkins DS. Rhabdomyosarcoma: Review of the Children's Oncology Group (COG) soft-tissue Sarcoma committee experience and rationale for current COG studies. *Pediatr Blood Cancer*. 2012;59(1):5-10. doi:10.1002/pbc.24118
298. Hawkins DS, Anderson JR, Mascarenhas L, et al. Vincristine, dactinomycin, cyclophosphamide (VAC) versus VAC/V plus irinotecan (VI) for intermediate-risk rhabdomyosarcoma (IRRMS): A report from the Children's Oncology Group Soft Tissue

Sarcoma Committee. *J Clin Oncol*. 2014;32(15_suppl):10004-10004. doi:10.1200/jco.2014.32.15_suppl.10004
299. Weigel BJ, Lyden E, Anderson JR, et al. Intensive Multiagent Therapy, Including Dose-Compressed Cycles of Ifosfamide/Etoposide and Vincristine/Doxorubicin/Cyclophosphamide, Irinotecan, and Radiation, in Patients With High-Risk Rhabdomyosarcoma: A Report From the Children's Oncology Group. *J Clin Oncol*. 2016;34(2):117-122. doi:10.1200/JCO.2015.63.4048
300. Schirrmacher V. From chemotherapy to biological therapy: A review of novel concepts to reduce the side effects of systemic cancer treatment (Review). *Int J Oncol*. 2019;54(2):407-419. doi:10.3892/ijo.2018.4661
301. Heske CM, Mascarenhas L. Relapsed Rhabdomyosarcoma. *J Clin Med*. 2021;10(4):804. doi:10.3390/jcm10040804
302. Vaddepally RK, Kharel P, Pandey R, Garje R, Chandra AB. Review of Indications of FDA-Approved Immune Checkpoint Inhibitors per NCCN Guidelines with the Level of Evidence. *Cancers (Basel)*. 2020;12(3):738. doi:10.3390/cancers12030738
303. Jenkins RW, Barbie DA, Flaherty KT. Mechanisms of resistance to immune checkpoint inhibitors. *Br J Cancer*. 2018;118(1):9-16. doi:10.1038/bjc.2017.434
304. Paston SJ, Brentville VA, Symonds P, Durrant LG. Cancer Vaccines, Adjuvants, and Delivery Systems. *Front Immunol*. 2021;12:985. doi:10.3389/fimmu.2021.627932
305. Zajac P, Schultz-Thater E, Tornillo L, et al. MAGE-A Antigens and Cancer Immunotherapy. *Front Med*. 2017;4(MAR). doi:10.3389/fmed.2017.00018
306. Chen YT, Scanlan MJ, Sahin U, et al. A testicular antigen aberrantly expressed in human cancers detected by autologous antibody screening. *Proc Natl Acad Sci U S A*. 1997;94(5):1914-1918. doi:10.1073/pnas.94.5.1914
307. Thomas R, Al-Khadairi G, Roelands J, et al. NY-ESO-1 Based Immunotherapy of Cancer: Current Perspectives. *Front Immunol*. 2018;9(MAY):947. doi:10.3389/fimmu.2018.00947
308. Arab A, Yazdian-Robati R, Behravan J. HER2-Positive Breast Cancer Immunotherapy: A Focus on Vaccine Development. *Arch Immunol Ther Exp (Warsz)*. 2020;68(1):2. doi:10.1007/s00005-019-00566-1
309. Antonarakis ES, Drake CG. Current status of immunological therapies for prostate cancer. *Curr Opin Urol*. 2010;20(3):241-246. doi:10.1097/MOU.0b013e3283381793
310. Bai R, Chen N, Li L, et al. Mechanisms of Cancer Resistance to Immunotherapy. *Front Oncol*. 2020;10:1290. doi:10.3389/fonc.2020.01290
311. Woodsworth DJ, Castellarin M, Holt RA. Sequence analysis of T-cell repertoires in health and disease. *Genome Med*. 2013;5(10):98. doi:10.1186/gm502
312. Zacharakis N, Chinnasamy H, Black M, et al. Immune recognition of somatic mutations leading to complete durable regression in metastatic breast cancer. *Nat Med*. 2018;24(6):724-730. doi:10.1038/s41591-018-0040-8
313. Vita R, Zarebski L, Greenbaum JA, et al. The Immune Epitope Database 2.0. *Nucleic Acids Res*. 2010;38(suppl_1):D854-D862. doi:10.1093/nar/gkp1004
314. Zhang L, Udaka K, Mamitsuka H, Zhu S. Toward more accurate pan-specific MHC-peptide binding prediction: a review of current methods and tools. *Brief Bioinform*. 2012;13(3):350-364. doi:10.1093/bib/bbr060
315. Nelson N, Lopez-Pelaez M, Palazon A, et al. A cell-engineered system to assess tumor cell sensitivity to CD8 + T cell-mediated cytotoxicity. *Oncoimmunology*. 2019;8(8):1-10. doi:10.1080/2162402X.2019.1599635

316. Fleri W, Paul S, Dhanda SK, et al. The Immune Epitope Database and Analysis Resource in Epitope Discovery and Synthetic Vaccine Design. *Front Immunol*. 2017;8(MAR):278. doi:10.3389/fimmu.2017.00278
317. Shugay M, Bagaev D V, Zvyagin I V, et al. VDJdb: a curated database of T-cell receptor sequences with known antigen specificity. *Nucleic Acids Res*. 2018;46(D1):D419-D427. doi:10.1093/nar/gkx760
318. Joglekar A V., Li G. T cell antigen discovery. *Nat Methods*. 2021;18(8):873-880. doi:10.1038/s41592-020-0867-z
319. Mann SE, Zhou Z, Landry LG, et al. Multiplex T Cell Stimulation Assay Utilizing a T Cell Activation Reporter-Based Detection System. *Front Immunol*. 2020;11:633. doi:10.3389/fimmu.2020.00633
320. Balan S, Radford KJ, Bhardwaj N. Unexplored horizons of cDC1 in immunity and tolerance. In: *Advances in Immunology*. Vol 148. Academic Press; 2020:49-91. doi:10.1016/bs.ai.2020.10.002
321. Trimble CL, Morrow MP, Kraynyak KA, et al. Safety, efficacy, and immunogenicity of VGX-3100, a therapeutic synthetic DNA vaccine targeting human papillomavirus 16 and 18 E6 and E7 proteins for cervical intraepithelial neoplasia 2/3: a randomised, double-blind, placebo-controlled phase 2b trial. *Lancet*. 2015;386(10008):2078-2088. doi:10.1016/S0140-6736(15)00239-1
322. Sahin U, Derhovanessian E, Miller M, et al. Personalized RNA mutanome vaccines mobilize poly-specific therapeutic immunity against cancer. *Nature*. 2017;547(7662):222-226. doi:10.1038/nature23003
323. Baumgaertner P, Costa Nunes C, Cachot A, et al. Vaccination of stage III/IV melanoma patients with long NY-ESO-1 peptide and CpG-B elicits robust CD8 + and CD4 + T-cell responses with multiple specificities including a novel DR7-restricted epitope. *Oncoimmunology*. 2016;5(10):e1216290. doi:10.1080/2162402X.2016.1216290
324. Perez CR, De Palma M. Engineering dendritic cell vaccines to improve cancer immunotherapy. *Nat Commun*. 2019;10(1):5408. doi:10.1038/s41467-019-13368-y
325. Butler M, Morel A-S, Jordan WJ, et al. Altered expression and endocytic function of CD205 in human dendritic cells, and detection of a CD205?DCL-1 fusion protein upon dendritic cell maturation. *Immunology*. 2007;120(3):362-371. doi:10.1111/j.1365-2567.2006.02512.x
326. Bhardwaj N, Friedlander PA, Pavlick AC, et al. Flt3 ligand augments immune responses to anti-DEC-205-NY-ESO-1 vaccine through expansion of dendritic cell subsets. *Nat Cancer*. 2020;1(12):1204-1217. doi:10.1038/s43018-020-00143-y
327. Ott PA, Hu Z, Keskin DB, et al. An immunogenic personal neoantigen vaccine for patients with melanoma. *Nature*. 2017;547(7662):217-221. doi:10.1038/nature22991
328. Shi T, Song X, Wang Y, Liu F, Wei J. Combining Oncolytic Viruses With Cancer Immunotherapy: Establishing a New Generation of Cancer Treatment. *Front Immunol*. 2020;11:683. doi:10.3389/fimmu.2020.00683
329. Li J, O'Malley M, Urban J, et al. Chemokine Expression From Oncolytic Vaccinia Virus Enhances Vaccine Therapies of Cancer. *Mol Ther*. 2011;19(4):650-657. doi:10.1038/mt.2010.312
330. Inoue T, Byrne T, Inoue M, et al. Oncolytic Vaccinia Virus Gene Modification and Cytokine Expression Effects on Tumor Infection, Immune Response, and Killing. *Mol Cancer Ther*. 2021;20(8):1481-1494. doi:10.1158/1535-7163.MCT-20-0863

331. Zemp F, Rajwani J, Mahoney DJ. Rhabdoviruses as vaccine platforms for infectious disease and cancer. *Biotechnol Genet Eng Rev*. 2018;34(1):122-138. doi:10.1080/02648725.2018.1474320
332. Chesney J, Puzanov I, Collichio F, et al. Randomized, Open-Label Phase II Study Evaluating the Efficacy and Safety of Talimogene Laherparepvec in Combination With Ipilimumab Versus Ipilimumab Alone in Patients With Advanced, Unresectable Melanoma. *J Clin Oncol*. 2018;36(17):1658-1667. doi:10.1200/JCO.2017.73.7379
333. Collins JM, Redman JM, Gulley JL. Combining vaccines and immune checkpoint inhibitors to prime, expand, and facilitate effective tumor immunotherapy. *Expert Rev Vaccines*. 2018;17(8):697-705. doi:10.1080/14760584.2018.1506332
334. Ji S, Lee J, Lee ES, Kim DH, Sin J-I. B16 melanoma control by anti-PD-L1 requires CD8+ T cells and NK cells: application of anti-PD-L1 Abs and Trp2 peptide vaccines. *Hum Vaccin Immunother*. 2021;17(7):1910-1922. doi:10.1080/21645515.2020.1866951
335. Danciu C, Oprean C, Coricovac DE, et al. Behaviour of four different B16 murine melanoma cell sublines: C57BL/6J skin. *Int J Exp Pathol*. 2015;96(2):73-80. doi:10.1111/iep.12114
336. Rausch J, Lopez PA, Bialojan A, et al. Combined immunotherapy: CTLA-4 blockade potentiates anti-tumor response induced by transcutaneous immunization. *J Dermatol Sci*. 2017;87(3):300-306. doi:10.1016/j.jdermsci.2017.06.013
337. Woo S-R, Turnis ME, Goldberg M V., et al. Immune Inhibitory Molecules LAG-3 and PD-1 Synergistically Regulate T-cell Function to Promote Tumoral Immune Escape. *Cancer Res*. 2012;72(4):917-927. doi:10.1158/0008-5472.CAN-11-1620
338. Dobson CC, Naing T, Beug ST, et al. Oncolytic virus synergizes with Smac mimetic compounds to induce rhabdomyosarcoma cell death in a syngeneic murine model. *Oncotarget*. 2017;8(2):3495-3508. doi:10.18632/oncotarget.13849
339. Leddon JL, Chen C-Y, Currier MA, et al. Oncolytic HSV virotherapy in murine sarcomas differentially triggers an antitumor T-cell response in the absence of virus permissivity. *Mol Ther - Oncolytics*. 2014;1:14010. doi:10.1038/mto.2014.10

Contributions of Collaborators

Dr. Silvia Boscardin (University of Sao Paulo) provided aDEC205-OVA and aDEC205-empty encoding plasmids. Dr. Boscardin also trained and assisted in the production of recombinant antibodies used in Chapters 2 and 4.

Patrick Murphy and Youra Kim from the lab of Dr. Shashi Gujar (Dalhousie University) performed MHC-I peptide elution, LC-MS/MS, *in silico* screening and provided raw output data for Table 2 and Table 3.

Dr. Robin Parks (The Ottawa Hospital Research Institute) provided all adenoviruses used in Chapter 2.

Dr. Fanny Tzelepis was crucial for performing, analysis and experimental assistance for the experiments in Figures 2-1 to 2-9, 3-1 to 3-7, and Appendix Figures 1-3.

Anna Jirovec was crucial for performing, analysis and experimental assistance for the experiments in Figures 2-1 to 2-9, 4-5C, 4-6, 4-7, 4-9, 4-10, 4-12 and Appendix 1-3, Appendix 11.

Andrew Chem assisted with all *in vivo* experiments for Chapters 2 and 4 and the production of VSV for Figure 4-7; this virus was also used in the experiments 4-9 to 4-12.

Christinao Tanese De Sousa from the lab of Dr. Rebecca Auer assisted with the *in vivo* experiments for Chapter 2.

Dr. Mohsen Hooshyar cloned and rescued the virus used in the experiment for Figure 2-9.

Dr. Serge Neault assisted in the molecular cloning of all engineered viruses used in Chapter 2, 3 and 4.

Keara Sutherland assisted in the cloning and rescue of the virus used in the experiment for Figure 2-9. Ms. Sutherland also assisted in the cloning of the virus depicted in Figure 4-8; this virus was also used in the experiments for Figure 4-9 to 4-12.

Dr. Daniel Serrano performed the experiments for Figure 3-11A, 4-7C and 4-11. Dr. Serrano also assisted with performing the experiments and analysis for Figure 3-11 and 4-10.

Nouf Alluqmani performed the experiments for Figure 4-9B, D and helped with experiments for Figure 4-2.

Anabel Bergeron helped with the experiment for Figure 4-2.

Zaid Taha assisted with performing the experiment for Figures 4-3 and 4-4 and rescued the virus depicted in Figure 4-8; this virus was also used in the experiments 4-9 to 4-12.

Boaz Wong performed the experiment for Figure 4-7B and assisting in performing the experiment for Figure 4-12B, C.

APPENDIX

Appendix I. Flow Cytometry Representative Gating Strategies

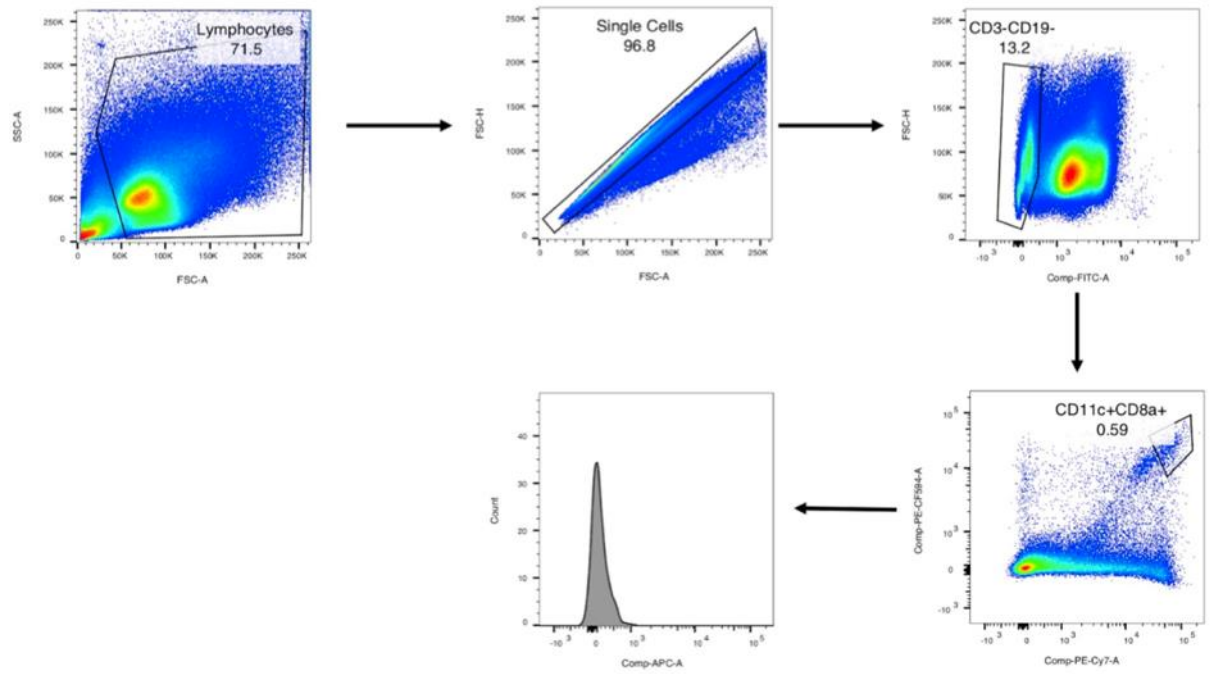

Appendix Figure 1. Gating strategy of binding assay to determine the binding efficacy of aDEC205-OVA to CD11c^{+}CD8^{+} DCs. The lymphocyte gate is set by the SSC-A v. FSC-A parameter. The next gates follow this order: singlets, CD3^{neg}CD19^{neg}, CD8^{+}CD11c^{+} then IgG^{+}

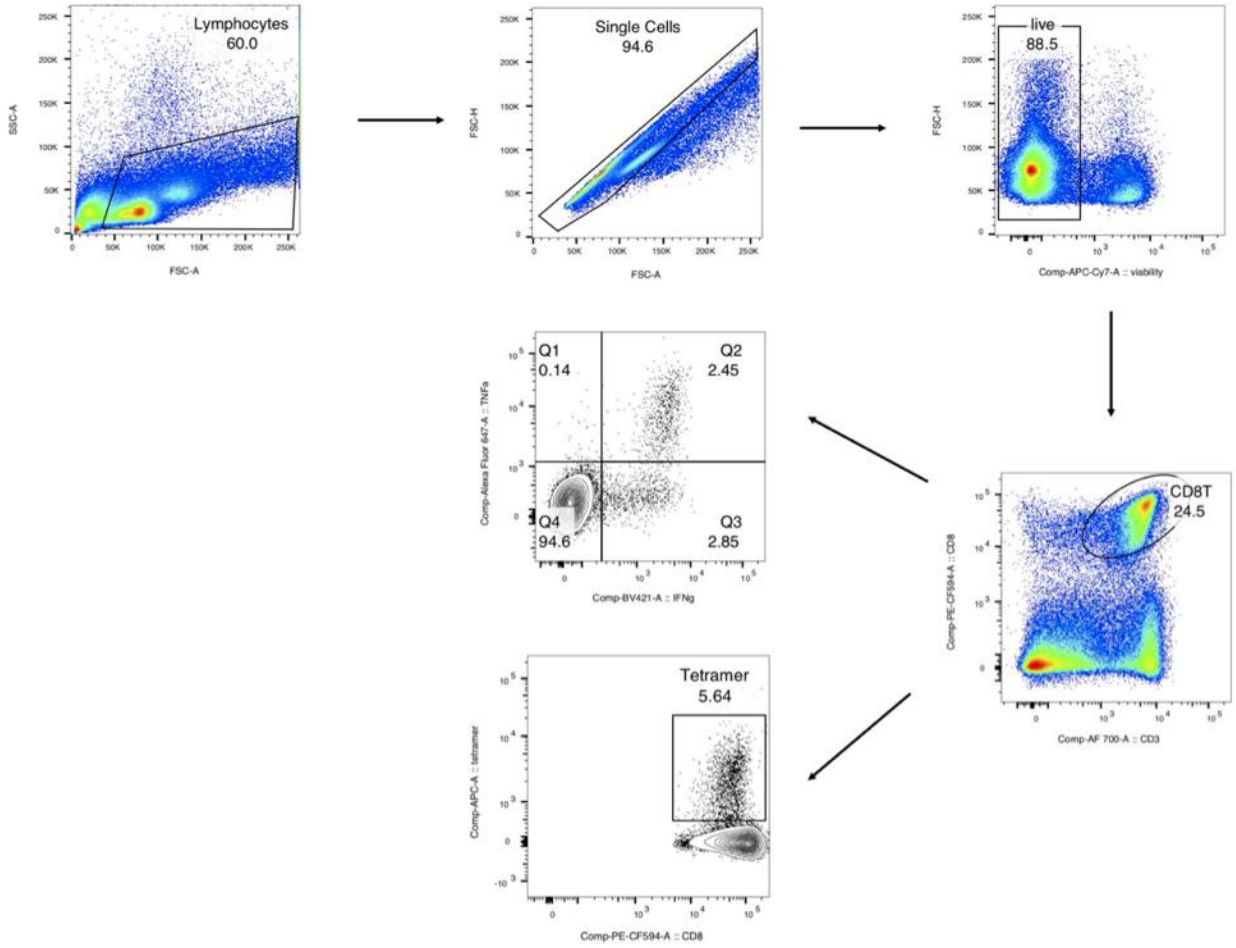

Appendix Figure 2. Gating strategy to determine percentage of $CD8^{+}CD3^{+}$ T cells producing IFNγ and TNFα or positive H2-K^{b}-SIINFEKL pentamer staining. The lymphocyte gate is set by the SSC-A v. FSC-A parameter. The next gates follow this order: singlets, live,$CD3^{ne+}CD8^{+}$,then either tetramer^{+} OR IFNγ^{+} and/or TNFα^{+}

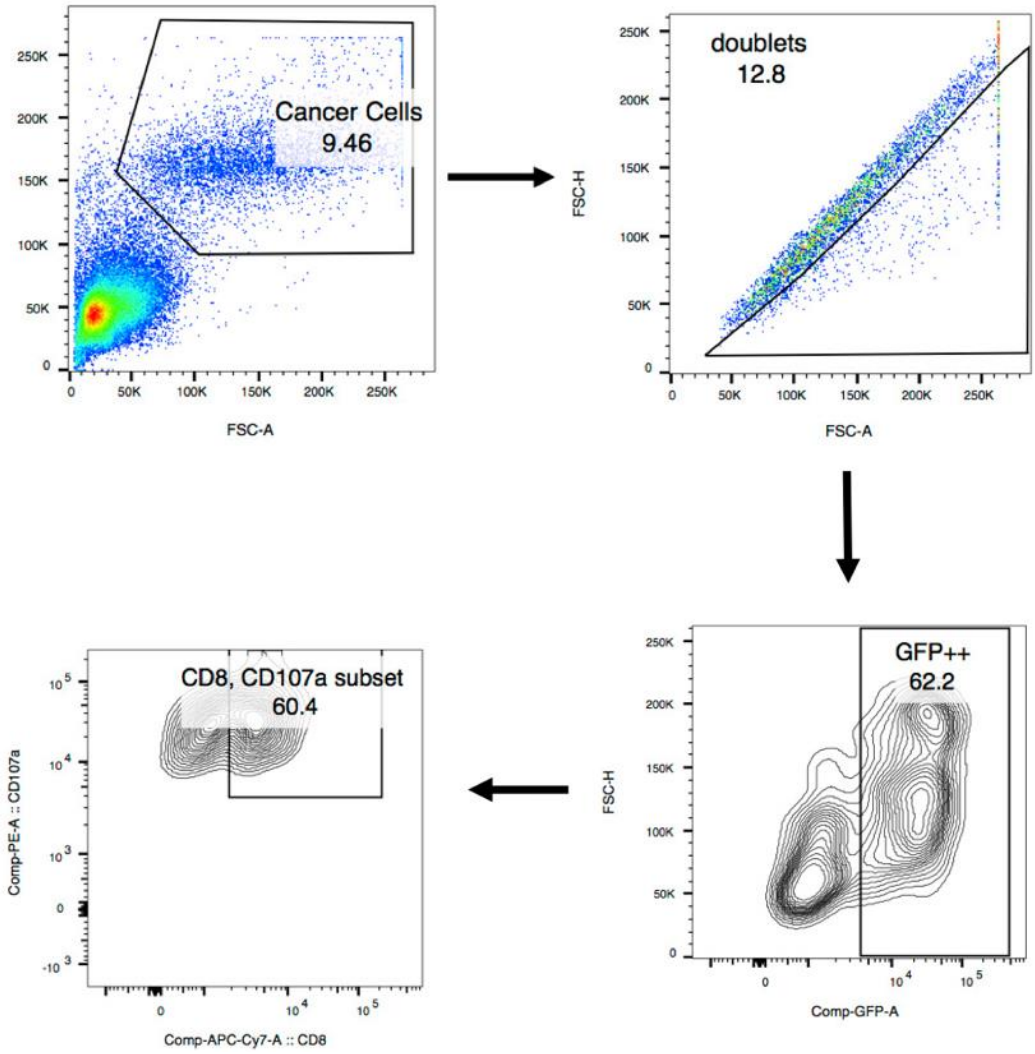

Appendix Figure 3. Representative gating strategy for the assessment of activated CTLs in immunological synapse (doublet). The target cell (B16 cancer cells) gate is set by the SSC-A v. FSC-A parameter. Doublet cells are visualized as populations with a diagonal shift in area and height parameters relative to singlets. The constituents of the doublet cells are determined by first gating on GFP+ cells, denoting target cells from which attached CTLs are characterized by the expression of CD8 and CD107a.

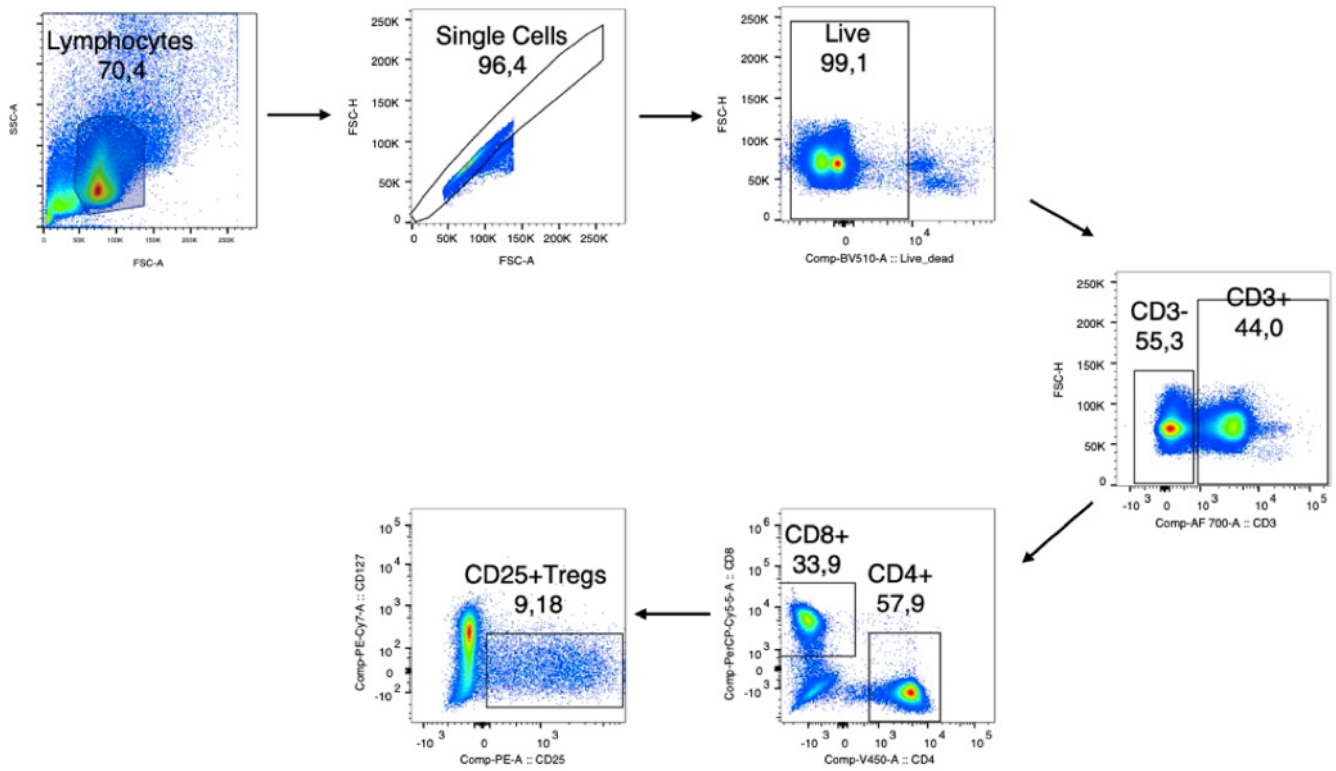

Appendix Figure 4. Gating strategy for Treg, CD4+ and CD8+ T cell visualization from spleen. The lymphocyte gate is set by the SSC-A v. FSC-A parameter. The next gates follow this order: singlets, live, $CD3^+$, then either $CD8^+$ or $CD4^+$ from which $CD25^+CD127^+$ Tregs are visualized.

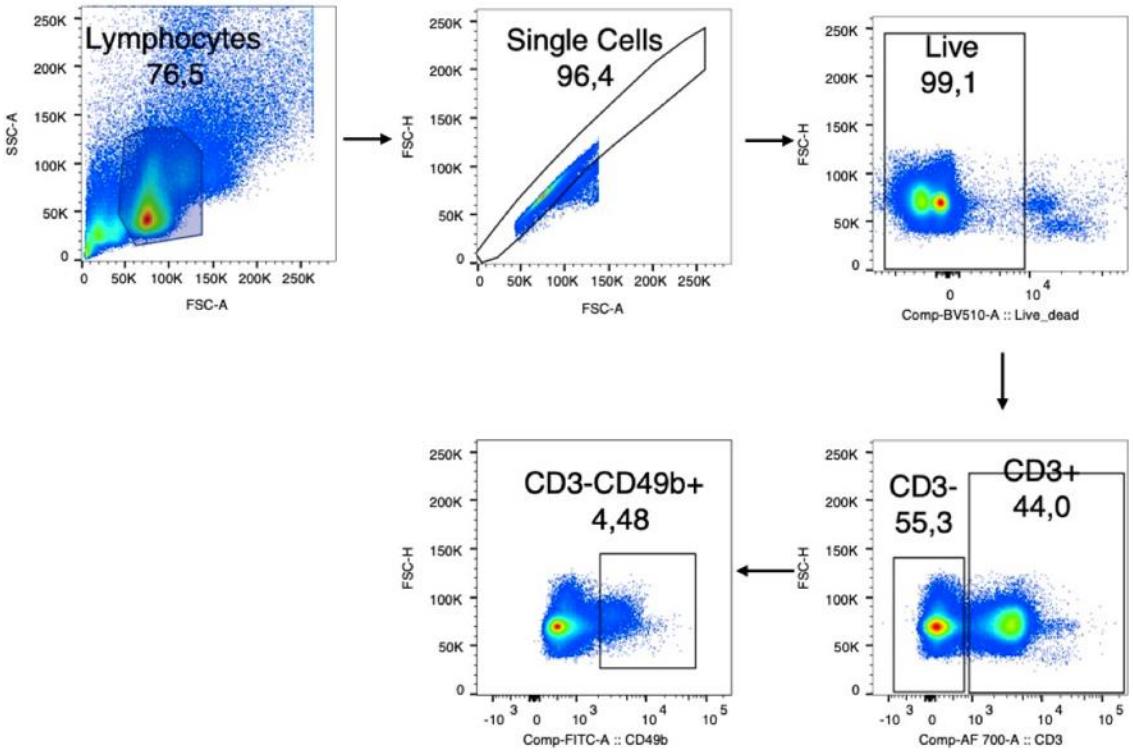

Appendix Figure 5. Gating strategy for NK cell visualization from spleen by flow cytometry. The lymphocyte gate is set by the SSC-A v. FSC-A parameter. The next gates follow this order: singlets, live, $CD3^-$, $CD49b^+$

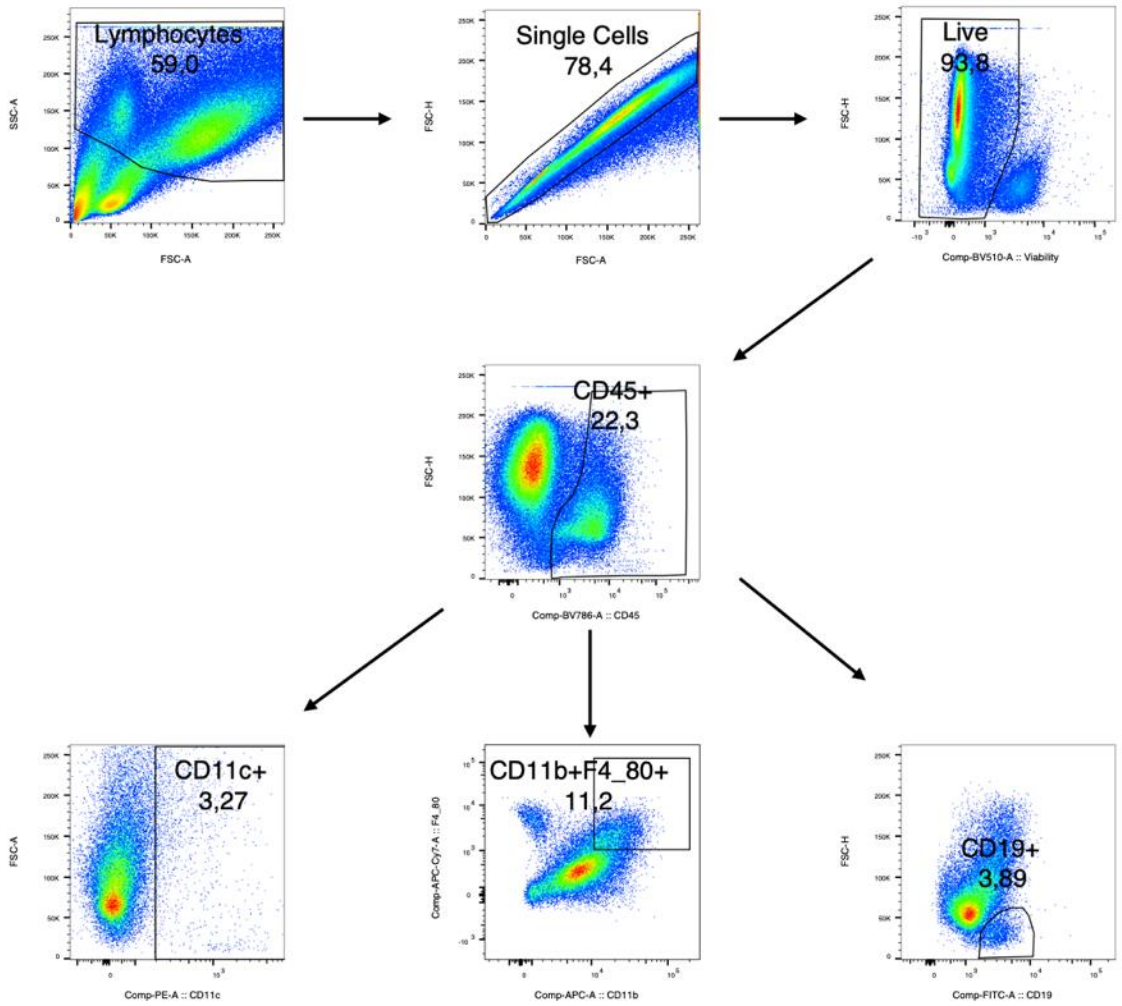

Appendix Figure 6. Gating strategy for leukocyte visualization in spleen by flow cytometry. The lymphocyte gate is set by the SSC-A v. FSC-A parameter. The next gates follow this order: singlets, live, $CD45^+$ then $CD11c^+$ for dendritic cells, $CD11b^+F4/80^+$ for macrophages and $CD19^+$ for B cells.

Appendix II. Supplemental Figures

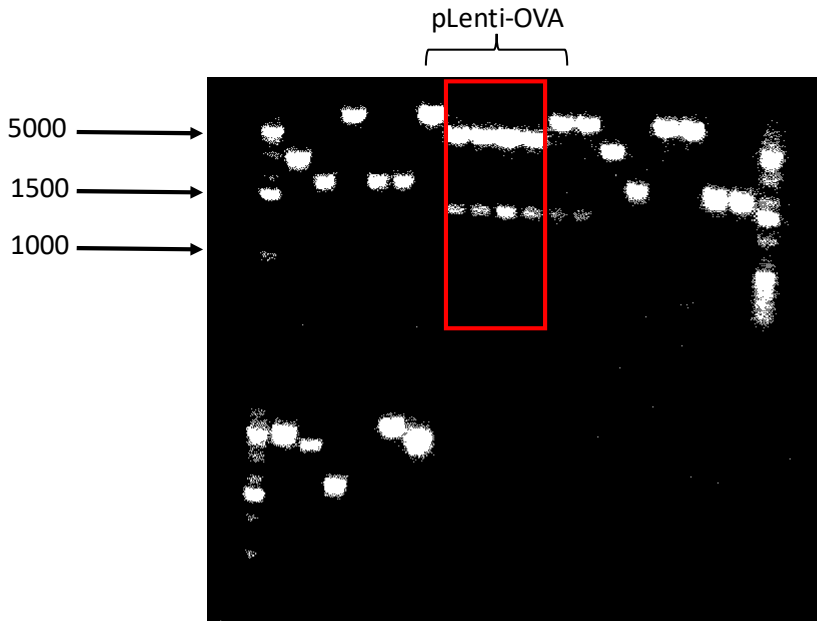

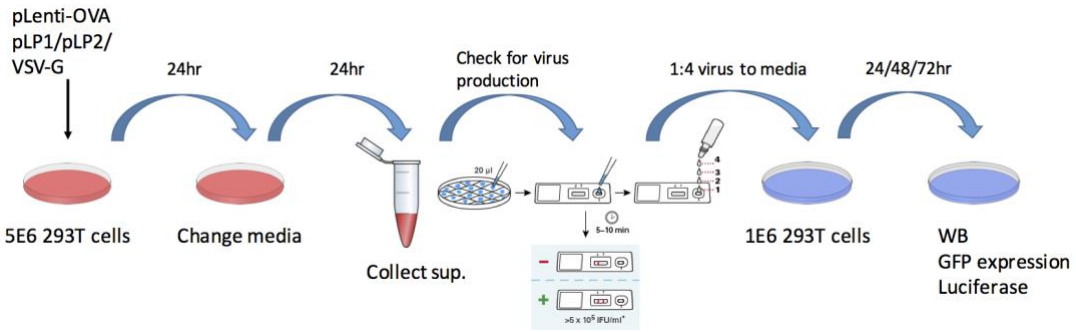

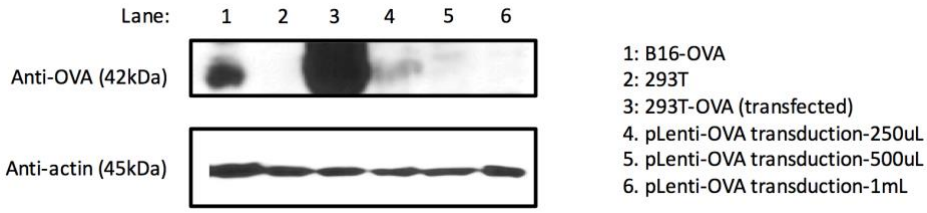

Appendix Figure 7. Molecular cloning and generation of lentivirus expressing OVA. Agarose gel with fragments of DNA from a restriction enzyme digest (BamHI, XbaI) of 4 predicted pLenti-OVA colonies. Lane 1: ladder, lanes 7-10: pLenti-OVA. b) Lentivirus production protocol following transfection using a standard lipofectamine method. c) Immunoblot for ovalbumin protein to confirm the presence of the protein in transfected (lane 3) and transduced (lanes 4-5) 293T cells.

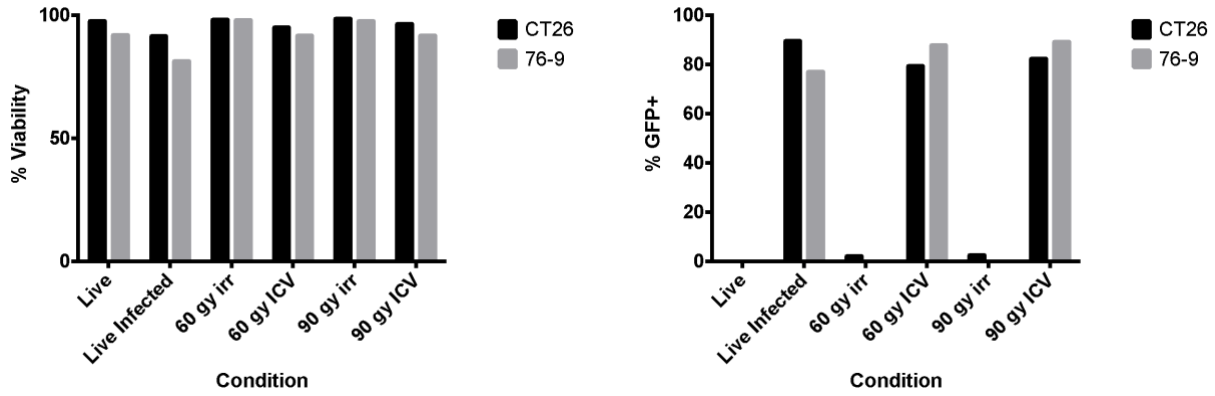

Appendix Figure 8. Irradiated and irradiated+VSVΔ51-GFP infected CT26WT and 76-9 cells retain viability after 60gy or 90gy of radiation as compared to live and also show GFP positivity. Briefly, $5x10^6$ CT26WT or 76-9 cells were subjected to 60gy or 90gy irradiation, stained with viability dye APC-Cy7 and acquired by flow cytometry. Previously irradiated CT26WT or 76-9 cells were also infected with VSVΔ51-GFP at an MOI of 10 for 2 hours and GFP+ signal was evaluated by flow cytometry.

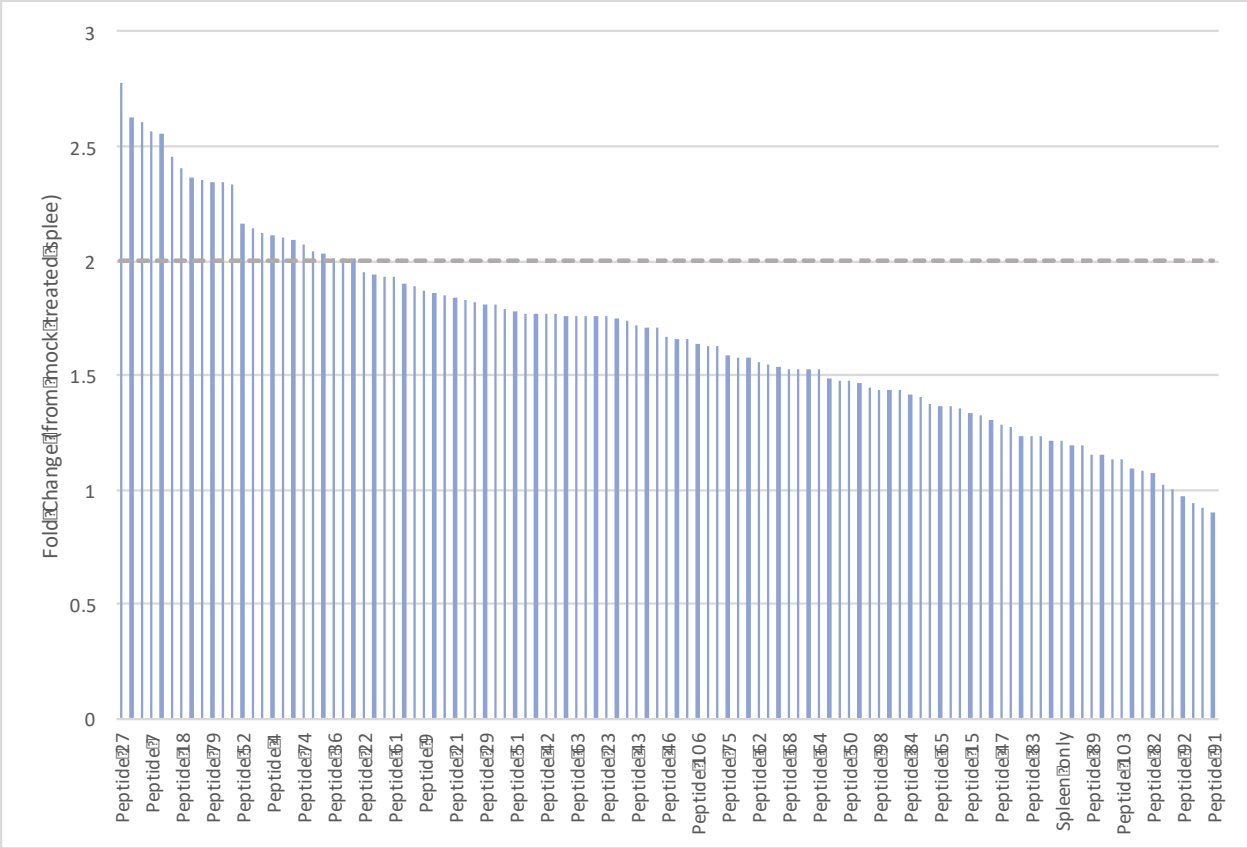

Appendix Figure 9. Fold change over mock of IFNγ production from splenocytes after stimulation with peptides. Lymphocytes from 76-9 ICV immunized mice were stimulated *in vitro* with 10ug/mL of each peptide. After 48 hours, the supernatant was harvested and assessed for the production of IFN-γ by cytokine ELISA.

A

Antibody	Concentration	Specification	Quantity	Yield
aDEC205_empty	1.00 mg/ml	200ug/vial	9vials	1.80mg/30ml
aDEC205_769	0.20mg/ml	0.18ml/vial	1vial	0.036mg/30ml

B

Antibody	Concentration	Specification	Quantity	Yield
aDEC205_769	0.13mg/ml	1.66ml/vial	3vials	0.65mg/200ml

C

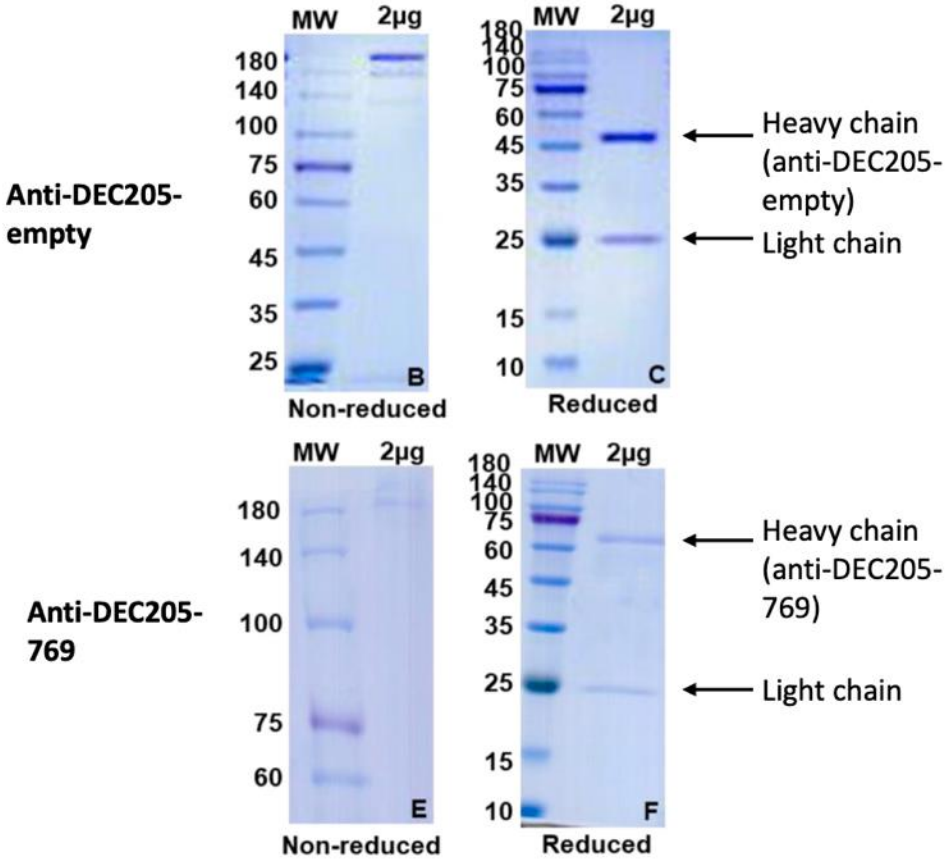

Appendix Figure 10. Proteogenix product report. Volumes and concentrations of aDEC205-empty and aDEC205-769 obtained in **A.** the first batch and **B.** the second batch. **C.** Immunoblotting of non-reduced (left) or reduced (right) antibodies depicting the heavy chain (50kDa in aDEC205-empty and 70kDa in aDEC205-769) and light chains (25kDa for both).

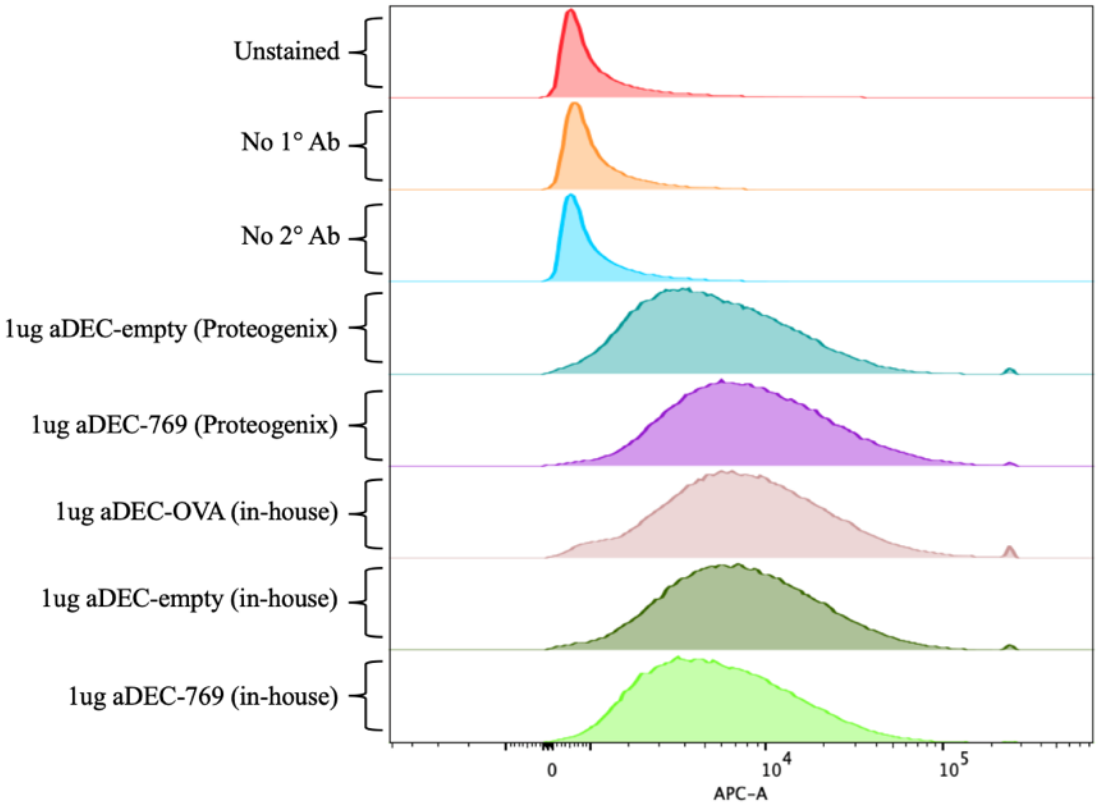

Appendix Figure 11. aDEC205-769 and aDEC205-empty produced by Proteogenix show similar binding capacity to the DEC205 receptor as the in-hosue produced antibodies. A binding assay was performed to verify the binding of 1ug of aDEC205-769 and 1ugaDEC205-empty from Proteogenix to the DEC205 receptor on JawsII cells, compared to the binding capacity of antibodies produced in-house (aDEC205-OVA, aDEC205-769 and aDEC205-empty). aDEC205 was probed with an anti-IgG1-APC antibody and detected by flow cytometry.

Appendix III. Sequences

DNA Sequence of Ovalbumin

ATGGGCTCCATCGGCGCAGCAAGCATGGAATTTTGTTTTGATGTATTCAAGGAGCTC
AAAGTCCACCATGCCAATGAGAACATCTTCTACTGCCCCATTGCCATCATGTCAGCT
CTAGCCATGGTATACCTGGGTGCAAAAGACAGCACCAGGACACAAATAAATAAGGT
TGTTCGCTTTGATAAACTTCCAGGATTCGGAGACAGTATTGAAGCTCAGTGTGGCAC
ATCTGTAAACGTTCACTCTTCACTTAGAGACATCCTCAACCAAATCACCAAACCAAA
TGATGTTTATTCCTTCAGCCTTGCCAGTAGACTTTATGCTGAAGAGAGATACCCAAT
CCTGCCAGAATACTTGCAGTGTGTGAAGGAACTGTATAGAGGAGGCTTGGAACCTA
TCAACTTTCAAACAGCTGCAGATCAAGCCAGAGAGCTCATCAATTCCTGGGTAGAA
AGTCAGACAAATGGAATTATCAGAAATGTCCTTCAGCCAAGCTCCGTGGATTCTCAA
ACTGCAATGGTTCTGGTTAATGCCATTGTCTTCAAAGGACTGTGGGAGAAAACATTT
AAGGATGAAGACACACAAGCAATGCCTTTCAGAGTGACTGAGCAAGAAAGCAAACC
TGTGCAGATGATGTACCAGATTGGTTTATTTAGAGTGGCATCAATGGCTTCTGAGAA
AATGAAGATCCTGGAGCTTCCATTTGCCAGTGGGACAATGAGCATGTTGGTGCTGTT
GCCTGATGAAGTCTCAGGCCTTGAGCAGCTTGAGAGTATAATCAACTTTGAAAAACT
GACTGAATGGACCAGTTCTAATGTTATGGAAGAGAGGAAGATCAAAGTGTACTTAC
CTCGCATGAAGATGGAGGAAAAATACAACCTCACATCTGTCTTAATGGCTATGGGC
ATTACTGACGTGTTTAGCTCTTCAGCCAATCTGTCTGGCATCTCCTCAGCAGAGAGC
CTGAAGATATCTCAAGCTGTCCATGCAGCACATGCAGAAATCAATGAAGCAGGCAG
AGAGGTGGTAGGGTCAGCAGAGGCTGGAGTGGATGCTGCAAGCGTCTCTGAAGAAT
TTAGGGCTGACCATCCATTCCTCTTCTGTATCAAGCACATCGCAACCAACGCCGTTC
TCTTCTTTGGCAGATGTGTTTCCCCTCTAGAGGGCCCGCGGTTCGAACAAAAACTCA
TCTCAGAAGAGGATCTGTAGTGA

Base DNA Sequence of aDEC205 antibody

ATG GGA TGG TCA TGT ATC ATC CTT TTT CTA GTA GCA ACT GCA ACT GGA GTA
CAT TCA GAG GTG AAG CTG TTG GAA TCT GGA GGA GGT TTG GTA CAG CCG GGG
GGT TCT CTG AGA CTC TCC TGT GCA GCT TCT GGA TTC ACC TTC AAT GAT TTC
TAC ATG AAC TGG ATC CGC CAG CCT CCA GGG CAG GCA CCT GAG TGG TTG GGT
GTT ATT AGA AAC AAA GGT AAT GGT TAC ACA ACA GAG GTC AAT ACA TCT GTG
AAG GGG CGG TTC ACC ATC TCC AGA GAT AAT ACC CAA AAC ATC CTC TAT CTT
CAA ATG AAC AGC CTG AGA GCT GAG GAC ACC GCC ATT TAC TAC TGT GCA AGA
GGC GGT CCT TAT TAC TAC AGT GGT GAC GAC GCC CCT TAC TGG GGC CAA GGA
GTC ATG GTC ACA GTC TCC TCA GCC ACC ACC AAG GGC CCA TCT GTC TAT CCA
CTG GCC CCT GGA TCT GCT GCC CAA ACT AAC TCC ATG GTG ACC CTG GGA TGC
CTG GTC AAG GGC TAT TTC CCT GAG CCA GTG ACA GTG ACC TGG AAC TCT GGA
TCC CTG TCC AGC GGT GTG CAC ACC TTC CCA GCT GTC CTG CAG TCT GAC CTC
TAC ACT CTG AGC AGC TCA GTG ACT GTC CCC TCC AGC ACC TGG CCC AGC GAG
ACC GTC ACC TGC AAC GTT GCC CAC CCG GCC AGC AGC ACC AAG GTG GAC AAG
AAA ATT GTG CCC AGG GAT TGT GGT TGT AAG CCT TGC ATA TGT ACA GTC CCA
GAA GTA TCA TCT GTC TTC ATC TTC CCC CCA AAG CCC AAG GAT GTG CTC ACC
ATT ACT CTG ACT CCT AAG GTC ACG TGT GTT GTG GTA GCA ATC AGC AAG GAT
GAT CCC GAG GTC CAG TTC AGC TGG TTT GTA GAT GAT GTG GAG GTG CAC ACA
GCT CAG ACG CAA CCC CGG GAG GAG CAG TTC AAC AGC ACT TTC CGC TCA GTC
AGT GAA CTT CCC ATC ATG CAC CAG GAC TGG CTC AAT GGC AAG GAG TTC AAA
TGC AGG GTC AAC AGT GCA GCT TTC CCT GCC CCC ATC GAG AAA ACC ATC TCC
AAA ACC AAA GGC AGA CCG AAG GCT CCA CAG GTG TAC ACC ATT CCA CCT CCC
AAG GAG CAG ATG GCC AAG GAT AAA GTC AGT CTG ACC TGC ATG ATA ACA GAC
TTC TTC CCT GAA GAC ATT ACT GTG GAG TGG CAG TGG AAT GGG CAG CCA GCG
GAG AAC TAC AAG AAC ACT CAG CCC ATC ATG GAC ACA GAT GGC TCT TAC TTC
GTC TAC AGC AAG CTC AAT GTG CAG AAG AGC AAC TGG GAG GCA GGA AAT ACT
TTC ACC TGC TCT GTG TTA CAT GAG GGC CTG CAC AAC CAC CAT ACT GAG AAG
AGC CTC TCC CAC TCT CCT GGT AAA

DNA sequence of 76-9 synthetic polypeptide

GCT AGC GAC ATG GCC AAG AAG GAG ACA CTC GAG GAG TTC GGT AGG TTC
CAT ACC TAC GTT CAT GCC ACC CTG GGC CCT GGC CCT GGC
AGC CAA CCC AAG AAT CTC GAC CCC GCG GGC CCT GGC CCT GGC
CGC TCA GTA CCC AAC TCT AGG GGC GAC TAT ATG GGC CCT GGC CCT GGC
GCG GGG CAT CGA AAC CGA GAG GTG CTG GGC CCT GGC CCT GGC
AGC GCT ACC AGT AAC CAG GAT ATA CTG GGC CCT GGC CCT GGC
AGC CAA TAC GTT TTC ACC GAA ATG GGC CCT GGC CCT GGC
ACC ATC TTC AAC TTT ATA ATC ACC GTG GGC CCT GGC CCT GGC
GTG CAA TAT ACT TTC GAT CTT CAA CTG GGC CCT GGC CCT GGC
AGC GGT CCA ATC AAT TTT ACT GTG TTT GGC CCT GGC CCT GGC
GCG ATC TTC GCC TTC CGC TGG GTG

Black: DEC heavy chain
Green: Peptide
Blue: Linker (GPGPG)

Amino Acid Sequence of aDEC205-769

Orange: CH1	Green: heavy chain-to-peptide linker
Pink: Hinge	Black: peptide(s)
Purple: CH2	**Bold: glycine-proline linker between**
Blue: CH3	**peptides**

MGWSCIILFLVATATGVHSEVKLLESGGGLVQPGGSLRLSCAASGFTFNDFYMNWIRQP
PGQAPEWLGVIRNKGNGYTTEVNTSVKGRFTISRDNTQNILYLQMNSLRAEDTAIYYCA
RGGPYYYSGDDAPYWGQGVMVTVSSATTKGPSVYPLAPGSAAQTNSMVTLGCLVKGY
FPEPVTVTWNSGSLSSGVHTFPAVLQSDLYTLSSSVTVPSSTWPSETVTCNVAHPASSTK
VDKKIVPRDCGCKPCICTVPEVSSVFIFPPKPKDVLTITLTPKVTCVVVAISKDDPEVQFS
WFVDDVEVHTAQTQPREEQFNSTFRSVSELPIMHQDWLNGKEFKCRVNSAAFPAPIEKT
ISKTKGRPKAPQVYTIPPPKEQMAKDKVSLTCMITDFFPEDITVEWQWNGQPAENYKNT
QPIMDTDGSYFVYSKLNVQKSNWEAGNTFTCSVLHEGLHNHHTEKSLSHSPGKASDMA
KKETLEEFGRFHTYVHATL**GPGPG**SQPKNLDPA**GPGPG**RSVPNSRGDYM**GPGPG**AGH
RNREVL**GPGPG**SATSNQDIL**GPGPG**SQYVFTEM**GPGPG**TIFNFIITV**GPGPG**VQYTFDL
QL**GPGPG**SGPINFTVF**GPGPG**AIFAFRWV

Appendix IV. Publications

Molecular Therapy
Oncolytics
Original Article

Oncolytic Rhabdovirus Vaccine Boosts Chimeric Anti-DEC205 Priming for Effective Cancer Immunotherapy

Fanny Tzelepis,[1,7] Harsimrat Kaur Birdi,[1,2,7] Anna Jirovec,[1,2,7] Silvia Boscardin,[3,4] Christiano Tanese de Souza,[1] Mohsen Hooshyar,[1] Andrew Chen,[1] Keara Sutherland,[1,2] Robin J. Parks,[2,6] Joel Werier,[5] and Jean-Simon Diallo[1,2]

[1]Centre for Innovative Cancer Research, Ottawa Hospital Research Institute, Ottawa, ON, Canada; [2]Department of Biochemistry, Microbiology and Immunology, University of Ottawa, Ottawa, ON, Canada; [3]Laboratory of Antigen Targeting to Dendritic Cells, Department of Parasitology, University of São Paulo, São Paulo, Brazil; [4]Institute for Investigation in Immunology (iii)-INCT, São Paulo, Brazil; [5]Department of Surgery, The Ottawa Hospital, Ottawa, ON, Canada; [6]Regenerative Medicine Program, Ottawa Hospital Research Institute, Ottawa, ON, Canada

Prime-boost vaccination employing heterologous viral vectors encoding an antigen is an effective strategy to maximize the antigen-specific immune response. Replication-deficient adenovirus serotype 5 (Ad5) is currently being evaluated clinically in North America as a prime in conjunction with oncolytic rhabdovirus Maraba virus (MG1) as a boost. The use of an oncolytic rhabdovirus encoding a tumor antigen elicits a robust anti-cancer immune response and extends survival in murine models of cancer. Given the prevalence of pre-existing immunity to Ad5 globally, we explored the potential use of DEC205-targeted antibodies as an alternative agent to prime antigen-specific responses ahead of boosting with an oncolytic rhabdovirus expressing the same antigen. We found that a prime-boost vaccination strategy, consisting of an anti-DEC205 antibody fused to the model antigen ovalbumin (OVA) as a prime and oncolytic rhabdovirus-OVA as a boost, led to the formation of a robust antigen-specific immune response and improved survival in a B16-OVA tumor model. Overall, our study shows that anti-DEC205 antibodies fused to cancer antigens are effective to prime oncolytic rhabdovirus-boosted cancer antigen responses and may provide an alternative for patients with pre-existing immunity to Ad5 in humans.

INTRODUCTION

As knowledge of the important role played by the immune system in preventing tumor growth in healthy individuals has expanded over the last decades, immunotherapy has emerged as a viable treatment option for cancer.[1] One form of immunotherapy that has gained recent regulatory approval employs oncolytic viruses (OVs). OVs are live, replicating viruses selected or genetically modified to preferentially target and kill cancer cells while leaving healthy cells relatively unharmed.[2] This is possible owing to the fact that cancers exhibit many characteristics that are conducive to successful viral replication, such as resistance to apoptosis, increased nucleotide synthesis, and an impaired antiviral response.[3] OVs elicit their anti-cancer effects through multiple mechanisms and following tumor cell lysis and immunogenic cell death, can trigger anti-cancer immune responses.[4] In addition to Imlygic, an intratumorally delivered oncolytic herpes simplex virus 1 (HSV-1) strain approved for treatment of late-stage melanoma, many different viruses have been clinically evaluated for their potential as OVs, including many that can be delivered intravenously (i.v.), such as (but not limited to) measles virus,[5] coxsackie virus,[6] and rhabdoviruses, like vesicular stomatitis virus (VSV) and the closely related Maraba virus (MG1).[7] Additional attenuating genetic modifications are generally introduced into OVs in order to increase their safety profile. For example, oncolytic rhabdoviruses are attenuated by deletion of the matrix protein in VSV (termed VSVΔ51) and mutation of components of the matrix and glycoproteins in MG1.[8] In addition, OVs can be genetically manipulated to encode proteins that either help to establish a productive infection of cancer cells or encode cytokines and/or immunogenic antigens, such as cancer antigens.

It is known that OVs can elicit *in situ* cancer vaccine effects and relieve local immunosuppression through the induction of immunostimulatory cytokines. In this environment, dendritic cells (DCs) can phagocytose dead/dying infected tumor cells and prime an anti-tumor as well as antiviral immune response in the draining lymph node.[9] However, the heterogeneous nature of cancer has resulted in limited efficacy of OVs as monotherapies and has steered researchers to investigate combinations of these biologics with other therapies that not only enhance OV infection of tumors but also enable anti-tumor immune responses.[10,11]

Typical vaccination regimens are generally not limited to a single dose and can be made more effective by multiple immunizations. This can involve the administration of additional homologous (matched

Received 15 January 2020; accepted 9 October 2020;
https://doi.org/10.1016/j.omto.2020.10.007.

[7]These authors contributed equally to this work.

Correspondence: Jean-Simon Diallo, Centre for Innovative Cancer Research, Ottawa Hospital Research Institute, 501 Smyth Road, C3128, Ottawa, ON K1H8L6, Canada.
E-mail: jsdiallo@ohri.ca

vaccine) or heterologous (unmatched vaccine) doses.[12] In the context of cancer vaccines, it has been recently shown that a heterologous prime-boost strategy, where an initial priming dose of an adenovirus virus encoding a cancer antigen is administered, followed by a boosting dose of an oncolytic rhabdovirus encoding the same antigen, can be effective to eradicate tumors.[13] This strategy has been shown to induce robust and long-term effector T cell responses[14,15] and is currently undergoing clinical evaluation for multiple antigens and indications (ClinicalTrials.gov: NCT02285816, NCT02879760, NCT03618953, and NCT03773744).

As a boosting component, oncolytic rhabdoviruses are thought to be uniquely effective because in addition to infecting tumor and breaking local immunosuppression, they efficiently, but nonproductively, infect splenic B cells, which provides an additional source for antigen presentation to DCs, resulting in secondary expansion of T cells.[16]

To prime the oncolytic rhabdovirus boost, current clinical trials employ a nonreplicating adenovirus serotype 5 (Ad5) vector expressing a shared cancer antigen (e.g., MAGE-A3, ClinicalTrials.gov: NCT02285816). Questions regarding the importance of vector seropositivity were raised recently following Merck's failed phase II clinical trial of a trivalent human immunodeficiency virus (HIV) vaccine delivered in an Ad5 vector.[17] Indeed, Ad5 seropositivity is sometimes an exclusion criterion in vaccine and gene-therapy clinical trials employing this vector.[18] Approximately 30%–40% of the North American population is seropositive for Ad5, and this proportion approaches an 85% average globally, posing a potential limitation to the widespread use of Ad5 as a priming vector for the oncolytic rhabdovirus heterologous prime-boost cancer immunotherapy strategy.[19–21]

DEC205 is a C-type lectin endocytic receptor highly expressed on certain DC subtypes.[22] Chimeric antibodies specific to DEC205 fused with an antigen of interest (anti-DEC205 [aDEC205]) have been shown to be an effective strategy to target fused antigens directly to DCs, inducing robust cellular and humoral responses when combined with adjuvants.[23,24] To overcome potential issues with Ad5 and other viruses that could be used as priming vectors but that may have the potential to be affected by pre-existing immunity, we hypothesized that chimeric aDEC205 antibodies could provide an effective alternative. In this study, we modeled and evaluated the impact of pre-existing immunity on Ad5-based priming. As proof of concept, we also evaluated a heterologous prime-boost vaccine strategy employing aDEC205-ovalbumin (OVA) as the priming agent, followed by a boost with OVA-expressing oncolytic rhabdoviruses in an experimental model of OVA-expressing B16 melanoma.

RESULTS

Pre-existing Immunity to Wild-Type Ad5 (WTAd5) Impairs Generation of a SIINFEKL-Specific Immune Response to Recombinant Ad5-SIINFEKL (rAd5-SIINFEKL)

We hypothesized that pre-existing immunity to WTAd5 may negatively affect priming of the immune response induced by rAd5-expressing antigens. To investigate this, we evaluated the capacity of Ad5 encoding the OVA epitope rAd5-SIINFEKL to generate an antigen-specific immune response in mice with pre-existing immunity to WTAd5. To model pre-existing immunity, we immunized naive C57BL/6 mice with 10^{10} plaque-forming units (PFU) of the WTAd5 virus. After 35 days, mice were administered 10^{8} PFUs rAd5-SIINFEKL intramuscularly (i.m.) (Figure 1A). Generation of anti-adenovirus neutralizing antibodies (AdNAbs) in sera of preimmunized mice 40 days postadministration of WTAd5 was confirmed by neutralization assay and was elevated in preimmunized mice (Figure 1B). SIINFEKL-specific $CD8^+$ T cell responses were measured 10 days after rAd5-SIINFEKL immunization, the peak time of the adaptive immune response elicited by adenovirus vectors.[25] We observed a statistically significant decrease from 10% to approximately 5% of splenic SIINFEKL-specific $CD8^+$ T cells, depicted by $H2K^b$-SIINFEKL pentamer staining, from preimmunized mice compared to control phosphate-buffered saline (PBS) mice (Figures 1C and 1D). To assess $CD8^+$ T cell functionality, splenocytes from preimmunized mice and PBS mice were restimulated with SIINFEKL peptide *in vitro* and followed by intracellular cytokine staining (ICS) for interferon (IFN)-γ and tumor necrosis factor (TNF)-α. Again, there was a reduction from an average of 6% to 2% of IFN-γ- and TNF-α-producing $CD8^+$ T cells specific to SIINFEKL detected in the splenocytes from preimmunized mice compared to control PBS (Figures 1E and 1F). Together, these results indicate that modeled pre-existing immunity to WTAd5 limits the generation of SIINFEKL-specific cellular responses following rAd5-SIINFEKL immunization in C57BL/6 mice.

Production and Characterization of aDEC205-OVA

Impaired SIINFEKL-specific immune responses following rAd5-SIINFEKL immunization of C57BL/6 mice modeling pre-existing immunity led us to consider employing an alternative priming agent that would be better able to overcome pre-existing immunity to WTAd5 and other potential alternative viral vectors. Several studies have shown the ability of chimeric aDEC205 antibodies fused to antigens, such as OVA (aDEC205-OVA) or tumor antigens, to elicit strong antigen-specific immune responses in mice when administered with an adjuvant.[26,27] To evaluate the use of antigen-fused aDEC205 antibodies as alternative priming agents for heterologous boosting with Oncolytic rhabdovirus (ORV) vectors, we used aDEC205 fused to the model antigen OVA.

To generate the aDEC205 antibodies used in this study, human embryonic kidney (HEK)293T cells were cotransfected with plasmids containing the mouse aDEC205-kappa light chain and the aDEC205 heavy chain fused to the full OVA protein sequence at the carboxyl terminus (or no antigen as a control [aDEC205-empty]). The recombinant antibodies produced following transient transfection in HEK293T cell were purified on protein G Sepharose columns.

The resulting antibodies were characterized by western blot using anti-immunoglobulin G (IgG) antibodies on SDS-PAGE under reducing conditions (Figure 2A). Figure 2A shows that heavy and light chains of the purified recombinant antibodies had the expected size for both the fused antibody (Ab) aDEC205-OVA (~95 kDa and 25 kDa, respectively) and control antibody aDEC205-empty (50 kDa

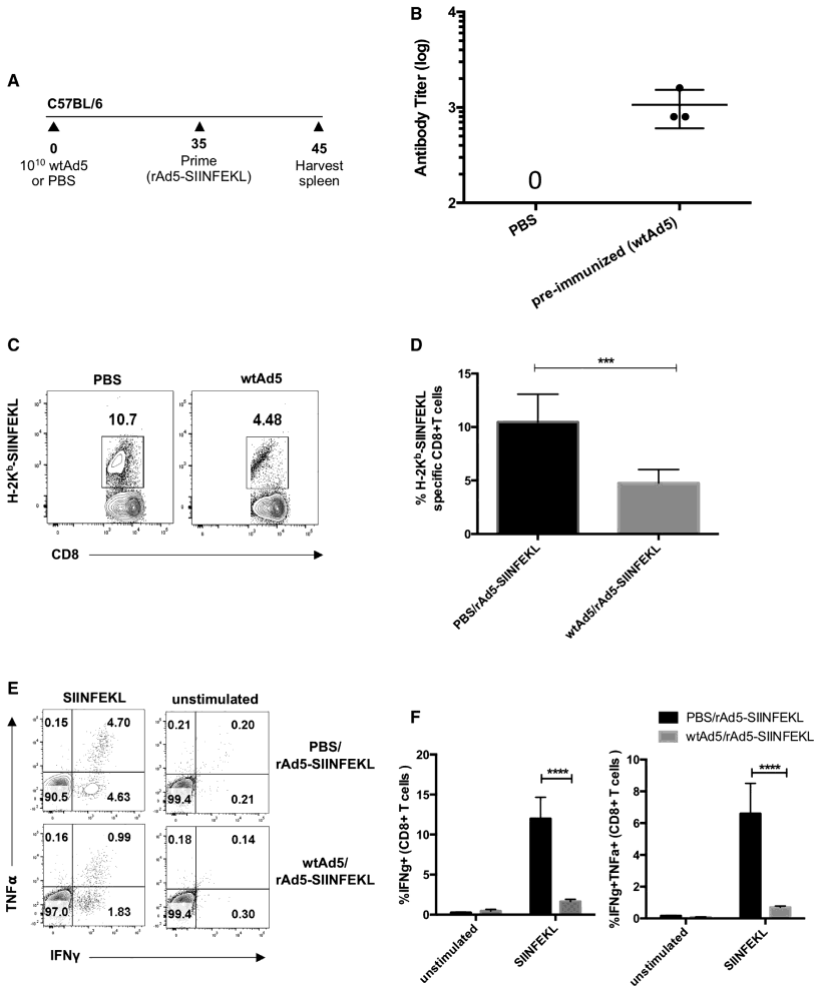

Figure 1. Comparing the SIINFEKL-Specific T Cell Response after i.m. Injection of Priming Agent Recombinant Adenovirus Expressing the SIINFEKL Transgene (rAd5-SIINFEKL) in Mice Modeling Pre-existing Immunity to WTAd5

(A) Naive C57BL/6 mice were injected i.m. on day 0 with 10^{10} PFUs of WTAd5 (n = 7) or PBS (n = 5). After 35 days, mice were injected i.m. with rAd5-SIINFEKL. (B) Anti-adenovirus neutralizing antibody (AdNAbs) titers in mouse sera (n = 3) were determined by neutralization assay, 40 days after administration of WTAd5.10 days after prime, the representative gating (C) and total percentage of (D) SIINFEKL-specific $CD8^+$ T cells in the spleen was determined by H2-K^b-SIINFEKL pentamer staining.The representative gating (E) and percentage of (F) OVA-specific T cells producing IFN-γ and TNF-α in the spleen was evaluated by flow cytometry. Briefly, splenocytes were stimulated *in vitro* with MHC-I epitope (SIINFEKL) for 5 h, subsequently stained for intracellular production of IFN-γ and TNF-α, and assessed by flow cytometry. $^{***}p < 0.001$ and $^{****}p < 0.0001$ (two-way ANOVA).

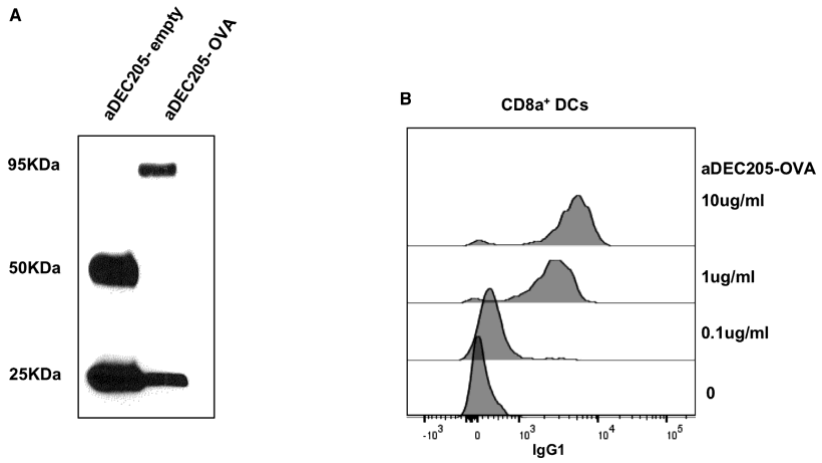

Figure 2. Production and Characterization of aDEC205-OVA

(A) aDEC205-OVA and aDEC205-empty were generated by transfection of 293T cells *in vitro* and subsequent purification of the antibody. (A) Final antibody product was reduced by β-mercaptoethanol and verified by immunoblotting for the heavy and light chains. aDEC205-empty shows a heavy chain at 50 kDa and light chain at 25 kDa. aDEC205-OVA shows the heavy chain linked with OVA at 95 kDa, indicating the presence of OVA antigen and a light chain at 25 kDa. (B) A binding assay was performed to verify effective binding of aDEC205-OVA to the DEC205 receptor on $CD11c^+CD8^+$ dendritic cells (DCs) isolated from murine splenocytes. aDEC205-OVA is probed with an anti-IgG1-APC antibody and detected by flow cytometry. The histogram overlay depicts high binding of aDEC205-OVA to $CD11c^+CD8^+$ DCs at concentrations of 10 μg/mL and 1 μg/mL and low binding at 0.1 μg/mL.

and 25 kDa, respectively). The capacity of the aDEC205-OVA and aDEC205-empty antibodies to bind to its receptor on the surface of splenic DCs $CD11c^+CD8a^+$ was confirmed with a binding assay.[28] Incubation of splenocytes from naive C57BL/6 mice with different concentrations of aDEC205-OVA (0.1, 1, or 10 μg/mL) resulted in a dose-dependent binding (Figure 2B) on the surface of splenic $CD11c^+CD8a^+$ DCs (gating strategy shown in Figure S1) expressing the DEC205 receptor. These results indicate that aDEC205-OVA and aDEC205-empty were successfully purified from culture supernatants and that aDEC205-OVA and aDEC205-empty (Figure S2) retain binding capacity to the DEC205 receptor as expected.

aDEC205-OVA Administered via Intraperitoneal (i.p.) and i.v. Routes Generates Cellular Immune Responses against SIINFEKL

Several studies demonstrated the influence of the route of immunization on immune response and disease outcome.[29] To determine which route of aDEC205-OVA administration leads to the most potent T cell response systemically, we immunized naive C57BL/6 mice i.p. or i.v. with 10 μg aDEC205-OVA or aDEC205-empty, both in combination with 50 μg poly(I:C) and 50 μg anti-CD40. SIINFEKL-specific T cells were evaluated by flow cytometry at 10 and 21 days postimmunization (Figure 3A; gating strategy shown in Figure S3). ICS, after *in vitro* restimulation of lymphocytes with the SIINFEKL peptide, showed that i.v. and i.p. routes of administration elicited statistically similar percentages of IFN-γ- and TNF-α-producing $CD8^+$ T cells in the lung and spleen of mice immunized with aDEC205-OVA at days 10 and 21 postimmunization (Figures 3B–3D; Figure S4). Additionally, staining with the $H2K^b$-SIINFEKL pentamer showed statistically similar percentages of SIINFEKL-specific $CD8^+$ T cells at day 21 in the spleen and lung of mice immunized with aDEC205-OVA when comparing i.v. and i.p. routes of administration (Figures 3E; Figure S4). As expected, no SIINFEKL-specific $CD8^+$ T cells were detected in the spleen or lungs of animals immunized with control aDEC205-empty. These results indicate that either route of administration elicits a strong anti-SIINFEKL primary immune response. Ultimately, to model a preferred route of administration in humans, we proceeded to administer aDEC205-OVA i.v. for the remainder of this study.

aDEC205-OVA Overcomes Barriers Posed by Pre-existing Immunity and Generates Cellular and Humoral Immunity against OVA

We next evaluated the ability of aDEC205-OVA to overcome pre-existing immunity to WTAd5 in a C57BL/6 murine model. To model pre-existing immunity, all naive C57BL/6 mice were immunized with WTAd5 35 days prior to the injection of priming agents (Figure 4A). As previously observed, AdNAbs were detected by a neutralization assay in mouse sera 40 days postadministration of WTAd5 and were elevated in preimmunized mice around time of prime

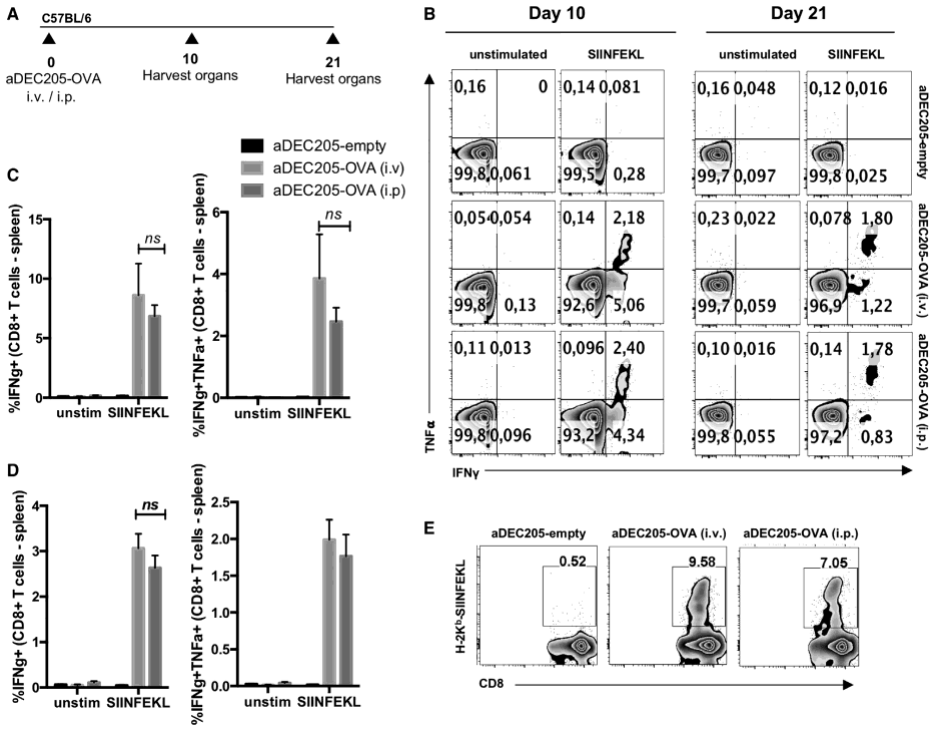

Figure 3. aDEC205-OVA Administered i.v. or i.p. Elicits OVA-Specific T Cells in the Spleen of Immunized Mice

(A) Naive C57BL/6 mice were primed with 10 μg of aDEC205-OVA or aDEC205-empty + 50 μg poly(I:C) + 50 μg anti-CD40 i.v. or i.p. The percentage of SIINFEKL-specific T cells producing IFN-γ and TNF-α in the spleen (B) on day 10 (C) and on day 21 (D) was evaluated by flow cytometry. (E) Quantification of SIINFEKL-specific T cells by pentamer staining (H-2K^b-SIINFEKL) was also assessed in the spleen by flow cytometry at day 21 postinjection. p value was considered nonsignificant (ns) when >0.05 (two-way ANOVA).

(Figure 1B). Pre-existing immunity to WTAd5 did not affect priming with aDEC205-OVA; approximately 9% of SIINFEKL-specific CD8$^+$ T cells were observed in the spleen of preimmunized mice and control PBS mice 10 days after prime (Figures 4B and 4C). Furthermore, a similar percentage of splenic IFN-γ- and TNF-α-producing CD8$^+$ T cells specific to SIINFEKL was also detected by intracellular staining (Figures 4D and 4E). Together with Figure 1, these results suggest that adjuvanted aDEC205 is an effective prime in the face of pre-existing immunity to WTAd5.

Heterologous Boosting of aDEC205-OVA Prime with Rhabdovirus-Encoding OVA Potentiates a Cellular and Humoral Immune Response

Priming with Ad5 encoding a cancer antigen, followed by boosting with ORV vectors, such as MG1 or VSV, expressing the same antigen, induces strong antigen-specific responses, providing survival benefit in various tumor models.[11–15] Therefore, we tested the ability of the combination aDEC205-OVA prime and MG1-OVA boost in the generation of a SIINFEKL-specific T cell response. To this end, naive C57BL/6 mice were primed (i.v.) with 10 μg aDEC205-OVA or aDEC205-empty, both in combination with 50 μg poly(I:C) and 50 μg anti-CD40 and boosted (i.v.) 14 days later with 10^8 PFUs of MG1-OVA or 10 μg aDEC205-OVA with 50 μg poly(I:C) and 50 μg anti-CD40 or PBS. 7 and 14 days after boost, lymphocytes were harvested from the spleen and lung and then stained with the H2K^b-SIINFEKL pentamer. At days 7 and 14 postboost, the greatest expansion of SIINFEKL-specific T cells was observed in the spleen (Figures 5A–5E) and lungs (Figure S5) of animals boosted with MG1-OVA. Similar results were obtained using VSV-OVA (Figures S6A and S6B). Although boost with aDEC205-OVA expanded the

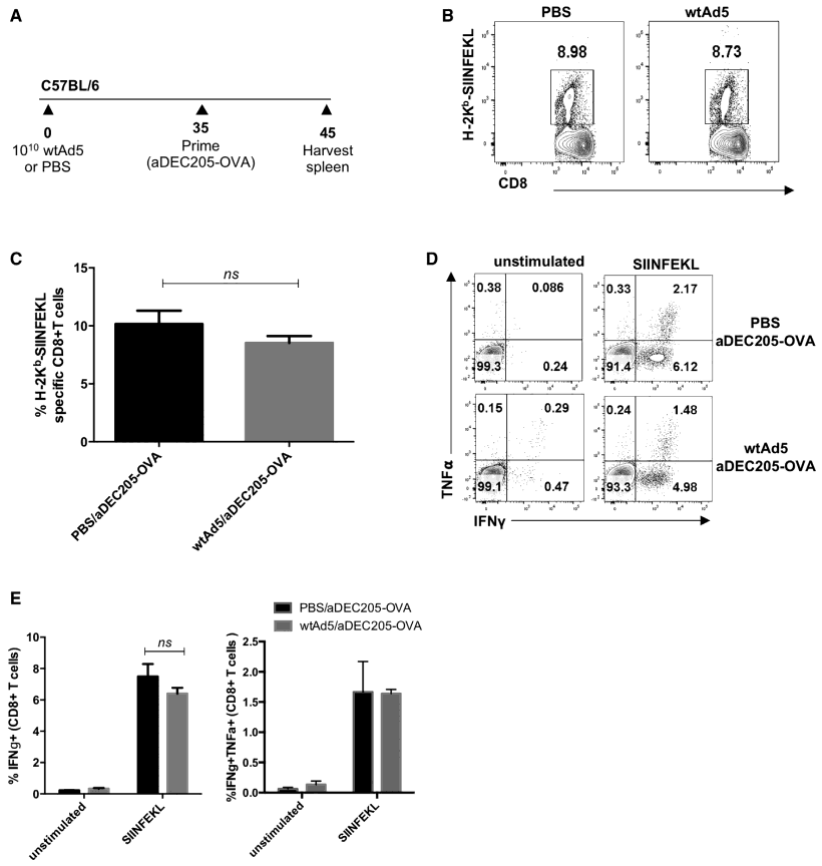

Figure 4. Pre-existing Immunity to Adenovirus Does Not Affect an Immune Response Elicited by aDEC205-OVA Prime

(A) Naive C57BL/6 mice were injected i.m. on day 0 with 10^{10} PFUs of WTAd5 or PBS. (B and C) After 35 days, mice were injected i.v. with 10 μg of aDEC205-OVA + 50 μg poly(I:C) + 50 μg anti-CD40. 10 days after priming, the representative gating (B) and percentage of (C) SIINFEKL-specific $CD8^+$ T cells in the spleen was determined by H2-K^b-SIINFEKL pentamer staining. The representative gating (D) and percentage of (E) SIINFEKL-specific T cells producing IFN-γ and TNF-α in the spleen was also evaluated by ICS and flow cytometry. p value was considered nonsignificant when >0.05 (two-way ANOVA).

antigen-specific cells compared to the group only primed with aDEC205-OVA, the level of expansion was significantly lower compared to MG1-OVA. Humoral immunity was also assessed using mouse sera to quantify OVA-specific IgG by ELISA. The combination of aDEC205-OVA/MG1-OVA prime-boost generated the highest anti-OVA antibody titers compared to other combinations and control groups (Figure 5F). Immunization with aDEC205-OVA/VSV-OVA prime-boost generated similar antibody titers compared to aDEC205-OVA/MG1-OVA prime-boost at day 7 postboost (Figure S6C).

Heterologous Prime-Boost Vaccine with aDEC205-OVA and Rhabdovirus-Encoding OVA Confers a Survival Advantage in Tumor-Bearing Mice

We next evaluated the therapeutic efficacy of the aDEC205-OVA/MG1-OVA prime-boost vaccine in an experimental model of lung

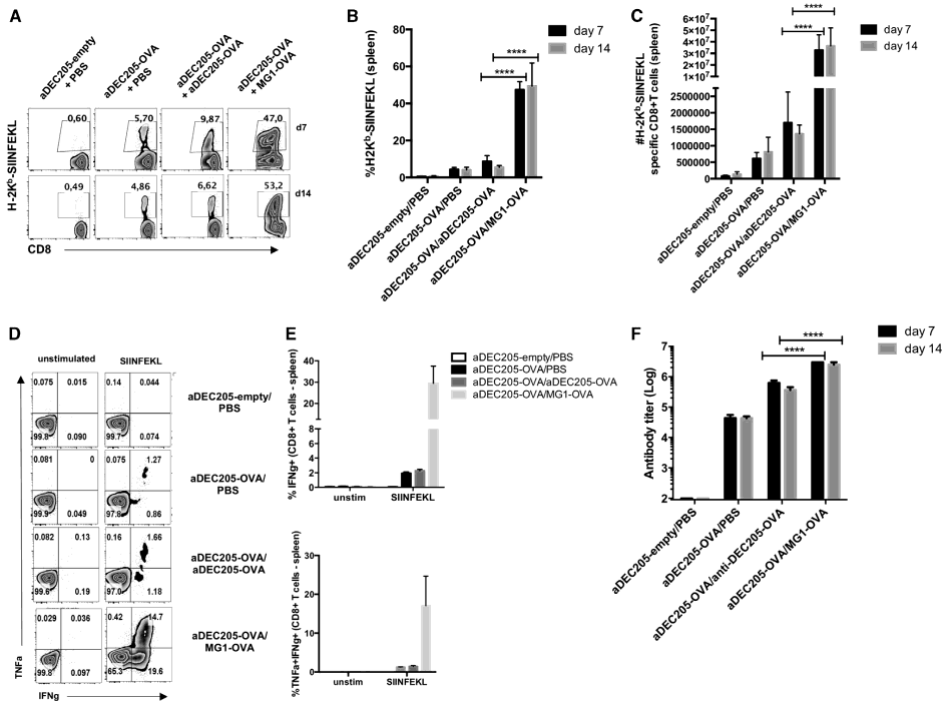

Figure 5. Induction of a Potent Cellular and Humoral OVA-Specific Immune Response after aDEC205-OVA Prime and MG1-OVA Boost

C57BL/6 mice were immunized i.v. with 10 μg of aDEC205-OVA or aDEC205-empty + 50 μg poly(I:C) + 50 μg anti-CD40 at day 0. 14 days later, mice were immunized with a boosting dose of PBS, 10 μg aDEC205-OVA i.v. + 50 μg poly(I:C) + 50 μg anti-CD40, or 10^8 PFUs of MG1-OVA. Spleens were harvested 7 and 14 days following boost to evaluate cellular immune response to prime-boost regimens by flow cytometry (A). The percentage (B) and total number of (C) SIINFEKL-specific $CD8^+$ T cells were determined by H2-K^b-SIINFEKL pentamer staining. At day 14, the representative gating (D) percentage of (E) splenic IFN-γ- and TNF-α-producing $CD8^+$ T cells in response to *in vitro* stimulation with 5 μM SIINFEKL peptide was evaluated. (F) The titers of anti-OVA antibodies in the sera of mice were determined by ELISA at day 7 and day 14 after boost. These results are representative of two independent experiments. ****$p < 0.0001$ (two-way ANOVA).

metastasis. Briefly, 3×10^5 B16-OVA cells were injected i.v. in C57BL/6 mice, and different primes were administered 5 days post-B16-OVA tumor implantation (Figure 6A). Generation of SIINFEKL-specific T cell responses was evaluated by H2-K^b-SIINFEKL pentamer staining of blood 7 days after boost. The heterologous prime-boost combination employing aDEC205-OVA or rAd5-OVA as a prime generated the greatest percentage of circulating antigen-specific T cells. Interestingly, whereas different routes of administration of the aDEC205-OVA prime (i.v. versus i.p.) did not significantly impact priming responses (Figure 3), there was a trend for a higher magnitude of a SIINFEKL-specific $CD8^+$ T cell response generated after prime with aDEC205-OVA administered i.v. compared to aDEC205-OVA prime administered i.p. (Figures 6B and 6D). In general, all OVA-targeted heterologous prime-boost regimens led to improved survival of tumor-bearing mice, with rAd5-OVA/MG1-OVA and aDEC205-OVA/MG1-OVA regimens being the most effective (30% complete remission). The administering of a prime-boost of aDEC205-OVA/VSV-OVA also resulted in the generation of greater SIINFEKL-specific $CD8^+$ T cells and improved survival of tumor-bearing mice (Figures S6B, S6D, and S6E). Cured mice were rechallenged with a subcutaneous injection of 2×10^6 B16-OVA cells (data not shown); no mice previously cured by any prime-boost regimen developed tumors, thus confirming that anti-SIINFEKL responses were long lasting and conferred protection against recurrent tumors.

DISCUSSION

Cancer immunotherapy has emerged as a promising alternative to conventional cancer treatments. Therapeutic strategies that actively

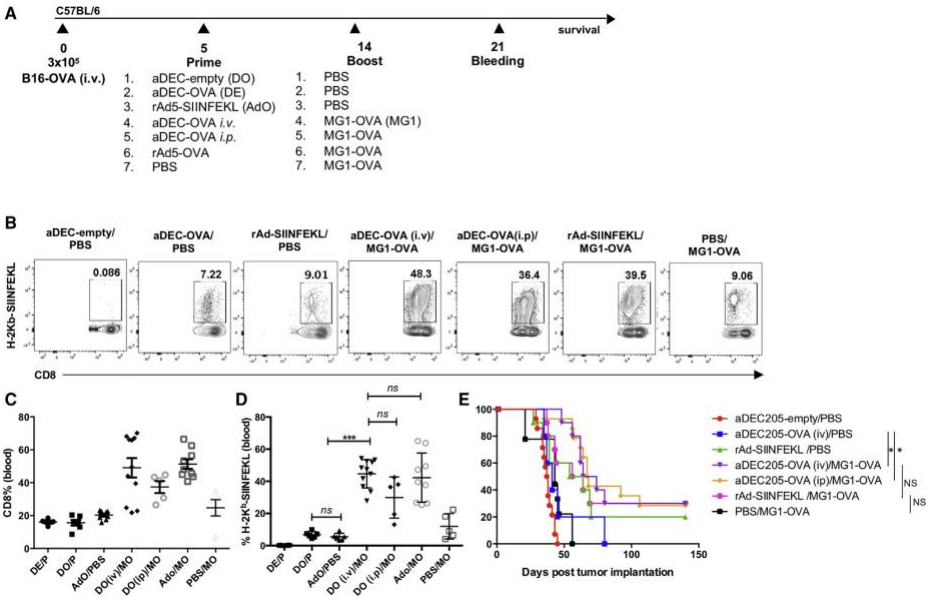

Figure 6. Therapeutic Efficacy of an aDEC205/OVA Prime-Boost Vaccine

(A) Schematic representation of immunization schedule. Briefly, C57BL/6 mice received 3×10^5 B16-OVA cells i.v. At day 5, mice were immunized i.v. or i.p. with 10 μg of aDEC205-OVA or aDEC205-empty + 50 μg poly(I:C) + 50 μg anti-CD40, 10^8 rAd5-SIINFEKL, or PBS. At day 14, mice were immunized with a boosting dose of either PBS or 10^8 MG1-OVA. (B–D) At day 21 saphenous (saph) bleeds were performed to assess the percentage, by flow cytometry (B), of bulk-circulating $CD8^+$ T cells (C) and SIINFEKL-specific $CD8^+$ T cells (D), the latter determined by H2-K^b-SIINFEKL pentamer staining. p value was considered nonsignificant when >0.05; ***$p < 0.001$ (one-way ANOVA). (E) Mice were monitored for survival 140 days post-B16-OVA implantation. Data from three independent survival experiments are pooled. p value was considered nonsignificant when >0.05; *$p < 0.05$ (log-rank Mantel-Cox).

stimulate the immune system to reject tumors have grown to include diverse platforms, including immune-modulating antibodies,[30] small molecules,[31,32] as well as genetically engineered bacteria,[33] cells,[34] and viruses.[7] OVs are attracting increasing interest as multi-mechanistic platforms for immunotherapy, owing, in part, to the recent approval of Imlygic for the treatment of melanoma and to the possibility of combining OVs with antibodies targeting immune checkpoints.[35] Indeed, it is increasingly recognized that OVs have significant potential as part of combination therapy regimens.[36]

In this study, we have further explored one such combination strategy consisting of a heterologous prime-boost, where the priming and boosting vectors share a similar tumor antigen and where the boosting vector is an oncolytic rhabdovirus.[37] This is a strategy that is now under phase I/II clinical evaluation using a nonreplicating Ad5 as a priming vector and oncolytic MG1 as a boosting vector. In contrast with repeat dosing with the same vector (homologous vaccination), this heterologous prime-boost approach has been shown to skew the immune response from antiviral to anti-tumor, promoting long-lasting anti-tumor immunity.[12,38] The secondary immunization with rhabdovirus, which preferentially infects tumors, not only induces oncolysis but also boosts the primary anti-tumor adaptive immune response and breaks immune tolerance.[8]

Although nonreplicating Ad5 is an effective and well-validated vector for vaccination, pre-existing immunity to Ad5, resulting from prior exposure to WT adenoviruses in humans, can potentially limit its effectiveness in clinical trials.[16,17] Indeed, we found that administration of rAd5-SIINFEKL in preimmunized mice led to both significantly lower percentages of SIINFEKL-specific $CD8^+$ T cells (Figures 1C and 1D) and a reduction in their functionality (Figures 1E and 1F).

As an alternative to Ad5, we demonstrate here, in line with other studies, that i.p. or i.v. administration of aDEC205-OVA generates antigen-specific and functionally robust anti-SIINFEKL T cells, as well as humoral immunity toward OVA.[22,25,39] However, as a standalone vaccination agent, we observed that aDEC205-OVA did not perform as well as rAd5-SIINFEKL in terms of controlling

B16-OVA tumors (Figure 6E) and generating activated (IFN-γ^+, TNF-α^+), SIINFEKL-specific $CD8^+$ T cells, even though the numbers of SIINFEKL-specific T cells were similar with both primes (Figure 6B). This difference could relate to dosing inequivalence between aDEC205 relative to Ad5, however something that is difficult to establish, owing to differences in how immune responses are initiated with the two vaccination methods. However, the dose of aDE205-OVA used in this study is within the range of the human equivalent dose of what is being evaluated in clinical trials employing aDEC205 (ClinicalTrials.gov: NCT01834248 and NCT01127464).[40,41] In comparison, Ad5 was administered at a higher human equivalent dose than what is administered in current clinical trials, further illustrating the potential of aDEC205 over Ad5. Additionally, pre-existing immunity to WTAd5, as evidenced by the presence of AdNAbs (Figure 1B), strongly decreased the ability of rAd5-SIINFEKL to produce an immune response against the SIINFEKL antigen but predictably bore no impact on the ability of aDEC205-OVA to generate functional anti-SIINFEKL $CD8^+$ T cells.

Consistent with other studies, we found that heterologous boosting with an oncolytic rhabdovirus, such as MG1-OVA, amplifies antigen-specific immunity in the spleen at days 7 and 14 to a higher extent than homologous boosting, for example, with aDEC205-OVA (Figure 5; Figure S5).[15,36] All heterologous regimens tested conferred a survival advantage in B16-OVA-bearing mice (Figure 6), and in this regard, primes using chimeric aDEC205 or Ad5 were essentially equivalent. This suggests that aDEC205 chimeric antibodies are a feasible alternative to Ad5 in the context of heterologous prime-boost with an oncolytic rhabdovirus. In addition to overcoming pre-existing immunity, which may be a barrier when using certain viral priming vectors, chimeric aDEC205 antibodies can provide additional practical advantages, including, but not limited to, ease of manufacturing, storage, and the possibility of repeat dosing. This last point is a notable limitation for viral vectors encoding antigens, which generally induce an antiviral immune response after the first dose.

Vaccines employing DCs loaded *ex vivo* with tumor lysate or major histocompatibility complex class I (MHC-I) peptides for re-administration to patients have been studied for decades and have been shown to generate robust memory $CD8^+$ T cell responses.[42] Following research in the 1990s on antigen-loaded DC vaccines, many clinical trials carried out to this end have been unable to achieve significant clinical responses.[43,44] Objective response rates for a range of DC vaccines loaded with antigens, such as tyrosinase, gp100, MART-1, and MAGE-A3, and autologous peptides in melanoma patients did not exceed 5%–10%.[45] With the consideration of limitations and logistical challenges in producing DC vaccines, DC targeting using chimeric antibodies, like aDEC205, may be more feasible for treating a diverse population of patients.[46] However, as observed in this study (Figure 6E), chimeric aDEC205 antibodies may be insufficient as standalone anti-cancer vaccines.

One key feature of chimeric aDEC205 antibodies is that they deliver a specific antigen directly to DCs, which in turn, present antigen and activate $CD4^+$ T cells, as well as cross present antigen to $CD8^+$ T cells. However, this approach is also not without limitations. For example, there can be antibody/protein engineering challenges restricting the choice of antigen and how many antigens can be fused to a given aDEC205 antibody. This can be somewhat addressed by using more restricted epitopes in tandem or using multiple different chimeric antibodies.

Another consideration for use of chimeric aDEC205 antibodies is the requirement for an adjuvant.[47] In our study, we found that aDEC205-OVA, administered with poly(I:C) and anti-CD40 adjuvants, was effective in generating anti-OVA responses in mice; however, whereas anti-CD40 antibodies (that target the costimulatory receptor CD40 on DCs to induce their maturation) are highly effective in mice, they have displayed severe toxicity in human cancer immunotherapy trials.[48,49] Although this regimen was selected for modeling purposes in mice, we expect adjuvants that are amenable to human use and that have been used in clinical trials (e.g., poly(I:C) stabilized with polylysine and carboxymethylcellulose [poly ICLC] Hiltonol) to be similarly effective in combination with aDEC205.[50] Indeed, many human-compatible adjuvants are known and available and routinely used in the context of cancer vaccines. These include, but are not limited to, alum, poly(I:C), CpG, lipopolysaccharide (LPS), T helper (Th)1-specific cytokines, and growth factors, like Flt3L, important for the development of classical DCs.[40,51] These adjuvants, cytokines, and growth factors may be further combined. For example, CDX-301, a soluble recombinant human (rhu)Flt3L, has been used in combination with poly ICLC in the context of a phase II human trial, testing an aDEC205-NY-ESO-1 melanoma vaccination strategy.[52]

Altogether, our study indicates that a vaccine consisting of an aDEC205-OVA prime, followed by a rhabdovirus boost, is a promising alternative to the current heterologous prime-boost that employs Ad5-OVA as a priming agent. To our knowledge, this study is the first of its kind to showcase a combination of the well-studied aDEC205 antibody in combination with an OV. Additional studies in other tumor models and antigenic targets will be necessary to assess the applicability of this novel approach to a broad range of disease models.

MATERIALS AND METHODS

Cell Lines

HEK 293T cells, kindly donated by the Oncolytic Virus Manufacturing Facility (OVMF; Ottawa, Canada) for antibody production and purification, were cultured in HyQ high-glucose Dulbecco's modified Eagle's medium (HyClone), supplemented with 10% ultra-low IgG fetal bovine serum (FBS; Gibco), 5% penicillin/streptomycin (pen-strep; Gibco), and 5% L-glutamine (Gibco). B16-F10-OVA cells, kindly gifted by Dr. Yonghong Wan (McMaster University), were cultured in Roswell Park Memorial Institute (RPMI; HyClone), supplemented with 10% FBS, pen-strep, 1 M HEPES buffer, and 50 μg/mL geneticin sulfate (G148 sulfate) (Gibco). All cell lines were incubated at 37°C in a 5% CO_2 humidified incubator.

All cells were tested by PCR and Hoechst staining to ensure that they are free of mycoplasma contamination.

Mice

6- to 8-week-old female C57BL/6J mice were obtained from Charles River Laboratories. All animals were handled in strict accordance with good animal practice and approved by the appropriate committee in collaboration with the Office of Animal Ethics and Compliance.

Antibody Production and Purification

The pcDNA plasmids expressing the heavy-chain aDEC205, aDEC205-OVA, and aDEC205-empty and the light-chain DEC205-kappa sequences were generated by Dr. Silvia Boscardin (University of São Paulo). The plasmid DNA was individually transformed in competent DH5-α, and DNA was purified using the QIAGEN Plasmid Maxi Kit (catalog [Cat.] 12165). Transfection of 90% confluent HEK293T cells in 150 mm tissue-culture dishes, collection of antibody from culture supernatant, and antibody purification were performed as previously described.[53]

Peptides

Peptides corresponding to the immunodominant epitope of OVA (SIINFEKL) that binds to H-2K^b were synthesized by New England Peptide (lot number 3001-1/48-21) and have >95% purity.

Tissue Processing

SIINFEKL-specific T cell responses were measured in blood, spleen, and lung. Briefly, saphenous bleeds of mice from hindlimb were performed, and blood (70–100 μL) was collected in sterile heparin tubes. Red blood cells were lysed using ammonium-chloride-potassium (ACK) lysis buffer. Spleens were excised from sacrificed mice and filtered through a 100-μm plastic cell strainer (Fisherbrand; 352360, 22-363-549) for cell collection. The cell viability of the resulting white blood cells was determined using Trypan blue staining. Lungs were also excised from sacrificed mice after lung perfusion and dissociated using the Lung Dissociation Kit-Mouse (Miltenyi Biotec; 130-095-927), according to the manufacturer's instructions. Upon resuspension in R10 buffer (RPMI, 10% FBS), the cells from blood, spleen, and lung were counted, and 1×10^6 cells per condition were stained for flow cytometry.

Immunoblotting

After aDEC205-OVA antibody quantification by the NanoDrop ND-1000 spectrometer, 1 μg of antibody was run on NuPAGE Novex 4%–12% Bis-Tris precast gels (Thermo Fisher Scientific) under reducing conditions using the XCell SureLock Mini-Cell System (Thermo Fisher Scientific) and transferred to nitrocellulose membranes (Hybond-C; Bio-Rad). Blots were blocked with 2% milk and probed with a goat anti-mouse peroxidase-conjugated antibody (1:2,000) (Jackson ImmunoResearch Laboratories). Bands were visualized using the SuperSignal West Pico Chemiluminescent substrate (Thermo Fisher Scientific).

ELISA

Murine serum was collected from blood for detection of OVA-specific antibodies. Briefly, blood (500 μL) from immunized mice was collected in sterile, 1.5 mL Eppendorf tubes. Collected blood was centrifuged for 10 min at 2,000 × *g*, and the resulting serum in the supernatant was collected and frozen at −20°C for downstream use. Murine serum samples were evaluated for presence of OVA-specific antibodies by ELISA for all groups. 96-well enzyme immunoassay (EIA)/radioimmunoassay (RIA) microplates (Corning; Cat. CLS3590) were coated with albumin (Sigma-Aldrich; A5503-1G) at a concentration of 2 ng/μL in PBS and incubated overnight at 4°C. Plates were washed twice with PBS-Tween 20 0.02% and blocked with blocking buffer (PBS-Tween 20 0.02%, 5% nonfat milk, and 1% BSA) for 1 h at room temperature (RT). Blocking buffer was removed, and serum dilutions (1:500–1:1,000,000 dilution in PBS-Tween 20 0.02%, 5% nonfat milk, and 0.25% BSA) were added to wells and incubated for 2 h at RT. Plates were washed three times with PBS-Tween 20 0.02%, and horseradish peroxidase (HRP)-AffiniPure goat anti-mouse IgG (Jackson ImmunoResearch), diluted 1:4,000, was added to wells and incubated for 1 h at RT. Plates were washed six times with PBS-Tween 20 0.02%, developed with substrate solution (R&D Systems; Cat. DY99), and incubated for 20 min in the dark (RT); development was stopped by addition of 2 N sulfuric acid, and absorbance was read at 510 nm on a Multiskan Ascent plate reader (Thermo LabSystems).

Neutralization Assay

A neutralization assay was performed to quantify the amount neutralizing antibodies against WTAd5, present in serum samples of preimmunized murine, and is based on the ability of serum antibodies to block adenovirus infection of A549 cells. Adenovirus used carries the firefly luciferase (Fluc) reporter gene, E1 deletion, and cytomegalovirus (CMV) promoter. 2-fold serum dilutions (1:100; 1:200; 1:400; 1:800; 1:1,600; 1:3,200; 1:6,400; 1:12,800; 1:25,600; 1:51,200; 1:102,400) were tested. In 96-well flat-bottom plates, the Ad-Fluc virus (MOI 100) was combined with different serum dilutions and incubated for 1 h at 37°C. Contents of this plate were transferred to a 96-well flat-bottom plate, previously seeded with 2×10^5 A549 cells per well, washed 3× with PBS, and incubated for 48 h at 37°C. To read plate, luciferin was added at a final concentration of 2 mg/mL luciferin per well and imaged/read by the Biotek Synergy Mx Microplate Reader. The antibody neutralizing unit (NU) was defined as the minimum serum dilution required to achieve at least an 80% reduction in luciferase activity, which was assumed to correlate directly to an inhibition of vector infection.

Mouse Tumor Model and Injections

B16-OVA lung tumors were established in 8-week-old female C57BL/6 mice by i.v. injection of 3×10^5 cells in 100 μL PBS. For adenovirus injections, mice were anesthetized with 5% isoflurane. WTAd5 (10^{10} PFUs) and rAd5-SIINFEKL (10^8 PFUs) were administered i.m. in 50 μL PBS. For aDEC205 injections, a solution containing 10 μg of aDEC205, 50 μg poly(I:C), and 50 μg anti-CD40 ligand (CD40L) in 150 μL of PBS was administered either i.v. or i.p. Oncolytic

rhabdoviruses (MG1-OVA and VSVΔ51-OVA) were administered i.v. in 100 μL of PBS.

Detection of Antigen-Specific T Cell Responses

OVA-specific T cell responses were measured 7 days and 14 days postboost in blood, spleen, and lung. Splenocytes and lung-resident lymphocytes were isolated and stained for the presence of SIINFEKL-specific T cells using a H-2K^b-SIINFEKL pentamer. For SIINFEKL-specific CD8$^+$ T cell *in vitro* restimulation, 1×10^6 splenocytes and lung-resident lymphocytes were incubated in RPMI medium, supplemented with 10% FBS and 5% pen-strep containing 5 μM of SIINFEKL peptide and brefeldin A (Golgi plug) for 4 h. ICS was performed as described below.

Virus Preparation

The adenoviruses were made using standard techniques.[54] The Indiana serotype of VSV (VSVΔ51 or VSVΔ51-OVA) and the Brazilian MG1 (or MG1-OVA) were used throughout this study and were propagated in Vero cells. VSVΔ51-expressing and MG1-expressing OVA are recombinant derivatives of VSVΔ51 and MG1, described previously.[55] All viruses were propagated on Vero cells and purified on 5%–50% OptiPrep (Sigma) gradient, and all virus titers were quantified by the standard plaque assay on Vero cells, as previously described.[56]

Antibody Binding Assay

A flow cytometry-based binding assay was performed for evaluation of aDEC205-OVA and aDEC205-empty binding specificity to the target DEC205 receptor on DCs. Bulk splenocytes were isolated from spleens of naive C57BL/6J mice. Red blood cells were lysed, and 5×10^6 bulk splenocytes were incubated with graded concentrations of antibody (0.1 μg/μL, 1 μg/μL, and 10 μg/μL) in a 96-well plate for 45 min (4°C). After incubation, cells were stained for flow cytometry.

Flow Cytometry

After processing the tissues as described above, cells were then stained with the FVS780 viability dye (BD Biosciences, San Jose, CA) PBS for 15 min at RT. Following washes, cells were incubated with anti-CD16/32 in 0.5% BSA/PBS at 4°C to block nonspecific antibody interaction with Fc receptors. Subsequently, the following protocols were used for staining.

Staining for Antibody Binding Assay

Anti-CD11c-phycoerythrin (PE)-Cy7, anti-MHC-I-PE, anti-CD8-PE-CF594, anti-IgG-allophycocyanin (APC), anti-CD3-fluorescein isothiocyanate (FITC), and anti-CD19-FITC antibodies were added to cells and incubated for 30 min (4°C).

Staining for ICS

First, 1×10^6 cells were incubated with antibodies targeting T cell surface markers CD3-AF700 and CD8-PE-CF594 for 30 min (4°C). Cells were washed twice with fluorescence-activated cell sorting (FACS) buffer. Next, the mouse Cytofix/Cytoperm Plus (BD Bioscience) was used for permeabilization and ICS. Cells were incubated with Cytofix for 20 min to permeabilize cells for ICS (4°C). Cells were washed twice with PermWash and incubated with anti-IFN-γ-BV650 and anti-TNF-α-AF647 diluted in PermWash for 30 min (4°C).

Staining for OVA-Specific T Cells/Pentamer Staining

Cells were washed with FACS buffer. In a 96-well plate, 3 μL of H-2K^b-SIINFEKL pentamer-APC (Proimmune) in 50 μL of FACS buffer was added per well and incubated for 10 min (RT) in the dark. Cells were washed twice with FACS buffer and stained with fixable viability stain for 30 min (4°C). Subsequently, the cells were washed with FACS buffer and incubated with anti-CD16/32 in FACS buffer for 5 min (4°C). Next, cells were stained with anti-CD8-PE-CF594 and anti-CD3-AF700 for 30 min (4°C)

After staining, cells were washed with FACS buffer and fixed in 1% paraformaldehyde. Cells were acquired on Becton Dickinson (BD) flow cytometry (Fortessa), and analyses were performed using FlowJo software version (v.)9.

VSV-OVA Cloning and Rescue

Phagemid cloning vector, also known as BlueScribe SK (pBSSK)-VSVΔ51, plasmid-containing viral genome, was used to construct VSVΔ51-OVA. In brief, the OVA gene was PCR amplified from pcDNA expressing aDEC205-OVA using the following primers: forward: 5′-AATTCTCGAGATGGGCTCCATCG-3′ and reverse: 5′-CATCGCTAGCTCACTACAGATCCTC-3′. PCR amplicon was digested by XhoI and NheI and cloned into the multiple cloning site (MCS) of pBSSK-VSVd51 between G and L open reading frames (ORFs). Positive clones were screened by restriction digestion mapping and verified by sequencing.

Statistics

Statistical significance was calculated using Student's t test or one-way or two-way ANOVA test, using Tukey's multiple comparison test, as indicated in the figure legends. The log rank (Mantel-Cox) test was used to determine significant differences in plots for survival studies. Error bars represent standard error of the mean. Significance is based on a p value <0.05. Statistical analyses were performed using GraphPad Prism 6.0 and Excel.

SUPPLEMENTAL INFORMATION

Supplemental Information can be found online at https://doi.org/10.1016/j.omto.2020.10.007.

AUTHOR CONTRIBUTIONS

F.T. conceived the project. F.T. and J.-S.D. designed the study. All authors participated in the acquisition, analysis, and/or interpretation of data and have read and approved the final manuscript. A.J., H.K.B., and J.-S.D. drafted the manuscript with editorial contributions from F.T. S.B. provided plasmids and protocols. C.T.d.S. and A.C. performed all animal work. M.H. and K.S. constructed and rescued viral vectors. R.J. P. provided adenovirus. J.-S.D. supervised the study.

CONFLICTS OF INTEREST

The authors declare no competing interests.

ACKNOWLEDGMENTS

We thank Dr. Brian Lichty (McMaster University) for providing the recombinant adenovirus encoding the epitope SIINFEKL (rAd5-SIINFEKL). We thank Turnstone Biologics for providing Maraba MG1 constructs. J.-S.D. is supported by the Canadian Institute for Health Research (CIHR) through a new investigator award in Infection and Immunity. J.-S.D. holds grants from the Terry Fox Research Institute (INI-147824). This project was supported by BioCanRx (FY18/CAT17) and Valerie's Flutter Foundation, as well as by the Canadian Cancer Society (grant 705952) and Canadian Institutes of Health Research–Institute of Cancer Research (grant 705952). F.T. was supported by a BioCanRx Travel Exchange Award. H.K.B. and A.J. were supported by the MITACS Accelerate Canadian Partnership in Immunotherapy Manufacturing Excellence PhD Internships.

REFERENCES

1. Strausberg, R.L. (2005). Tumor microenvironments, the immune system and cancer survival. Genome Biol. *6*, 211.
2. Russell, S.J., Peng, K.W., and Bell, J.C. (2012). Oncolytic virotherapy. Nat. Biotechnol. *30*, 658–670.
3. Ilkow, C.S., Swift, S.L., Bell, J.C., and Diallo, J.-S. (2014). From scourge to cure: tumour-selective viral pathogenesis as a new strategy against cancer. PLoS Pathog. *10*, e1003836.
4. Gujar, S., Bell, J., and Diallo, J.S. (2019). Snapshot: cancer immunotherapy with oncolytic viruses. Cell *176*, 1240–1240.e1.
5. Russell, S.J., and Peng, K.W. (2009). Measles virus for cancer therapy. Curr. Top. Microbiol. Immunol. *330*, 213–241.
6. Miyamoto, S., Inoue, H., Nakamura, T., Yamada, M., Sakamoto, C., Urata, Y., Okazaki, T., Marumoto, T., Takahashi, A., Takayama, K., et al. (2012). Coxsackievirus B3 is an oncolytic virus with immunostimulatory properties that is active against lung adenocarcinoma. Cancer Res. *72*, 2609–2621.
7. Chiocca, E.A., and Rabkin, S.D. (2014). Oncolytic viruses and their application to cancer immunotherapy. Cancer Immunol. Res. *2*, 295–300.
8. Brun, J., McManus, D., Lefebvre, C., Hu, K., Falls, T., Atkins, H., Bell, J.C., McCart, J.A., Mahoney, D., and Stojdl, D.F. (2010). Identification of genetically modified Maraba virus as an oncolytic rhabdovirus. Mol. Ther. *18*, 1440–1449.
9. Lichty, B.D., Breitbach, C.J., Stojdl, D.F., and Bell, J.C. (2014). Going viral with cancer immunotherapy. Nat. Rev. Cancer *14*, 559–567.
10. Zamarin, D., Ricca, J.M., Sadekova, S., Oseledchyk, A., Yu, Y., Blumenschein, W.M., Wong, J., Gigoux, M., Merghoub, T., and Wolchok, J.D. (2018). PD-L1 in tumor microenvironment mediates resistance to oncolytic immunotherapy. J. Clin. Invest. *128*, 1413–1428.
11. Selman, M., Rousso, C., Bergeron, A., Son, H.H., Krishnan, R., El-Sayes, N.A., Varette, O., Chen, A., Le Boeuf, F., Tzelepis, F., et al. (2018). Multi-modal potentiation of oncolytic virotherapy by vanadium compounds. Mol. Ther. *26*, 56–69.
12. Lu, S. (2009). Heterologous prime-boost vaccination. Curr. Opin. Immunol. *21*, 346–351.
13. Pol, J.G., Zhang, L., Bridle, B.W., Stephenson, K.B., Rességuier, J., Hanson, S., Chen, L., Kazdhan, N., Bramson, J.L., Stojdl, D.F., et al. (2014). Maraba virus as a potent oncolytic vaccine vector. Mol. Ther. *22*, 420–429.
14. Bridle, B.W., Boudreau, J.E., Lichty, B.D., Brunellière, J., Stephenson, K., Koshy, S., Bramson, J.L., and Wan, Y. (2009). Vesicular stomatitis virus as a novel cancer vaccine vector to prime antitumor immunity amenable to rapid boosting with adenovirus. Mol. Ther. *17*, 1814–1821.
15. Le Boeuf, F., Selman, M., Son, H.H., Bergeron, A., Chen, A., Tsang, J., Butterwick, D., Arulanandam, R., Forbes, N.E., Tzelepis, F., et al. (2017). Oncolytic Maraba Virus MG1 as a Treatment for Sarcoma. Int. J. Cancer *141*, 1257–1264.
16. Bridle, B.W., Nguyen, A., Salem, O., Zhang, L., Koshy, S., Clouthier, D., Chen, L., Pol, J., Swift, S.L., Bowdish, D.M.E., et al. (2016). Privileged antigen presentation in splenic B cell follicles maximizes T cell responses in prime-boost vaccination. J. Immunol. *196*, 4587–4595.
17. Sekaly, R.P. (2008). The failed HIV Merck vaccine study: a step back or a launching point for future vaccine development? J. Exp. Med. *205*, 7–12.
18. Barnes, E., Folgori, A., Capone, S., Swadling, L., Aston, S., Kurioka, A., Meyer, J., Huddart, R., Smith, K., Townsend, R., et al. (2012). Novel adenovirus-based vaccines induce broad and sustained T cell responses to HCV in man. Sci. Transl. Med. *4*, 115ra1.
19. Mast, T.C., Kierstead, L., Gupta, S.B., Nikas, A.A., Kallas, E.G., Novitsky, V., Mbewe, B., Pitisuttithum, P., Schechter, M., Vardas, E., et al. (2010). International epidemiology of human pre-existing adenovirus (Ad) type-5, type-6, type-26 and type-36 neutralizing antibodies: correlates of high Ad5 titers and implications for potential HIV vaccine trials. Vaccine *28*, 950–957.
20. Nwanegbo, E., Vardas, E., Gao, W., Whittle, H., Sun, H., Rowe, D., Robbins, P.D., and Gambotto, A. (2004). Prevalence of neutralizing antibodies to adenoviral serotypes 5 and 35 in the adult populations of The Gambia, South Africa, and the United States. Clin. Diagn. Lab. Immunol. *11*, 351–357.
21. Saxena, M., Van, T.T.H., Baird, F.J., Coloe, P.J., and Smooker, P.M. (2013). Pre-existing immunity against vaccine vectors–friend or foe? Microbiology (Reading) *159*, 1–11.
22. Trombetta, E.S., and Mellman, I. (2005). Cell biology of antigen processing in vitro and in vivo. Annu. Rev. Immunol. *23*, 975–1028.
23. Bonifaz, L., Bonnyay, D., Mahnke, K., Rivera, M., Nussenzweig, M.C., and Steinman, R.M. (2002). Efficient targeting of protein antigen to the dendritic cell receptor DEC-205 in the steady state leads to antigen presentation on major histocompatibility complex class I products and peripheral CD8+ T cell tolerance. J. Exp. Med. *196*, 1627–1638.
24. Moriya, K., Wakabayashi, A., Shimizu, M., Tamura, H., Dan, K., and Takahashi, H. (2010). Induction of tumor-specific acquired immunity against already established tumors by selective stimulation of innate DEC-205(+) dendritic cells. Cancer Immunol. Immunother. *59*, 1083–1095.
25. Yang, T.C., Dayball, K., Wan, Y.H., and Bramson, J. (2003). Detailed analysis of the CD8+ T-cell response following adenovirus vaccination. J. Virol. *77*, 13407–13411.
26. Bonifaz, L.C., Bonnyay, D.P., Charalambous, A., Darguste, D.I., Fujii, S., Soares, H., Brimnes, M.K., Moltedo, B., Moran, T.M., and Steinman, R.M. (2004). In vivo targeting of antigens to maturing dendritic cells via the DEC-205 receptor improves T cell vaccination. J. Exp. Med. *199*, 815–824.
27. Dudziak, D., Kamphorst, A.O., Heidkamp, G.F., Buchholz, V.R., Trumpfheller, C., Yamazaki, S., Cheong, C., Liu, K., Lee, H.W., Park, C.G., et al. (2007). Differential antigen processing by dendritic cell subsets in vivo. Science *315*, 107–111.
28. Mukherjee, G., Geliebter, A., Babad, J., Santamaria, P., Serreze, D.V., Freeman, G.J., Tarbell, K.V., Sharpe, A., and DiLorenzo, T.P. (2013). DEC-205-mediated antigen targeting to steady-state dendritic cells induces deletion of diabetogenic $CD8^+$ T cells independently of PD-1 and PD-L1. Int. Immunol. *25*, 651–660.
29. Zhang, P., Andorko, J.I., and Jewell, C.M. (2017). Impact of dose, route, and composition on the immunogenicity of immune polyelectrolyte multilayers delivered on gold templates. Biotechnol. Bioeng. *114*, 423–431.
30. Scott, A.M., Allison, J.P., and Wolchok, J.D. (2012). Monoclonal antibodies in cancer therapy. Cancer Immun. *12*, 14.
31. Liu, M., Wang, X., Wang, L., Ma, X., Gong, Z., Zhang, S., and Li, Y. (2018). Targeting the IDO1 pathway in cancer: from bench to bedside. J. Hematol. Oncol. *11*, 100.
32. Zhao, Y., and Adjei, A.A. (2014). The clinical development of MEK inhibitors. Nat. Rev. Clin. Oncol. *11*, 385–400.
33. Liang, K., Liu, Q., Li, P., Luo, H., Wang, H., and Kong, Q. (2019). Genetically engineered Salmonella Typhimurium: Recent advances in cancer therapy. Cancer Lett. *448*, 168–181.

34. Miliotou, A.N., and Papadopoulou, L.C. (2018). CAR T-cell therapy: a new era in cancer immunotherapy. Curr. Pharm. Biotechnol. *19*, 5–18.

35. Zamarin, D., Holmgaard, R.B., Subudhi, S.K., Park, J.S., Mansour, M., Palese, P., Merghoub, T., Wolchok, J.D., and Allison, J.P. (2014). Localized oncolytic virotherapy overcomes systemic tumor resistance to immune checkpoint blockade immunotherapy. Sci. Transl. Med. *6*, 226ra32.

36. Phan, M., Watson, M.F., Alain, T., and Diallo, J.S. (2018). Oncolytic viruses on drugs: achieving higher therapeutic efficacy. ACS Infect. Dis. *4*, 1448–1467.

37. Bridle, B.W., Stephenson, K.B., Boudreau, J.E., Koshy, S., Kazdhan, N., Pullenayegum, E., Brunellière, J., Bramson, J.L., Lichty, B.D., and Wan, Y. (2010). Potentiating cancer immunotherapy using an oncolytic virus. Mol. Ther. *18*, 1430–1439.

38. Pol, J.G., Acuna, S.A., Yadollahi, B., Tang, N., Stephenson, K.B., Atherton, M.J., Hanwell, D., El-Warrak, A., Goldstein, A., Moloo, B., et al. (2018). Preclinical evaluation of a MAGE-A3 vaccination utilizing the oncolytic Maraba virus currently in first-in-human trials. Oncoimmunology *8*, e1512329.

39. Mahnke, K., Guo, M., Lee, S., Sepulveda, H., Swain, S.L., Nussenzweig, M., and Steinman, R.M. (2000). The dendritic cell receptor for endocytosis, DEC-205, can recycle and enhance antigen presentation via major histocompatibility complex class II-positive lysosomal compartments. J. Cell Biol. *151*, 673–684.

40. Miller, G., Pillarisetty, V.G., Shah, A.B., Lahrs, S., and DeMatteo, R.P. (2003). Murine Flt3 ligand expands distinct dendritic cells with both tolerogenic and immunogenic properties. J. Immunol. *170*, 3554–3564.

41. Nair, A.B., and Jacob, S. (2016). A simple practice guide for dose conversion between animals and human. J. Basic Clin. Pharm. *7*, 27–31.

42. Tacken, P.J., de Vries, I.J., Torensma, R., and Figdor, C.G.G. (2007). Dendritic-cell immunotherapy: from ex vivo loading to in vivo targeting. Nat. Rev. Immunol. *7*, 790–802.

43. Nestle, F.O., Alijagic, S., Gilliet, M., Sun, Y., Grabbe, S., Dummer, R., Burg, G., and Schadendorf, D. (1998). Vaccination of melanoma patients with peptide- or tumor lysate-pulsed dendritic cells. Nat. Med. *4*, 328–332.

44. Hsu, F.J., Benike, C., Fagnoni, F., Liles, T.M., Czerwinski, D., Taidi, B., Engleman, E.G., and Levy, R. (1996). Vaccination of patients with B-cell lymphoma using autologous antigen-pulsed dendritic cells. Nat. Med. *2*, 52–58.

45. Lesterhuis, W.J., Aarntzen, E.H.J.G., De Vries, I.J.M., Schuurhuis, D.H., Figdor, C.G., Adema, G.J., and Punt, C.J.A. (2008). Dendritic cell vaccines in melanoma: from promise to proof? Crit. Rev. Oncol. Hematol. *66*, 118–134.

46. Caminschi, I., Maraskovsky, E., and Heath, W.R. (2012). Targeting dendritic cells in vivo for cancer therapy. Front. Immunol. *3*, 13.

47. Kato, M., McDonald, K.J., Khan, S., Ross, I.L., Vuckovic, S., Chen, K., Munster, D., MacDonald, K.P.A., and Hart, D.N.J. (2006). Expression of human DEC-205 (CD205) multilectin receptor on leukocytes. Int. Immunol. *18*, 857–869.

48. Wen, P.Y., Reardon, D.A., Armstrong, T.S., Phuphanich, S., Aiken, R.D., Landolfi, J.C., Curry, W.T., Zhu, J., Glantz, M., Peereboom, D.M., et al. (2019). A Randomized Double-Blind Placebo-Controlled Phase II Trial of Dendritic Cell Vaccine ICT-107 in Newly Diagnosed Patients with Glioblastoma. Clin. Canc. Res. *25*, 5799–5807.

49. Vonderheide, R.H., Flaherty, K.T., Khalil, M., Stumacher, M.S., Bajor, D.L., Hutnick, N.A., Sullivan, P., Mahany, J.J., Gallagher, M., Kramer, A., et al. (2007). Clinical activity and immune modulation in cancer patients treated with CP-870,893, a novel CD40 agonist monoclonal antibody. J. Clin. Oncol. *25*, 876–883.

50. Bowen, W.S., Svrivastava, A.K., Batra, L., Barsoumian, H., and Shirwan, H. (2018). Current challenges for cancer vaccine adjuvant development. Expert Rev. Vaccines *17*, 207–215.

51. Anandasabapathy, N., Feder, R., Mollah, S., Tse, S.W., Longhi, M.P., Mehandru, S., Matos, I., Cheong, C., Ruane, D., Brane, L., et al. (2014). Classical Flt3L-dependent dendritic cells control immunity to protein vaccine *211*, 1875–1891.

52. Bhardwaj, N., Pavlick, A.C., Ernstoff, M.S., Hanks, B.A., Albertini, M.R., Luke, J.J., Yellin, M.H., Keler, T., Davis, T.A., Crocker, A., et al. (2016). A Phase II Randomized Study of CDX-1401, a Dendritic Cell Targeting NY-ESO-1 Vaccine, in Patients with Malignant Melanoma Pre-Treated with Recombinant CDX-301, a Recombinant Human Flt3 Ligand. J. Clin. Oncol. *34*, 9589, 9589.

53. Henriques, H.R., Rampazo, E.V., Gonçalves, A.J.S., Vicentin, E.C., Amorim, J.H., Panatieri, R.H., Amorim, K.N.S., Yamamoto, M.M., Ferreira, L.C.S., Alves, A.M.B., and Boscardin, S.B. (2013). Targeting the non-structural protein 1 from dengue virus to a dendritic cell population confers protective immunity to lethal virus challenge. PLoS Negl. Trop. Dis. *7*, e2330.

54. Ross, P.J., and Parks, R.J. (2009). Construction and characterization of adenovirus vectors. Cold Spring Harb. Protoc. *2009*, pdb.prot5011.

55. Stojdl, D.F., Lichty, B.D., tenOever, B.R., Paterson, J.M., Power, A.T., Knowles, S., Marius, R., Reynard, J., Poliquin, L., Atkins, H., et al. (2003). VSV strains with defects in their ability to shutdown innate immunity are potent systemic anti-cancer agents. Cancer Cell *4*, 263–275.

56. Diallo, J.S., Vähä-Koskela, M., Le Boeuf, F., and Bell, J. (2012). Propagation, purification, and in vivo testing of oncolytic vesicular stomatitis virus strains. Methods Mol. Biol. *797*, 127–140.

Curriculum Vitae

EDUCATION

Doctorate of Science (PhD) (*Microbiology and Immunology)* **May 2016-Present**
University of Ottawa, Ottawa, ON

Honours Bachelor of Science (*Honours Life Science*) **September 2011-June 2015**
McMaster University, Hamilton, ON

RESEARCH EXPERIENCE

Graduate Student **May 2016-Present**
Ottawa Hospital Research Institute, Cancer Center
Supervised by Dr. Jean-Simon Diallo

- Project: Identification and evaluation of novel cancer targets, or antigens, from sarcoma for use with a new vaccine therapy using cancer-fighting viruses called oncolytic viruses
- MITACS CanPrime Internship (academia-industry partnership with Turnstone Biologics) as of May 2019
- Experience in the following research techniques:
    - Basic microscopy
    - Molecular cloning and viral rescue (transfections, transductions)
    - PCR
    - Tissue culture (cancer cells, T cells, dendritic cells)
    - Animal handling and mouse work (intraperitoneal, subcutaneous injections, saphenous bleeds, tumour measurements)
    - Protein extraction and western blot
    - Flow cytometry (panel design, staining, acquisition and analysis)
    - Tissue processing and immune profiling
    - Viral assays (*in vitro* infections, cytotoxicity assays, plaque assays)
    - Recombinant antibody production and purification

Research Assistant **September 2015-April 2016**
McMaster Immunology Research Centre 5071, McMaster, Hamilton, ON
Supervised by Dr. Yonghong Wan

- Project: Molecular cloning of gp33 cancer specific target into lentivirus vector for antigen targeting studies in B16, MCA205 and ID8 tumour cell lines
- Experience in the following research techniques:
    - Basic microscopy
    - Molecular cloning and viral rescue (transfections, transductions)
    - PCR
    - Tissue culture (cancer cells)

PUBLICATIONS

Arulanandam, R., Garcia, V., Taha, Z., Selman, M, Chen, A., Varette, O., McDonald, E., Birdi, H.K., Jirovec, A., Tzelepis, F., Landry, A., Bergeron, A., Vanderhyden, B., Diallo JS. "Strategic combination of trastuzumab emtansine with oncolytic rhabdoviruses leads to therapeutic synergy." *Communications Biology,* May 2020.

Tzelepis, F.,*Birdi, H.K.,* Jirovec, A.,* Boscardin, S., Tanese de Souza, C., Hooshyar, M., Chen, A., Sutherland, K., Parks, R., Werier, J., Diallo, JS. "Oncolytic rhabdovirus vaccine boosts chimeric anti-DEC205 priming for effective cancer immunotherapy." *Molecular Therapy Oncolytics*. 19; P240-252 (December 2020) doi: 10.1016/j.omto.2020.10.007.

Birdi, HK.,* Jirovec, A.,* Cortes-Kaplan, S.,* Diallo, JS., Ardolino, M. "Immunotherapy for sarcomas: new frontiers and unveiled opportunities." *Journal for Immunotherapy of Cancer*, November 2020.

In preparation: Selman, M., Bergeron, A., Birdi, HK., Chen, A., Tzelepis, F., Werier, J., Abelbary H., Diallo, JS. "Potentiating oncolytic virotherapy in sarcoma using vanadium compounds."

VOLUNTEER AND INTERSHIPS

Public Health Agency of Canada (PHAC) **May-November 2021**
PHAC (Remote), Ottawa, Ontario

- Federal Student Work Experience Program (FSWEP)
- Student analyst in the Immunization Program and Emergency Preparedness: COVID-19 Preparedness

Ximbassador for Ximbio **September 2020-May 2021**
OHRI, Ottawa, Ontario

- Ximbassador internship at the OHRI, working in partnership with the UK based not-for profit organization Ximbio, aims to facilitate reagent and material procurement from academic laboratories at the OHRI and deposit into a global repository
- Some of the tasks of a Ximbassador include: literature review of home institute publications to identify novel reagents/materials, communication with affiliated scientists, doctors and inventors, completion of procurement documentation, learn and apply intellectual patent law and work with home institute TTO staff

Antibuddies Podcast Host **May 2020-May 2021**

- Created immunology focused content (scripts, presentations, research) for 3 podcast segments: Career Talks, video Journal Club, and Immunology 101

Ottawa Hospital Technology Transfer Office (TTO) Volunteer **December 2019-May 2020**
OHRI, Ottawa, Ontario

- Volunteer executing prior-art patent searches for the OHRI with Leah Labib

Graduate Student Experience Committee **September 2019-Present**
University of Ottawa, Ottawa, Ontario

- Part of the committee that strives to enhance the graduate school experience at the University as part of the Biochemistry, Microbiology and Immunology program
- Plan research nights, school merchandise, workshops, and seminars relevant to the program

Valerie's Flutter Foundation Sarcoma Lab Tour **October 17, 2019**
Cancer Centre, OHRI, Ottawa, Ontario

- Organized and planned information night and lab tour for donators to the Valerie Flutter Foundation that fund our sarcoma research

Guest Lecturer for Cell Biology and Biochemistry, BIOL 2201 **June 14, 2018**
Carleton University, Ottawa, Ontario

- Instructor: Dr. Mohsen Hooshyar
- Gave an introductory lecture on cancer biology, cancer immunotherapy, and oncolytic viruses

Let's Talk Science Volunteer **September 2017-2018**
University of Ottawa, Ottawa, Ontario

- OHRI Grade 9 Job Shadowing Day (Lab Tour)
- Cancer Centre Lab Tour
- The Ottawa Hospital (TOH) 'Behind the Scenes'
- Canada Wide Science Fair (CWSF) Judge
- Science outreach at Golf Quest for 4 Clinical Trials

SCHOLARSHIPS AND AWARDS

2017-2021	University of Ottawa Entrance Scholarship	5x$15,000
2018-2021	MITACS Accelerate CanPRIME Internship	3x$2000
2018/2019	BioCanRx Travel Award	2x$1000
2018/2019	FGPS Travel Award	2x$400
2018	1st place BMI Seminar Day	$100
2011	McMaster Honours Award	$1200

CONFERENCE ATTENDANCE

Year	Venue: Date	Type	Title
2021	Biochemistry, Microbiology and Immunology Seminar Day, University of Ottawa; April 1, 2021	Virtual Oral Presentation	Identification and evaluation of novel sarcoma antigens for use with oncolytic vaccines
2020	Connective Tissue Oncology Society (CTOS) Online Annual Conference. November 18-21, 2020	Virtual Poster	Identification and evaluation of novel sarcoma antigens for use with oncolytic vaccines
2020	Ottawa Hospital Research Institute Research Day 2020; November 20, 2020	Virtual Poster	Identification and evaluation of novel sarcoma antigens for use with oncolytic vaccines
2020	Biochemistry, Microbiology and Immunology Seminar Day, University of Ottawa; April 30, 2020	5-minute virtual Oral presentation	Identification and evaluation of novel sarcoma antigens for use with oncolytic vaccines
2019	Ottawa Hospital Research Institute Research Day 2019; November 7, 2019	Poster	Identification and evaluation of novel sarcoma antigens for use with oncolytic vaccines
2019	BioCanRx Summit for Cancer Immunotherapy, Victoria, British Columbia; October 20-23, 2019	Poster+ 2 minute oral presentation	Identification and evaluation of novel sarcoma antigens for use with oncolytic vaccines
2019	Biochemistry, Microbiology and Immunology Poster Day, University of Ottawa; May 2, 2019	Poster	Identification and evaluation of novel sarcoma antigens for use with oncolytic vaccines
2018	Ottawa Hospital Research Institute Research Day 2018; November, 2018	Poster	Identification and evaluation of novel sarcoma antigens for use with oncolytic vaccines
2018	BioCanRx Summit for Cancer Immunotherapy, Banff, Alberta; October 27-30, 2018	Poster	Identification and evaluation of novel sarcoma antigens for use with oncolytic vaccines
2018	Keystone Symposium Cancer Immunotherapy: Combinations (C5), Montreal, Quebec; March 23-27, 2018	Poster	Identification and evaluation of novel sarcoma antigens for use with oncolytic vaccines
2018	Biochemistry, Microbiology and Immunology Seminar Day, University of Ottawa; February 23, 2018	Oral presentation	Identification and evaluation of novel sarcoma antigens for use with oncolytic vaccines
2017	Ottawa Hospital Research Institute Research Day 2017; November 9, 2017	Poster	Identification and evaluation of novel sarcoma antigens for use with oncolytic vaccines
2017	BioCanRx Summit for Cancer Immunotherapy, Gatineau, Quebec; June 25-28, 2017	Poster	Identification and evaluation of novel sarcoma antigens for use with oncolytic vaccines

2017	Biochemistry, Microbiology and Immunology Poster Day, University of Ottawa; May 11, 2017	Poster	Identification and evaluation of novel sarcoma antigens for use with oncolytic vaccines
2016	Ottawa Hospital Research Institute Research Day 2016; November 10, 2016	Poster	Identification and evaluation of novel sarcoma antigens for use with oncolytic vaccines

CERTIFICATIONS

Animal Care Training
Flow Cytometry Training
Radiation Training
WHMIS

LANGUAGE SKILLS

Proficient in reading, writing and speaking English